Classical biotechnological and analytical techniques in combination with FTIR spectroscopy: A study of protein hydrolysates from poultry residual raw materials

Linn Maria Gundersen Hunnes

Thesis for the Masters Degree in Chemistry

60 credits

Department of Chemistry
Faculty of Mathematics and Natural Sciences
UNIVERSITY OF OSLO

November 2020

Classical biotechnological and analytical techniques in combination with FTIR spectroscopy: A study of protein hydrolysates from poultry residual raw materials

Linn Maria Gundersen Hunnes

Thesis for the Master's Degree in Chemistry

60 credits

Department of Chemistry

Faculty of Mathematics and Natural Sciences

UNIVERSITY OF OSLO

November 16th 2020

2020

Classical biotechnological and analytical techniques in combination with FTIR spectroscopy: A study of protein hydrolysates from poultry residual raw materials

Linn Maria Gundersen Hunnes

http://www.duo.uio.no/

Printed at reprosentralen, University of Oslo

Abstract

Enzymatic protein hydrolysis (EPH) is a well-established process with the potential to produce sustainable protein-rich products from residual raw materials (RRM) deriving from the food industry (1). However, in the EPH today, one protease is usually used to separate a fat phase, a liquid phase with soluble protein, and a solid phase with mineral-rich sediment from the RRM. The challenge of the industry is that this technology cannot release all the proteins found in complex residuals. Annually, poultry processing industries produce large amounts of RRM, with a high potential for a value increase (2). Moreover, while helping the industry with a sustainable valorization of the RRM, new products with high nutritional content can be produced and used to nourish the globally growing population. **Figure 1** show some examples of products that could contain protein hydrolysates. The present study aimed to optimize the utilization of the poultry RRM by optimizing the EPH process on a lab-scale, with the purpose of releasing a wide variety of peptides, obtain an increased protein yield and gain substantial information about the released peptides. A combination of classical biotechnological and analytical techniques, such as high performance size-exclusion chromatography (HP-SEC), Dumas combustion analysis, degree of hydrolysis (DH%), raw material analysis (RMA), and sodium dodecyl sulfate – polyacrylamide gel electrophoresis (SDS-PAGE) was used to obtain quality parameters, such as protein yield, mass average molar mass (M_W), and degree of hydrolysis, as well as structural information of the peptides in the hydrolysate products using fourier-transform infrared spectroscopy (FTIR). MDPR treated with a combination of both proteases did increase the protein yield by 13-20 %, with a % RSD of $1.6 \geq 7.4$ %, relative to the EPH using either Bromelain or Endocut-02. The HP-SEC analyses showed that the hydrolysates from chicken fillet and tendons treated with Bromelain or Endocut-02 constituted peptides in the MW range of approximately 1100-3000 and 3000-5000, or 2000-6700 and 2000-12000, respectively. The information obtained through the work of this study have lead to a higher protein yield and contributed valuable information about the peptide composition of the hydrolysate products that will be useful in further EPH studies.

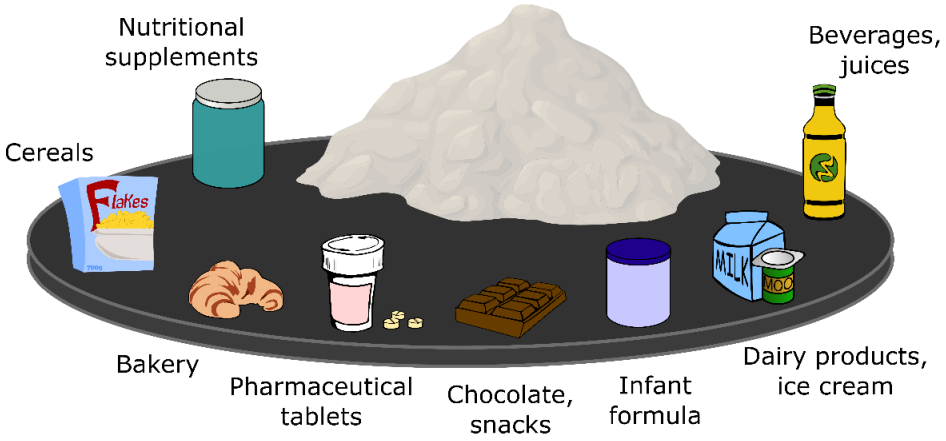

Figure 1. Example products where protein hydrolysates can be used. The picture is borrowed from Kristoffersen, K.A. (1).

Preface

The present work was performed at Nofima, department Ås, from January 2018 until November 2020. My supervisors have been Dr. Diana Lindberg and Dr. Nils Kristian Afseth at Nofima and Prof. Elsa Lundanes at the Department of Chemistry, University of Oslo. First of all, I want to thank Nofima for letting me be part of their team and their exciting project, Notably. It has been really interesting work where I've been challenged and earned a lot of knowledge in new areas. Also, thank you for allowing me to attend the Bioprosp_19 conference «Unlocking the potential of biomolecules from marine environments» in Tromsø, with financial support through the Notably project. The presented poster is given in **Appendix 8**.

I want to thank Diana for sharing her thoughts and knowledge during the lab work and the constructive feedback during the writing of the thesis. Also, for always being available for conversations, both work-related and others. She has also shown me care and support during a somewhat difficult period during the study where "life happened," which I have hugely appreciated.

I would also like to thank project manager Nils Kristian. I'd probably still be working at the lab if it wasn't for your down-on-earth thinking. I have also appreciated his FTIR and multivariate analysis expertise. A huge thank you to the other fantastic people at Nofima, especially MSc. Katinka Dankel, for helping with HP-SEC, Dumas, and just being available for a chat. MSc. Lene Øverby, for all the help with the biotechnological part, Dr. Shiori Koga for sharing her knowledge on SDS-PAGE, and last but not least, Dr. Kenneth Aase Kristoffersen for all the help, good discussions, mental support, and for being a good friend.

The fantastic students and interns I have worked with also deserve a big thank you, especially MSc. Marte Dalsnes, Julia Döring, and Helena Weits Nielsen. It's been a pleasure to work with you.

A huge thank you to Elsa for letting me be a part of the bioanalytical group, for always responding with fast and concrete answers to my questions, and for the constructive feedback on the thesis. Also, I would like to thank the Bioanalytics group at the Department of Chemistry for their sharing of knowledge and good energy.

My colleagues at Thune also deserve a humble thank you for all their patience when the lab work or the train from Ås has been delayed.

Finally, I want to send my gratitude to my family and friends who have endured me throughout this time. A humble thank you to those who persuaded me to continue with the studies and convinced me that it is possible to be a chemist even if life suddenly presents you with a few physical challenges. To Kenneth, my other half who has occasionally had to be a single father to our little ones; from the bottom of my heart, you are simply the best! And to my beloved children, I can't wait to spend more time with you! ❤️

Oslo, Norway, november 2020

Linn Maria Gundersen Hunnes

Table of content

1 Abbreviations 1
1.1 Definitions 2
2 Introduction 3
2.1 A notably project 3
2.2 Amino acids 4
2.3 Proteins 5
2.3.1 Collagen 7
2.3.1.1 Gelatin 9
2.3.2 Proteases 11
2.4 Enzymatic protein hydrolysis 12
2.5 Residual raw materials from poultry 15
2.5.1 Poultry protein composition and its changes over time 16
2.6 Analytical techniques 17
2.6.1 Raw material analysis methods 17
2.6.2 Protein content 18
2.6.3 Degree of hydrolysis 20
2.6.4 Hydroxyproline content 21
2.6.5 Sodium dodecyl sulfate – polyacrylamide gel electrophoresis 21
2.6.6 Liquid chromatography 22
2.6.6.1 Size-exclusion chromatography 23
2.6.7 Fourier-transform infrared spectroscopy 25
2.6.7.1 Fourier-transform infrared spectroscopy in characterization of proteins, peptides, and amino acids 26
2.7 Aim of study 28
3 Experimental 30
3.1 Small equipment 30
3.2 Chemicals 30
3.2.1 Solvents 30
3.2.2 Reagents 30
3.2.3 Solutions 31
3.2.3.1 Solutions used in the EPH 31
3.3 Sample preparation of the hydrolysates 34
3.3.1 Protease activity screening of 25 proteases on azo-casein 34
3.3.2 Enzymatic protein hydrolysis of poultry residual raw material 35
3.3.3 Fourier-transform infrared spectroscopy 36
3.3.4 High performance size-exclusion chromatography 36

3.3.5 Sodium dodecyl sulfate – polyacrylamide gel electrophoresis *36*
3.3.6 Degree of hydrolysis assay *37*
3.3.7 Dumas Combustion Analysis *38*
3.3.8 Determination of hydroxyproline in collagen-rich samples *38*
3.4 Instrumentation and settings, data acquisition and processing of data 39
3.4.1. Spectrophotometer used for measuring the protease activity *39*
3.4.2 Spectrophotometer used for measuring the degree of hydrolysis *39*
3.4.3 Sodium dodecyl sulfate – Polyacrylamide gel electrophoresis *39*
3.4.4 Fourier-transform infrared spectroscopy *39*
3.4.5 High performance size – exclusion chromatography *41*
3.4.6 Dumas combustion analysis – nitrogen content *42*
3.4.7 Raw material analysis *43*
4 Results and discussion 44
4.1 Framework of study 46
4.1.1 Preliminary study – proteolytic activity towards azo-casein *47*
4.1.2 Preliminary study – selectivity screening on poultry raw material residues *50*
4.2 Enzymatic protein hydrolysis in small- and lab-scale experiments 51
4.2.1 Verification of the small-scale selectivity screening experiment *51*
4.2.1.1 High performance size-exclusion chromatography – mass average molar mass distribution analysis of the small-scale hydrolysates from the verification 55
4.2.1.2 Optimization – collagen-rich hydrolysate analysis 55
4.2.1.3 High performance size-exclusion chromatography – small-scale EPH analysis 56
4.2.1.4 Fourier-transform infrared spectroscopy – structural characterization of the small-scale hydrolysates from the verification 59
4.2.2 Scaling up the enzymatic protein hydrolysis to lab-scale *63*
4.2.2.1 Raw material analysis 63
4.2.2.2 Lab-scale enzymatic protein hydrolysis 64
4.2.2.3 Optimization of the lab-scale enzymatic protein hydrolysis 67
4.2.2.4 Lab-scale enzymatic protein hydrolysis – combining Endocut-02 and Bromelain 68
4.2.3 Lab-scale enzymatic protein hydrolysis – optimization and its effects on the hydrolysate composition studied by analytical techniques *72*
4.2.3.1 Peptide fragments from myofibrillar proteins and collagen analyzed by Sodium dodecyl sulfate – polyacrylamide gel electrophoresis 74
4.2.3.2 High performance size-exclusion chromatography – mass average molar mass distribution of the lab-scale hydrolysates 76
4.2.3.3 High performance size – exclusion chromatography – lab-scale EPH combining Endocut-02 and Bromelain 80
4.2.3.4 Degree of hydrolysis and protein content % in the lab-scale hydrolysates 85

4.2.3.5 Hydroxyproline analysis of mechanically deboned poultry residues treated with Endocut-02 and Bromelain *89*

4.2.3.6 Degree of hydrolysis and protein content % in the lab-scale hydrolysates from combining Endocut-02 and Bromelain *90*

4.2.3.7 Fourier-transform infrared spectroscopy – analysis of the lab-scale hydrolysates *93*

4.2.3.8 Fourier-transform infrared spectroscopy – lab-scale enzymatic protein hydrolysis combining Endocut-02 and Bromelain *98*

5 General discussion, with challenges and improvements 102

6 Conclusion and future work 106

6.1 Future work 108

References 110

7 Appendix 117

7.1 Proteases used during the activity screening 117

7.1.1 Protease concentration calculated from the activity screening *118*

7.2 Protocols developed during the study 121

7.2.1 Protocol – Small-scale enzymatic protein hydrolysis *121*

7.2.2 Protocol – Lab-scale enzymatic protein hydrolysis *123*

7.2.3 Protocol – Sodium dodecyl sulfate – Polyacrylamide gel electrophoresis *125*

7.3 Raw material analysis provided by ALS laboratories UK 127

7.4 Dumas combustion analysis – nitrogen content in the lab-scale hydrolysates. 128

7.4.1 Nitrogen content in the lab-scale hydrolysates treated with Bromelain or Endocut-02 ..... *128*

7.4.2 Nitrogen content in the lab-scale hydrolysates treated with a combination of Bromelain and Endocut-02 ..... *135*

7.5 Calculations of the small- and Lab-scale hydrolysates 138

7.5.1 Values for determining the ER % for the small-scale hydrolysates *138*

7.5.2 Values for determining the protein yield % for the lab-scale hydrolysates *139*

7.5.3 F-test and student`s t-Test for the lab-scale hydrolysates treated with a combination of Endocut-02 and Bromelain *140*

7.6 Degree of hydrolysis during hydrolysis time 143

7.7 Fourier-transform infrared analysis of the small- and lab-scale series 148

7.7.1 The variation during hydrolysis time revealed by principle component-1 ..... *156*

7.8 High performance size – exclusion chromatography 158

7.9 Images from the enzymatic protein hydrolysis process 162

8 Poster presented at Bioprosp_19 «Unlocking the potential of biomolecules from marine environments,» Tromsø 2019. 163

1 Abbreviations

B.rx %	Background reaction
CF	Chicken fillet
Da	Dalton
DAD	Diode array detector
DH%	Degree of hydrolysis
EPH	Enzymatic protein hydrolysis
ER%	Enzymatic reaction yield
F1-F4	Fraction 1-4
FTIR	Fourier-transform infrared spectroscopy
HP-SEC	High performance size-exclusion chromatography
Hyp	Hydroxyproline
KB	Chicken fillet treated with Bromelain
KE	Chicken fillet treated with Endocut-02
LC	Liquid chromatography
MB	Mechanically deboned poultry residues treated with Bromelain
MBE	Mechanically deboned poultry residues treated with Bromelain+Endocut-02
MB+E	Mechanically deboned poultry residues treated with Bromelain 30 minutes before Endocut-02
MDPR	Mechanically deboned poultry residues
ME	Mechanically deboned poultry residues treated with Endocut-02
ME+B	Mechanically deboned poultry residues treated with Endocut-02 30 minutes before Bromelain
MS	Mass spectrometry
MP	Mobile phase
M_W	Mass average molar mass
NMR	Nuclear magnetic resonance
PC-1	Principle component one
PC-2	Principle component two
PCA	Principle component analysis
RMA	Raw material analysis

RRM	Residual raw material
RSD	Relative standard deviation
rt	Room temperatur
SB	Tendons treated with Bromelain
SD	Standard deviation
SDS-PAGE	Sodium dodecyl sulfate – polyacrylamide gel electrophoresis
SE	Tendons treated with Endocut-02
SKB	Tendons+CF treated with Bromelain
SKE	Tendons+CF treated with Endocut-02
SNV	Standard Normal Variate
SP	Stationary phase
TCD	Thermal conductivity detector
t_R	Retention time
UV	Ultraviolet-visible
Xaa	Amino acid in X-position
Yaa	Amino acid in Y-position

1.1 Definitions

Dalsnes 12mL	Selectivity screening in small-scale by Marte Dalsnes
Dalsnes 40mL	Up-scale selectivity screening by Marte Dalsnes
End-product	The hydrolysate product after ending the entire reaction (deactivation *with* materials) after 60 minutes
Lab-scale	Up-scale EPH reaction (1000 mL)
Sediment	The solid phase from the hydrolysate separation (primarly lipids, hydrophobic proteins and inorganic matter)
Small-scale	Small-scale EPH (12 mL)
Time series	The collected samples between 0.5 - 60 minutes
Vibrations	When molecules absorb and are exited by infrared radiation

2 Introduction

2.1 A notably project

In 2011 the world's population reached 7 billion people, and **Figure 2** illustrates that the United Nations expects this number to be around 11.2 billion by 2100. Estimated, we will need a 70 % increase in food production to be able to feed the population in 2100 (3). The most significant debate until now has been whether the earth has enough resources and food. However, considering this growth, the critical question is, what can the people do to achieve and preserve a more sustainable development of the environment. Food production has become one of the more critical global challenges. Meat is used as the primary protein source in human consumption all over the world, although the production often is very energy-demanding as well as being a large pollution-source (4). A common consensus among nations is that food production links to climate change and reduced biodiversity (5-10). It seems like there is a need and a demand for finding new nutritious resources in a way that benefits the growing population and the environment.

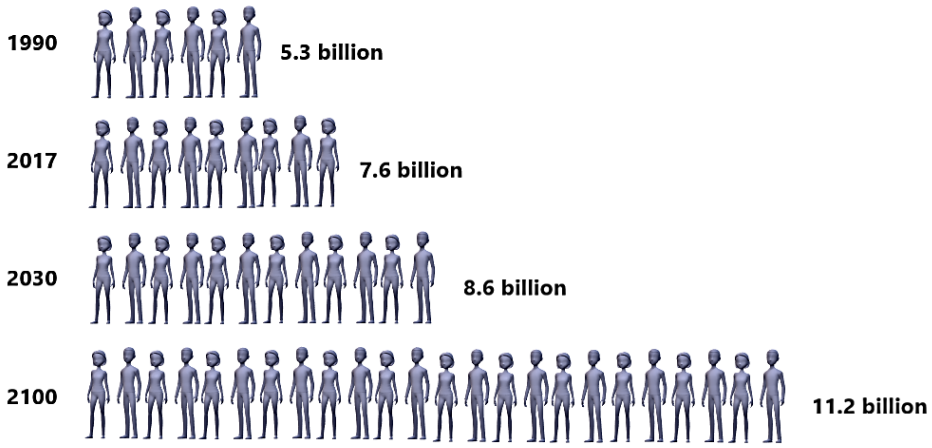

Figure 2. illustrates the global population growth from this day until the year 2100. The figure is adapted from United Nations (7).

Nofima is a leading food research institute that conducts research and development for the aquaculture industry, fisheries, and the food industry, with the vision "Sustainable food for all." With Nofimas` project, Notably, the goal is to use the proteins that are already produced, such as RRM from the poultry industry, to reduce overproduction and help the industries to generate

less waste. Notably is funded by the research council of Norway and Bionær, and is a collaboration with Sintef Industry, Simula, Lunds University, Brødrene Karlsen, Biomega group, Norilia, and Bioco. Animal and marine processing industries produce large amounts of RRM every day. With this project, Nofima will strive to reach full utilization of these materials, using EPH. This research can provide proteins, protein derivatives, and other biological molecules, which can be included in human food, as seasoning, in animal food, cosmetics, health food, and as medicine (11).

Development of an EPH process is likely to help the industry generate less waste than many of the current technologies do. Furthermore, a valorization of poultry RRM can provide an additional nutritious resource for humans and animals, produce biologically active molecules that can be used in different fields, and give the producers an economic gain instead of costs regarding the residual waste.

2.2 Amino acids

Twenty amino acids usually occur in all proteins, where eight of the amino acids are essential for the cells to perform protein synthesis and need to be consumed through food (12). As shown in **Figure 3**, almost all amino acid contains a central α-C atom attached to an H-atom, a -NH_2, a -COOH and a side group (-R) that varies for each amino acid. Alanine (Ala), valine (Val), leucine (Leu), isoleucine (Ile), and proline (Pro) are non-polar aliphatic amino acids that help stabilize protein formation through van der Waals interactions. Glycine (Gly), serine (Ser), threonine (Thr), cysteine (Cys), methionine (Met), asparagine (Asn), and glutamine (Gln) are polar, but uncharged amino acids (13). In an oxidizing reaction, two cysteines can be linked covalently to each other forming a disulfide bond. This is due to the highly reactive thiol in the cystein side chain (12). Phenylalanine (Phe), tyrosine (Tyr), and tryptophan (Trp) all have an aromatic side group, which absorbs ultraviolet (UV) light. Aspartic acid (Asp) and glutamic acid (Glu) are both negatively charged, while lysine (Lys), arginine (Arg), and histidine (His) have a net positive charge. Since His is a tertiary amine, it can donate its lone pair of electrons to an electrophile, and the side chain has an essential role under the catalysis due to its location in the active site in some enzymes, e.g., subtilisin (13).

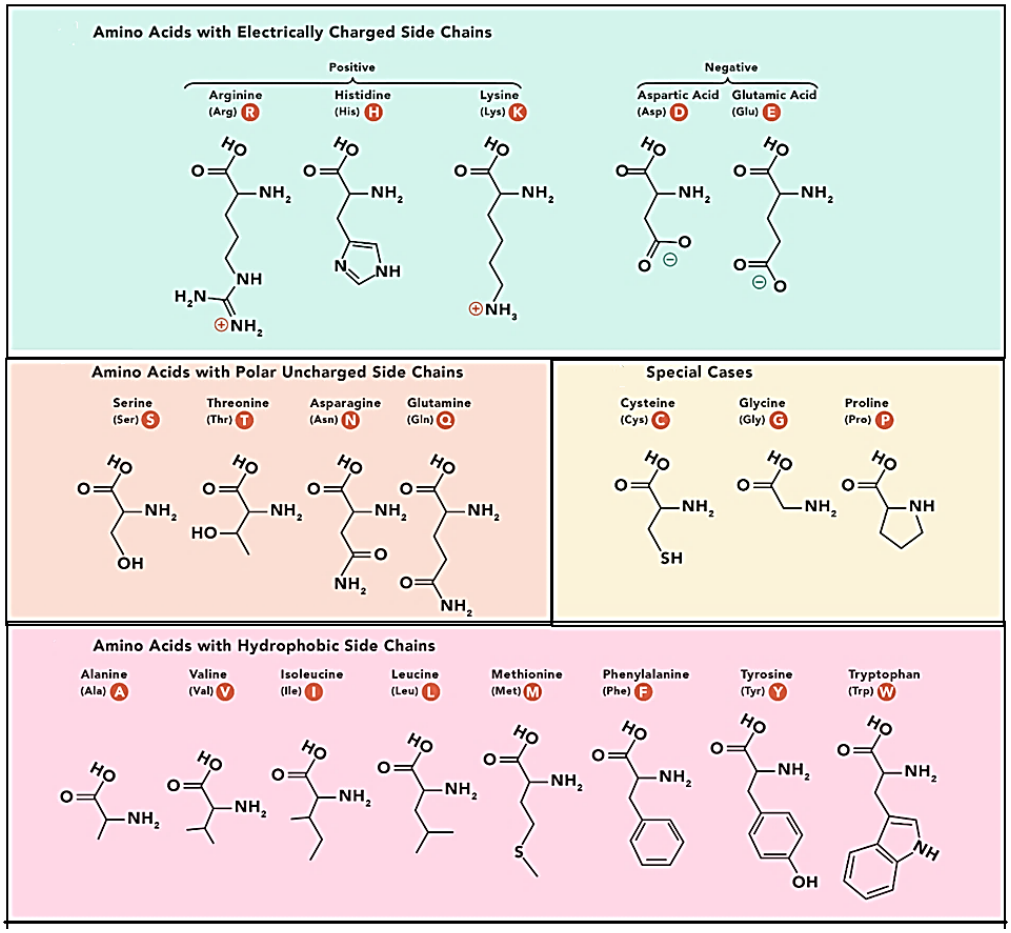

Figure 3. The 20 most common amino acids in proteins, which are divided according to their functional groups that gives them different charge, hydrophobicity, and polarity. The figure is adapted from Technology Network (14).

2.3 Proteins

Proteins are found in all living materials, and there are countless variations of proteins that each has their purpose (15). These macromolecules have a specific amino acid composition linked together by rigid peptide bonds between the α-amino (NH_2) and α-carboxylic (COOH) groups of two adjacent amino acids. This formation occurs in a condensation reaction during the protein synthesis, creating the polypeptide chains. The protein consists of one or several polypeptide chains formed into a three-dimensional structure which defines the protein functionalities. **Figure 4** shows the free amino acids before the primary and secondary polypeptide chain is formed. Further, the polypeptide chain is folded into a tertiary structure, which give the protein its identity and characteristics. However, some proteins are made up of two or more folded polypeptide chains, referred to as subunits that stabilize the protein structure through covalent or noncovalent cross-linking and creates a quaternary structure (16).

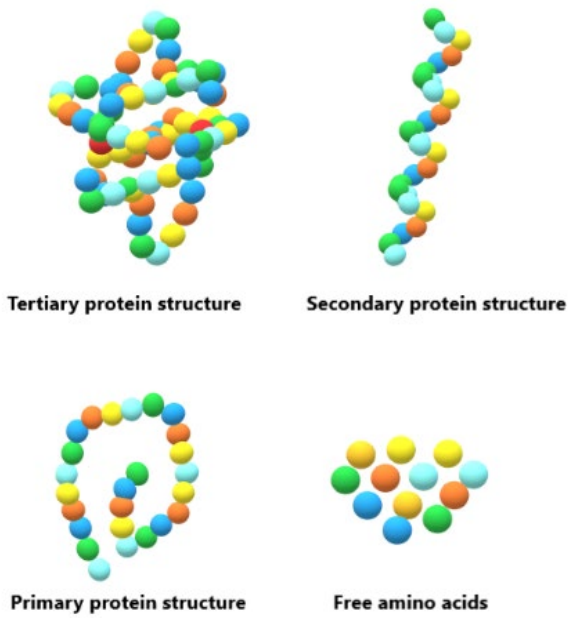

Figure 4. Free amino acids, the primary polypeptide chain, the secondary structure, and the characteristic folded tertiary structure that makes up the protein's nature.

In a water phase, the hydrophobic parts of the protein will be folded into the center of the molecule, while most hydrophilic parts are faced outwards. Although the peptide bonds in the polypeptide backbone are rigid, bonds between the $C_{\alpha\text{-}1}$ and C atoms and the N and $C_{\alpha\text{-}2}$ are free to rotate relative to each other. The polypeptide chain also contains a free NH_2 - or COOH group at each end, which is called the N- and C-terminal ends, respectively (13). Complete hydrolysis of a protein can provide information about which amino acids it holds (12). However, denatured, the unique structure of the protein folds out, and with a large variety of amino acids, the protein can be challenging to characterize. X-ray crystallography analysis (XRC) and nuclear magnetic resonance (NMR) have long been helpful in this characterization. Through XRC, the unfolded protein can be identified through crystallization, and NMR can reveal the carbon and hydrogen atoms relative to each other in a protein structure (17, 18). However, analytical approaches like FTIR, liquid chromatography (LC), and mass spectrometry (MS) have also proven to be useful tools in protein characterization. FTIR can provide structural information with known bands appearing in the same area for similar proteins. LC can separate and characterize proteins based on their molar mass or retention time, and with MS, the proteins can be identified based on their molar mass. These methods alone can provide misleading interpretations due to the lack of information, but in combination, they can provide quality parameters with good accuracy (18, 19).

Globular and fibrous proteins

Proteins can be divided into three categories, globular, fibrous, and membrane proteins. However, this study focuses on the globular and fibrous proteins found in muscle and tendons, where myofibrillar protein and collagen are of importance. Globular proteins, like enzymes, are large with irregular surfaces (13). Globular proteins are soluble in water or solutions with low ionic strength (20) and are particularly important in biological processes. Fibrous proteins with some exceptions like, e.g., small gelatin peptides, are usually not water-soluble. The fibrous proteins are essential in the formation of tissue, where collagen, keratin, and elastin can be mentioned (12).

The group of myofibrillar proteins found in muscle, constitute a variety of different proteins, where myosin and actin accounts for as much as 70% of the total amount of proteins in this group. Furthermore, whereas actins are globulins and hence water-soluble in liquids with minimal salt content, myosin, which are large proteins with a fibrous structure and a mass of about 500 000 Da, can be solved in salt solutions. Myosin consists of a hydrophilic and a hydrophobic part, which in total comprises two heavy (~250 kDa) and four light chains (~24 kDa).

After pre-rigor meat treatment, when the meat has been removed from the carcass before cooling, groups of actins are linked to each other as long chains or become cross-linked to myosin. This actin-myosin complex is called actomyosin and is the dominant protein complex in processed meat (20). Many proteins involved in constructing the actomyosin complex, with actin as the most prominent, are observed in young poultry. Myosin has not been identified as a significant constituent in the actomyosin complex, using gel electrophoresis that is (21), which can be explained by the fact that larger proteins like myosin are more easily degraded. Fibrous proteins included in connective tissues, like the collagen found in bones, cartilage, and tendons, can be dissolved in acidic or alkaline solutions (12). Since collagen has distinctive characteristics and qualities, it is necessary to describe these proteins in more detail.

2.3.1 Collagen

Collagen is arranged in tissue-specific fibrils, and the fibril-arrangement takes place extracellularly. Fibrils act as tension elements and are especially suitable to withstand tensile stress. In tendons, collagen fibers are arranged in long parallel bundles and have a tensile

strength equal to that of light steel wire (22). Previous research shows that ultimate tensile strength is more significant in larger fibrils with a broader cross-section (23). **Figure 5** shows how collagen is formed from a single polypeptide chain to the assembled fibers.

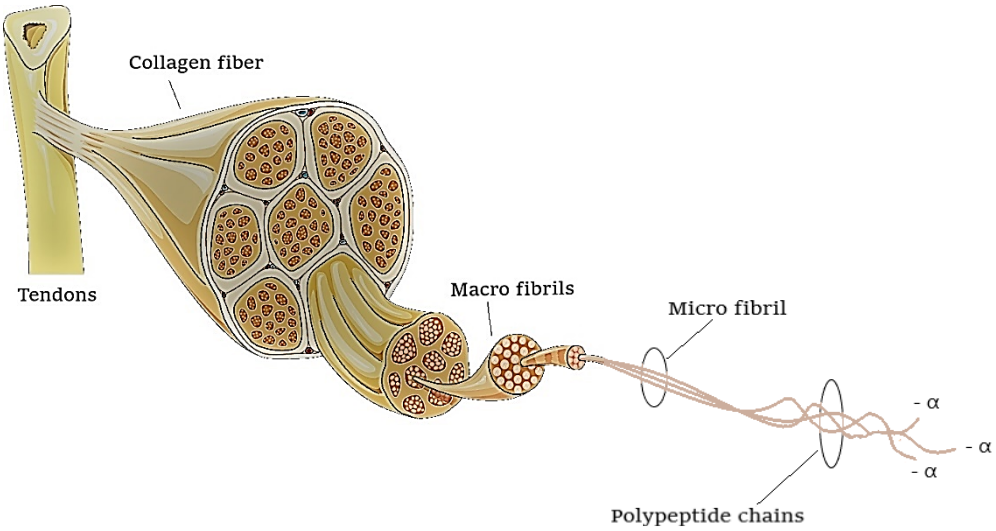

Figure 5. Collagen molecules with its α-polypeptide chains, is arranged in fibrils and constitute hierarchically aggregated fibers. Figure adapted from Istock (24).

There are several types of collagen, and so far, 29 types have been identified (25). The most common are types I and II, where type I constitutes the majority of collagen in both vertebrates and invertebrates. Type I collagen is found throughout the body and particularly in connective tissue, such as skin and bone. In cartilage tissue, type II is the most abundant collagen (11). The collagen molecule consists of three α-chains, containing approximately 1 000 amino acids each and has a mass of about 100 kDa. The single α-chain twists as a right-handed helical structure connecting intercellular cross-bindings before forming a rigid left-handed helix, which gives the characteristic triple superhelical collagen structure (25). The main structure of the molecule is built up by the amino acid triplet Gly-Xaa-Yaa, which repetitively continues throughout the helix, with molecular flanks that contain short non-helical conformation telopeptides rich in Lys and hydroxylysine (Hyl). Consequently, Gly appears in every third position (26), and with only a hydrogen atom in the side chain combined with a small molecular size, Gly will not cause steric hindrance. Gly is thus essential for the tightly packed superhelical structure and contributes to its hydrophobic core (27). The Xaa and Yaa positions consist mainly of the amino

acids Pro and hydroxyproline (Hyp), which is uncommon in proteins other than collagen and elastin (25). **Figure 6** shows the collagen molecule with its repeating Gly-Xaa-Yaa triplet.

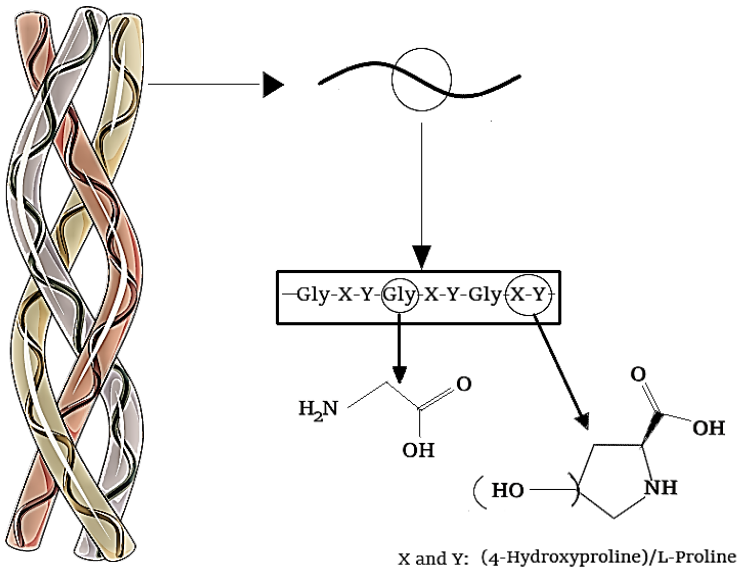

Figure 6. The three-dimensional super helical structure of a collagen molecule with the Gly molecule and its two most abundant amino acids for the Xaa and Yaa – positions, Hyp and Pro. The hydroxy-group which sits in the fourth position on the Pro molecule, in brackets, indicates that 4-hydroxyproline is formed by a hydroxylation of Pro.

Hyp and Hyl are post-translationally modified amino acids formed by hydroxylation of Pro and Lys, respectively. Both Pro and Hyp are particularly crucial for the gelling effect of gelatin when extracted from collagen (28). With XRC, Kempka, A. P. et al. revealed that the amino acids in the most significant quantity in four tested gelatins were Gly, followed by Pro, Hyp, Glu, Arg, and Ala (29). Since Hyp is uncommon in other proteins, the Hyp content can be used as an indicator to determine collagen and gelatin amount in samples, as shown in section **4.2.1** (Equation 2) (28, 30).

2.3.1.1 Gelatin

Gelatin is a high molar mass macromolecule that is extracted from collagen through, e.g., thermal hydrolysis (11) and is an essential biopolymer that has extensive application in many industrial fields (31). Peptides from gelatin have the potential of providing antioxidative, antihypertensive, antiphotoaging, cholesterol-lowering, cryoprotective, and having anticancer properties (32, 33). Biologically active gelatin-peptides could, with advantage, replace many of

the synthetically made antioxidants, which in many cases, provide unhealthy side effects (34). The gelatins functional characteristics such as water-binding capacity, film-forming properties, foaming capacity, and emulsifying capabilities (28), makes gelatin a functional ingredient in, e.g., food, pharmaceuticals, cosmetics, and photographic industries (31). Today, most of the commercial gelatins are derived from the skin or bone of porcine or bovine origin, but recently other possible sources have been explored, like fish and poultry (35). The utilization of raw materials from fish and poultry in gelatin production has recently received a great deal of attention. However, there are still limitations in the current technologies, making poultry and fish less competitive than mammals. One drawback of especially fish gelatins is that the gels tend to be less stable. Also, there are more challenges concerning the rheological parameters with poultry and fish gelatins than with land mammals (28, 36). Du et al. extracted gelatin from poultry heads, which is highly collagen-rich but still received a low yield due to the complexity of the material, including non-collagenous proteins and other impurities. However, comparing turkey and chicken gelatins showed that turkey-derived gelatins revealed better rheological, textural, and functional properties than chicken head gelatins (37).

Hydrolytic conversion from collagen to gelatin leads to breakage of several intra-and extra molecular cross-bindings, as well as hydrolysis of some peptide bonds in the primary structure of the collagen (38). These arrangements give gelatin-fragments in the range of 16-150 kDa, dependent on which collagen the gelatin derived from and where the collagen structure has been cleaved (11). Gelatin contains 8-13 % moisture and has a relative density of 1.3-1.4 kg/m^3. Gelatin particles in water will begin to hydrate and swell with decreasing temperature. How quickly the consistency of the gelatin solution changes from liquid to gel and the gelatins final structure, will vary based on the concentration and molecular size of the gelatin and its properties in a solution. That is, pH, temperature, and solvents will affect the viscosity of the gelatin solution (39). If a solution with more than 0.5 % gelatin contains no other non-colloidal ions than H^+ and OH^-, it is known as isoionic gelatin, and the solution is likely to become more viscous at a temperature of 35 - 40 ºC (11). In aqueous solutions heated above its melting point, the gelatin will change its structure from triple-helical conformation to random coils. When the solution cools, the gelatin structures partially go back to the ordered triple-helical collagen-like sequences but will reform in a disordered coil conformation (40).

Gelatin is ampholytic and is, therefore, able to act either as an acid or a base. This means that the gelatin will behave like cations in acidic solutions and anions in alkaline solutions (39).

During denaturation and hydrolysis, collagen can be transformed into two different gelatin types, commercially known as type A and B, and are obtained with acid and alkaline pretreatment, respectively (20). Type A gelatin has its isoelectric point in the pH-range 8-9, while that of type B lies between pH 4-5, after an acid or alkaline pretreatment, respectively. Since the cross-linking in collagen is relatively sensitive to acid, especially within young species, a weak acid with gentle stirring is often enough to break the non-covalent bonds, disorganize the protein structure, and increase the solubility of collagen (28). Very polar organic solvents that form hydrogen bonds are preferable to solve gelatin; such as acetic acid, trifluoroethanol, and formamide. Less polar solvents, such as benzene, acetone, primary alcohols, and dimethylformamide, will not dissolve the collagen and gelatin structure (36).

In many cases, proteolytic enzymes used in hydrolysis of collagen have shown to result in improved protein yield, reduced processing time, and less generated waste compared to alkaline and acidic processes. The use of proteolytic enzymes can lead to enhanced gelatin solubilization efficiency (11) since gelatins with a peptide size smaller than approximately 2000 kDa usually are water-soluble. The findings in Gray, V.A. et al., showed that Bromelain was suitable for the dissolution of cross-linked gelatin in the pH range from 4.0 to 6.8 (41). Proteolytic enzymes, also referred to as proteases, proteinases, and peptidases, will further in the text go under the designation of proteases. These proteases catalyze the hydrolysis of peptide bonds in proteins during the EPH (27).

2.3.2 Proteases

One way to divide the various proteases is to categorize them as cysteine proteases, serine proteases, threonine proteases, aspartate proteases, glutamate proteases, and metalloprotein proteases, where the mechanism and functional amino acids in the proteases active seat decides which category (42). Proteases exist naturally in both eukaryotic and prokaryotic organisms and are therefore found in plant material, animal tissue, archaea, and microorganisms (43). They can have exopeptidase, endoprotease, or in some cases, both activities. Exopeptidases cut from one to three amino acids at a time from one or the other terminal end, working as amino- or carboxyl proteases, depending on which end it cleaves. Endoproteases such as serine- and cysteine protease, cleave peptide bonds in the interior of the polypeptide chain near specific amino acids (44).

Bromelain is a cysteine protease found in pineapple and is one of the two essential proteases in this study. In 1493 Columbus found the pineapple in Guadeloupe. In 1876, Peckold et al. observed the proteases activity, and already in 1891, bromelain was isolated from pineapple juice (45). Commercial Bromelain was marketed when Heinecke et al. in 1957 found that pineapple stem contained more protease than the fruit itself (46). Bromelain's proteolytic activity has been evaluated and analyzed on gelatin, casein, and other protein substrates (45). Bromelain has many beneficial properties (47). It seems that its proteolytic activity can be correlated to, e.g., platelet aggregation inhibition and clinically as anti-inflammatory agents in rheumatoid arthritis, soft tissue injuries, colonic inflammation, chronic pain, and asthma. Other beneficial observations regarding bromelain have been documented, like anti-cancer effect and debridement of burns. Bromelain has proven to be one of the leading proteases on the market to this day (45, 47).

In the present study, bromelain in powder form from Taylorzyme has been used. According to the producer its optimum temperature lies in the range 40-65 ^{o}C with a pH range between pH 4.0-9.0 (48). Endocut-02 is the other important protease utilized in the study, and as its name implies, it is also an endoprotease. Endocut-02 is an alkaline protease with broad selectivity, and it is extracted from the bacteria *Bacillus licheniformis* after a controlled fermentation process (48). In biotechnological fields, there is a substantial market for enzymes, and proteases account for more than 40 % of the total enzyme distribution in biotechnological applications. Alkaline proteases with broad selectivity are particularly interesting in the process-industry. They have high activity and stability in a wide alkaline pH-range and good activity within a high temperature-range. Many different microorganisms produce alkaline proteases used in the industry today, but they often derive from Bacillus species (49). They are used as cleaners in detergents to facilitate the release of proteins in stains. Endocut-02 comes in liquid form and has, according to Taylorzyme, its optimum temperature range between 55-65 ^{o}C and pH-range between pH 7.0-10 (48). However, various experiments made with these proteases have shown different optimum temperatures and -pH than stated above, which may be a consequence of different substrate effects altering these parameters (49-51).

2.4 Enzymatic protein hydrolysis

Several commercial proteases have been used for EPH, such as trypsin, pepsin, Alcalases, collagenases, Bromelain, papain, different Corolases, and others (28). Hydrolytic enzymes are

referred to as hydrolases, which cleave bonds in the respective compound at the expense of a water molecule (52). There are many different types of enzymes in this group. Still, proteases are separated from other hydrolases in that they hydrolyze and cleave peptides and peptide bonds in proteins and peptides into smaller peptides and free amino acids. **Figure 7** illustrates the reaction of EPH.

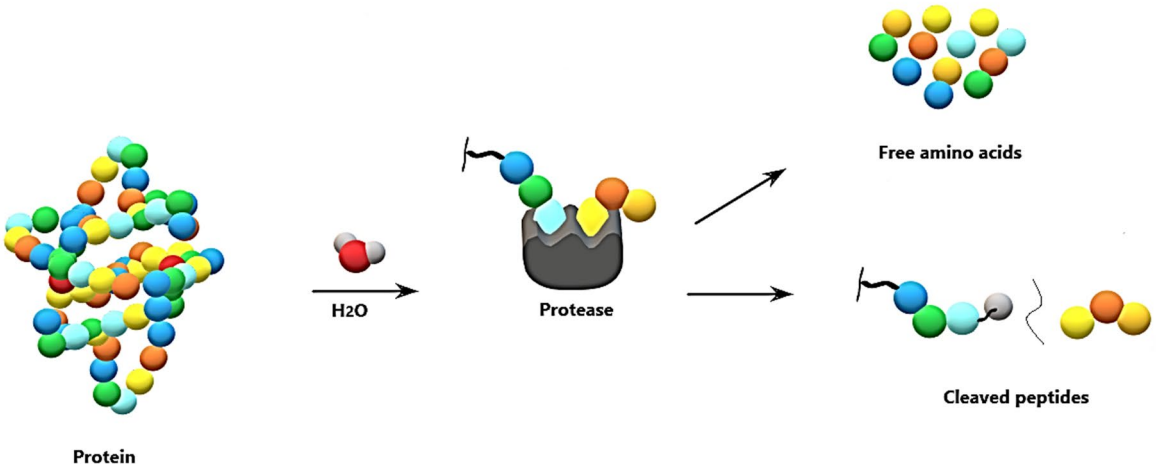

Figure 7. Illustrates the EPH reaction, where a part of the proteins three-dimensional structure binds to the protease's active site, the peptide chain is cleaved, which provides smaller peptides and/or free amino acids.

Some proteases are versatile and can be used for hydrolysis of proteins from many species. These are of great interest in hydrolysis reactions of animal RRM when the purpose is to extract a wide variety of peptides. Proteases with a high selectivity for selected binding sites are preferred when aiming at producing bioactive peptides. It has been known that peptides of smaller sizes may possess bioactive properties (28, 53-55). Peptides that consist of 2-30 amino acids and a mass lower than 3000 Da could potentially be biologically active and possess many functionalities (56). If bioactive peptides from poultry RRM can be released through an EPH process, this can be advantageous for both the producers and the consumers. Peptides used for this purpose provide a higher profit than larger peptides used in the food industry (57).

According to information found in Banan-Mwine Daliri et al., it is not shown that specific proteases provide bioactive peptides. However, hydrolysis with Subtilisin tends to yield low molar mass peptides that often have higher antioxidants and antihypertensive properties than

peptides with high molar mass (58). In 2019, Lima et al. showed that peptides obtained from MDPR had a potential of anti-diabetic activity. By using Corolase 2TS, which is an endoprotease produced by *Bacillus stearothermofilus*, they extracted peptides that could be an ingredient in multi-functional food with aim of inhibiting dipeptidyl peptidase IV and stimulate the uptake of muscle glucose (19).

Since proteases are more or less specific (43), they can, in theory, be selectively used to extract any product of interest. However, this is rarely the case in practice. Several parameters are influencing the hydrolysis, like the proteases pH dependency, heat stability, catalytic selectivity as well as product inhibition, where peptides formed during the reaction inhibit the protease (27, 59). For the endoproteases to reach the peptide bonds inside the folded protein structure, reagents, as well as temperature and pH-changes, can help defold the compound before adding protease (2). However, adjusting the pH usually requires acidic or alkaline solutions, which could influence the product quality. The addition of, e.g., alkali usually results in high salt concentrations in the hydrolysates, which can reduce the nutritional content in the product and is unwanted in the consumer industry (58). The proteases have different optimum temperature and pH and therefore the activity will be affected by changes in these parameters. Regulation of temperature within the temperature range can either change the speed of the reaction or, if the temperature is too low for the protease to work or too high, denature the protein structure or deactivate the protease completely. Other parameters that may affect the process are the substrate concentration, the protease-substrate ratio (E-S), which is an essential factor to consider obtaining a reasonable degree of hydrolysis, and the reaction time. For an optimal EPH process, substrate specific factors such as origin, age, food intake, and complexity, as well as protein-specific factors such as selectivity, stability, and sensitivity to inhibitors, must also be considered (2).

The degree of hydrolysis (DH%) is a measure of the number of cleaved peptide bonds in hydrolysates, and can be determined by using different approaches (44). One method, suggested by Adler-Nissen in 1984, is based on the amount of alkaline solution consumed during hydrolysis, where the equation gives the percentage of cleaved peptide bonds (30). EPH is gentle and widely used in the valorization of RRM in the food industry (30). Also, the pet food industry uses a broad range of protein sources, e.g., proteins from poultry residues (60). EPH can contribute to the reduction of allergens in feed and food by destroying the proteins and induce a loss or change in the respective proteins' functional properties (61).

2.5 Residual raw materials from poultry

High amounts of poultry are consumed every year, and with this, large amounts of RRM from the poultry processing industries are produced, and which has a high potential for a value increase (2). A report from 2015 presented that 56 550 tons of chicken RRM and 7 200 tons of turkey residuals were produced in Norway in 2014. Residuals are, according to the Norwegian meat industry, everything on the butchered animal that is not meat used for human consumption. The amount of residuals from chicken is about 51 %, and approximately 45 % of the turkey is classified as residuals (4). Mechanically deboned poultry residues are shown in **Figure 8**, with some of the essential materials that can be utilized.

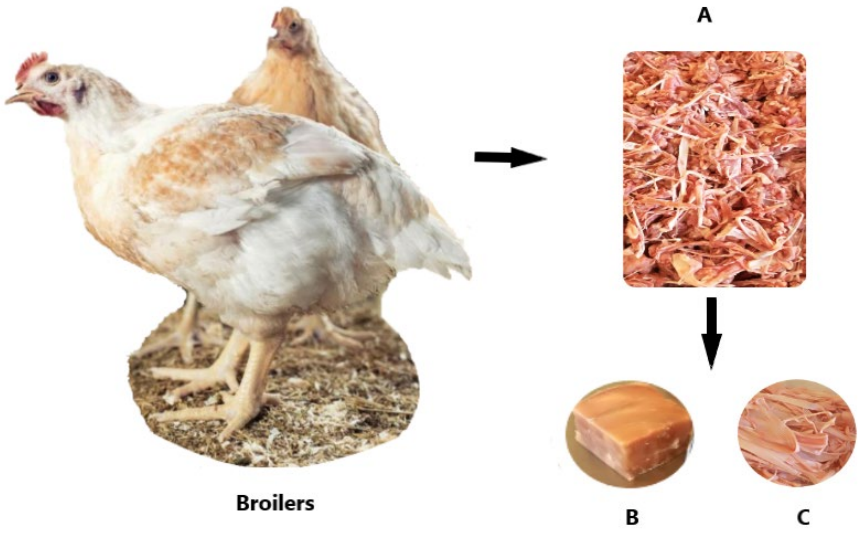

Figure 8. A**)** MDPR containing B) muscle and C) tendons, as well as some skin and bone. The picture of the broilers are adapted from (62).

An Optimized EPH process where proteases selective towards different protein groups are being used can contribute valuable research for utilizing the full potential of the RRM. In the current EPH processes, one protease is used to separate a fat phase, a liquid phase with soluble protein, and a solid phase with mineral-rich sediment of lipids, insoluble proteins, and inorganic matter. The challenge with the current EPH is that it cannot release all the various components found in complex raw material residuals (2). As mentioned in section **2.3**, there are many different proteins in RRM, and the release of all the various proteins from the complex poultry RRM can benefit from a more targeted approach.

2.5.1 Poultry protein composition and its changes over time

As poultry age, the relative content of collagen versus myofibrillar proteins change. Muscle proteins from cattle, pig, chicken, and sheep have been mapped in several studies over the last few years (21), and the distribution of different proteins are, to a varying degree, species-specific. In the study done by Montowska et al., they found that the difference in the amino acid composition between cattle and chicken was 35 %, but that differences within poultry species like chicken and turkey are minimal (63). It has been observed that most of the soluble protein in muscle, and particularly from older poultry, consists of relatively few proteins. However, the highest degree of specialization in protein expression is in skeletal muscle. Several soluble proteins commonly associated with myofibrillar structure, have been seen in chicken immediately after hatching. These proteins are most likely to incorporate in the more maturing myofibrillar structure while the bird is aging. From 1-27 days old, the composition of myofibrillary proteins in skeletal muscle increased from 30 to 80 % (21), and with their aging there was also an increase in mechanical resistance which Baeza et al. explained with a decrease in collagen solubility (64).

According to Montowska et al., heating of the meat worsened the quality of high molar mass proteins more than for proteins with low molar mass, which was revealed by weak staining intensity of the myosin heavy chain fragments during SDS-PAGE. The volume of proteins went considerably down, and some degraded when the meat was aging due to high microbiological activity, where especially the muscle proteins were highly degraded. Their study showed that there are significant differences in proteins in terms of stability when exposed to external stress, but that low molar mass proteins could, in general, withstand more compared to those with high molar mass (63).

It is necessary to have in mind that the complexity in the protein composition of poultry RRM can produce very inconsistent results and provide peptides with various functional and biological properties even if the same processing conditions are applied due to the information introduced in this section. Also, environmental changes, feeding programs, and the poultry's origin are factors that can influence the protein composition (1). With analytical techniques, the various proteins released during the EPH process can be followed, and reveal the different proteins in the hydrolysates.

2.6 Analytical techniques

Usually, it is not enough to use one technique alone to provide information on all aspects of the peptide composition in hydrolysates from complex RRM. However, when combining several biotechnological and analytical techniques, it is possible to describe the composition of hydrolysates more accurately (65). DH% provides a relative degree of hydrolysis in the hydrolysates during an EPH but needs to be corrected for the protein content determined by, e.g., Dumas combustion analysis, as explained in section **2.6.2** (not everything in the hydrolysates are proteins). The protein yield relative to the protein content in poultry RRM can be determined by combining the protein content found in the hydrolysates from the Dumas method with the protein content found in the RRM from the RMA. HP-SEC and FTIR are nearly complementary methods. However, by looking at the M_W relative to the corrected DH% during hydrolysis time, this may expose an unexpected or abnormal degradation pattern in the EPH. Also, the fragments appearing in SDS-PAGE can support the structural information of the hydrolysates provided by FTIR and HP-SEC.

2.6.1 Raw material analysis methods

Several analytical techniques are used in RMA, depending on the desired information. The RRM composition and quality are two major factors influencing an EPH process and the resulting hydrolysate products (66, 67). RMA can be done to reveal the composition of the RRM. An RMA can provide quality information about the different parts of the poultry RRM, such as the amount of protein, ash, fat, Hyp, water, and carbohydrate content. By analyzing the raw materials, it is often possible to predict their subsequent behavior during processing. The processing conditions can then be altered to produce a final product with the desired properties. The analytical procedure must be selected based on the property to be measured, the type of food to be analyzed, and the reason for carrying out the analysis (68). An RMA may already be routinely used in the laboratory, or the materials can be transferred to a company that can perform the RMA (69). The determination of proteins in food can be done using, e.g., IR, NMR, MS, and polymerase chain reaction (PCR), often in combination with separation techniques like LC or capillary electrophoresis (CE). For the separation of fat compounds, supercritical fluid chromatography (SFC) can be used. Since food analysis is related to the matrix's complexity, coupled techniques such as gas chromatography (GC)-MS, GC-FTIR, or HPLC-MS are often required. To receive information about large and thermolabile compounds such

as peptides and proteins, HPLC-MS is the more suitable choice since the GC only can be applied to volatile, non(to semi-)-polar, and/or thermostable compounds (70).

2.6.2 Protein content

Dumas combustion analysis determines the total amount of carbon (C), hydrogen (H), nitrogen (N), and sulfur (S) in solid or liquid organic and inorganic samples, generally using 4.500-5.200 mg of sample. The method is optimized for small samples, but it is possible to analyze semi-macro samples up to 800 mg soil and 20 mg of organic material (71). A combustion process of the material releases elementary nitrogen (72), and a thermal conductivity cell measures the total nitrogen content (1). In greater detail, simultaneous CHNS analysis requires high-temperature combustion in an oxygen-rich environment. In the combustion pipe where the temperature reaches 1150 ºC, carbon is converted into CO_2, hydrogen to H_2O, nitrogen to N_2 and various nitric oxides N_XO_Y, and sulfur to SO_2. Various adsorption columns are used to remove combustion products from other elements, such as halogens. The products are then carried through a reduction pipe with inert helium gas in a temperature of 850 ºC. The tube is filled with copper that removes the excess of oxygen simultaneously as it reduces N_XO_Y to N_2. The gas mixture is then transferred to three different columns, and components are separated before they are detected using a thermal conductivity detector (TCD) (71). The instrument used in the Dumas analysis, a vario EL cube, with visible parts in the front interior when opening the instrument, the sample inlet on the top, and the necessary sample preparation tools is shown in **Figure 9**.

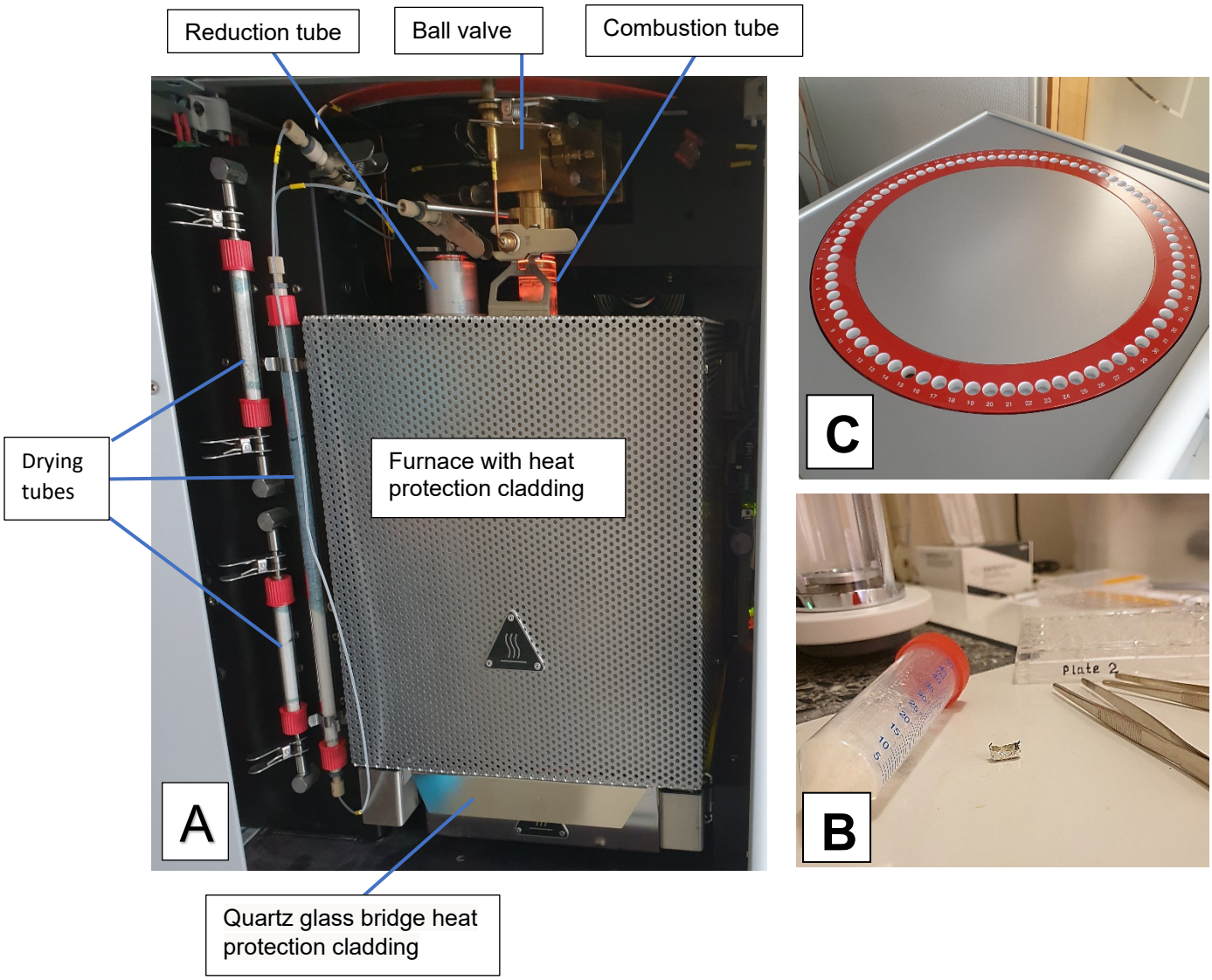

Figure 9. Picture of a Vario El instrument A) the front interior of a vario EL instrument can be seen when opened. B) Small aluminum trey where the sample is added before it is wrapped into a small inert piece with tweezers and placed in C) sample inlet for combustion.

An average protein consists of about 16 % nitrogen, and based on this knowledge, a conversion factor of 6.25 is often used to determine the protein content in the raw material (1). The Kjeldahl method is also widely used for measuring the nitrogen content, but Dumas is more straightforward, provides higher levels of nitrogen, and is more environmentally friendly. Several studies are supporting this (73-75), e.g., the empirical study done by Thompson, M. et al. in 2002, which showed that the Dumas method typically provided more correct levels of nitrogen than the Kjeldahl method (72).

2.6.3 Degree of hydrolysis

The degree of hydrolysis (DH%) is a measure of the number of cleaved peptide bonds and provides information about the extent of hydrolysis in a reaction. **Equation 1)** is used to calculate the DH%, which is defined as the percentage of cleaved peptide bonds relative to the total amount of peptide bonds in the sample (76).

$$DH\% = \frac{h}{htot} \times 100 \qquad \textbf{Eq. 1)}$$

where h is the number of cleaved peptide bonds and htot is the total number of peptide bonds in the sample. There are several known approaches for calculating DH%. Still, the assays utilizing o-phthaldialdehyde (OPA) or trinitrobenzenesulfonic acid (TNBS) to measure the number of free N-terminals are the most common for determining DH% in protein hydrolysates. Through N-terminals derivatization with respective reagent, spectrophotometric measurement with ultraviolet-visible (UV)- or fluorescent detection can be achieved. OPA, which creates strongly fluorescent OPA – amino acid derivatives, can be measured by fluorescence detection (excitation at 350 nm, emission at 450 nm), and TNBS, creating trinitrophenyl – amino acid derivatives, can be determined by UV detection (340 nm) (77, 78). **Figure 10** shows the OPA and TNBS reaction mechanisms with an amino acid.

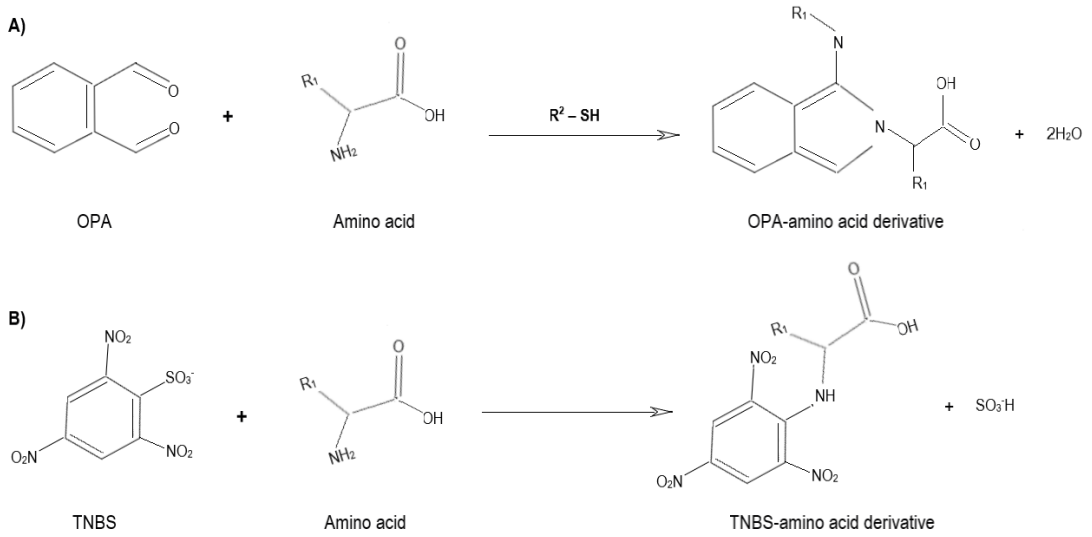

Figure 10. A) OPA is reacting with an amino acid in the presence of a reducing agent (R^2-SH). B) TNBS reacts with the primary amine of lysine by a nucleophilic aromatic substitution reaction and converts it into a trinitrophenyl-amino acid derivative that absorbs long-wavelength UV-light.

The OPA – DH% is a well-known technique that has been used for a long time and is often preferred due to the rapid reaction. However, OPA does not react with Pro, reacts poorly with cysteine-rich hydrolysates, and may not derivatizes insoluble peptides or proteins. TNBS – DH% has some of the same disadvantages as OPA, like reacting poorly with Pro. Nevertheless, TNBS often provides slightly higher DH% values than OPA (44). Spellman et al. found that the difference between the DH% values obtained after using either the OPA- or TNBS – DH was about 15%. With the utilization of OPA, the DH% was underestimated by 13% (79). However, the results obtained from using either OPA or TNBS in DH% analysis vary based on the composition of the hydrolysates to be derivatized. Often, there is a good correlation between these two methods (44).

2.6.4 Hydroxyproline content

Hyp is found primarily in collagen. In animals, collagen contains approximately 12–14 % Hyp, and the number in this knowledge can be used to quantify the collagen content in tissue or biological fluids like serum and urine. A large proportion of Hyp in the urine derives from bone collagen. An increase in urinary Hyp excretion is a marker for altered collagen metabolism, which can be caused by, e.g., very high rates of bone turnover such as in Paget's disease of bone (80, 81). The collagen metabolism can conceivably relate to several other diseases, such as tumor invasion and rheumatic arthritis. Several commercial assays for determining the Hyp content are available on the market. Sigma Aldrich have developed a Hyp assay that is straightforward, and with spectrophotometric detection at 560 nm Hyp can be measured in the hydrolysates at a minimum of 0.05 μg per well in a 96 well format (82).

2.6.5 Sodium dodecyl sulfate – polyacrylamide gel electrophoresis

Sodium dodecyl sulfate – polyacrylamide gel electrophoresis (SDS-PAGE) separates proteins, peptides, and nucleic acids based on size, and the migration and separation are carried out under an electric field. The anionic detergent, SDS, denatures the compounds and creates ionic and hydrophobic interactions, forming a protein-SDS complex. When the SDS bind to the unfolded proteins, they get a total negative charge. The charge-to-mass ratio becomes the same for all proteins, leading to separation of the proteins with size as the migrating factor. The negatively charged compounds are drawn through the gel matrix towards the positively charged anode (83). In many cases, a reducing agent, e.g., dithiothreitol (DTT), is added during sample

preparation to break intra- and inter-molecular disulfide bonds within the proteins. The reducing agent provides complete unfolding of all the proteins and maintains them in a reduced state (84). The gel matrix is chemically inert, electrically neutral, hydrophilic, and are built up by a synthetic polymer formed by polymerization of the monomer acrylamide, cross-linked to the co-monomer, N, N'-methylenebisacrylamide (85). The electrophoretic separation thus occurs in a porous matrix available with various pore densities (gel%). The gel% is dependent on the ratio of the monomer and crosslinker. Smaller peptides require smaller pores not to be washed out of the gel during migration (83, 86). With hydrolysates containing similar sized peptides, a narrow range gel, meaning a single-percentage gel, can separate the peptides in the lower half of the gel, e.g., 12%. Unknown or new samples can be separated through a gel with a broad range, e.g., 4-20%, before optimizing the separation by narrowing down the gel% range. Molecular size markers, containing several proteins with known molecular size, can be used to estimate the relative size of the proteins and peptides in the hydrolysates. The protein and peptide bands can be visualized with protein stains after the electrophoresis, e.g., using Coomassie blue stains (84, 87).

2.6.6 Liquid chromatography

As the name implies, in liquid chromatography (LC), a liquid is used as a mobile phase. The mobile phase carries analytes through a column, containing a stationary phase. Which mobile phase to use depends on the choice of stationary phase, as well as the solubility of the sample. The stationary phase is chosen based on which analytes to be separated and comes in various forms and materials. Some give a high degree of interaction with the analytes, others providing almost none (86, 88). Which detector to use is also dependent on which analytes to separate, as well as the use of solvents. Although UV still is the predominant detector in LC analysis, many detectors are available that are highly more sensitive and selective (89, 90). A great variety of different separation principles make LC a powerful analytical tool and often the pre-choice in several research fields.

Although there are many different separation principles within LC, the two most known techniques are probably normal-phase (NPLC), using a polar stationary phase (SP), and a nonpolar mobile phase (MP), and reversed-phase (RPLC). RPLC is one of the most popular separation principles, which also applies to protein and peptide separations. RPLC is based on hydrophobicity. The SP in RPLC often consists of C18 or C8 ligands chemically bound to the surface of totally porous silica particles. The analytes are separated according to the

hydrophobic interactions between analytes and the hydrocarbon chains attached to the silica particles surface. According to the solvophobic theory, the retention of the analytes in the column depends on the interactions between analytes and SP (86). C18, which is more hydrophobic than C8, generally provides higher retention of the analytes. The MP is aqueous with an organic modifier. In protein and peptide separations, a small amount of acid is added to the MP to keep the proteins and peptides positively charged and reduce undesirable interactions with the stationary phase (91). Another separation principle in LC, different from the principle of RPLC but widely used in protein and peptide separation, is size-exclusion chromatography (SEC).

2.6.6.1 Size-exclusion chromatography

Size-exclusion chromatography (SEC) is based on size distribution of compounds using a stationary phase of particles with defined pore size (86). The separation principle is based on how the hydrodynamic volume of the components, which means the space a particular compound occupies in a solution, contributes to the time spent in the column (92). The SP and the MP should, in principle, not interact with the analytes. SEC is well suited for the separation of macromolecules and is thus widely used in protein and peptide analysis (66, 86). Molecules, in the current study proteins and peptides, that are larger than the pores will elute first, traveling between the particles along with the aqueous mobile phase. Smaller proteins and peptides will, to a varying degree, diffuse into the particle pores and get retained (93, 94) as shown in **Figure 11**.

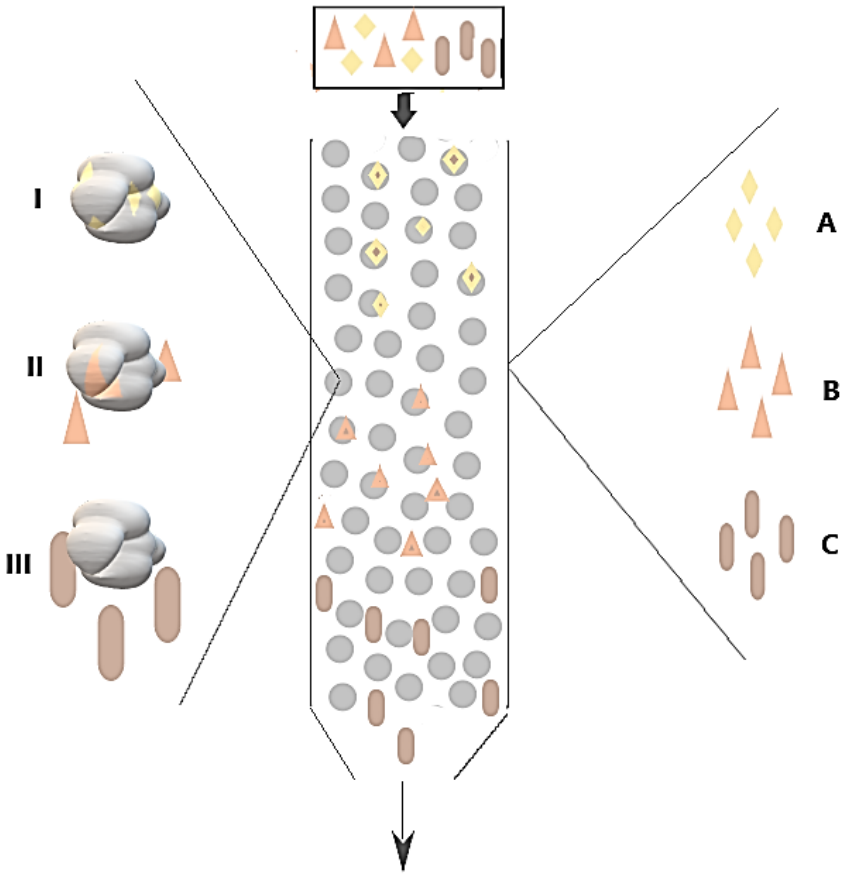

Figure 11. Illustration of a SEC column and the distribution of molecular size. I/A) The smallest components will travel into the particle pores and be delayed, II/B) the medium size particles will somewhat be delayed, while III/C) is too large to fit into the pores and will be transported by the mobile phase between the particles and elute first.

Achieving good separation of the compounds requires a column with appropriate pore size, and the particles are often silica-based with surface functionalities that are suitable for protein and peptide analysis. Surface modifiers, such as a diol functional group, or the porous hybrid bridged ethyl hybrid (BEH) particles modified with diol groups, are commonly used (95). The pore sizes are usually between 6-100 nm and are selected based on the size-range of molecules to be separated. The mobile phase is chosen based on the solubility of the analyte, and an aqueous mobile phase is often infused with small amounts of acid as well as salt to reduce hydrophobic and ionic interactions (86). For analysis of proteins and peptides derived from EPH, an aqueous mobile phase containing organic modifiers, like acetonitrile or methanol with small amounts of trifluoroacetic acid (TFA), is often used in combination with UV detection (88). Lower UV wavelengths, in the range 210-220 nm, provides enhanced sensitivity towards the amide peptide bonds. Higher UV wavelengths between 270-280 nm, provide a greater linear

dynamic range, and are more selective for the aromatic amino acids. A diode array detector (DAD), able to measure a range of wavelengths at the same time, is the preferred UV detector, since proteins, peptides, and free amino acids absorb UV at different wavelengths (89, 90). However, other detectors have been used with today's SEC columns with good results. One example is fluorescence detectors, improving both sensitivity and selectivity (89).

Even if the hydrodynamic volume of a molecule is affected by the surroundings, giving molecules with the same molar mass different hydrodynamic properties, previous studies have shown that the molecular size and hydrodynamic volume do correlate. However, the molar mass of one protein may be lower than another protein and still elute first; therefore, some differences should be expected to occur. Calibration curves are hence an important tool for estimating the molar mass of the proteins relative to proteins and peptides with known mass (1, 96, 97).

2.6.7 Fourier-transform infrared spectroscopy

Infrared spectroscopy (IR) has been utilized in the characterization of inorganic, organic, and biological analytes in complex matrices for a long time (98). Commercial FTIR spectrometers have been available for almost 50 years. However, the signal-to-noise ratio is sufficiently higher in FTIR spectrums compared to the original IR instruments (more of the energy reaches the sample, hence the detector) (99). FTIR has been extensively used for protein analysis and can be used to analyze everything from small soluble proteins to large membrane proteins, with high time resolution (1μs) and low costs, making FTIR a valuable tool for hydrolysate analysis (100). The instrument uses a system called an interferometer instead of the monochromator used in conventional dispersive spectrometers (101). The interferometer consists of a radiation source, a beam splitter (usually a thin film of germanium supported on a potassium bromide substrate), two mirrors, a sample cell, and a detector. The radiation from a heated element or glower goes to the beam, creating two separate optical paths where one part is transmitted to a moving mirror and the other to a fixed mirror. The radiation that hits the two mirrors will partially be reflected towards the splitter, transferred through the sample cell, and what is not absorbed by the sample hits the detector (102). The signal's intensity (I) will be at a maximum when the two beams reaching the detector are in phase. In greater detail, the optical path in both legs of the interferometer is identical (optical retardation (δ) = wavelength (λ) = 0). The sum of the two beams combined constitute the energy that reaches the detector, and an interference pattern is created, which provides an interferogram (102), as shown in **Figure 12**. The computer

performs fourier-transformation on the interferogram after receiving the detector signal to convert it into a single beam spectrum and create an infrared spectrum that can be interpreted (102).

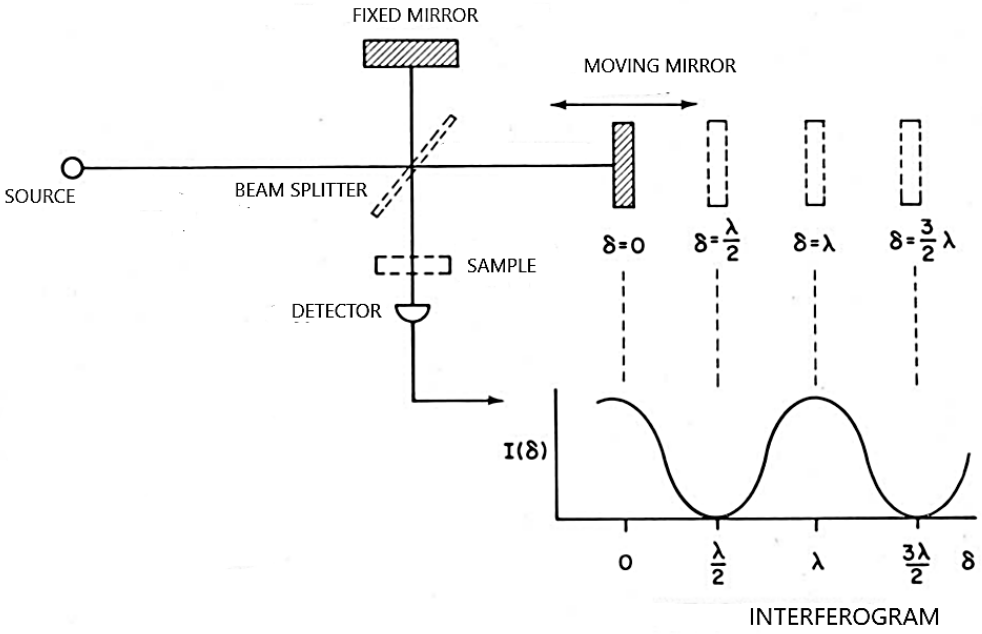

Figure 12. Illustration of a FTIR instrument. The interferogram is made of how the two mirrors and the beam splitter is reflecting radiation trough different angels. Maximum detection is achieved when the beams are in phase and minimum when the beams are out of phase, as the cosine wave implies. δ is the optical retardation, I(δ) is the intensity of the detector signal as a function of optical retardation, and λ is the wavelength. This picture is adapted from Perkins, W.D., 1986 (102).

2.6.7.1 Fourier-transform infrared spectroscopy in characterization of proteins, peptides, and amino acids

FTIR spectroscopy is an almost universal, rapid, non-destructive technique (86), and the analysis can be performed with relatively small amounts of sample (10 – 100 μg) with little restriction in terms of solvents (52, 65, 100). An IR spectrum, usually referred to as a fingerprint, can identify known functional groups on the molecule. FTIR is thus a useful instrument for identifying a protein structure and following changes in the protein due to internal or external modifications (103). The frequency absorbed by the molecule corresponds to the specific movements of the atoms (104). Nine distinctive bands can be seen from peptide groups, called amide A, B, I, II, through VII. While amide I and II bands are the two major

bands of the protein IR spectrum, amide III and IV are very complex bands resulting from a mixture of several coordinate displacements (103). Studies done in the 1950s showed that for proteins with the α-helix structure, the amide I and II absorbed in the spectral range 1652 – 1657, or in 1545 - 1551 cm^{-1} for aqueous solutions, while proteins with β-sheet structure showed similar absorptions of 1628 - 1635 and 1521 - 1525 cm^{-1}, respectively. The length of the hydrogen bonds formed in α-Helix becomes slightly longer and weaker than in an antiparallel β-sheet, which increases the frequency of amide I bands (15).

As previously mentioned, several variables affect wherein the spectrum of the different bands occur. The characterization of proteins is primarily interpreted based on amide bands I and II from the peptide groups. While the C = O stretching vibration contributes to the amide I bands, the amide II bands are mainly N-H bending with contributions from C-N stretching vibrations. The somewhat weaker absorbance that provides amid III bands occurs mainly from the N-H bending and C-N stretching vibrations (65). Inter-, intra-, and extra-molecular interactions will affect the occurrence of the bands through the spectral range. Observations made by Hong et al. (105), as well as Prystupa et al. (106), showed that heat treatment disturbed intramolecular hydrogen bonds in collagen so that the helical structure, to some extent, was unwounded. Collagen with a helical structure tends to appear in a specific range in the FTIR spectrum. When the collagen-derived peak intensity decreases after heat treatment, this indicates changes in the collagen secondary structure (105, 106).

Absorption and frequency depend on the polarity and strength of the various bonds in a molecule, the dipole moment, and the electron-withdrawing and -donating capabilities (100). With these affecting features in mind, all polar bonds absorb IR radiation, including nearly all biomolecules. However, large compounds, like proteins, can provide overlapped bands in the spectrum, where information is hidden beneath broad bands (100). Broad bands in the spectrum can be analyzed in detail by using, e.g., the Savitzky-Golay algorithm, creating a second derivative of the spectrum. Furthermore, corrections with data processing tools can reveal the overlapped components within the broad bands (65). In EPH, it is useful to follow the fragmentation during the reaction. FTIR analysis allows us to follow the protein structure's breakdown during the EPH, the molecular mechanisms in protein reactions, and protein unfolding occurrences (100).

2.7 Aim of study

Raw materials from poultry residuals are not utilized to its full potential as of today. Although EPH has gained a more central role in the industrial utilization of residuals now in recent years, new and better biotechnological and analytical approaches are needed to be able to reach the full potential in utilization of these raw materials. Therefore, the aim of this MSc thesis was to investigate if the use of two different proteases with a preference for myofibrillar or collagen proteins, added in different arrangements, can enhance the yield and quality of protein hydrolysates. Also, through the characterization of process intermediates and the resulting hydrolysates, the aim was to understand more about the causes for the obtained results. **Figure 13** illustrates the aim and sub-goals of the present study.

Sub-goals:

- Perform enzymatic protein hydrolysis on various poultry raw material residues using two proteases, alone and in different arrangements, to produce time-series and product hydrolysates

- Use a combination of classical biotechnological and analytical techniques to obtain process and product quality parameters, such as mass average molar mass, protein content, peptide size distribution, degree of hydrolysis, hydroxyproline content, and structural information of the protein and peptides within the hydrolysates.

- Develop a sample preparation method so that collagen-rich hydrolysates can be analyzed using high performance size-exclusion chromatography

- Use the obtained data to evaluate which process-choice resulting in the highest yield and explain when and how the various components are released during the enzymatic protein hydrolysis process.

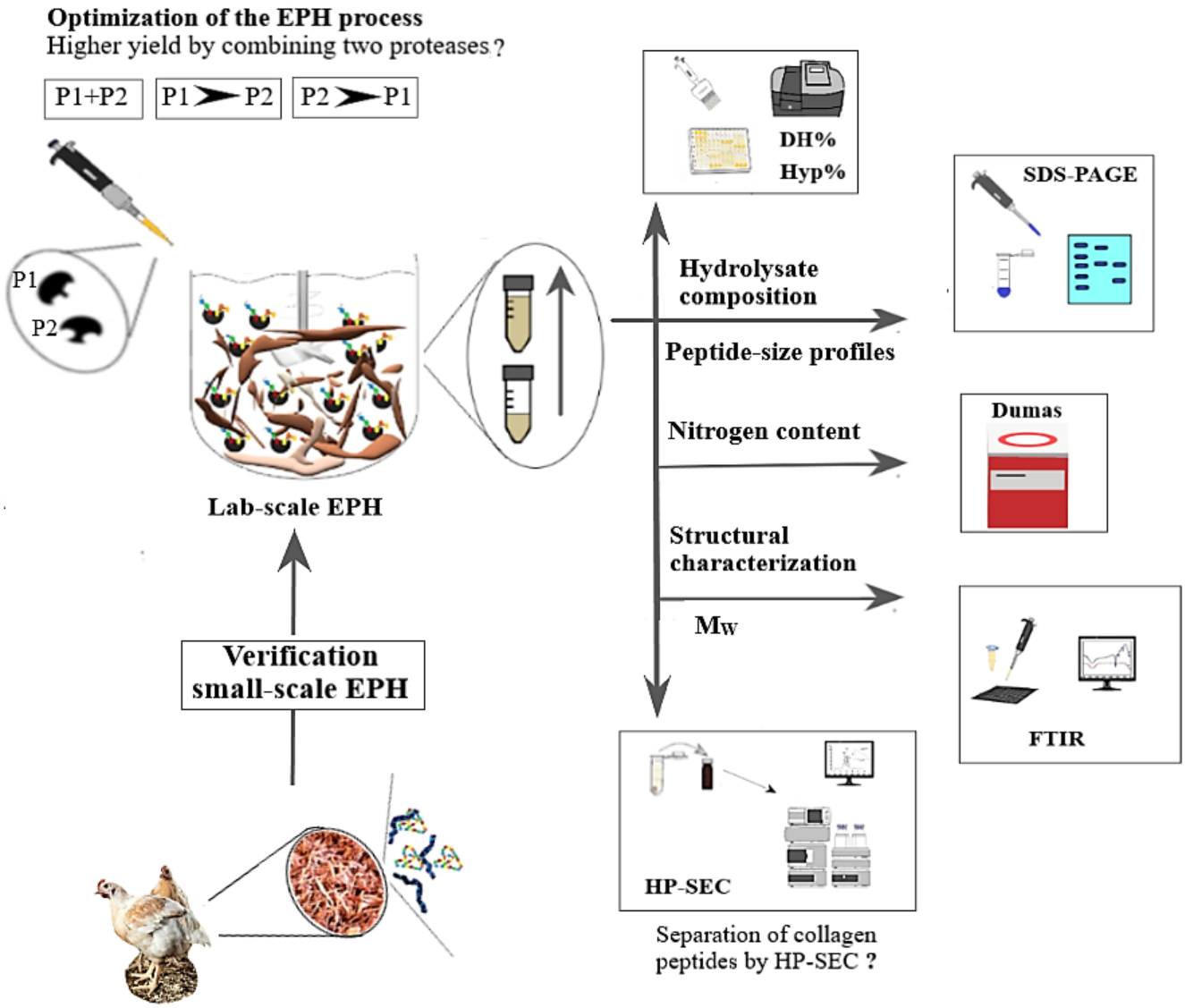

Figure 13. Overview of the aim and sub goals, with factors that were evaluated during the present study. Abbreviation: P1) protease one, P2) protease two.

3 Experimental

3.1 Small equipment

Automatic pipettes, serological pipettes, powerpette Plus, and other small glass and plastic equipment were from VWR chemicals (Radnor, PA, USA). Vortex mixer MS 3 series was from IKA (Staufen im Breisgau, Germany). The analytical balance used in hydrolysis sample preparation was AG 204 from Mettler-Toledo (Columbus, OH, USA). Millex-HV PVDF syringe and Millipore filter with pore size 0.45 mm were from Merck (Billerica, MA, USA). The 597 Whatman (Ø 125 mm) filters were from VWR.

3.2 Chemicals

3.2.1 Solvents

Methanol (MeOH) (≥ 99.9% purity) and acetonitrile (MeCN) (≥ 99.9% purity) were obtained from VWR. Acetic acid (AcOH) (100%) was obtained from Merck. Water used was type 3 water or type 1 water (resistivity of 18.2 MΩ•cm at 25 ˚C) taken from a Millipore type 1 purification system with a Q-guard cartridge, a Quantum cartridge and a filter membrane with 0.22 µm pores purchased from Merck.

3.2.2 Reagents

Trifluoroacetic acid (TFA) (≥ 99.0%), trichloroacetic acid (TCA) (≥ 99.0%), hydrochloric acid (HCl) (≥ 99.0%), L-cysteine hydrochloride monohydrate (≥ 98.0%) and ethylenediaminotetra acetic acid (EDTA) (98.5-101.5%) were obtained from Sigma Aldrich, (Dramstadt, Germany). Monosodium phosphate (NaH_2PO_4) and Sodium dihydrogen phosphate dihydrate ($NaH_2PO_4•2H_2O$) were obtained from Merck. Coomassie brilliant blue – R250 (825.99 g/mol) was obtained from Thermo Fisher scientific (Rockford, USA). Azo-casein (Casein dyed with sulphanilic acid) was obtained from Megazyme (Wicklow, Ireland). NuPAGE MOPS SDS Running Buffer (20x) from Novex by life technologies was obtained from Thermo Fisher scientific. The 13 calibration standards bovine albumin (Mw 66000), albumin from chicken egg white (Mw 44287), carbonic anhydrase (Mw 29000), lysosyme (Mw 14300), cytochrome c from bovine heart (Mw 12327), aprotinin from bovine lung (Mw 6511), insulin chain B oxidized from bovine pancreas (Mw 3496), renin substrate tetradecapeptide porcine (Mw 1759), angiotensin II human (Mw 1046), bradykinin fragment 1-7 (Mw 757), [D-Ala2]-leucine

enkephalin (Mw 570), valine-tyrosine-valine (Mw 379) and tryptophan (Mw 204) were obtained from Sigma Aldrich (St. Louis, MO). Column performance check standard Protein Mix (ALO-3042) was obtained from Phenomenex (Torrance, USA). The standard Sulfanilamide was obtained from Elementar Analysensysteme GmbH (Langenselbold, Germany). 2,4,6-trinitrobenzenesulfonic acid (TNBS, $C_6H_3N_3O_9S$) was obtained from Sigma Aldrich. The 25 proteases were obtained from various producers and are given in **Appendix 7.1**.

3.2.3 Solutions

3.2.3.1 Solutions used in the EPH

Protease screening using the azo-casein assay from Megazyme and the protease screening using different parts of the MDPR, on a small-scale, was done in cooperation with master student Marte Dalsnes from NTNU (107).

Poultry RRM used in the EPH reactions

The poultry RRM was a mixture of chicken and turkey deboned residues referred to as mechanical debone poultry residues (MDPR) and CF provided by Nortura (Hærland, Norway). The materials were delivered frozen, and before defrosting, they were cut into cubes and minced under semi-frozen conditions with a Mado 723 Meatgrinder from MADO GmbH (Dornhan, Germany). The minced materials were vacuum packed in 500 g packages before being stored at -40 °C.

Buffer solutions for the protease activity screening on azo-casein / – small-scale EPH reactions

Of 1 M, buffer A was made by solving 178 g $Na_2HPO_4 \cdot 2H_2O$ in 900 mL of type 3 water, during heated stirring at 45 °C until solved. Then the pH was adjusted to 7.0 with 5M HCl, and the volume was adjusted to 1000 mL. The buffer could stay at room temperature for a few weeks.

0.1M buffer B was made by solving 8.9 g Na2HPO4 • 2H2O in 450 mL of type 3 water, following the same procedure as for Buffer A. Then 2.65 g L-cysteine hydrochloride monohydrate and 5.6 g EDTA were added before pH was adjusted to 7.0 with 1M NaOH. The volume was adjusted to 500 mL. This buffer had to be used within two days (108).

Protease solutions for the protease activity screening on azo-casein

In cooperation with Dalsnes et al., protease activity screening of 25 different proteases were done using the azo-casein assay from Megazyme (108). To obtain a dilution of 1:50, 20 mg of the solid proteases were dissolved in 1000 µL of buffer, while 20 µL of the liquid proteases were dissolved in 980 µL buffer. A dilution row with three tubes per protease was created with decreasing protease concentration, where the third tube also was used in the blank sample. The optimum dilution range for both liquid and powder proteases was customized according to the results from the spectrophotometric analysis at 440 nm until absorbance between 0-1.5 was achieved.

Protease solutions for small- and lab-scale EPH

The protease concentrations used in the small-scale EPH are presented in **section 4.4.1, Table 8**, and prepared according to the protocol in **Appendix 7.2.1**. The concentration of two selected proteases, Endocut-02 from Tailorzyme ApS (Denmark) and Bromelain from Ultra Bio-logics (Canada), was upscaled with the protease- and substrate amounts as given in **Table 1**. The protease solutions were stirred for 30 minutes before use and could be stored for ≤ 2 hours.

Table 1. The amount of protease and substrate in the lab-scale reactions.

Protease	Amount of protease	Amount of substrate
Bromelain	1515 mg	333.0 g
Endocut-02	1149 µL	333.0 g
Mixed proteases	(x 2.5) / 2	250.0 g

Substrate solutions for protease activity screening on azo-casein

0.5 g azo-casein was added to a 50 mL tube with 1 mL ethanol, vortexed until homogenized before mixed well with 24 mL of sodium phosphate buffer. The substrate could stay for several weeks when stored at 4 ºC (108).

Substrate solution for poultry RRM used in the small- and lab-scale EPH

The amount of RRM used in the small-scale EPH was 2.000-2.050 mg and prepared according to the protocol in **Appendix 7.2.1**. The amount of RRM in the lab-scale reaction using single protease-treatment, and mixed proteases are given in **Table 1** and prepared as given in section **3.3**.

3.2.3.2 High performance – size-exclusion chromatography

Size calibration solutions and standard solution

Both the size calibration solutions, shown in **Table 2**, and the check standard were prepared in type 1 water at a concentration of 2 mg/mL.

Table 2. The 13 calibration standards used, with the proteins molar mass.

Molecules	M_W
Bovine serum albumin	66000
Albumin from chicken egg white	44287
Carbonic anhydrase	29000
Lysosyme	14300
Cytochrome c from bovine heart	12327
Aprotinin from bovine lung	6511
Insulin chain B oxidized from bovine pancreas	3496
Renin substrate tetradecapeptide porcine	1759
Angiotensin II human	1046
Bradykinin fragment 1-7	757
[D-Ala2]-leucine enkephalin	570
Valine-tyrosine-valine	379
L-Tryptophan	204

Buffer solution

To wash the column, 1 L buffer was made by preparing a 0.10 M monosodium phosphate solution.

Mobile phase

The aqueous mobile phase was consisted of type 1 water/CAN/TFA (70/30/0.05 v/v/v), prepared in a 5 L volumetric flask.

3.2.3.3 Sodium dodecyl sulfate – polyacrylamide gel electrophoresis

Buffer solution

A tracking dye buffer of 8 mL was made by mixing 2 mL 1M DTT and 500 µL of a 0.8 % Bromophenol blue solution in type 1 water. This solution was pre-made and stored in a freezer. 500 mL running buffer was made with 25 mL of NuPAGE MOPS SDS Running Buffer (20x) in type 1 water.

Staining solution

A staining solution of 1000 mL was made with MeOH/Coomassie brilliant blue R/ type 1 water/AcOH (50/25/15/10 v/v/v/v).

Destaining solution

The 1000 mL destaining solution was type 1 water/MeOH/AcOH (73/20/7 v/v/v).

3.3 Sample preparation of the hydrolysates

3.3.1 Protease activity screening of 25 proteases on azo-casein

Megazyme has developed an assay to be able to measure the activity of endo-proteases when these are added to the substrate azo-casein at different conditions. The procedure from Megazyme was followed, with some modifications (108). Two sets of Eppendorf tubes were prepared and placed in a thermomixer at 42 °C and 500 rpm for pre-equilibration (TermoMixer F1.5 from Eppendorf, Germany). One set of Eppendorf tubes contained 250 µL of the protease solutions and another 200 µL of the substrate solution. After 20 minutes in the thermomixer, 200 µL from the set with protease solutions was added to the set with the substrate, from high to low protease-concentration. The protease-substrate solutions were then vortexed and incubated at 42 °C for precisely 10 minutes, before deactivation with 1.2 mL 5 % (w/v) TCA followed by an additional 3 seconds of vortexing. The protease solution with the lowest concentration was added to the blank sample immediately after the TCA to deactivate the protease while being added. After 5 minutes of cooling, the solutions were centrifuged at 5200 rpm for 10 minutes in a microcentrifuge (MICRO-STAR 17R from VWR, Radnor, PA, USA), leaving precipitated non-hydrolyzed azo-casein pellets at the bottom of the tubes. The supernatant was transferred to cuvettes, and the absorbance was read against the reaction blank at 440 nm using a spectrophotometer.

3.3.2 Enzymatic protein hydrolysis of poultry residual raw material

The small-scale EPH reactions was performed with 2.000 – 2.050 g of material (bones, tendons, CF, and artificial MDPR) in 12 mL falcon tubes. The materials were added to the tubes in one batch, whereafter, the tubes were frozen until the day of hydrolysis. Before hydrolysis, the materials were thawed. Further, 7.5 mL of buffer A was added to each tube before being placed in a water bath at 45 ºC. The small-scaled reaction was a study done in cooperation with Dalsnes et al. in 2019, and experimental details can be found in Dalsnes` thesis (107).

The lab-scale EPH reactions were performed using a Reactor-Ready jacketed reaction vessel heated with a JULABO circulator pump to 50 °C (Radleys, Saffron Walden, Essex, UK). 333 g of previously frozen and homogenized poultry RRM were thawed at room temperature (rt) and mixed with 667 mL of type 3 water in the reactor. The suspension was stirred at 300 rpm until it reached 50 °C. Before adding the proteases, 1149 µL of Endocut-02 or 1515 mg of Bromelain was mixed in 10 mL water. At time (t) = 0, proteases were added to the preheated raw material suspensions. 10-15 mL of the reaction mixtures was collected at t = 0.5, 2.5, 5, 7.5, 10, 15, 20, 30, 40, and 50 minutes using a rubber hose attached to an electric pipette. The samples were transferred directly into a microwave oven from Menumaster Commercial (Iowa, USA) and heated for 6 seconds at 1800 W before being placed in a water bath at 95 °C for 15 minutes to inactivate the protease preparations. Finally, after 60 minutes, the total reaction was stopped by thermal inactivation using the microwave oven to reach 95 °C quickly. The reaction mixtures were then kept at 95 °C for 15 minutes. Following the thermal inactivation, the solutions were left to cool down to rt, and centrifuged at 4400 rpm at 25 °C for 15 minutes (HERAEUS MULTIFUGE 4KR Centrifuge from VWR). The product hydrolyzed for 60 minutes was separated into three phases, i.e., fat-, water- and solid-phase. All products were weighed. The total water phase was vacuum filtrated using Pall XX filters (Port Washington, NY, USA) and stored at -40 °C. The water phase of the time-series samples was vacuum filtrated using 597 Whatman filters from General electric Life Sciences (Marlborough, MA, USA) and stored at -40 °C. The amount of dry matter in the water phases was determined by freeze-drying of the samples using a Laboratory freeze dryer, Gamma 1 – 15 from CHRIST (Osterode am Harz, Germany).

3.3.3 Fourier-transform infrared spectroscopy

The water phase from the time series samples taken during hydrolysis was filtrated through a Millex-HV PVDF syringe attached to a Milli-pore filter with pore size 0.45 mm before applied to the sample plate in 5 replicates with a volume of 5-10 µL Some were diluted due to concentration differences in the samples, while others were loaded undiluted and at lower volumes, depending on how the FTIR spectra turned out. Often, several runs were done to produce satisfying spectra from the hydrolysates. The MDPR hydrolysates treated with Bromelain contained fat, which gave interferences in the spectra and was, therefore, freeze-dried and reconstituted in water before analysis (15 mg/mL). 70 % isopropanol and type 1 water were used to wash the FTIR 96 wells plate between the analysis.

3.3.4 High performance size-exclusion chromatography

The hydrolysate's water phase was filtrated through a Millex-HV PVDF syringe attached to a Milli-pore filter with pore size 0.45 mm into 15 mL tubes before being freeze-dried. 25 mg of dried samples were transferred to Eppendorf tubes and reconstituted in 1 mL of the MP before being vortexed and placed in the fridge at 4 ºC overnight. The following day, samples were vortexed again and centrifuged at 3500 rpm for 5 minutes, and the supernatant was transferred to SEC-vials ready for injection.

3.3.5 Sodium dodecyl sulfate – polyacrylamide gel electrophoresis

The samples were prepared by solving peptides from the solid phase after hydrolysis due to the experiments were done before the freeze-drying of the water phase was done. 15 mg of the sediment was solved in 1 mL type 1 water, using heated stirring at 45 ºC and 700 rpm before being centrifuged in 10 minutes at 4400 rpm. 20 µL of the supernatant was mixed with a 20 µL tracking dye buffer before 5-15 µL of the mixed sample was applied to the 12 % polyacrylamide wells. A few experiments were conducted after freezing-drying of the water phase in which 2 mg was resolved in type 1 water and with an equal concentration-ratio of the tracking dye buffer. 7-15 µL of the mixed sample was applied to the wells

3.3.6 Degree of hydrolysis assay

The Degree of hydrolysis (DH%) was measured using a TNBS method based on descriptions by Adler-Nissen, J., and Satake et al. (78, 109). An example of the calibration solutions and corresponding calibration curve from the DH% analyses are shown in **Table 3** and **Figure 14**.

The freeze-dried hydrolysates were diluted in a 0.21 M phosphate buffer, reaching a concentration of 10 mg/mL. After dilution, the sample solutions were vortexed and refrigerated overnight. 50 µL of each sample solution was transferred to new Eppendorf tubes and further diluted to 0.5 mg/mL with 950 µL 1% SDS solution before being vortexed again. Further, 15 µL of calibration solutions (0, 0.075, 0.15, 0.3, 0.6, 0.9, 1.2, and 1.5 mM leucine in 1 % SDS), and each hydrolysis sample was added to a 96 wells plate (Thermo Immunoplate F96 MAXISORP from VWR). An additional 45 µL of phosphate buffer was added to each well. 0.05 % (w/v in water) TNBS solution was then added to the wells before the plates were stirred, wrapped in aluminum foil, and incubated for 1 hour at 50 ºC. After incubation, the solutions were quenched with 90 µL 0.1 M HCl, stirred, and analyzed in triplicates at 340 nm using a BioTek Synergy H1 Spectrophotometer (BioTek Instruments, Winooski, VT, USA). According to **Equation 1,** in section **2.6.3**, the DH% values were calculated using htot estimated from literature values (74, 79, 110) and protein content measurements from Dumas combustion analysis. The DH% during hydrolysis time of all the EPH series are presented in **Appendix 7.6** (Figure 51-55).

Table 3. The concentration and absorbance of the calibration solutions used in the DH% analyses, example from one of the measured lab-scale series.

Calibration consentration of leucine (mM)	Absorbance at 340 nm
0	0.337
0.075	0.381
0.15	0.423
0.3	0.503
0.6	0.664
0.9	0.830
1.2	0.993
1.5	1.131

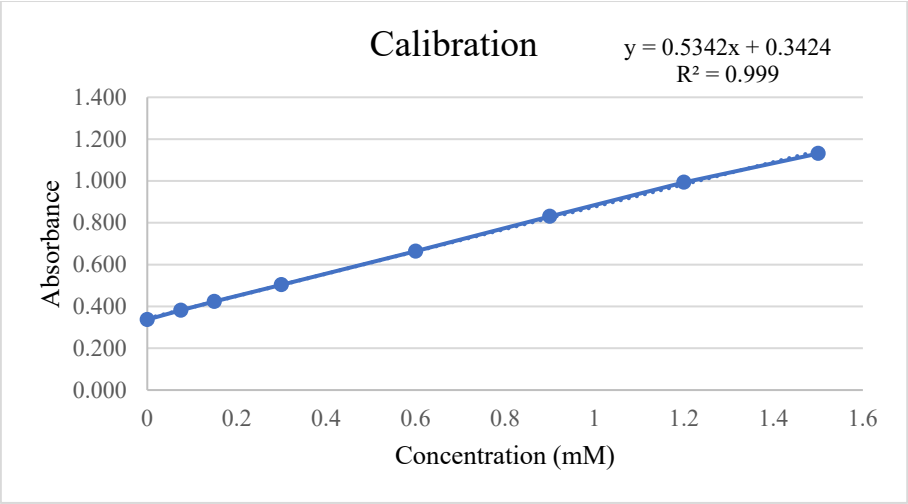

Figure 14. The calibration curve of leucine used in the calculations of DH%, with concentration (mM on the x-axis and Absorbance on the y-axis (corresponds with the calibration solutions in **Table 3**). Includes trendline and R-value.

3.3.7 Dumas Combustion Analysis

The Dumas method was used to determine the protein content (%) in the hydrolysates. Between 4.500-5.300 mg of sample was weighed into small aluminum trays using a METTLER MT5 analytical scale (Bergman AS, 2001 Lillestrøm, Norway). Tweezers were used to wrap the aluminum trays into small inert parcels, ready to be placed in the instruments sample inlet. 3 x standards containing Sulfanilamide (N 16.26%; C 41.81% and S 18.62%) were prepared the same way as the samples for each 60-70 sample analyzed and were used to calculate adjustment factors for C, N, and S.

3.3.8 Determination of hydroxyproline in collagen-rich samples

The Hyp content was determined in the two duplicated MDPR series using a Hydroxyproline Assay Kit from Sigma Aldrich. These experiments were performed in collaboration with Kristoffersen, K.A. (111). 1.0 mg of the freeze-dried hydrolysates were applied to Eppendorf tubes and diluted in 1 mL type 1 water. The sample preparation was conducted as presented in the technical bulletin from Sigma Aldrich (82) and transferred to 96 wells plates before spectrophotometric analysis at 560 nm.

3.4 Instrumentation and settings, data acquisition and processing of data

3.4.1. Spectrophotometer used for measuring the protease activity

Using a spectrophotometer (Pharmacia Ultrospec 3000) with plastic cuvettes, absorbance at 440 nm (108) was measured for each sample with an optimized diluent row, given in **Appendix 7.1.2** (Table 19-21). By plotting the absorption as a function of the dilution, providing an approximate linear graph, the calculation of dilution factors for each protease could be determined. Only absorbance between 0.1-1 OD was approved since values above 1.5 - 2 diverged from the linear range. The calculations and linear graphs of Bromelain and Endocut-02 are shown in **Appendix 7.1.2** (Figure 49-50).

3.4.2 Spectrophotometer used for measuring the degree of hydrolysis

Using a BioTek Synergy H1 spectrophotometer from BioTek Instruments, and 96 well plates, absorbance at 340 nm was measured for each sample in triplicates, providing values within the range of the calibration curve.

3.4.3 Sodium dodecyl sulfate – Polyacrylamide gel electrophoresis

Invitrogen Power Ease 500, Invitrogen XCell SureLock, and Novex Mini-Cell from life technologies (Carlsbad, California, USA) were used when performing the gel electrophoresis. The gels were scanned using EPSON PERFECTION 4990 PHOTO from EPSON (Long Beach, California, USA) with both colored and grey scaled settings.

3.4.4 Fourier-transform infrared spectroscopy

The FTIR instrumentation used was a High Throughput Screening eXTension (HTS-XT) connected to a Tensor 27 spectrometer (Bruker Optics, Germany). The data acquisition was controlled using Opus v6.5 (Bruker Optics, Germany), and the data were analyzed using the computer software Unscrambler (Camo Analytics, Norway). The FTIR instrument was used continuous, providing rapid information about the hydrolysates during the EPH process. The proteases' ability to break down the RRM could be monitored during the run. From each EPH

sample, five replicates with the filtered liquid phase were pipetted onto a 96-well microplate of graphite and dried at room temperature overnight. The amount of applied sample varied a lot, considering the differences in the RRM as well as in peptide-concentration. Volumes between 4-15 µL were applied to the 96-well microplate. The raw data were preprocessed using the Savitzky-Golay algorithm to create a second derivative with 13 smoothing points and a polynomial degree of two. For normalization of the spectra, Standard Normal Variate (SNV) was used, followed by creating an average of the replicates of each sample. Then, principal component analysis (PCA) was conducted to the hydrolysates within the spectral region from 1800-400 cm^{-1}.

Data processing in FTIR

The goal of data processing is to translate the signals with fourier-transformation into IR spectra that can be interpreted based on similar protein and peptide-peaks. Correcting the spectrum after the deconvolution can be done with several modifying tools such as Multiplicative Scatter Correction (MSC) and SNV, which are multi-wavelength, pre-processing concepts for optical correction that helps to separate the chemical light absorption from the physical light scatter (52, 112). Even if MSC is the most commonly used preprocessing treatment, the SNV can be applied to every spectrum individually and is often used to remove the scatter when processing complex data sets in multivariate methods like PCA (98, 113, 114). To obtain useful models from multivariate regression such as PCA analytes must be separated from the interferants appearing from contaminants in the sample or instrument, atmospheric CO_2 and H_2O reacting with the sample prior analysis, or interference caused by instrumental variations. Preprocessed data suppress these interferant signals and therefore enhance the analyte signals (98).

Principal component analysis

PCA is an unsupervised multivariate analytical tool that can be used to emphasize variations and bring out strong patterns in a dataset (115, 116) and thus identify the underlying structure in a data set such as outlier identification, identification of trends and groups, and exploration of similarities (52, 117). The score plot of the PCA is dimensionally reduced, and consists of score vectors plotted against one another, and the most common plot is the score vector of principal component one (PC-1) on the x-axis against principal component (PC-2) on the y-axis, where the distance between the points indicates the difference between them (118). PC-1

describes the direction in the data set with the most significant variance, and PC-2 (PC-3 ..PC-n), which is orthogonal to the previous, accounts for the remaining variance (1).

3.4.5 High performance size – exclusion chromatography

The HP-SEC instrumentation used was an Agilent 1200 series instrument (Santa Clara, CA, USA) with a quaternary pump, a degasser, a thermostatic column compartment, a photodiode array detector, an autosampler, and a BioSep-SEC-s2000 column from Phenomenex (300 x 7.8 mm, particle size 5 µm, pore size 145 Å). Only the size calibration solutions and the column performance check standard (Aqueous SEC 1, Ea, protein mix) were analyzed in triplicates, but all the solutions were injected with the same volume and at the same column temperature. The instrument set-up was carried out as the procedure found in Wubshet et al. (119, 120) and is given in **Table 4 and 5**. An isocratic elution at a flow rate of 0.900 mL/min were carried out for 17.0 minutes. Between 17.0 and 17.1 minutes, the MP was changed to the 0.10 M monosodium phosphate buffer and maintained in 3 minutes for column cleaning. The elution conditions were then restored, and the column was equilibrated for an additional 25 minutes. Cromatograms were collected for all the hydrolysates using a UV-DAD recording wavelength at 214 nm. Calculations of the Mw were performed using PSS winGPC UniChrom V 8.00 (Polymer Standards Service, Mainz, Germany).

Table 4. Instrument setup for the HP-SEC used in all analyses

Parameter	Setting
Mobile phase (A)	Type 1 water/ACN/TFA (70/30/0.05 v/v/v)
Washing buffer (B)	0.10 M monosodium phosphate
Injection volume	10 µL
Column temperature	25 ºC
Flow rate	0.900 mL/min
Detector	Photodiode array (UV), 214 nm
Total analysis time	45 minutes
Re-equilibriation time	25 minutes

Table 5. Isocratic elution setup, with A and B an for **Table 3**.

Time [min.]	A (100 %)	B (100 %)
0	0.900 mL/min	
17 - 17.1		0.900 mL/min
20	0.900 mL/min	

The **HP-SEC system** needs to be periodically cleaned and frequently calibrated which can provide changes in the analytical method over time, especially in long runs. Frequently use of a control standard can be used to monitor variations in the method set-up and changes in the instrument performance during the runs (121).

Data processing in HP– SEC

The purpose of the data processing is mainly to convert chromatograms into a molecular size distribution, where calculations can be done based on a slicing method. In greater detail, this means that the distribution of peptides can be divided into fractions according to their molar mass based on the use of a defined calibration range. Also, when collecting time-series samples during the EPH, it is possible to find an association between the calculated M_W and the hydrolysis time (120), using the collected data from the analyses in the creation of analytical graphs and models.

3.4.6 Dumas combustion analysis – nitrogen content

The instrument used for nitrogen content analysis was an Elemental Vario EL cube from Elementar Analysensysteme GmbH (Langenselbold, Germany). The Vario EL cube was operated using software with Laboratory information management system (LIMS). The instrument held an auto sleep and wake-up function for automated and unattended overnight operations and was monitored by the lab manager. The analysis was performed with the parameter settings as shown in **Table 6**. As presented in **Table 7**, each sequence started with; three blank samples without O_2 followed by five blank samples with O_2, and finally, three analytically weighed standards. The eight first places in the carousel sample inlet were left empty, representing the blank samples. Further, the hydrolysate samples were placed in the carousel after a numbered order, and a TCD recorded the nitrogen content in the hydrolysates.

Table 6. Instrumental setup for elemental nitrogen analysis with vario El cube.

Parameter	Setting
Temperature combustion	1150 ºC
Temperature, reduction	850 ºC
Temperature, CO_2 column	27 ºC
Temperature, SO_2 column	96 ºC
Flow, helium	230 mL
Flow in standby, oxygen	12 mL
Pressure	1200-1250 mbar

Table 7. Sample setup for the elemental nitrogen analysis with vario EL cube.

Sample	Run
Blank without O_2	1 - 3
Blank with O_2	4 - 8
Standard, Sulfanilamid	9 - 11
Sample	12 - 72

The **Dumas instrument** needs to be cleaned and have the drying columns replaced about every three months. Calibration with control standards can regulate for the differences that may occur after cleaning and replacement of the columns (122).

3.4.7 Raw material analysis

RMA of the poultry RRM used during the present study was done to determine the amount of protein, Hyp, ash, fat, water, carbohydrates, and energy content in the materials. 100 g of tendons, CF, and MDPR were sent to ALS Laboratories UK for the RMA completion (69). The materials were analyzed in duplicates, and the results were presented in mg/100g of material presented as mg/100g of material.

4 Results and discussion

New and better biotechnological and analytical approaches are needed to be able to reach the full potential in the utilization of poultry RRM. The RRM composition and quality are two major factors influencing an EPH process and the resulting hydrolysate products. According to Wubshet et al., low solubilization of proteins from connective tissue during EPH has previously led to decreased protein yield of poultry RRM due to the high amounts of connective tissue and bones in these materials (66, 120). In the present study, an optimization of the original EPH process was done. During the EPH optimization, it was investigated whether two different proteases with a preference for myofibrillar or collagen proteins added in different orders could enhance the protein yield. A combination of classical biotechnological and analytical techniques was used to understand more about the reasons for the obtained results, focusing on the characterization of process intermediates and the resulting hydrolysate products. The flow chart of the optimized EPH process is presented in **Figure 15** and an overview of the methods used for evaluation of the resulting hydrolysate products as shown in **Figure 16**.

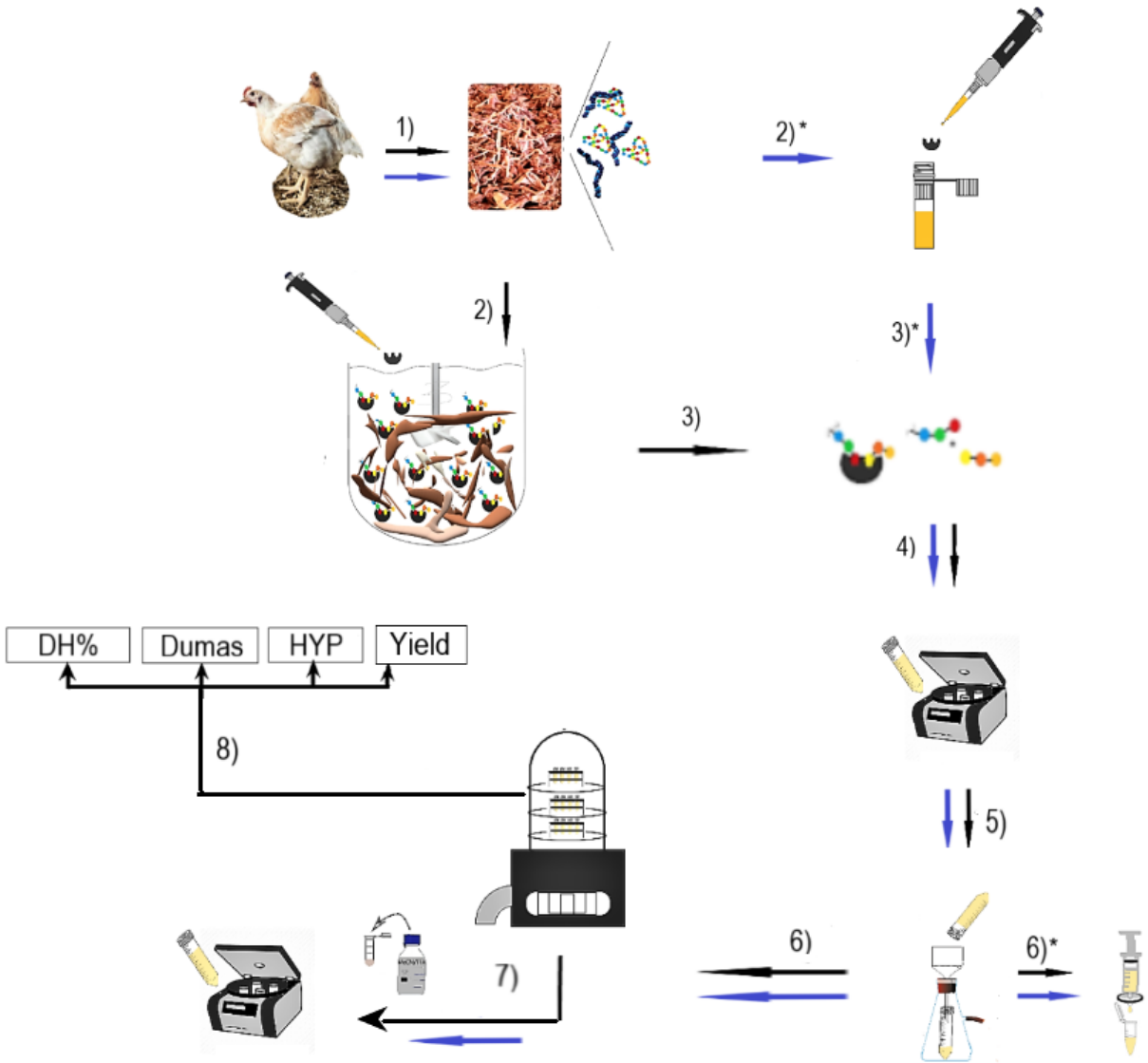

Figure 15. Flow chart over the process of optimizing the EPH process aiming at better utilization of poultry RRM. Small- and up-scale EPH is followed by the necessary steps to measure protein hydrolysates and calculate the protein yield of the reactions (blue arrows: small-scale EPH and black arrows: lab-scale EPH); 1) MDPR containing different proteins, 2)/2)* adding proteases to the substrate solutions, 3)*/3) proteases are cleaving the peptide chains in the substrate, 4) centrifugation of the total hydrolysate solutions, 5) vakuum filtration of the supernatant, 6)* Milli-pore filtration of the liquid hydrolysate before FTIR analysis, 6) freeze-drying of the liquid hydrolysate, 7) re-solving the hydrolysates in MP followed by centrifugation before SEC analysis, 8) DH%, Dumas, Hyp, and calculation of protein yield were done of all the lab-scale hydrolysate products.

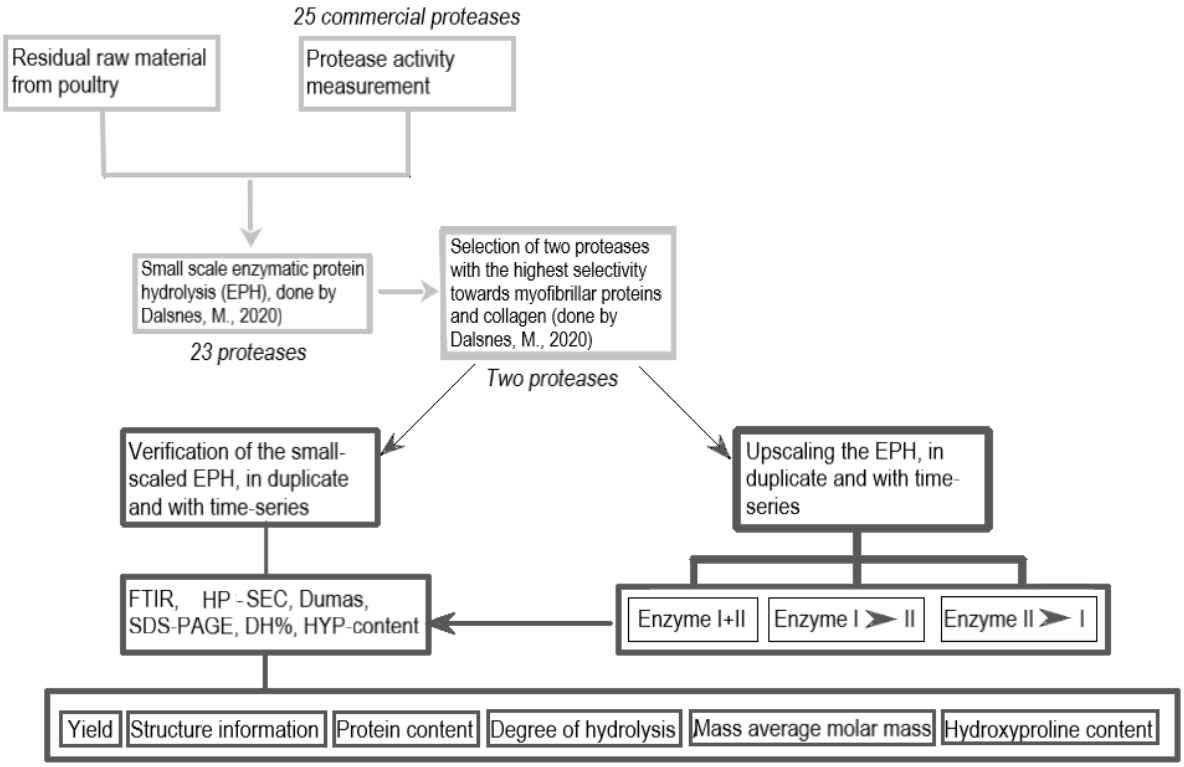

Figure 16. overview of the techniques used in the preliminary study (in gray frames) and the present study (in black frames).

4.1 Framework of study

As mentioned in the introduction, large amounts of poultry RRM are produced every year. The valorization of the poultry RRM would induce less generated waste and could result in a broad range of proteins and protein derivatives that can be used in different fields, including nutritious sources for a globally growing population. Hence, if a complete utilization of poultry RRM can be accomplished, this would contribute to a more sustainable environment (2). The possibility of reaching complete utilization of poultry RRM could be higher by using targeted EPH, e.g., by using a combination of two proteases, Endocut-02 and Bromelain, which are selective towards myofibrillar proteins and collagen, the two main substrates in poultry RRM. Since various commercial proteases have different activities and selectivity, a preliminary study was carried out in two steps. In the first step, an activity screening of 25 different proteases was done on the unspecific substrate azo-casein to reduce the concentration differences before the selectivity screening was done on the poultry RRM (108). That means, the first step was to find a suitable protease concentration based on the proteases activity and selectivity towards azo-casein (some commercial proteases are highly more concentrated and hence more active than

others). Each protease would then have approximately the same starting point when the selectivity screening against myofibrillar protein and collagen in poultry RRM was done in the second step of the preliminary study.

4.1.1 Preliminary study – proteolytic activity towards azo-casein

As the first step, an activity screening of 25 different proteases using an assay that measured their activities towards a nonspecific substrate, azo-casein, was done in collaboration with Dalsnes, M. (107, 108). The assay is frequently used for studying protease activity (123, 124) and was therefore used even though casein is a different protein than collagen and myofibrillar proteins. The dilution series aimed to find protease activities that showed spectrophotometric values between OD 0.5 and OD 1.0. The optimal dilution coefficient for each protease was found within the linear range of the graph between OD 1.0 - 1.5. The measured values were then used to find a relationship between the absorbance and dilution coefficient using linear regression, as illustrated in **Figure 17**.

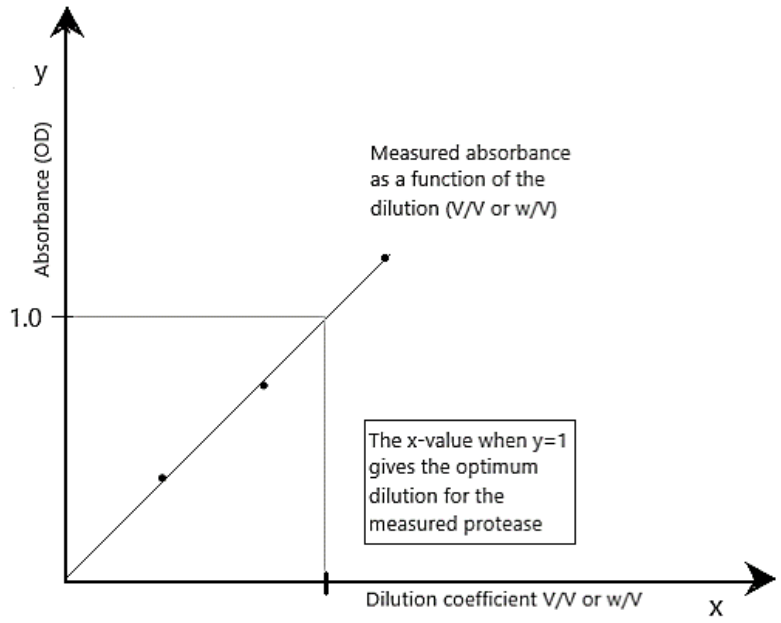

Figure 17. Absorbance as a function of dilution coefficient. The x-value where y equals 1 gives, in theory, the optimal dilution for each protease.

The mean dilution coefficient for liquid and solid proteases was used for calculating the protease concentrations used further. The screening showed that the amount of protease needed to find approximately the same activity measured as OD value varied between 6.93-199 µL or mg per 1000 µL substrate solution, as shown in **Table 8**. The 25 proteases showed quite different activity in degradation of azo-casein, and 23 of them were further used during the second step of the preliminary study, in the selectivity screening on MDPR. The two proteases that were not used further in the selectivity screening, marked with gray in table 8, were rejected due to the need of using excessive protease concentrations to obtain a usable protease activity.

The second screening aiming at finding differences in selectivity on different RRM from poultry using the 23 proteases done in Dalsnes' experiment, led to the finding of two proteases, Endocut-02 and Bromelain, which were further used in the lab-scale EPH (107).

Table 8. The protease concentrations determined from the protease screening. Neutrase and MaxiPro NPU, marked in gray, required too high concentrations to be included in the present study.

Protease	Concentration of protease based on the protease screening (µL or mg/1000 µL)
Alcalase[1]	17.4
Bromelain[2]	7.27
Corolase 2TS[3]	82.9
Corolase 7090[3]	50.0
ENDOCUT-01[4]	77.8
ENDOCUT-02[4]	6.93
ENDOCUT-03[4]	9.92
Flavourzyme[1]	48.3
FoodPro 30L[5]	10.2
FoodPro 51 FP[5]	55.9
FoodPro PNL[5]	51.1
Protamex[1]	45.5
Neutrase[1]	157
MaxiPro NPU[6]	199
PROMOD 144GL-100TU[7]	65.2
PROMOD P950L[7]	15.0
TAIL-10 [4]	7.01
Tail-189 [4]	7.23
Tail-190[4]	36.7
Tail-191[4]	23.7
Tail-192[4]	17.8
Tail-193[4]	18.1
Tail-194[4]	83.0
Tail-197[4]	54.0
VERON L[3]	20.8

Protease reference list:

Novozymes ApS (Denmark)[1]

Ultra Bio-logics (Canada)[2]

AB Proteases GmbH (Germany)[3]

Tailorzyme ApS (Denmark)[4]

DuPont-Danisco (USA)[5]

DSM (The Netherlands)[6]

Biocatalysts LtD (UK)[7]

4.1.2 Preliminary study – selectivity screening on poultry raw material residues

In a second step, done by Dalsnes, M. (107) (hereafter called Dalsnes 12mL and Dalsnes 40mL), selectivity screening was performed on four different poultry RRM (tendons, bones, meat and MDPR) using 23 of the 25 initial proteases from the first screening on azo-casein with the associated concentrations are listed in **Table 8**. The Dalsnes 12mL was done in a small-scale EPH to observe which of the proteases showed similar activity aimed at RRM from poultry and had the highest selectivity against myofibrillary proteins or collagen, and according to Dalsnes (107), Bromelain, and Endocut-02 were more interesting than the other proteases. PCA of the proteases enzymatic reaction yield (ER %) combined with their M_W profiles and the structural information obtained from FTIR, showed that Endocut-02 was predominant when it came to tendons and bones. At the same time, Bromelain was more selective towards muscle and MDPR and less selective to tendons and bones. However, when Dalsnes was studying the reactions at different time points and in more substantial volumes in a follow-up experiment on a larger scale (Dalsnes 40mL), Bromelain appeared to be the better protease regarding digestion of tendons and muscle. Endocut-02 showed better digestion of the more complex RRM, such as MDPR and artificial MDPR in the same experiment (107). In the second step during the Dalsnes 12mL, samples were collected at time points (t) t = 15, 30, 60, and 180 minutes. Little change concerning both the ER % and the peptides structural changes between 60 and 180 minutes was found (107), and based on that, the maximum hydrolysis time in the lab-scale EPH reactions in the present study was chosen to be 60 minutes. Also, even though the optimal hydrolysis time to obtain the highest yield is raw-material specific (125), according to Nchienzia et al., most of the dissociation of peptides happens within the first hour of hydrolysis (30).

To sum up; proteases could be used in tailored EPH towards different substrates in complex materials. Better utilization of RRM could be achieved by using customized proteases to release more of the proteins, resulting in an increased yield and a broad range of proteins and protein derivatives.

4.2 Enzymatic protein hydrolysis in small- and lab-scale experiments

The main aim of the present study was optimization of the EPH process to obtain higher protein yield and sufficient information regarding the peptide composition in the hydrolysate products of such quality that it could be used for further research in the Notably project and, perhaps, in industrial applications later. Hence, a single- and multi-step cascade in which proteases selective towards myofibrillar proteins and collagen was used to extract a wide range of peptides of different sizes and characteristics and provide a high protein yield.

4.2.1 Verification of the small-scale selectivity screening experiment

To verify the Dalsnes 12mL experiments a duplicate of the small-scale EPH was performed at 60 minutes using Bromelain and Endocut-02. New batches of RRM were obtained from Nortura, making it difficult to achieve the same ER % even if the same settings in the protocol (**Appendix 7.2.1**) was followed. Thus, the focus was to find whether the proteases showed similar degradation patterns in the FTIR spectra and SEC chromatograms after hydrolysis — concerning the proteases selectivity towards myofibrillar proteins and collagen. Various materials from Nortura were used because it would make the study more industrially representative. The batches from Nortura contained a mixture of the poultry of different sizes, gender, and ages. As mentioned in section **2.3.1**, several studies have investigated how biological factors could impact protein composition and structure both before and after the slaughter (21, 63, 64, 126-128).

Three replicates of the raw materials used (tendons, CF, MDPR, and artificial MDPR), were dried to determine the water content in each material. As shown in **Table 9**, the water content also matched the materials water content obtained from ALS laboratory (marked in grey), where RMA of larger quantities was carried out. The extended RMA by ALS laboratory with information about the raw material composition in the present study are given in **Table 22**, **Appendix 7.3**. Unfortunately, no RMA was performed on the materials from the preliminary study to compare the two separate batches.

Table 9. $\overline{X}$ water content (%) in all the raw materials, dried in small amounts, and the water content obtained by the ALS laboratory where larger quantities were analyzed (marked in grey).

Material	$\overline{X}$ water content (%)	$\overline{X}$ water content (%)
Tendons	58	59
Meat	75	74
MDPR	59	59
Artificial MDPR	66	66

As mentioned in section **2.2** and **2.4.3**, Hyp is primarily found in collagen and elastin-rich tissues and can be used to measure collagen content in a sample (25, 82). In 1950 Neuman, R.E. et al. determined the collagen content in various tissues based on the Hyp content in dried samples. A collagen conversion factor of 7.46, providing results within an uncertainty of ± 0.24 %, was developed through their study. In greater detail, Neuman, R.E. et al. found that the overall Hyp content in collagen was 13.4 ± 0.24 % (129). Other similar conversion factors have been found to convert the Hyp content in tissue into collagen content in hydrolysates (130), but the conversion factor determined by Neuman, R.E. et al. was used in the present study (129). Since the RMA from the ALS laboratory provided both protein content (g/100g material) and Hyp content (g/100g material) (marked in grey), the proportion of collagen (%) in the protein could be calculated for all materials using **Equation 2).** The results are shown in **Table 10**. Of the 30.9 g of protein found in 100 g of tendons, 73.6 % of the protein consisted of collagen. For MDPR, 38 % of the protein consisted of collagen, while the collagen content in CF only was 1.8 % of the protein.

Table 10. Protein (g/100g material) and Hyp % (marked in grey) from the RMA by the ALS laboratory. The proportion of collagen (%) in the protein were calculated for all the materials used in the present study.

Material	Protein (g/100g)	Hyp (g/100g)	Hyp (%)	Collagen (%)
Tendons	30.9	3.05	9.87	73.6
MDPR	20.0	1.02	5.09	38.0
Chicken fillet	22.4	0.06	0.25	1.8

$$Collagen(\%)\ in\ protein\ composition = \left(\left(\frac{g\ Hyp}{g\ protein}\right) * 100\%\right) * \left(\left(\frac{1}{13.4}\right) * 100\right) \quad \textbf{2)}$$

Table 11 shows the ER % (the yield with added enzymes) and the background reaction (B.rx %) for both Dalsnes 12mL (marked in grey) and the present verification. The ER % was calculated from the remaining sediment after the separation of the small-scale hydrolysate solutions. Meaning, the amount of solubilized proteins and peptides in the liquid phase after the EPH. **Equations 3-6** were used for these calculations, by Dalsnes (107). As shown in **Table 11**, the activity of the two proteases, aimed at the different substrates from the RRM, was quite different from the experiments performed by Dalsnes (107). The B.rx (%), which consists of the reaction without added protease, was much lower than in the earlier experiments. This is probably caused by the variaton in the RRM from the second batch obtained from Nortura, with more thick tendons, more skin, bones, and less meat. Only one of the data was close to the results in Dalsnes 12mL if seen relative to the other materials, where a higher yield was determined from MDPR treated with Endocut-02, compared to the treatment with Bromelain.

Table 11. The B. rx % and ER % in percent of solubilized raw material, for both the Dalsnes 12mL (marked in grey) and the present verification, calculated from the remaining sediment after the small-scale EPH reactions treated with Endocut-02 and Bromelain.

Material	B. rx %	B. rx %	ER % Endocut-02	ER % Endocut-02	ER % Bromelain	ER % Bromelain
Tendons	4.2	22	21	23	28	25
Meat	9.3	18	-3.6	15	19	37
Artificial MDPR	6.1	18	26	10	34	1.1
MDPR	6.8	3.9	23	33	18	34

$$Sample\ weight\ (dry)(mg) = Sample\ weight\ (wet)(mg) * \left(1 - \frac{Water\ content\ (\%)}{100\ \%}\right) \quad \textbf{Eq. 3)}$$

$$Background\ rx\ (\%) = \left(1 - \frac{Zero\ sample\ (dry)(mg)}{Sample\ weight\ (dry)(mg)}\right) * 100\ \% \quad \textbf{Eq. 4)}$$

$$Total\ yield\ (\%) = \left(1 - \frac{Weight\ after\ hydrolysis\ (dry)(mg)}{Sample\ weight\ (dry)(mg)}\right) * 100\ \% \quad \textbf{Eq. 5)}$$

$$Yield/Enzymatic\ rx\ (ER)(\%) = Total\ yield\ (\%) - Background\ rx\ (\%) \quad \textbf{Eq. 6)}$$

As shown in **Table 11**, the verification provided lower ER % from the materials with higher meat content than that of Dalsnes (107). The muscle meat used in Dalsnes 12mL and Dalsnes 40mL derived from the poultry carcass, where the meat was scraped from the bones and tendons. The meat used during the present verification was of pure chicken fillet, similar to the ones that can be bought in the supermarket. The difference between these types of muscle meat could be one reason for the variations in the yield from the two studies. The composition of proteins, salts, and other water-soluble components in the CF and carcass-muscle was probably very different. The abundance of endogenous enzymes in meat-based residues could have led to protein solubilization and contributed to the high ER % in Dalsnes's 12mL (125). In the present study, several analytical tools, such as the RMA, the Dumas combustion analysis, and the DH%, were used to calculate the protein yield. Calculations of the ER % based on the sediment, as done during the preliminary study in the Dalsnes 12mL and Dalsnes 40mL, did not provide an accurate yield from the hydrolysates. The analytical techniques mentioned above were used to calculate the protein yield % of the hydrolysates in the present study, which was more accurate than the ER % and hence provided more relevant measurement values for the industry. Not everything released into the water phase is proteins, peptides, and free amino acids. Other water-soluble components, e.g., salts and minerals, are being released into the liquid phase along with the proteins and protein derivatives (131).

More knowledge regarding the protein- and peptide composition in the hydrolysate products is essential for the industries to differentiate the products before further applications. In that regard, methods such as HP-SEC and FTIR are useful tools for obtaining information about the

peptide-size distribution and provide structural information that can reveal the inequalities of the various peptides.

4.2.1.1 High performance size-exclusion chromatography – mass average molar mass distribution analysis of the small-scale hydrolysates from the verification

HP-SEC was used to determine the M_W of the protein hydrolysates from various materials treated with the two proteases, Endocut-02 and Bromelain. SEC has proven to be a suitable technique for measuring the extent of hydrolysis and characterization of the peptide composition in protein hydrolysates. The peptide composition influences the functional qualities and usability of hydrolysates. For instance, reduced protein/peptide size is considered to reduce allergenicity risks and increase the safety associated with protein-transmitted diseases (125). All the hydrolysates from the verification of Dalsnes 12mL were analyzed by HP-SEC, eight small-scale EPH products in duplicate, a total of 16 hydrolysate samples. The analyses were done to see if the hydrolysates from Dalsnes 12mL and the verification experiments showed structural similarities and M_W profiles.

4.2.1.2 Optimization – collagen-rich hydrolysate analysis

Before the hydrolysates could be analyzed by HP-SEC, a sample preparation method of collagen-rich hydrolysates had to be optimized, as illustrated in **Figure 18**. Collagen-rich materials from poultry formed gels at temperatures between 25-30 ^oC, even highly diluted samples, which were probably caused by larger peptides and the low-temperature extraction. The gel viscosity was dependent on the peptide concentration and the size of the peptides in the hydrolysates. Peptides larger than 200 kDa contributes to gel formation, and even at low concentrations, cross-links could be formed. According to Kempka, A. P. et al., gelatin extracted at lower temperatures is more rigid and less water-soluble. Also, amino acid residues are united through covalent peptide bonds with side chains varying in structure, size, and electrical charge, influencing the solubility of the amino acids in water (29). Since most samples to be analyzed derived from collagen-rich materials, known to form gelatin, there was a great possibility that an SEC column would be clogged if these samples were injected into the system. In earlier studies and during the Dalsnes 12mL and 40mL, the hydrolysates were injected directly after filtration or after being resolved in water and collagen-rich hydrolysates could thus not be analyzed by SEC.

Since minimal amounts of acid are enough to solve gelatin (28), the samples could be resolved in the mobile phase, which contained 0.05 % TFA. There was a risk that protein precipitation could occur since the mobile phase also contained 30 % ACN. However, a small test to investigate if this was the case in the present settings was performed. The samples solubilized in the mobile phase were still transparent after 24 hours in the refrigerator and no pellet was formed after centrifugation. With that in mind, all the gelatin-rich samples were analyzed by SEC without the risk of damaging the column.

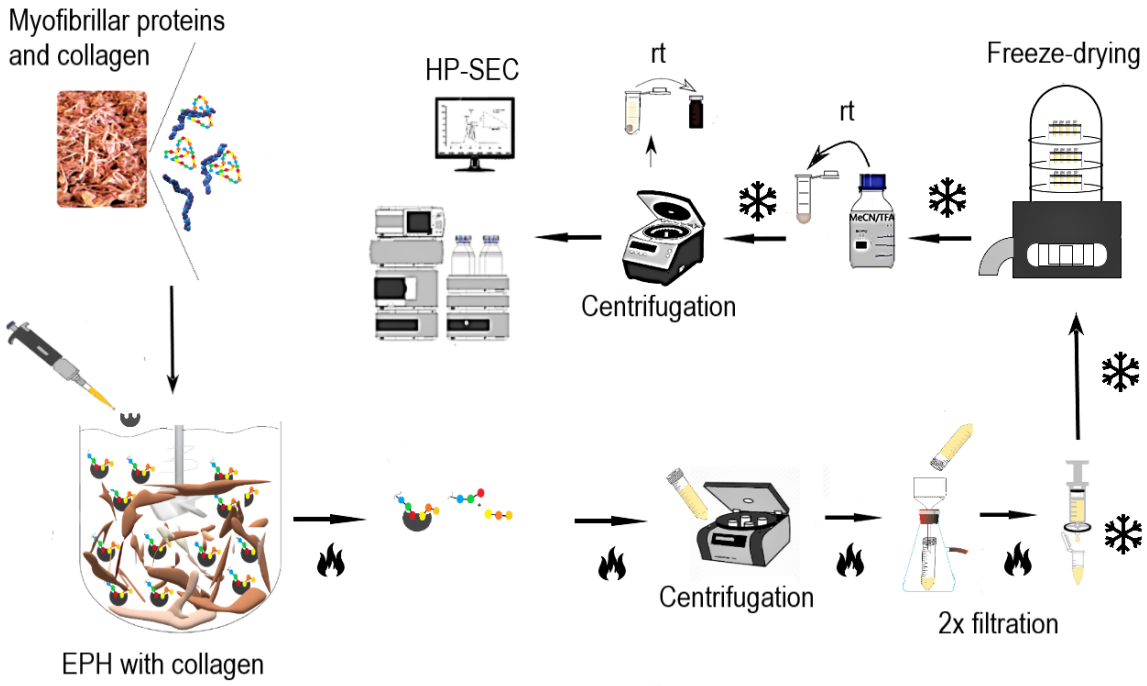

Figure 18. Overview of the sample preparation method with the necessary steps needed for determining the M_W of collagen-rich hydrolysates using HP-SEC. The symbols are indicating either heated or cooled sample preparation step.

4.2.1.3 High performance size-exclusion chromatography – small-scale EPH analysis

After optimizing the sample preparation method for collagen-rich samples, all the hydrolysate products from the small-scale EPH were analyzed by HP-SEC, and the chromatogram in **Figure 19** shows the retention time (t_R) of the peptides formed during the verification of Dalsnes 12mL. The fractions marked in the chromatogram (F1-F4), were sliced in separate fractions based on

the peptides Mw. The peptide size distributions in the fractions were set based on the approximate Mw range of the calibration solutions seen in **Table 12**. Although the retention time usually corresponds with the peptide's size, two of the calibration solutions used in the present study proved this wrong. While renin substrate tetradecapeptide porcine (1759 g/mol) had a retention time of 7.54 min., insulin chain B oxidized from bovine pancreas (3496 g/mol) eluted at 7.83 min. The hydrodynamic volume determines the compounds' retention time, which uncertainty should be in mind when doing protein analysis with HP-SEC.

Table 12. Peptide fractions 1 to 4 based on the corresponding size calibration solutions. The fractions are set based on the retention time of the size calibration solutions, with their approximate M_W.

Fraction	Time span (min)	Approximate M_W	Calibration solution range (based on their t_R)
F1	5.00-6.62	66000 - 6511	From bovine serum albumin to aprotinin from bovine lung
F2	6.62-7.83	6511 - 3496	From aprotinin from bovine lung to insulin Chain B Oxidized from bovine pancreas
F3	7.83-8.64	3496 - 204	From insulin Chain B Oxidized from bovine pancreas to L-tryptophan
F4	8.64-20.00	204 ≤ 0	L-tryptophan ≤ Free amino acids

As shown in **Figure 19**, there was a wide variation in the SEC chromatogram based on which material and protease that were used in the EPH. The distinct large peak in the front in F1 detected at the beginning of the analysis came from the fact that concentrated large-sized peptides were eluted first. In the small-scale EPH from the verification of Dalsnes 12mL, all samples were introduced to heat treatment with the materials still in the solution. As previously mentioned, that would trigger a heat-induced release of larger collagen-derived components. It was mainly in collagen-rich materials treated with Endocut-02 that a large peak in the front was observed. The collagen-rich materials treated with Bromelain also caused a large peak in the front by eluting larger peptides at the beginning of the run but not to the extent provided by the samples treated with Endocut-02. As viewed in the chromatogram, the composition of smaller peptides in F4 mostly came from the Bromelain-treated materials, and especially CF treated with Bromelain provided peptides in this fraction. **Figure 20** shows very clearly that Endocut-

02 primarily contributed to peptides in the F1-F3 fractions, while Bromelain provided most peptides within fractions F4-F2. However, the patterns were also material dependent, and the collagen-rich materials contributed to F1 even though they were treated with Bromelain.

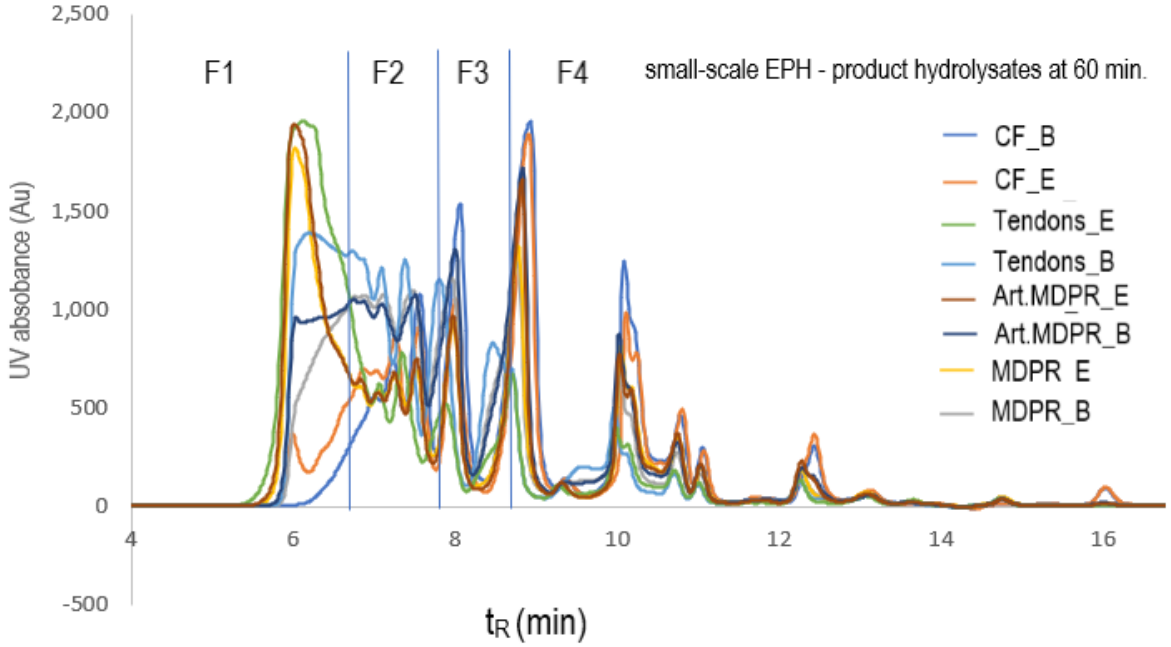

Figure 19. Chromatograms of the small-scaled EPH from the preliminary study's verification with the retention time in minutes (t_R) on the x-axis and the UV-absorbance on the y-axis. The chromatograms are divided into fractions, F1-F4, from large to small compounds, respectively. Abbreviations: Art.MDPR: Meat+tendons (50/50), B) Bromelain, and E: Endocut-02.

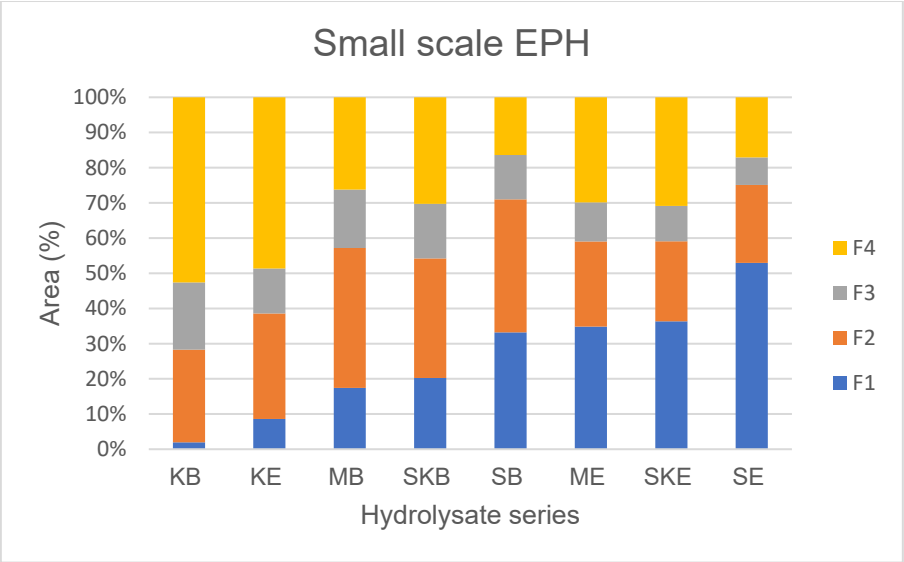

Figure 20. A bar chart of the area % versus hydrolysates from the verification of the small-scale EPH. The area below the peaks for each fraction in the chromatograms represents the amount of peptides in that respective fraction from the different hydrolysate series. The series are abbreviated as in **Figure 18**.

4.2.1.4 Fourier-transform infrared spectroscopy – structural characterization of the small-scale hydrolysates from the verification

FTIR was a useful tool for following protein degradation during the EPH process. The information obtained from the FTIR analysis can reveal both the chemical composition and the structure of the proteins (1). FTIR was therefore used as a complementary method to SEC, SDS-PAGE, DH%, and Hyp analysis to fill in with additional information of the hydrolysate products. However, the complexity of the materials made it challenging to apply the correct film thickness and concentration on the 96 well plates. This affected the quality of some of the spectra, such as the collagen-rich hydrolysates where the concentration of peptides varied considerably. Nevertheless, despite the concentration challenges, characteristic bond vibrations could be observed. The inequalities could be seen primarily by differences in the amide regions at ~1650 cm^{-1} and ~1550 cm^{-1}. PCA was conducted to all FTIR analyses to study variations and groupings within the data sets during hydrolysis time.

Fourier-transform infrared spectroscopy – small-scale enzymatic protein hydrolysis analysis

All hydrolysates from the verification of Dalsnes 12mL (107) were analyzed by FTIR. This was done to see if there were structural similarities between the hydrolysates from Dalsnes 12mL and the verification experiments. Although the ER % from Dalsnes 12mL and the verification experiments was quite different, the FTIR analyses showed many of the same patterns. The samples were prepared with the same conditions to achieve similar values and degradation patterns of the different products when treated with Bromelain and Endocut-02. In greater detail, that means that the same amount of material was used, the same protease concentration was added, the hydrolysate solutions held the same temperature and pH, and all of the hydrolysate products were collected after the 60 minutes. The only difference was that the duplicated EPH experiments were performed on different days. Due to the concentration differences in the hydrolysate products the intensity of the measured products could not be used to compare differences between hydrolysates in the raw spectra. The raw spectra from the small-scale EPH can be found in **Appendix 7.7** (Figure 55). The pure tendons hydrolysates had to be diluted extensively, while the samples containing CF treated with Bromelain had to be applied to the plate undiluted. The diluted samples with tendons also began crawling towards the center or edges of the well, as shown in **Figure 21**. An unevenly dried sample provided bad quality spectra, which was a problem throughout the study.

Figur 21. The collagen-rich samples crawling towards the center or edge of the 96 well plate.

Nevertheless, the raw spectra showed the same characteristic bond vibrations of collagen in the amide I region, with two distinct bands at ~1650 and ~1520 cm^{-1}, as in the Dalsnes 12mL and 40mL (107). The CF samples had one distinct stretch at 1650 cm^{-1}, which straightened out towards the ~1520 cm^{-1} region, which also could be seen in the normalized second derivative spectra in **Figure 22**. PCA was used to display the variations of the two proteases in degrading the poultry RRM materials. The PCA score plot in **Figure 23,** A) revealed that PC-1 held 61 % of the dataset variations and that 18 % came from PC-2. The loading in **Figure 23,** B) showed that the main variance was in the amide I and II regions at ~1650 cm^{-1} and ~1550 cm^{-1}, respectively, and in the -COO^- symmetric stretch region at ~1400 cm^{-1}.

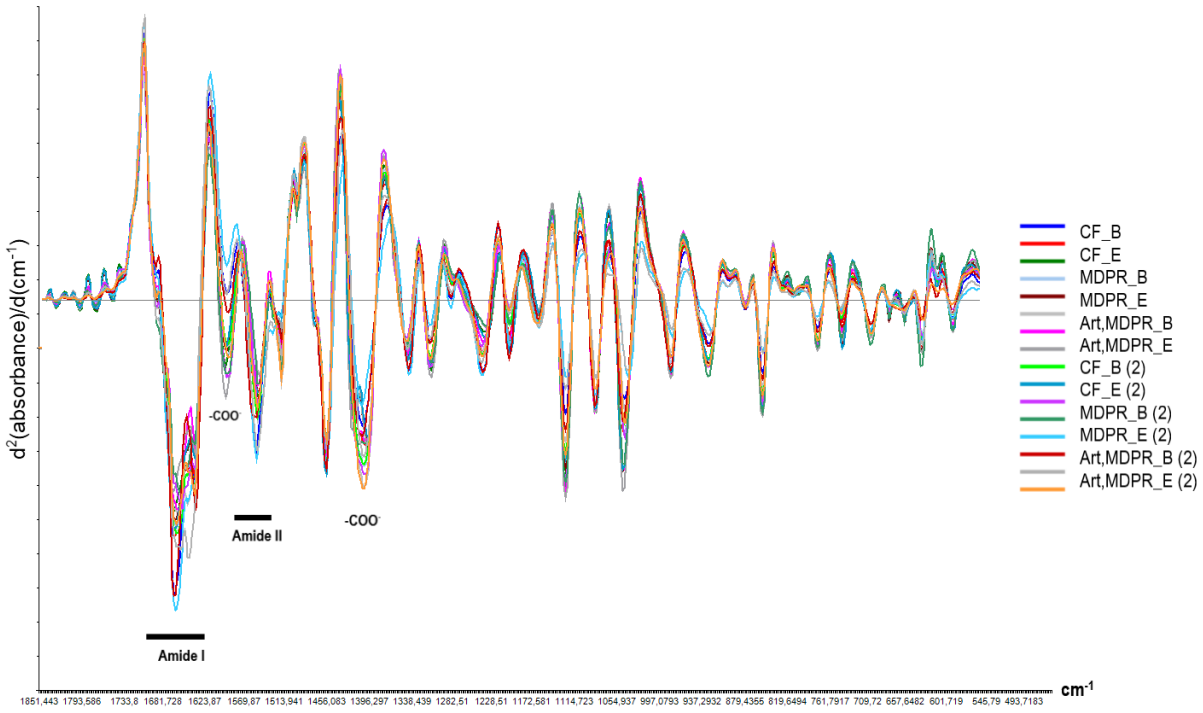

Figure 22. Second derivative and normalization with SNV FTIR spectrum of the duplicated small-scale EPH where the materials were treated with Bromelain or Endocut-02. Abbreviations: Art.MDPR: Meat+tendons (50/50), _B) Bromelain, _E: Endocut-02, and (2): duplicate.

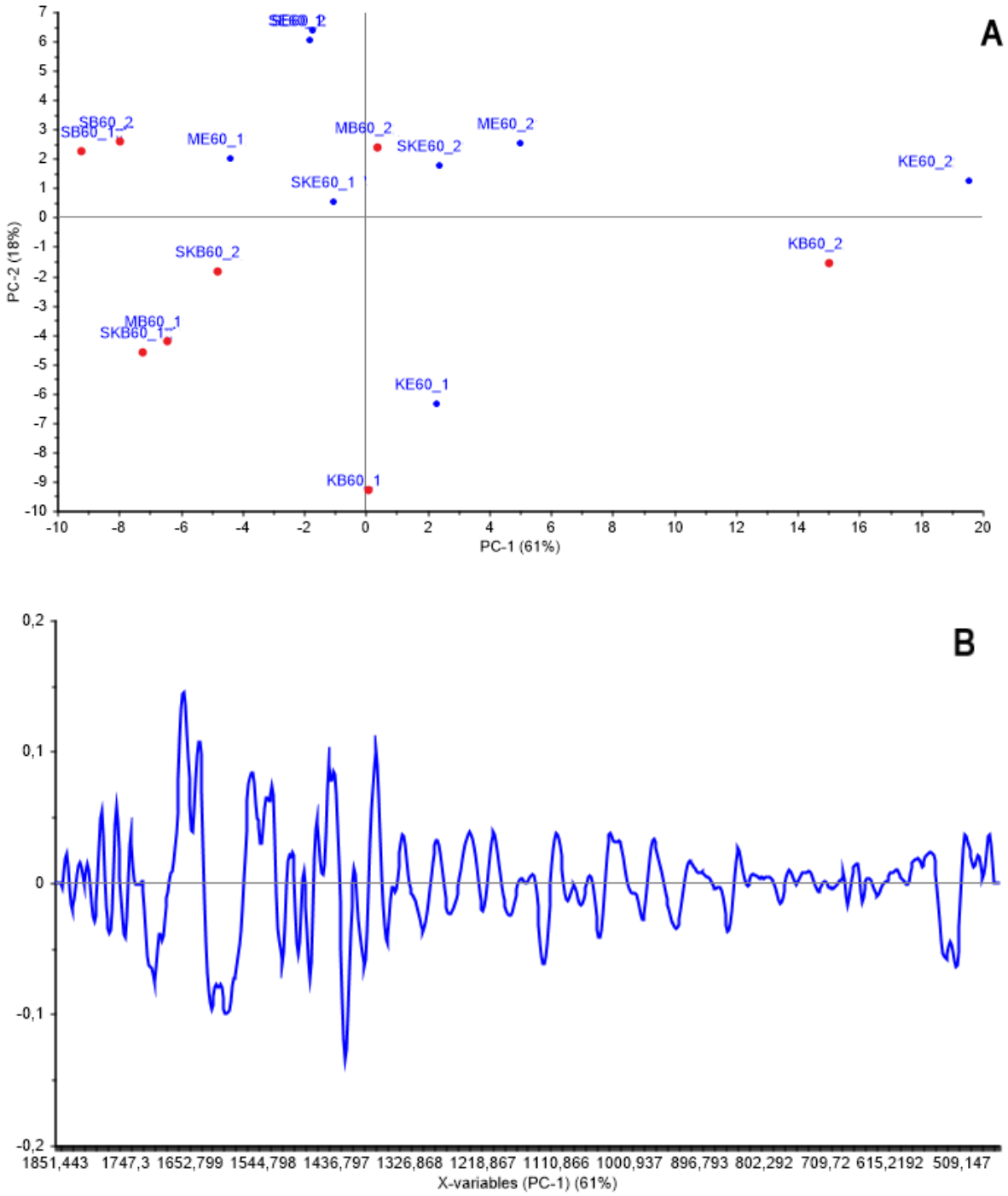

Figure 23. A) The score plot shows the groupings of the different samples, and B) loadings are showing the main variation in the spectra, with 61 %. PCA plot of the FTIR data for the duplicated small-scaled EPH reactions where Bromelain (marked in red) and Endocut-02 were added to the materials, CF, tendons, MDPR, and Art. MDPR.

The score plot to the left in A) showed that tendons treated with Endocut-02 and Bromelain from the duplicated reactions both ended up in about the same area. The fact that hydrolysates with artificial MDPR (tendons+CF) and MDPR ended up somewhere in between was expected.

However, the CF samples from the first and second reactions were quite spread, which was somewhat surprising since the meat was relatively homogenous. However, it has been observed that the rapid degradation of myofibrillar proteins happened from the reaction start, which probably has contributed to the uneven grouping in the PCA plot. These groupings would likely have become more and more related if the hydrolysis time had been sufficiently extended. Tendons, on the other hand, have shown to require high heat-treatment to release the peptides, where the large peptides have tended to be very similar. The characteristic structure of collagen helices would naturally be more intact with an increasing number of amino acids. Both the PC-1 and PC-2 scores clearly showed that the most considerable variation was between tendons and CF regardless of which protease was used, but that the most significant difference was between CF treated with Endocut-02 versus tendons treated with Bromelain.

To sum up; the small-scale EPH verification resulted in an ER % different than of Dalsnes 12mL and Dalsnes 40mL. The different batches of RRM from Nortura and the complexity of poultry RRM were probably the largest contributor to the variation in ER %. The materials B.rx % turned out to be a significant influencing factor in the resulting ER %. A combination of FTIR and HP-SEC gave a good indication of the peptide composition in the hydrolysate products. In the FTIR spectra and SEC chromatograms, many of the same patterns were observed in Dalsnes 12mL and the present study regarding the hydrolysate composition in the various RRM. Structural differences between especially tendons and CF materials were observed in the FTIR spectra. The peptide-size distribution from HP-SEC indicated that the collagen-rich hydrolysates provided large peaks in the front of the chromatograms, contributing to a large-sized peptide composition in F1.

4.2.2 Scaling up the enzymatic protein hydrolysis to lab-scale

4.2.2.1 Raw material analysis

RMA was carried out to obtain knowledge of the composition of the various materials in the poultry RRM used during the present study, as presented in **Table 13**. The Hyp content is related to the amount of collagen in the measured materials because Hyp almost exclusively exists in collagen and elastin. The amount of ash refers to the inorganic residue remaining after ignition or complete oxidation of organic matter, revealing the amount of inorganic elements in the raw materials and are often more eminent in bone-rich RRM. The fat content is one of the vital quality control parameters in the production of feed and food (1). Still, in the present study, the focus has been on proteins and protein-derivatives. Hence, the protein content obtained from

the RMA was the most important parameter and was used in the calculations of the protein yield % in the hydrolysates. The water content was used to determine the weight yield in the small- and lab-scale EPH, and the collagen content in the materials was calculated using the resulting Hyp content.

Table 13. RMA of the different materials in the poultry RRM, with the determined Hyp content (g/100g), ash (g/100g), water (g/100g), protein (g/100g), and fat content (g/100g) and the techniques used in the measurements with measurement uncertainty (MU) The analyses were done by ALS Laboratories UK (69).

Element	Unit	CF	Tendons	MDPR	Analysis technique	MU %
Hydroksyproline	g/100g	0.1	3.1	1.0	Spectrophotometric	17
Ash	g/100g	1.2	5.1	1.8	Gravimetric	6.5
Water content	g/100g	74	59	59	Gravimetric	1.1
Protein	g/100g	22	31	20	Dumas	2.0
Fat	g/100g	2.6	4.6	20	Pulsating NMR	6.5

4.2.2.2 Lab-scale enzymatic protein hydrolysis

In the Dalsnes 12mL and 40mL (107) experiments, the proteases showed different selectivity in targeting the various materials as opposed to when the EPH was performed in the lab-scale reactor.

The optimized EPH process in the present study was scaled-up to a lab-scale hydrolysis reactor, with the amount of substrate increased from 2.000 g to 333.0 g to approach an industrial scale. The reactor with a propeller could hold a larger volume and gave a better stirring of the materials, which made the substrate more accessible to the proteases. In theory, this should lead to a better degradation of the proteins and thus provide a higher yield. During the Dalsnes study, a scale-up experiment was carried out using 40 g material in a screw cap bottle using a magnetic stirrer (Dalsnes 40mL). Even though Dalsnes 40mL also provided an inadequate stirring of the material, it resulted in a higher yield than in Dalsnes 12mL (107).

The protein yield % in the present study was calculated using the **Equations 7-9** and can be found in **Table 14**. Nitrogen content obtained from the Dumas analysis and the nitrogen content in the raw material provided by the ALS laboratory, both converted to protein content using the

protein conversion factor of 6.25, were included. The ER % from the hydrolysates in the present study were also calculated, marked in grey. This was done to compare the ER % with the protein yield %. The differences between the ER % and the protein yield % were determined by comparing the values and reporting the difference in the percentage of deviation. The resulting ER % was higher for materials with high meat content, such as the muscle meat and MDPR, than the resulting protein yield %, as also shown in **Table 9,** section **4.2.1.** The combined ER % from the verification and the scaled-up EPH showed that more of the protein, peptides, and other water-soluble compounds were solubilized into the liquid phase from the meat-based materials. However, the Dumas measurements revealed that the collagen-rich hydrolysates contained slightly higher amounts of protein than the hydrolysates containing primarily myofibrillar proteins, as seen in **Appendix 7.4.1** (Table 23-29). Thus, more salts, minerals, and other water-soluble components were released from the meat-based materials into the liquid phase along with the proteins, peptides, and free amino acids, providing a negative percentage deviation for CF and MDPR. This means that the calculation approach in the present study was more accurate considering the hydrolysates yield and that a combination of different methods was necessary to obtain this information. For all the EPH reactions in the present study, Bromelain proved to be the most efficient protease providing the highest ER % and average protein yield %. In Dalsnes 40mL (107), Endocut-02 had provided a slightly higher ER % for MDPR and artificial MDPR. However, the ER % and protein yield % presented in **Table 14** showed the opposite.

Table 14. Protein yield from the lab-scale reactions in which the materials were treated with either Endocut-02 or Bromelain. The calculated ER % and protein yield % from the hydrolysates, with the percentage of deviation to compare the two calculation approaches within the same EPH reactions. The % RSD are included for the calculated protein yield within each duplicated series.

Endocut-02	n	ER (%)	Protein yield (%)	Deviation (%)	% RSD protein yield (%)
CF	2	38.5	36.7	-4.7	6.2
Tendons	2	34.4	40.1	14	10
Artificial MDPR	2	36.1	38	5	5.5
MDPR	2	54.1	52.6	-2.8	2.8
Bromelain	2	ER (%)	Protein yield (%)	Deviation (%)	% RSD protein yield (%)
CF	2	49.6	48.4	-2.4	7.9
Tendons	2	42.3	53.9	22	8.7
Artificial MDPR	2	34.8	51.1	32	5.8
MDPR	2	55.3	55.1	-0.4	2.7

$$\frac{Hydrolysate\ (g)}{Residual\ raw\ material\ (g)} = \frac{\left(\frac{Freeze-dried\ water\ phase\ (g)}{Water\ phase\ (g)}\right) * Total\ water\ phase\ (g)}{Residual\ raw\ material\ (g)} \quad \textbf{Eq. 7)}$$

$$\frac{Protein\ (g)}{Residual\ raw\ material\ (g)} = \frac{\left(\frac{Hydrolysate\ (g)}{Residual\ raw\ material\ (g)}\right) * Protein\ (\%)\ from\ Dumas}{100\ (\%)} \quad \textbf{Eq. 8)}$$

$$Yield\ \% = \left(\frac{\left(\frac{Protein\ (g)}{Residual\ raw\ material\ (g)}\right)}{\left(\frac{Protein\ (g)}{Residual\ raw\ material\ (g)\ from\ ALS}\right)}\right) * 100\ \% \quad \textbf{Eq. 9)}$$

Hydrolysates from the EPH with MDPR did not provide a significant difference in protein yield % by using Bromelain or Endocut-02, with an average protein yield of 55.1 % versus 52.6 %. Artificial MDPR had a more considerable difference, with 51.1 % for Bromelain and 38.0 % for Endocut-02. Tendons and CF showed the same trend, where Bromelain yielded 53.9 % and 48.4 %, respectively, against Endocut-02 with 40.1 % and 36.7 %. However, the relative standard deviation (% RSD) revealed a large spread within the duplicated series, and thus, no major differences in protein yield % could be concluded by using either Bromelain or Endocut-

02. Nevertheless, the lab-scale EPH in the present study provided higher overall yields than the Dalsnes 40mL, which also was expected due to the challenges of optimizing EPH reactions in a screw cap bottle. Also, if both studies' experiments were performed with the same conditions except for the two different batches of RRM, the variation of materials could probably contribute to many of the observed differences.

4.2.2.3 Optimization of the lab-scale enzymatic protein hydrolysis

Due to an unpredictable stirring of the materials during the scale-up of EPH, an optimization of the lab-scale reactor hydrolysis was performed. As shown in **Figure 24**, the lab-scale EPH reaction was optimized. By decreasing the amount of materials and increasing the amount of liquid, raising the propeller, and increasing the protease concentration, this led to a more available substrate. Also, an increased protease concentration helped solubilize the materials at an earlier stage during the hydrolysis, which further prevented the materials from wrapping around the propeller.

Better stirring has been necessary for the protease to access the materials. When the EPH was scaled-up from 2 g to 333 g substrate in the lab-scale reactions, that would theoretically make the substrate more accessible to the proteases because a higher volume with more space would lead to better stirring, where more of the peptides could be released. However, even if the materials were minced thoroughly before the experiments, there were some difficulties with the stirring in the EPH experiments with tendons. The tendons quickly accumulated around the propeller from the experimental start, resulting in some substrate becoming inaccessible to the proteases. Hence, the proteins, and peptides could presumably not be released to the extent that if completely dissolved. Adjusting the substrate amount down from 333 g to 250 g, raising the propeller in the reactor, and increasing the stirring rate from 280 to 300 rpm became the solution for this problem. Also, increasing the enzyme concentration 2.5 times, aiming at having the materials more degraded at an earlier stage in the reaction, could prevent the build-up of the densely packed materials around the propeller.

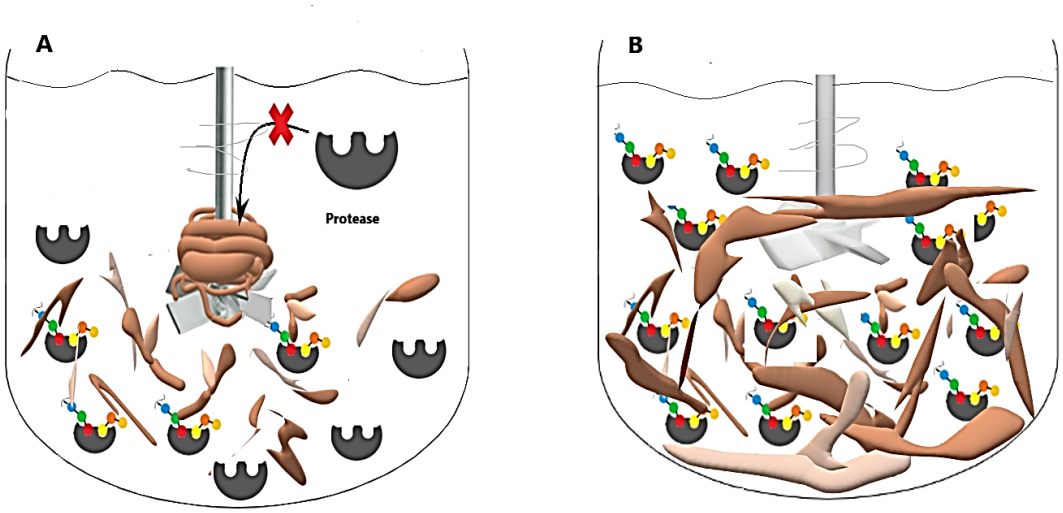

Figure 24. The reactors used in the lab-scale EPH with hydrolysate solutions including collagen-rich materials. A) Tightly packed material around the propeller makes the substrate inaccessible to the proteases and prevents them from performing the hydrolysis and releasing the proteins. B) When the reaction was optimized by a decreased amount of materials and increased amount of liquid, the propeller raised, and the protease concentration was increased, all substrate became available. An increased protease concentration helped solubilize the materials at an earlier stage during the hydrolysis, which further prevented the materials from wrapping around the propeller.

4.2.2.4 Lab-scale enzymatic protein hydrolysis – combining Endocut-02 and Bromelain

After the EPH process was scaled up to lab-scale and optimization of the initial lab-scale was performed, a combination of Endocut-02 and Bromelain was added to a second lab-scale reactor hydrolysis, in three different orders.

Since MDPR was the material that would eventually be used on an industrial scale, this RRM was used in the following where Bromelain and Endocut-02 were added to the same EPH reactions. During Dalsnes`s (107), the verification, and the lab-scale experiments, Bromelain and Endocut-02 were first investigated separately, and knowledge about their activity and selectivity towards myofibrillar proteins and collagen was obtained. In the last part of the present study, the two proteases were mixed in a 50/50 ratio to see how they worked together on the MDPR. Three different series, in duplicates, a total of six lab-scale EPH experiments were done using a total reaction time of 60 minutes. In the first series, called MBE, Endocut-02, and Bromelain was added from the experimental start. In the second series, called MB+E,

Bromelain was added first, followed by Endocut-02 after 30 minutes. At last, in the ME+B series, Endocut-02 was added 30 minutes before Bromelain. The protein yield % was calculated as in section **4.2.2** (Equation 7-9), and the protein yield % are shown in **Table 15** and **Figure 25**, along with the % RSD based on the variations *within* the three duplicated series. As presented in the table, there was a relatively large spread within the protein yields in the duplicated reactions, especially within the MBE and ME+B series.

Table 15. The protein yield % for the three series, the number of replicates (n), the average protein yield % of all six reactions, and % RSD *within* each series. MBE1(2): treated with 50/50 Endocut-02 and Bromelain from the experimental start, MB+E1(2): treated with Bromelain 30 minutes before Endocut-02 was added to the hydrolysis reaction, and ME+B1(2): treated with Endocut-02 30 minutes before Bromelain.

Series 1	Protein yield (%)	**Series 2**	Protein yield (%)	**Series 3**	Protein yield (%)
MBE1	60	MB+E1	68	ME+B1	76
MBE2	69	MB+E2	70	ME+B2	66
n	2		2		2
$\bar{X}$	64		69		71
% RSD	6.7		1.6		7.4

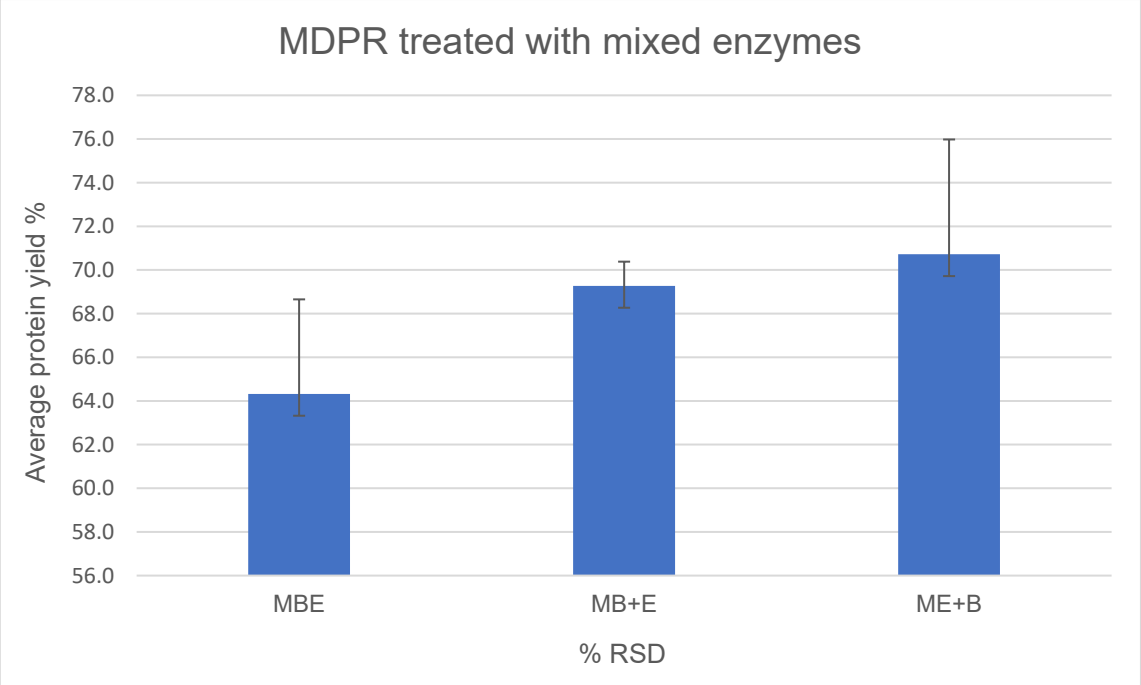

Figure 25. The calculated protein yield % of the six reactions with the % RSD within the three series.

The standard deviation (SD) *between* all three series were calculated, as presented in **Table 16**, including calculations from a student`s t-Test based on the protein yield % to see if there was a significant difference between the three ways of adding the proteases. An F-test followed by an unpaired one-tailed t-Test was done and can be seen in **Appendix 7.5.3** (Table 35-37). The bar chart in **Figure 26** shows the differences between the three series with the average protein yield %. The SD showed that the largest spread was between the MBE- and ME+B series. The least spread was observed between the ME+B- and MB+E series. However, the t-Tests showed no significant difference in the protein yield % between the three ways of adding the proteases, based upon the entire dataset. **Table 16** showed a relatively large spread between the protein yields *within* the duplicated series, especially within the MBE and ME+B series, which probably affected the t-Test values. Hence, the resulting t-Tests could have been more informative if a third lab-scale EPH of the series was done.

Table 16. Average protein yield % for the three series A) MBE treated with 50/50 Endocut-02, and Bromelain from the experimental start, B) MB+E treated with Bromelain 30 minutes before Endocut-02 was added to the hydrolysis reaction, and C) ME+B treated with Endocut-02 30 minutes before Bromelain. SD and P-values from the t-Tests between the three series are also given as A/B) MBE/MB+E, B/C) MB+E/ME+B, and A/C) MBE/ME+B.

Series	$\overline{X}$ Yield (%)	Series ratio	SD n = 2	From t-Test (*P*) *(P < 0.05)*
A: MBE	64.3	**A/B**	3.50	0.19
B: MB+E	69.3	**B/C**	1.03	0.22
C: ME+B	70.7	**A/C**	4.52	0.42

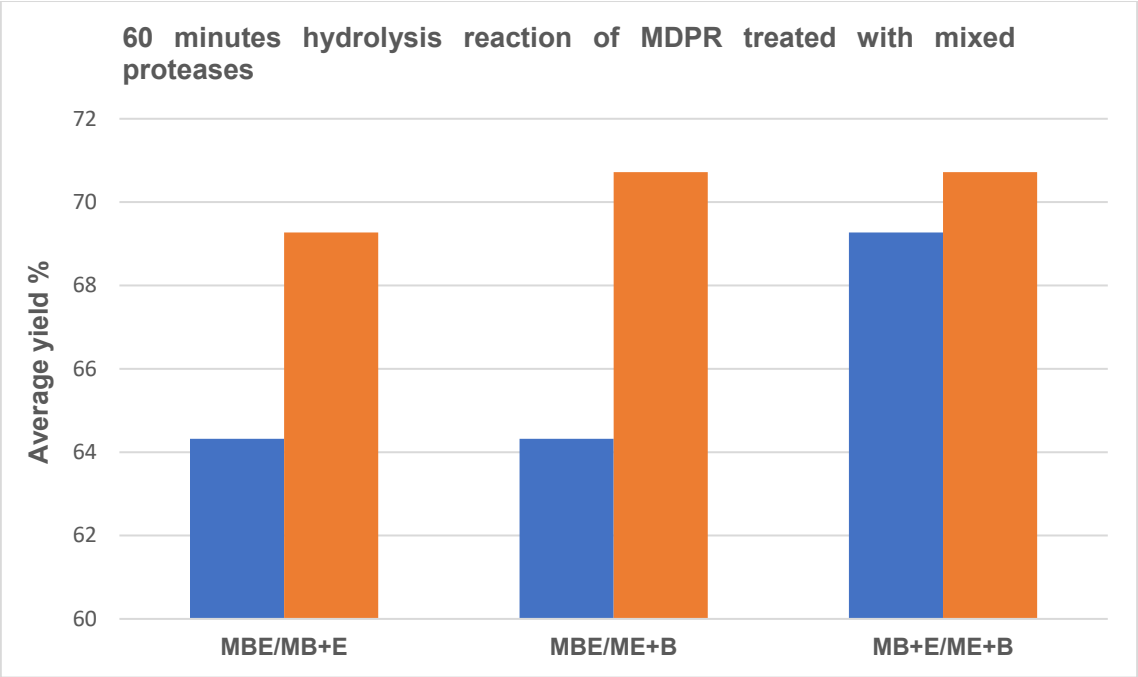

Figure 26. Bar chart showing the average protein yield % for the three series with the MDPR treated with mixed proteases, from the calculations given in **Table 16**.

It was expected that there would be a spread in the protein yield % *within* the same series. Although it has been mentioned earlier, most of the variations probably appeared due to the materials complexity. For many of the observed differences in-between the resulting ER % and protein yield % from the preliminary study (107) and the present lab-scale trial, the variety in the composition of the RRM and its origin could be a logical explanation. During the EPH reaction, the protein availability would give rise to specific peptides that directly affected the yield, dependent on the peptides' size.

Endogenous enzymes, such as cathepsins that are native proteases found in meat, could alter the peptide composition in the hydrolysates by interacting with the substrate as well as the proteases (125). According to the study by Xiong et al., these endogenous enzymes are involved in the postmortem degradation of myofibrillar proteins and have also shown activity against collagen (20). In one extreme case in the study of Lapeña et al., using salmon intestines, the reaction was carried out exclusively by endogenous enzymes, despite the addition of commercial enzymes, showing that the origin of the substrate and its composition are influencing the proteases and the hydrolysate products extensively (125). Aggregation of either the substrate or the products could alter the peptide structure and reduce the proteases' access

to the substrate or inhibit the proteases cleaving sites. Long, unfolded collagen peptides have a natural tendency to form aggregates (132). Product- and substrate-inhibition, autolysis, and thermal unfolding could, therefore, have affected the proteases activity during the EPH reaction (59).

4.2.3 Lab-scale enzymatic protein hydrolysis – optimization and its effects on the hydrolysate composition studied by analytical techniques

Several analytical techniques were used to obtain sufficient information about the protein hydrolysates during the small- and lab-scale EPH. A total of 294 hydrolysate samples have been prepared and analyzed using several instruments and methods. All the samples were analyzed using FTIR and SEC. DH% and Dumas were conducted on all protein hydrolysates from the lab-scale experiments. The RMA was performed by ALS laboratory on all the poultry RRM used during the study. Also, SDS-PAGE was used as an alternative to SEC, analyzing the peptide size distribution and observe differences in the protein degradation patterns when using the two proteases. **Figure 27** shows the analytical techniques that were used during the present study.

In the following, SDS-PAGE was used to study the peptide fragments in the hydrolysate products and to get an approximate identification of the proteins in the different RRM. HP-SEC could determine the size distribution of the proteins and peptides in the hydrolysate products. And in combination with the DH%, Dumas, and Hyp analyses, the correlation to the peptide sizes found in HP-SEC was used to reveal the degradation patterns of Endocut-02 and Bromelain towards myofibrillar protein and collagen. FTIR was used to fill in with information which the techniques mentioned above could not provide, such as information regarding changes in the secondary structure of hydrolysate products during hydrolysis time. Moreover, PCA displayed variations and groupings in the score plots and loadings that strengthened the information obtained by the classical analytical techniques.

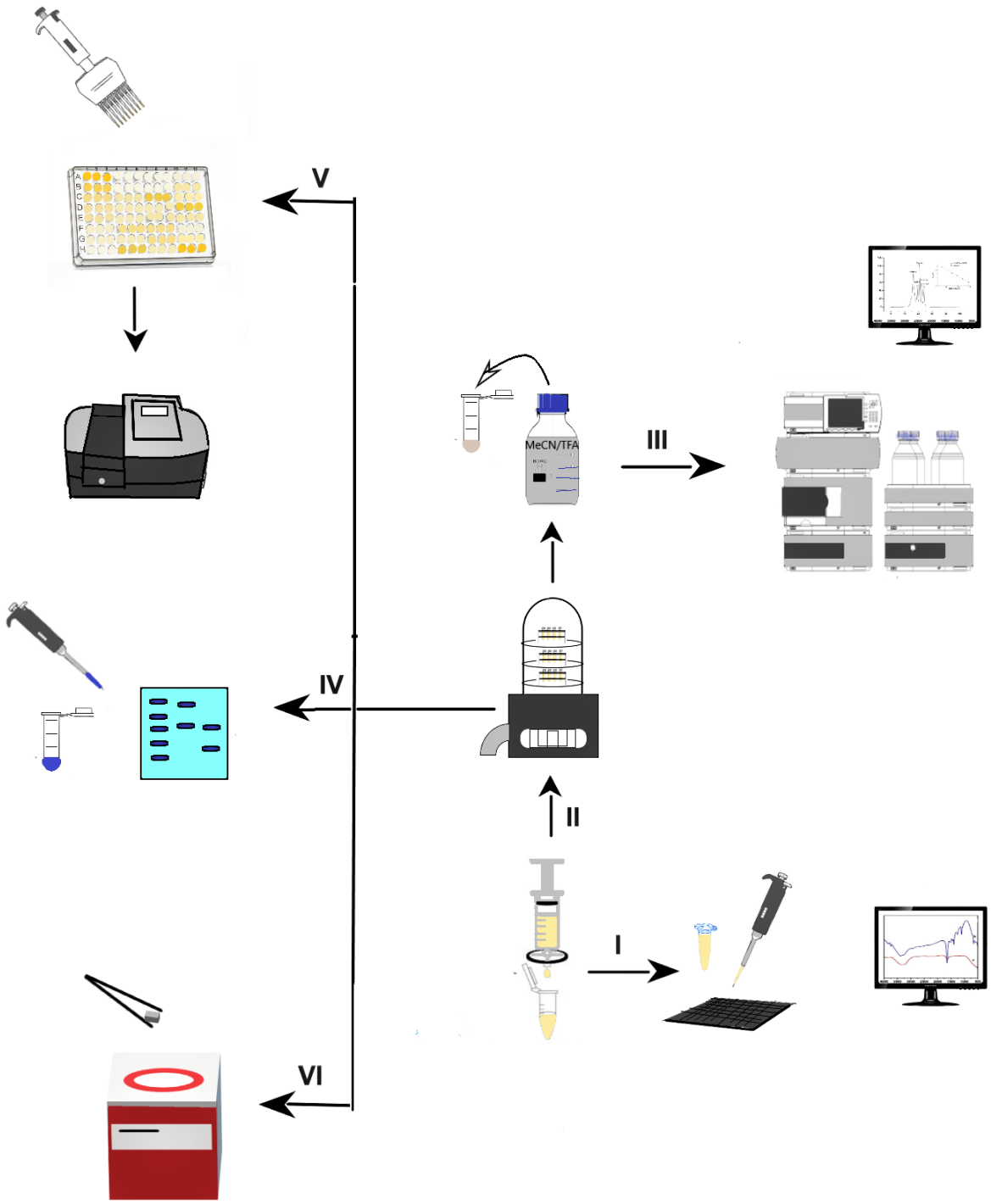

Figure 27. Overview of the analytical techniques that were used during the study. I: FTIR spectroscopy of the filtered hydrolysates, freeze-drying of the liquid phase was performed before either III: HP-SEC was performed after resolving in the mobile phase, or IV: powder was solved in sample buffer containing Coomassie blue and applied to SDS-PAGE, or V: DH%- or Hyo-assays analyzed with spectrophotometry, or lastly, was VI: packed in small aluminum trays with tweezer before Dumas combustion analysis. The figures of the small equipment were adapted from Lab-icons, 2020 (133).

4.2.3.1 Peptide fragments from myofibrillar proteins and collagen analyzed by Sodium dodecyl sulfate – polyacrylamide gel electrophoresis

SDS-PAGE was performed on the hydrolysate products from both the small- and lab-scale EPH to observe if there had been a degradation of myofibrillar proteins and collagen and if there was a noticeable difference between the peptide fragments from using Endocut-02 or Bromelain. SDS-PAGE, shown in **Figure 28**, confirmed that Bromelain gave more of the smaller peptides than Endocut-02, as evident by creating a smear in the applied gels. Endocut-02 were probably more selective towards specific binding sites, whereas Bromelain had a more relaxed selectivity with a broader cleaving range.

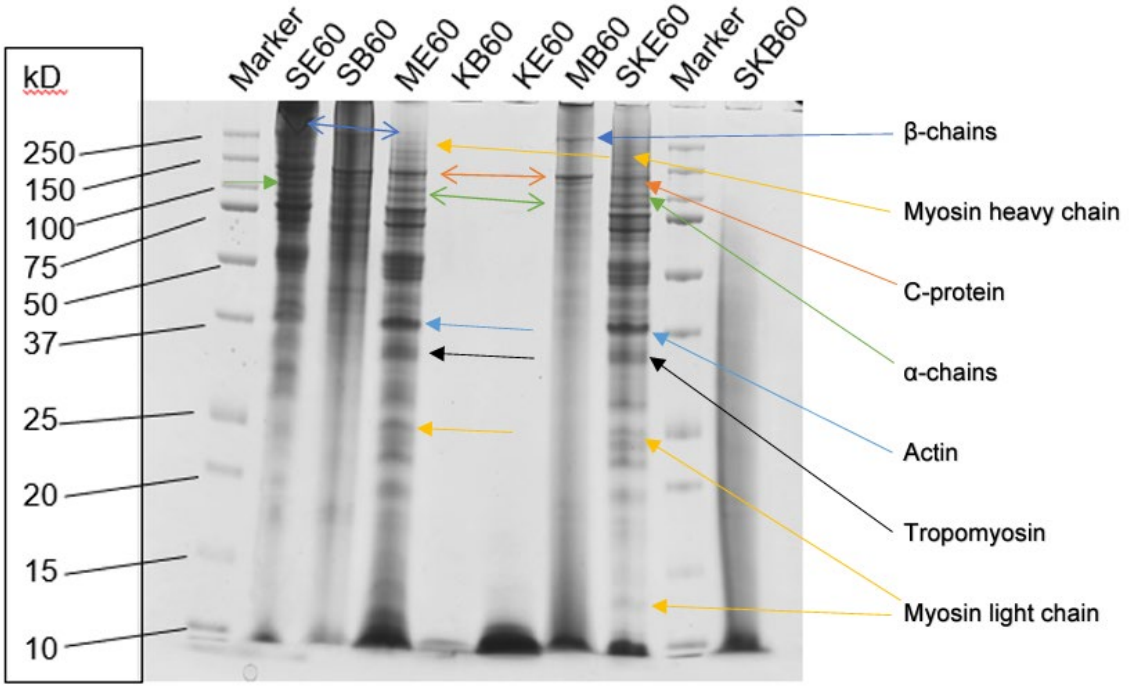

Figure 28. 12 % polyacrylamide gel SDS-PAGE analysis of the end-products in lab-scale hydrolysis. The marker yielded fragments of a given size in kDa, as marked in the figure. From the left; Marker, SE60: (tendons treated with Endocut-02), SB60: (tendons treated with Bromelain), ME60: (MDPR treated with Endocut-02), KB60: (CF treated with Bromelain), KE60: (CF treated with Endocut-02), MB60: (MDPR treated with Bromelain), SKE60: (tendons + CF (50/50) treated with Endocut-02), marker, and SKB60: (tendons + CF (50/50) treated with Bromelain).

Between 5-15 µl of 2.5mg/mL sample was applied to each well. It was challenging to find the right concentration so that the fragments were not under- or over-exposed by staining. Both 10% and 16% gels were tried, but 12% produced the best visible fragments. The peptide

fragments could be characterized by comparing the bands formed in the gel with a marker containing a mixture of several known proteins of known mass (87).

According to Deyl, et al. the individual α-chains of type I, II, III, and V collagens appear as fragments in the gel around 100 000–150 000 kDa (134). Sotelo et al. found β-chains of type I collagen in fish between 200-220 kDa, depending on the sample preparation technique (135). Still, according to Rabotyagova et al., the β-band of collagen is located at 250 kDa (136). This means that the collagen fragments appeared between 200-250 kDa depending on the sample preparation and the origin of the collagen. Claeys et al. found that the location of tropomyosin in the gels varied due to changes in myofibrillar protein composition and was found in the 30-50 kDa region. Actin appeared around 140 kDa, myosin heavy chains around 200 kDa, and myosin light chain around 20 kDa (137).

In the present study, the collagen fragments (in all lanes except those for KE/KB) were observed at ~100 kDa as the monomeric α1 and α2-chains, indicating collagen type I. The dimeric β-chains were found slightly above ~250 kDa, which also are characteristic for collagen. The presence of myosin heavy chain (~205 kDa), C-protein (~137 kDa), actin (~43 kDa), tropomyosin (~36 kDa), and myosin light chain (~24 kDa) was observed in the samples where meat was involved (all except SE/SB), all of which came from myofibrillar proteins (54). Samples where the materials were treated with Endocut-02, showed more defined fragments than those treated with Bromelain, where mostly a smear of peptides was apparent. Presumably, because the solution treated with Bromelain consisted of many different peptides where the protein fragments gradually increased in M_W, it appeared as a smear in the gel.

Both of the enzymes are endoproteases, but they obviously cleaved the peptide chains very differently. A protease with more selectivity, would provide more defined bands in the gel (138), whereas non-specific proteases often create a smear of peptide fragments in the gel (139). The CF materials showed no evident fragments of larger size, only peptides at the bottom of the well, possibly due to the fragments being too small, which led to them being washed out of the gel during the analysis. This trend appeared regardless of which gel % that was used. One possible reason for this could be autolysis, in which endogenous enzymes contribute to an increase in protein solubilization. The added commercial enzymes had a considerable effect on the M_W of the generated peptides from, especially meat-based residuals, by reducing the peptide lengths. However, according to, e.g., the study done by Lapeña et al., endogenous enzymes could drastically reduce the peptide size without adding commercial proteases, leading to

protein solubilization of around 30 % in CF residues (125). Samples of hydrolyzed tendons showed a good deal of peptides in the higher size-region of the gel, which can be explained by the fact that the end products contained larger collagen peptides released during heat-treatment in the deactivation step.

To sum up; SDS-PAGE was used to study the peptide composition in the hydrolysate products. It was observed that the various materials from RRM showed several visible fragments after treatment with Endocut-02, while after treatment with Bromelain, the fragments often appeared as a smear. By comparing the visible fragments with known markers and similar peptides identified in other studies, information of myofibrillar proteins and collagen was found in the hydrolysate products.

4.2.3.2 High performance size-exclusion chromatography – mass average molar mass distribution of the lab-scale hydrolysates

The lab-scale hydrolysates were analyzed by HP-SEC to examine the hydrolysates Mw profiles and their variations during the time. The chromatograms of CF treated with Endocut-02 A) and tendons treated with Bromelain B), shown in **Figure 29**, will be discussed in more detail in association with the PCA obtained from FTIR analyses in section **4.2.2** as the most significant variation appeared between these series. However, all chromatograms from the single protease-treated lab-scale EPH are of interest and can be viewed in **Appendix 7.8** (Figure 68-73).

The chromatograms A) and B) showed a significant difference in the peak heights where the hydrolysate product at 60 minutes in B) deviated from the other hydrolysates. This chromatogram confirmed the observations from SDS-PAGE in section **4.4.1** concerning the collagen peptides. In further explanation, larger collagen-peptides were released during the deactivation of the proteases due to the high heat-treatment. By comparing the relative area % of the fractions between the series, minor differences between the materials treated with the two proteases could be discovered. However, the inequalities between the peak heights in the two chromatograms were quite evident. The observed differences were expected due to the peptides' structural variations in the FTIR spectra from section **4.2.2**. Also, the variations in the corresponding PCA score plot revealed a distinct difference between the two series, in A and B.

In **Figure 29** C) and D), the Mw was plotted against the hydrolysis time to study the extent to which the Mw changed with hydrolysis time. **Figure 30** shows that CF treated with Endocut-02 produced a steady decreased Mw between approximately 3750-2000. However, for tendons

treated with Bromelain, seen in D), the Mw was relatively low from the beginning until the end product at 60 min, where large components with an Mw of approximately 6700 were released. Bromelain has been shown to produce smaller peptides than Endocut-02 in the EPH reactions. However, larger peptides were also released from the tendons when treated with Bromelain during deactivation with high heat-treatment at the end of the hydrolysis reaction.

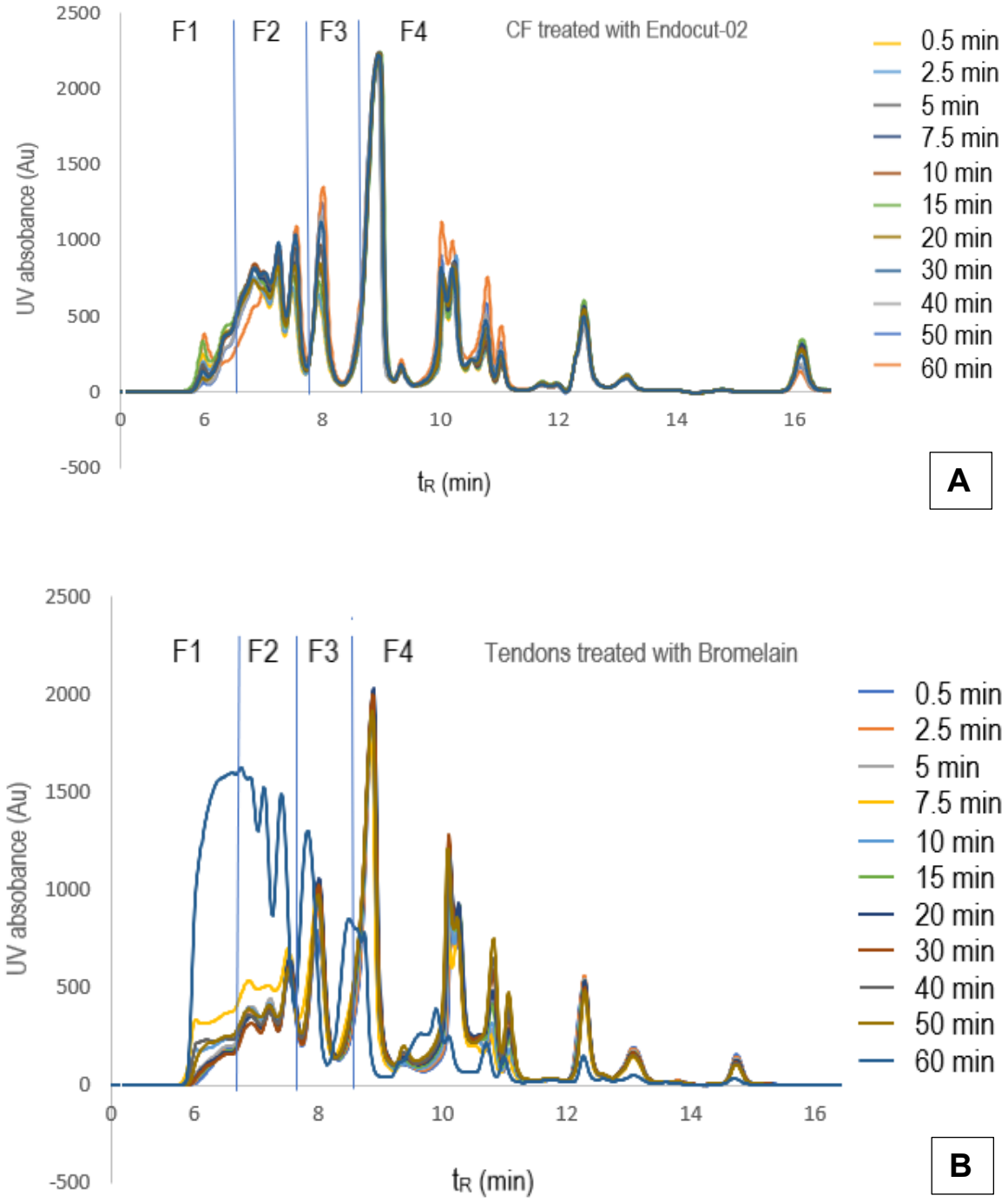

Figure 29. SEC-chromatograms of samples taken during the lab-scale EPH of A) CF treated with Endocut-02 and B) tendons treated with Bromelain, with the retention time in minutes (t_R) is on the x-axis and the UV absorbance (Au) on the y-axis. The peaks are divided into fractions, F1-F4, from large to small compounds, respectively. The hydrolysate series are color marked from 0.5-60 minutes (end-product at 60 minutes).

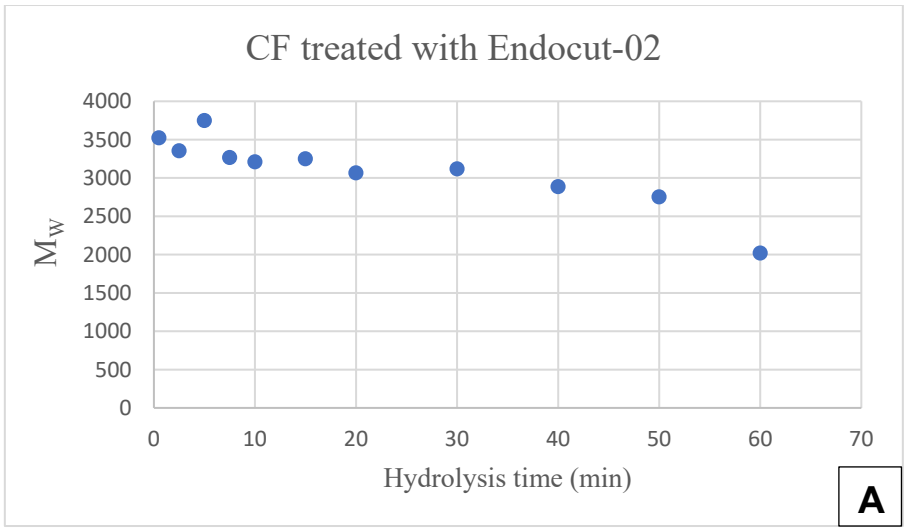

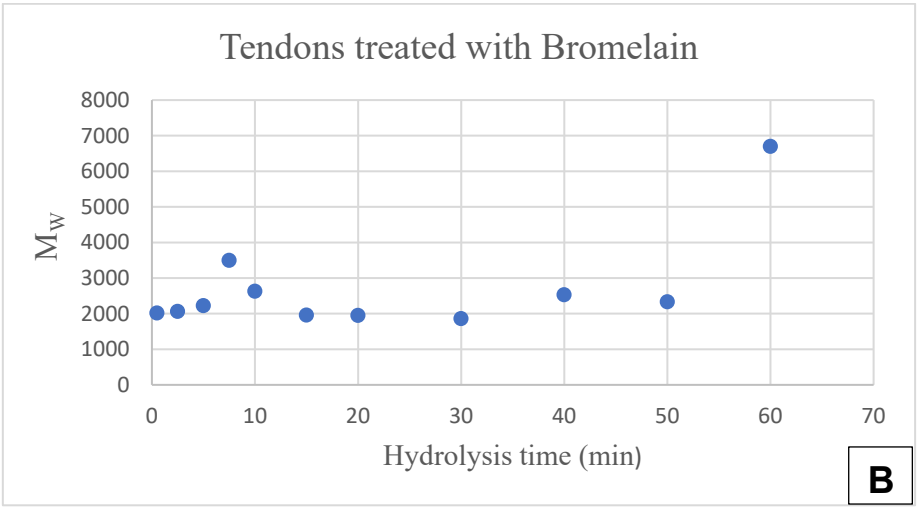

Figure 30. A) Plots of the Mw versus hydrolysis time from the same series as A) in figure 27, with hydrolysis time on the x-axis and the Mw on the y-axis revealing how the Mw decreases during the hydrolysis time. B) Plots of the Mw versus hydrolysis time from the same series as B) in figure 27.

Figure 31, A) and B) show bar charts for the two outer extremes in the F1-F4 fractions after hydrolysis during this study, which were CF treated with Bromelain, and tendons treated with Endocut-02. Fractions F1-F4 for each time series, from 0.5 to 60 min, were plotted against the hydrolysis time and revealed the hydrolysates peptide composition. The CF samples treated with Bromelain were relatively small throughout the hydrolysis reaction. However, the proportion in F1 became lower and lower, which corresponds with an Mw that was reduced during the reaction time, eventually causing F1 to become completely absent. For the samples where tendons were treated with Endocut-02, the fractions varied more, but the amount of

peptides in F1 compared to the total area increased significantly in the final product. Bar chart plot A) also shows that F1 contained a larger proportion of large-sized peptides at the beginning of the hydrolysis reaction, and also when solid material was collected during the sampling, at 0.5, 2.5, and 15 min.

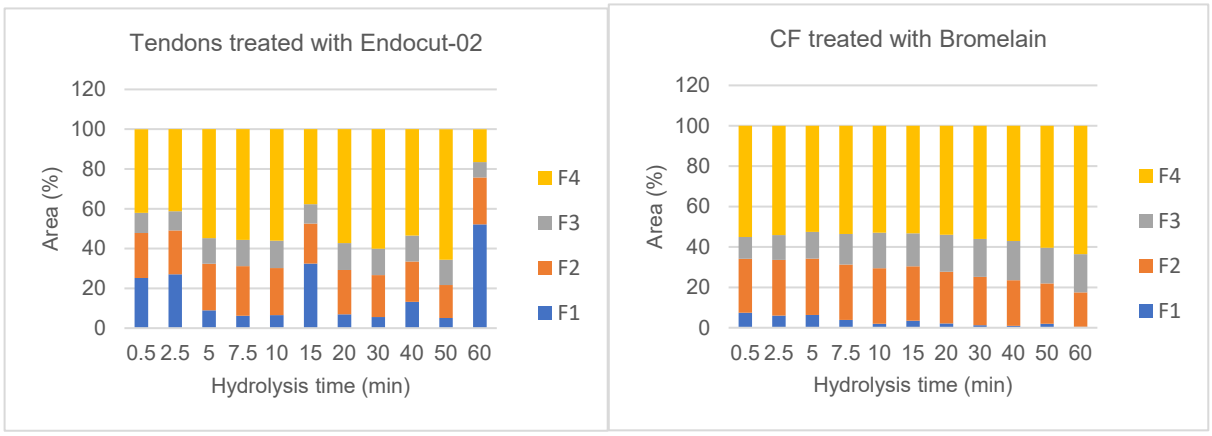

Figure 31. Bar charts of the percent of the total area of the chromatograms that were divided into fractions, F1-F4, for the most extreme EPH series. In A) CF treated with Bromelain and in B) tendons treated with Endocut-02. The area (%) of each faction, F1-F4, for each of the time series were plotted against the hydrolysis time and gave the peptide composition in each hydrolysate, from 0.5 min. to 50 min. as well as the hydrolysate end-product at 60 min.

4.2.3.3 High performance size – exclusion chromatography – lab-scale EPH combining Endocut-02 and Bromelain

When both Bromelain and Endocut-02 were added to the same solution, differences in the protein degradation were observed based on when the proteases were added to the reaction. The chromatograms in **Figure 32**, A) – C) and the bar charts in **Figure 33**, A) – C) show the corresponing F1-F4 distribution profiles. The hypothesis in the initial phase of the study was that by adding two proteases with different selectivity towards the myofibrillar proteins and collagen, such as Endocut-02 and Bromelain, to the same EPH reaction, the proteases would cleave the peptides in different locations and result in a broader range of peptides. After analyzing the hydrolysates from the small- and lab-scale EPH reactions, observing that endocut-02 primarily released large-sized peptides while Bromelain mainly was releasing small-sized peptides, the proteases clearly had different cleaving sites in the peptide chains. Still, it was uncertain how the two proteases would affect each other during the EPH.

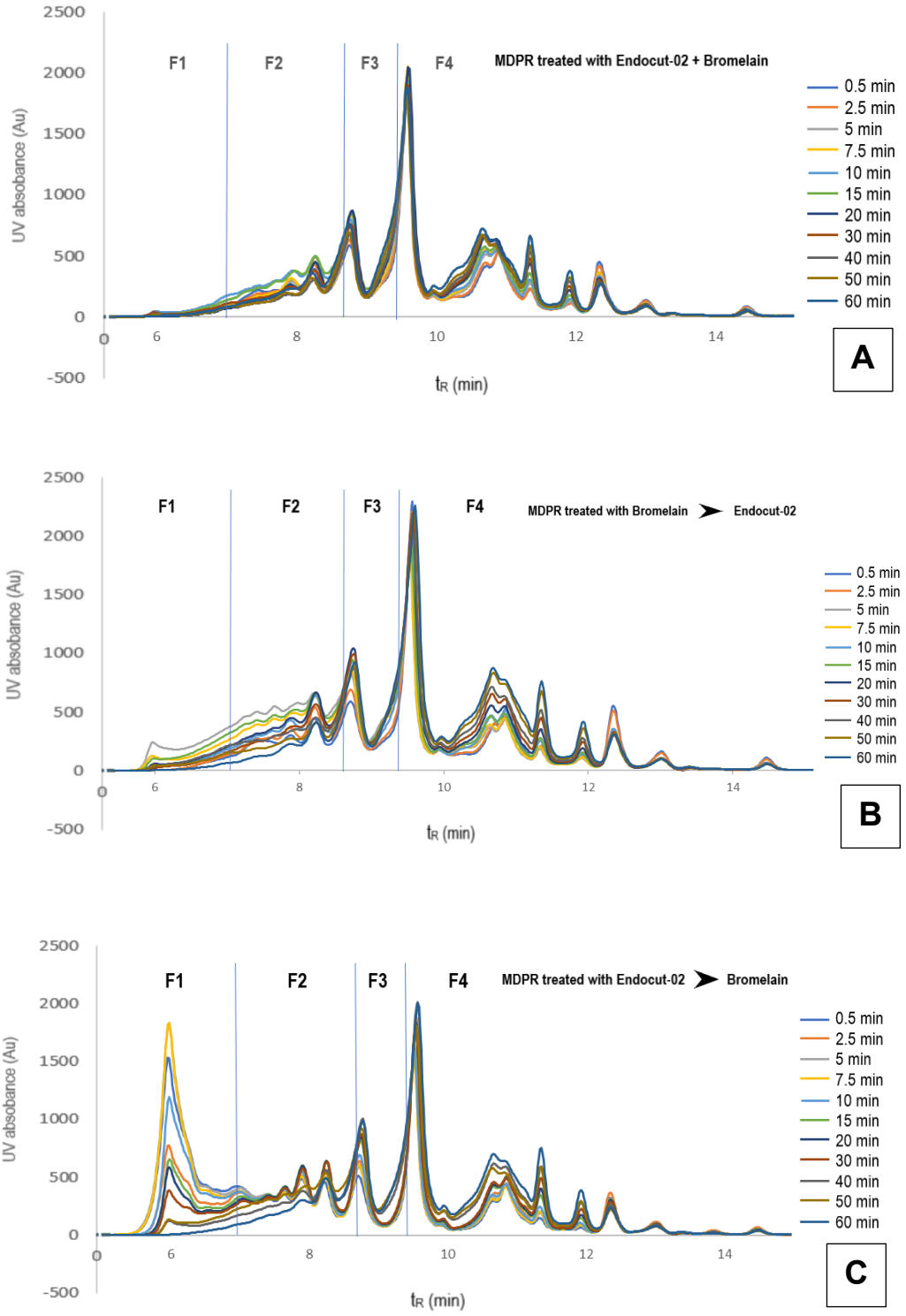

Figure 32. Chromatograms of the lab-scale EPH using a mix of proteases. A) MDPR was treated with Bromelain and Endocut-02 from the start, B) MDPR treated with Bromelain 30 minutes before adding Endocut-02, and C) MDPR treated with Endocut-02 30 minutes before adding Bromelain. The retention time in minutes (t_R) on the x-axis and UV absorbance (Au) on the y-axis. The peaks are divided into fractions, F1-F4, from large to small compounds, respectively. The hydrolysate series are color-marked with time-series from 0.5 to 60 minutes.

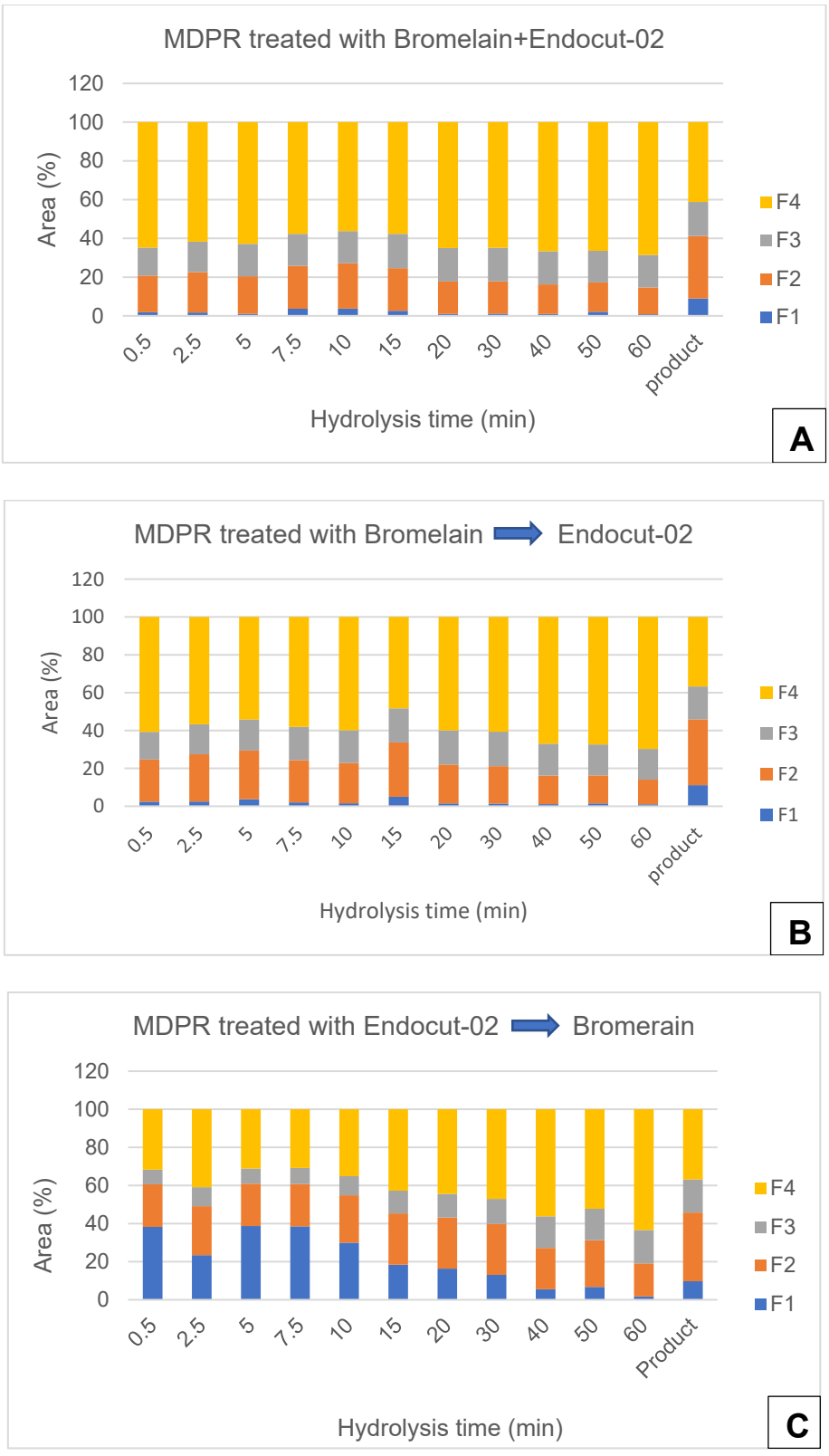

Figure 33. The area % versus hydrolysis time of hydrolysates from A) MDPR treated with Bromelain and Endocut-02 from the start, B) MDPR treated with Bromelain 30 minutes before adding Endocut-02, and C) MDPR treated with Endocut-02 30 minutes before adding Bromelain. The area (%) of each faction, F1-F4, for each of the time series were plotted against the hydrolysis time and gave the peptide size composition in each sample, from 0.5 min. to 60 min. The end-product is also included.

The chromatograms of the end-products at 60 minutes were inserted into a separate figure but the end-products were included in the bar charts to see if there was an increase of larger components when deactivating the reaction with the material still present in solution. There was a slightly increased F1 and F2 in the end-product compared to the time series hydrolysates, although the difference was not significant. The same distribution pattern in F1-F4 could be observed in the MB+E profile, in the B) chromatogram and the B) bar chart, where Bromelain was added 30 min before Endocut-02. Since Bromelain was added first and started to cleave the peptide chain in different locations, smaller peptides were released from the start and probably made it difficult for Endocut-02 to reach all of its cleaving sites.

The fractions in the MB+E series was almost identical to the MBE series. The last series, ME+B, had an interesting profile, as shown in the C) chromatogram in **Figure 32** and the C) bar chart **Figure 33**. Larger components were eluted at the beginning of the run and created high peaks in the front in F1 in the chromatograms. However, the high peaks in F1 did not appear for the samples collected at the end of the hydrolysis-time, like earlier when MDPR was treated with one single protease. In the ME+B series, the large-sized peptides came from the time series collected before Bromelain was added to the solution, between 0-30 minutes into the reaction.

As previously mentioned, the hypothesis was that Endocut-02 cleaved the peptide chain in more specific locations and released larger peptides. In contrast, Bromelain produced smaller peptides by cleaving several places in the peptide chain. By adding the proteases in the order done in ME+B, larger peptides would first be released. This means that Bromelain could easily access its accessible cleaving sites in the solubilized peptides and produce various smaller peptides with different properties than it would in single protease-treatment. The peptide profiles of MBE and MB+E showed a relatively similar degradation of the peptides from the initial phase of the reaction and throughout the hydrolysis. Both series had peptides with an M_W between approximately 4000-1300, while the ME+B series had an M_W profile between approximately 11000-1500.

Not much information was given about the proteases. However, the proteases could contain a mixture of enzymes. In greater detail, it means that when proteases such as Bromelain are extracted from pineapple, it could contain an enzyme system composed of various enzymes of different molar mass and molecular structures. With several proteases, where each has its own selectivity, Bromelain might have a slightly more relaxed selectivity than Endocut-02. Hence, Bromelain has been particularly active in the degradation of the materials. With that said, the

chromatograms and Mw distribution in **Figure 34** and **Figure 35** showed that the end-products were virtually identical.

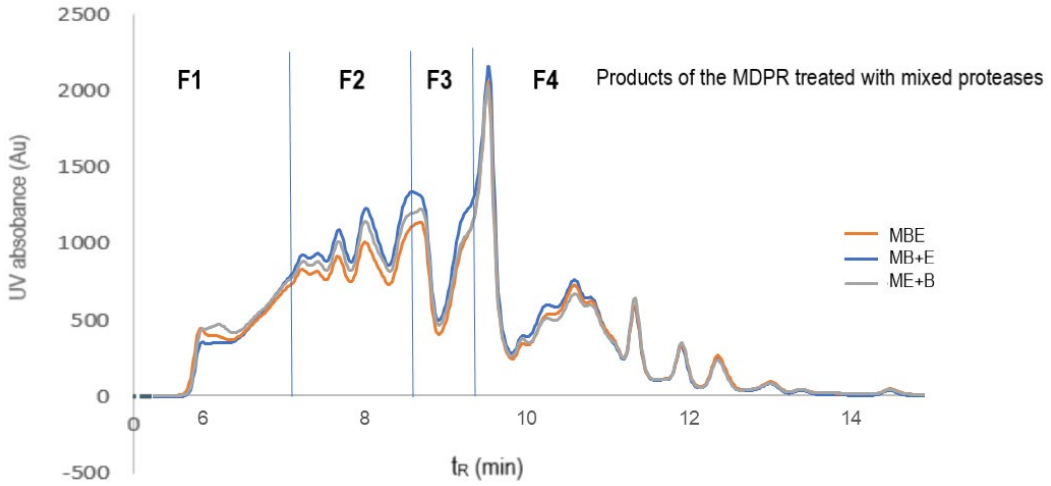

Figure 34. SEC-chromatograms of the end-products from the lab-scale EPH with mixed proteases. The retention time in minutes (t_R) on the x-axis and the UV absorbance on the y-axis. The chromatograms are divided into fractions, F1-F4, from large to small compounds, respectively. The hydrolysate series are abbreviated as MBE: Bromelain and Endocut-02 added simultaneously from the start MB+E: Bromelain was added 30 minutes before Endocut-02 ME+B: MDPR treated with Endocut-02 30 minutes before adding Bromelain.

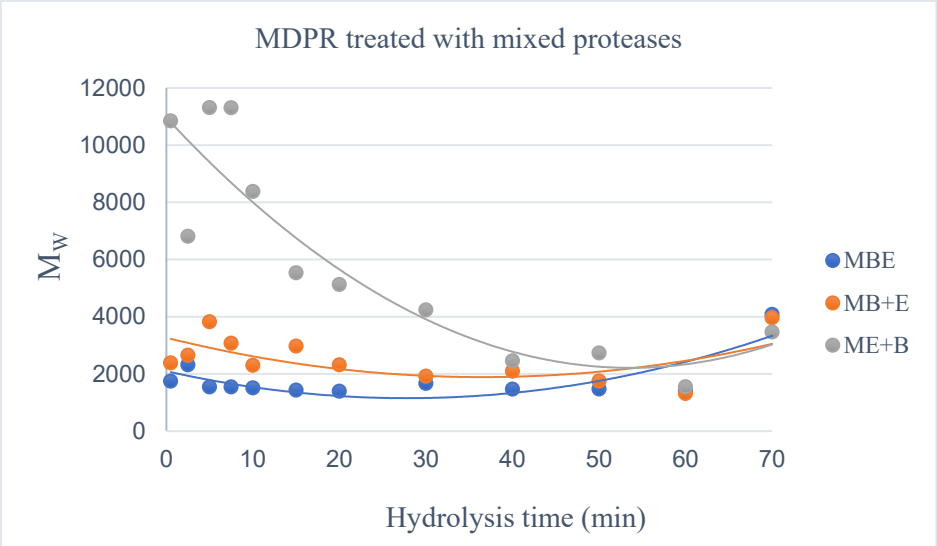

Figure 35. The M_W plotted against the hydrolysis time (min) for all three series of MDPR treated with mixed proteases. MBE: MDPR was treated with Bromelain and Endocut-02 from the start, MB+E: MDPR treated with Bromelain 30 minutes before Endocut-02 and ME+B: where Endocut-02 was added 30 minutes before Bromelain. Trendlines are included.

There may have been several reasons why the profiles became more and more similar and eventually ended up at about the same point. If the substrates' available surface area were too small, much of the proteins inside the material were unavailable, and the proteases would only have access to the outer part of the material. The protease concentration could have been too low relative to the amount of substrate. It may also be that the proteases were product-inhibited or that the hydrolysis time should have been extended. Alternatively, it could be as simple as Endocut-02 having access to its cleaving sites and Bromelain to its cleaving sites regardless of the order they were introduced to the substrate. In further explanation, none of the proteases hindered the other in cleaving at their respective locations in the peptide chain and hence degraded the myofibrillary proteins and collagen to the same extent in all three series. Nevertheless, further study on the composition of Endocut-02 and Bromelain should probably be done to exclude that a mixture of the proteases released peptides that prevented further degradation.

To sum up; HP-SEC provided valuable information regarding the size distribution of proteins and peptides in the hydrolysate products. It was observed that large peptides were released from the collagen-rich materials, especially when using Endocut-02 and that these were likely to be released during the heat-treated deactivation of the proteases. This was particularly notable when analyzing the end-products. When studying the M_W profiles of the MBE, MB+E, and ME+B series, the protein degradation patterns varied in terms of how the proteases were added to the solutions, but that the M_W profiles ended up with approximately the same M_W composition in the end-products.

4.2.3.4 Degree of hydrolysis and protein content % in the lab-scale hydrolysates

DH% and Dumas analyses were performed to obtain information about the number of cleaved peptide bonds and the protein content, respectively, and were conducted for all lab-scale EPH samples. The obtained values were used to calculate the protein yield and to determine the corrected DH%. **Table 17** shows an example of Dumas data, from the MB+E series, showing an increasing amount of nitrogen during hydrolysis time. Each of the hydrolysates from the collected time series from all hydrolysis rounds showed the same increasing amount of nitrogen in the Dumas measurements. This nitrogen content could be converted to a crude protein % using a conversion factor of 6.25, which is the most frequently used conversion factor due to the assumption that protein contains 16 % nitrogen and that all nitrogen in food comes from proteins (1, 71). An increase in the protein content during the hydrolysis time was expected

since more of the peptides were solubilized and released into the solution towards the end of the reaction. Slightly more variations of the protein content % were observed in the hydrolysates from complex materials such as MDPR because of non-repeatable collected samples from the reactor, with different amounts of solid material at each sampling. The somewhat variable data was, therefore, seen as a natural anomaly. All the Dumas data can be found in **Appendix 7.4.2** (Table 30-32).

Table 17. One example of a Dumas dataset with the amount of hydrolysate (mg), the measured nitrogen content (%), and the protein factor which was used to convert the nitrogen into protein content (%). The series shown is of MB+E, from 0.5 min. - product at 60 min. with an increasing amount of protein throughout the hydrolysis reaction.

Hydrolysis time (min)	Hydrolysate (mg)	Nitrogen content (%)	Protein factor	Protein content (%)
0.5	5.12	11.4	6.25	71.0
2.5	4.77	12.7	6.25	79.1
5	4.80	12.1	6.25	75.4
7.5	4.77	12.5	6.25	78.2
10	4.84	12.6	6.25	78.4
15	4.53	13.6	6.25	85.2
20	4.69	13.1	6.25	81.9
30	4.43	13.2	6.25	82.8
40	4.79	13.2	6.25	82.5
50	4.83	13.2	6.25	82.5
60	4.56	13.4	6.25	83.5
Product (60)	4.63	15.1	6.25	94.6

However, although the DH% increased during hydrolysis time, there was an abrupt decrease in the number of cleaved peptide bonds in the end-product. The more natural trend would be if the increased DH% continued throughout the EPH reaction. During the present study, gelatin was apparently released during the heated deactivation. The large-sized collagen peptides could cause this sudden decrease in DH%. Since DH% measures the number of free N-terminals in a solution, the number of cleaved peptide bonds could decrease as the protein content % increases. This study has shown that the DH% analysis alone was not enough to analyze what happens during an EPH process of a complex material like MDPR. A solution to this was to investigate whether there was a correlation between DH% and the M_W obtained from the HP-SEC analysis (section **4.4.2)**. During the typical course of a hydrolysis reaction, the Mw is

reduced over time as the proteins and peptides are digested. With the combination of techniques, further investigation could reveal if the resulting DH% matched the hypothesis about larger peptides being released at the end due to heat treatment. If this is true, it could be expected that this would affect the DH% in the opposite direction. In **Figure 36,** A), and B), the Mw of collagen-rich tendons treated with Endocut-02 and Bromelain, respectively, is plotted against the corresponding DH%, showing a defined decrease in DH% with an increasing Mw, which strengthened the truth of the hypothesis.

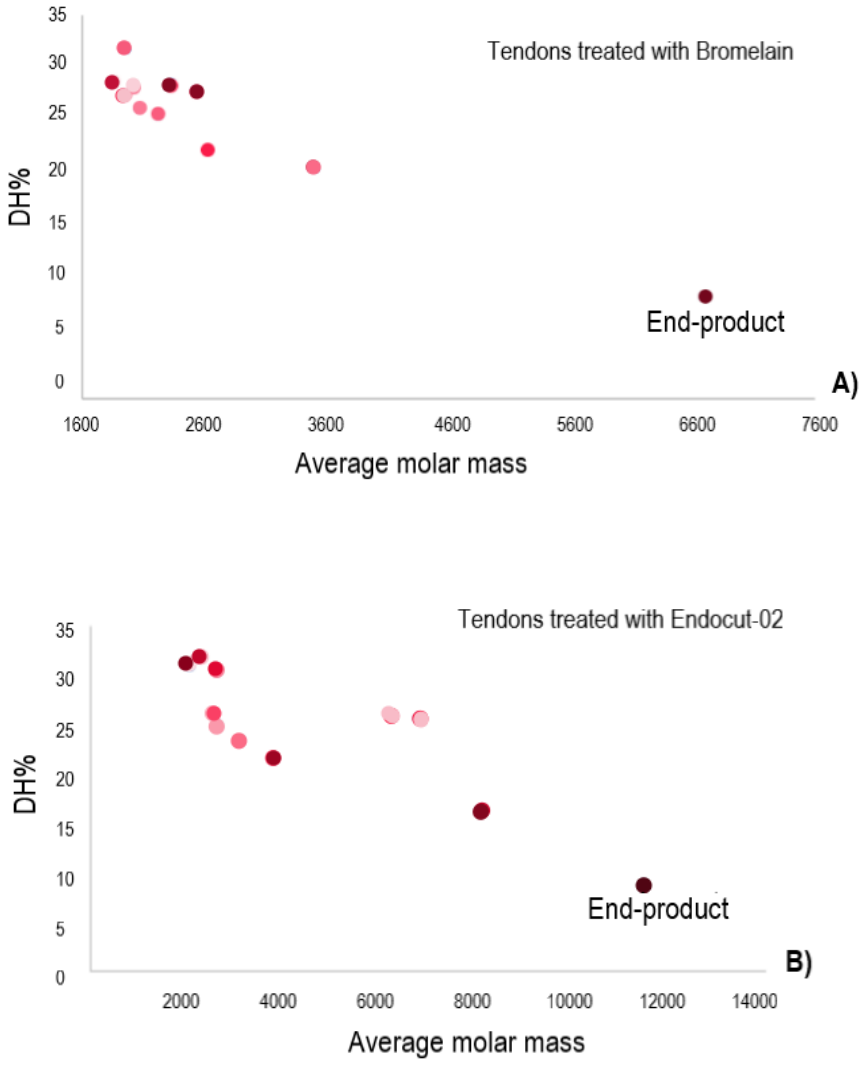

Figure 36. A) The correlation between the DH% and M_W for tendons treated with Bromelain, where the intensity of the red color in the plots increases by increased hydrolysis time. B) The correlation between the DH% and M_W for tendons treated with Endocut-02, with decreasing DH% when M_W increases.

The CF series in **Figure 37** showed a relatively flat curve, in which the hydrolysates in A), which derived from CF treated with Bromelain, showed M_W-values between approximately 1100-2800. The hydrolysates in B) where CF was treated with Endocut-02, showed M_W-values between approximately 3000-4900. In graph A), the end-product had a decreasing M_W, with an increasing DH%, which usually are seen in EPH reactions. Larger peptides were released from myofibrillar proteins when using Endocut-02 compared to when using Bromelain. Still, graphs A) and B) in **Figure 37** showed a more normal trend in the degradation profiles, which means that large-sized peptides were released at the initial phase of the EPH with a lower DH%, and the small-sized peptides at the end of reaction with a high DH%.

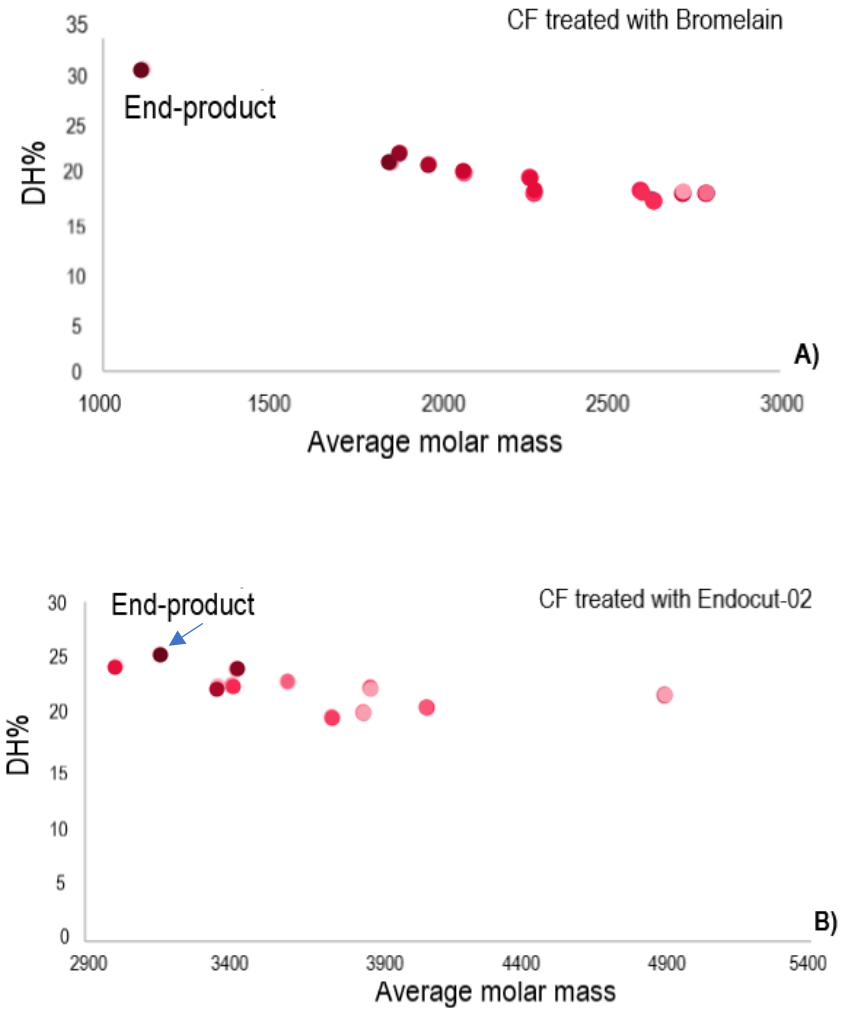

Figure 37. A) The correlation between the DH% and M_W in a time series of hydrolysates where CF was treated with Bromelain, with a relatively constant DH% and M_W over time. B) The correlation between the DH% and M_W for hydrolysates where CF was treated with Endocut-02, with a relatively constant DH% and M_W over time, except the end-product where a low M_W provided higher DH%.

4.2.3.5 Hydroxyproline analysis of mechanically deboned poultry residues treated with Endocut-02 and Bromelain

A Hyp analysis was performed in collaboration with Kristoffersen, K.A. (111) of MDPR treated with Bromelain and Endocut-02 to verify if the hypothesis assuming that larger peptides were released from collagen-rich materials during heat treatment was true. **Figure 38**, A) and B) shows the hydroxyproline determination in the MDPR samples treated with Bromelain and Endocut-02, respectively. The values of the samples were calculated based on a calibration curve from references with known hydroxyproline amounts. The Hyp profiles clearly showed that the collected samples contained minimal collagen, except in the end-products.

According to Shoulders, M. D., and Raines, R. T., 2009, the hydroxylation of Pro residues in the Yaa position of collagen increases the thermal stability of the triple helices dramatically. The hydroxyl group of Hyp stabilizes collagen through a stereoelectronic effect (132). The assumption that the collagen materials investigated during the present study required extensive heat-treatment to break the inter- and extracellular interactions to release the collagen peptides were strengthened after the Hyp analyses.

During the lab-scale EPH reactions, occasionally pieces of the solid phase were collected from the reactor with the liquid sample, which released more collagen peptides during the deactivation of the proteases. Therefore, small amounts of Hyp was revealed in some of the time series, such as the ME1 series at 7.5 minutes.

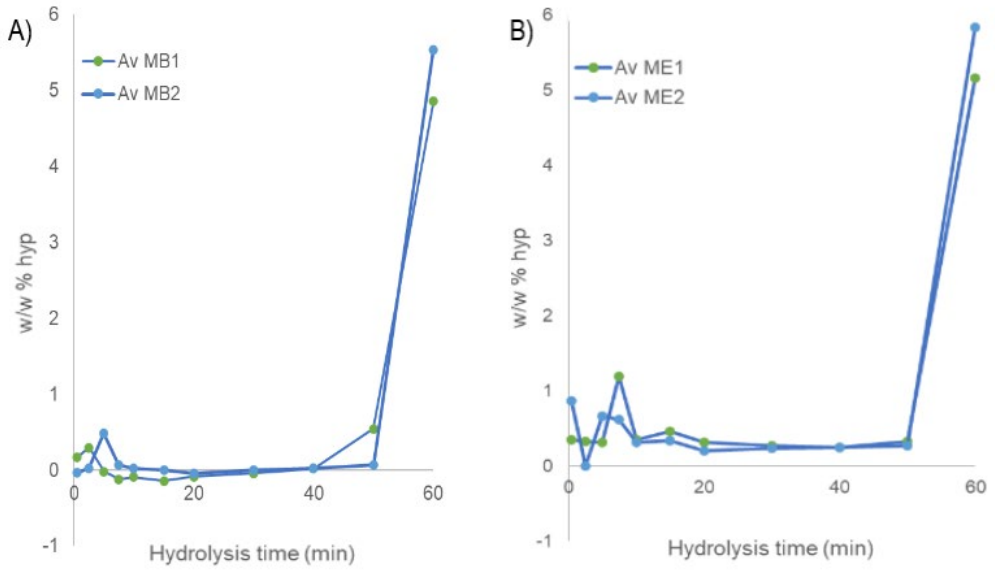

Figure 38. Hyp content (%) as a function of hydrolysis time in the duplicated MDPR series treated with Bromelain and Endocut-02. A) MB1 and MB2: two replicates of the first lab-scaled EPH reaction treated with Bromelain, B) ME1 and ME2: treated with Endocut-02. The graph's x-axis shows the hydrolysis time (min), and the y-axis shows Hyp content in (w/w %) (111).

4.2.3.6 Degree of hydrolysis and protein content % in the lab-scale hydrolysates from combining Endocut-02 and Bromelain

The MDPR treated with a combination of Endocut-02 and Bromelain was investigated by plotting the DH% against hydrolysis time, as shown in **Figure 39**. The hydrolysis series, MBE, MB+E, and ME+B showed an increase in cleaved peptide bonds from the collected samples. However, the end-products resulted in an abrupt decline in DH%, where the values went from about DH% 20 to DH% 30. It was observed that the similarity in DH% between the series, MBE, MB+E, and ME+B varied during the hydrolysis time concerning the number of cleaved peptide bonds. However, at the end of the hydrolysis reaction, it was MB+E and ME+B that ended up at the same point, which could indicate that regardless of the order in which the proteases were added to the reaction, MB+E and ME+B ended up with approximately the same number of cleaved peptide bonds in the hydrolysate product.

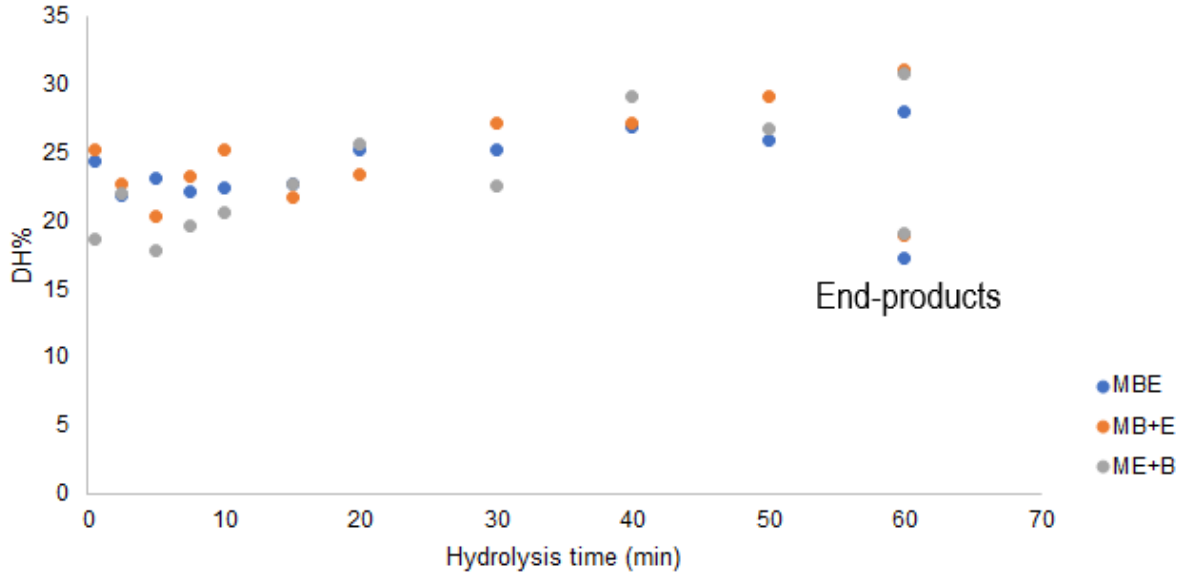

Figure 39. DH% plotted against the hydrolysis time (min) for all three series of MDPR treated with mixed proteases. MBE: MDPR was treated with Bromelain and Endocut-02 from the start, MB+E: MDPR treated with Bromelain 30 minutes before Endocut-02 and ME+B: where Endocut-02 was added 30 minutes before Bromelain.

The most notable variations between the three series relative to each other could be observed in the peptide profiles by plotting DH% against Mw, as shown in **Figure 40**, A) – C).

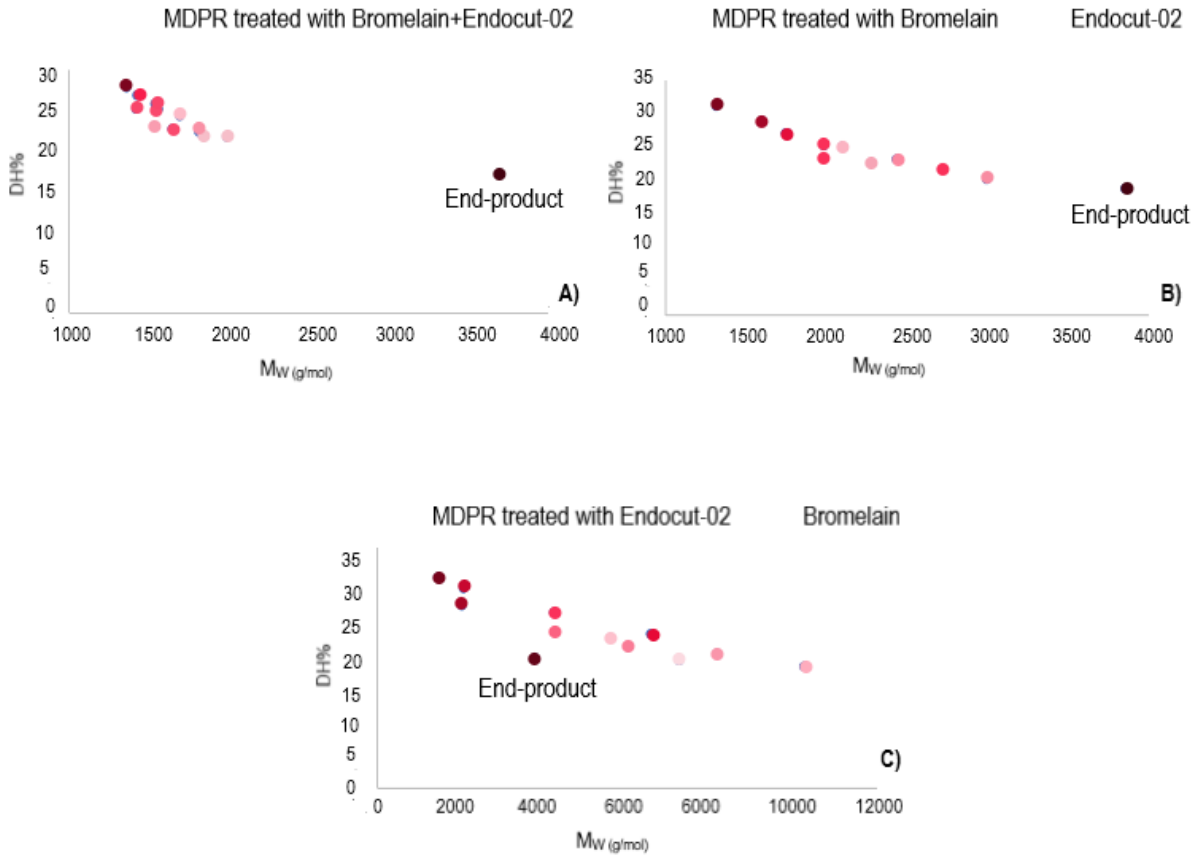

Figure 40. DH% plotted against the Mw for all three series of MDPR treated with mixed proteases. The intensity of the red color in the plots increases by increased hydrolysis time. A**)** MDPR was treated with Bromelain and Endocut-02 from the start, B**)** MDPR was treated with Bromelain 30 minutes before Endocut-02, and **C)** Endocut-02 was added 30 minutes before Bromelain.

In A), both proteases were added from the start. Most of the A)-samples had a DH% between 20-30 and with an Mw of approximately 1350-2000. When both proteases were added simultaneously from the experimental start, Bromelain could cleave the somewhat larger peptides solubilized by Endocut-02 into smaller peptides from the initial phase of the hydrolysis, which resulted in an overall small-sized peptide profile. Still, the span between the collected time-samples and the end-product, with 17 in DH% and an Mw of approximately 3700, certified that larger peptides were released during the heated deactivation. The

hydrolysates from the MB+E series in B) showed a more normal degradation pattern. Still, the end-product had a slightly higher M_W with a lower DH%, as seen in A).

Nevertheless, the series diverging the most from the other two hydrolysate-series could be seen in C), where Endocut-02 was added 30 minutes before Bromelain with a DH% between 17.8-30.8 and an M_W between approximately 1450-10000. Strangely, the ME+B plot showed a more normal trend, with an increasing DH% correlating with small-sized peptides. However, the end-product of ME+B did reveal a somewhat larger M_W with a lower DH%. All the three end-products from the three series had a similar M_W of approximately 3800-3900, as observed in the HP-SEC analysis, shown in **Figure 35**, section **4.4.2.1,** but the number of cleaved peptide bonds in the end-products were also similar with a DH% between 17-19. The MB+E and ME+B series, which ended up at the same point in the peptide profile in **Figure 39**, both had a DH% of 19, confirming that the end-products of these two series were independent of the order in which they were added to the hydrolysis reaction.

To sum up; The hypothesis that the collagen peptides in the present study needed high heat to be released from the materials was confirmed after the Hyp analyses showed a sudden increase of Hyp in the end-product and minimal amounts in the overall time series. However, it was somewhat surprising that no difference regarding the amount of Hyp in the end products was observed by using Bromelain and Endocut-02. This indicates that the amount of collagen released from the materials was independent of the used protease but that Endocut-02 releases more of the large-sized collagen peptides. The DH% analyses, along with the MW profiles obtained from HP-SEC, could reveal that the number of cleaved peptide bonds in the end-products from collagen-rich hydrolysates decreased with an increasing MW. This explained why the number of cleaved peptide bonds was reduced at the same time as Dumas presented an increased protein content in the end-products.

4.2.3.7 Fourier-transform infrared spectroscopy – analysis of the lab-scale hydrolysates

All the lab-scale hydrolysates were analyzed by FTIR to monitor the structural differences between the materials when they were treated with the two proteases. PCA plots were used to reveal any clear groupings or outliers. The scale-up of the EPH revealed the same differences as in the small-scale verification of the preliminary study, where differences in particularly the amide I and amide II regions were seen. The PCA data from the small-scale EPH verification revealed that the most significant differences were between CF treated with Endocut-02 (KE)

and tendons treated with Bromelain (SB). Therefore, these spectra including the spectra with the end-products are included in the this section, while all the remaining spectra can be found in **Appendix 7.7** (Figure 57-67). **Figure 41** shows the FTIR spectra of the lab-scale hydrolysates, A) KE and B) SB.

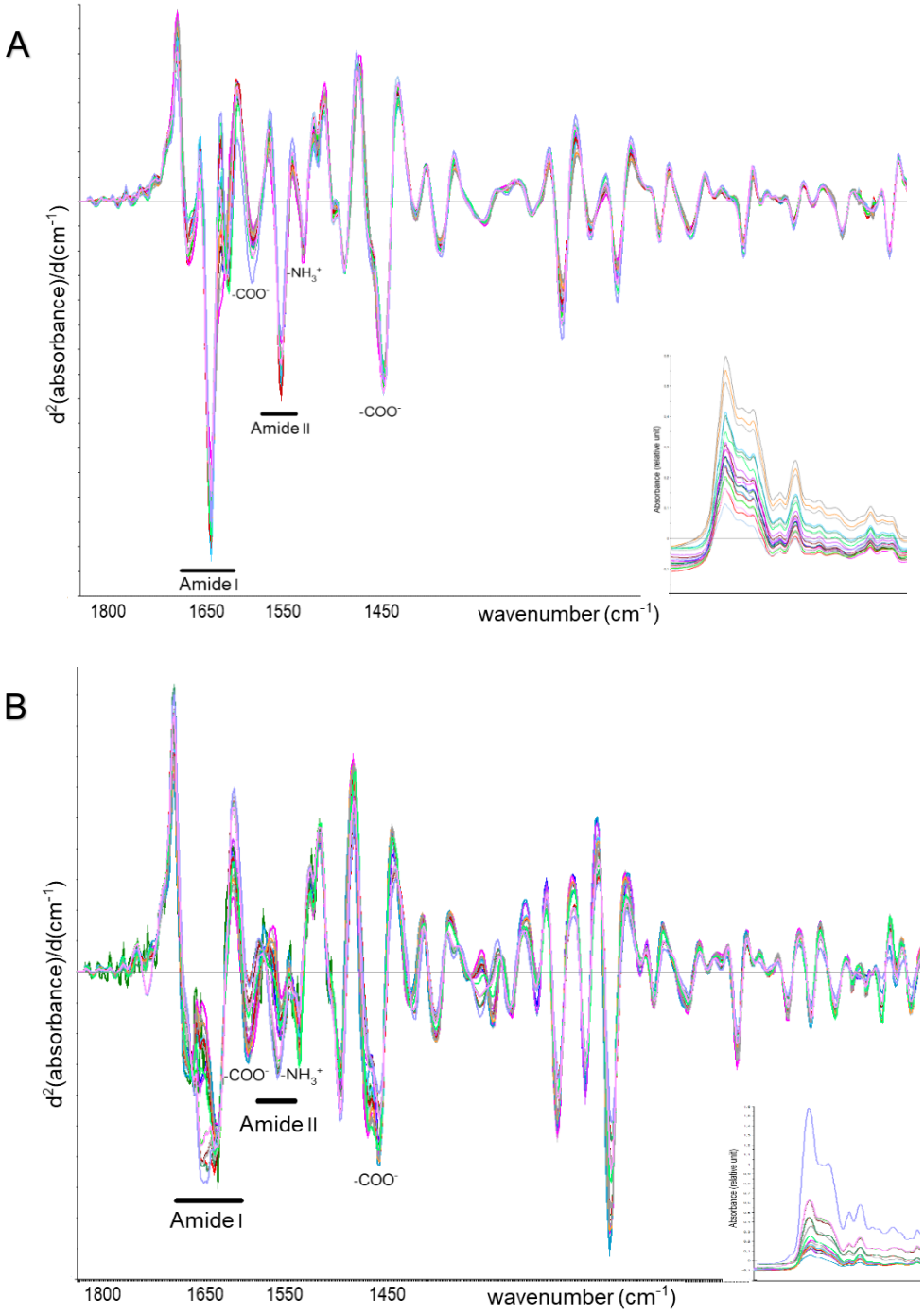

Figure 41. The SNV normalized second derivative FTIR spectra, including the raw spectra in the bottom right corner, of A) CF treated with Endocut-02, B) tendons treated with Bromelain.

Theoretically, there should have been decreasing absorption during the hydrolysis time in the amide I and amide II region at ~1650 cm^{-1} and ~1550 cm^{-1}. The bond vibrations in these regions would typically provide information about the secondary structure of the hydrolyzed proteins before degrading into smaller peptides and free amino acids. A formation of terminal amino and carboxyl groups would be shown with increasing absorption at ~1580 cm^{-1} for $-COO^-$ (asymmetric stretch), ~1400 cm^{-1} for $-COO^-$ (symmetric stretch), and $-NH_3^+$ at ~1500 cm^{-1} relative to the decreasing amide regions (116, 120). However, this pattern did not occur in all spectra. After normalizing the spectra with SNV, the relative changes could be observed, not necessarily the assumed increase or decrease of the vibrational bonds. The DH% and Dumas method showed apparent degradation of the proteins during time. As shown in section **4.4.3**, the DH% analysis showed a slightly rise in the number of cleaved peptide bonds during hydrolysis time for most of the collected time series hydrolysates. Also, the Dumas analysis of the same samples divulged that increasing hydrolysis time provided a higher protein content, as shown in the data presented in **Appendix 7.4.1** (Table 23-29).

PCA was performed on both datasets of the lab-scale series KE and SB, as shown in **Figure 42** A) – D). The PCA score plots showed that the duplicated series of SB appeared at the same place, as it did in the small-scale verification, with a PC-1 score of 82 % standing for most of the variations in the dataset. Also, an apparent spread between the duplicated KE reactions, also as it did in the verification. This means that two duplicated reactions performed on four different days, showed similar groupings in the PCA score plots. The solid material was collected with the liquid phase at each sampling during the KE reaction since CF constituted a more homogeneous phase. The tendons consistency was bulkier than CF, and it was only collected a few small pieces occasionally during the EPH reactons. The most logical explanation for this grouping or dispersion in the PCA score plots has already been discussed in the verification, section **4.2.3**.

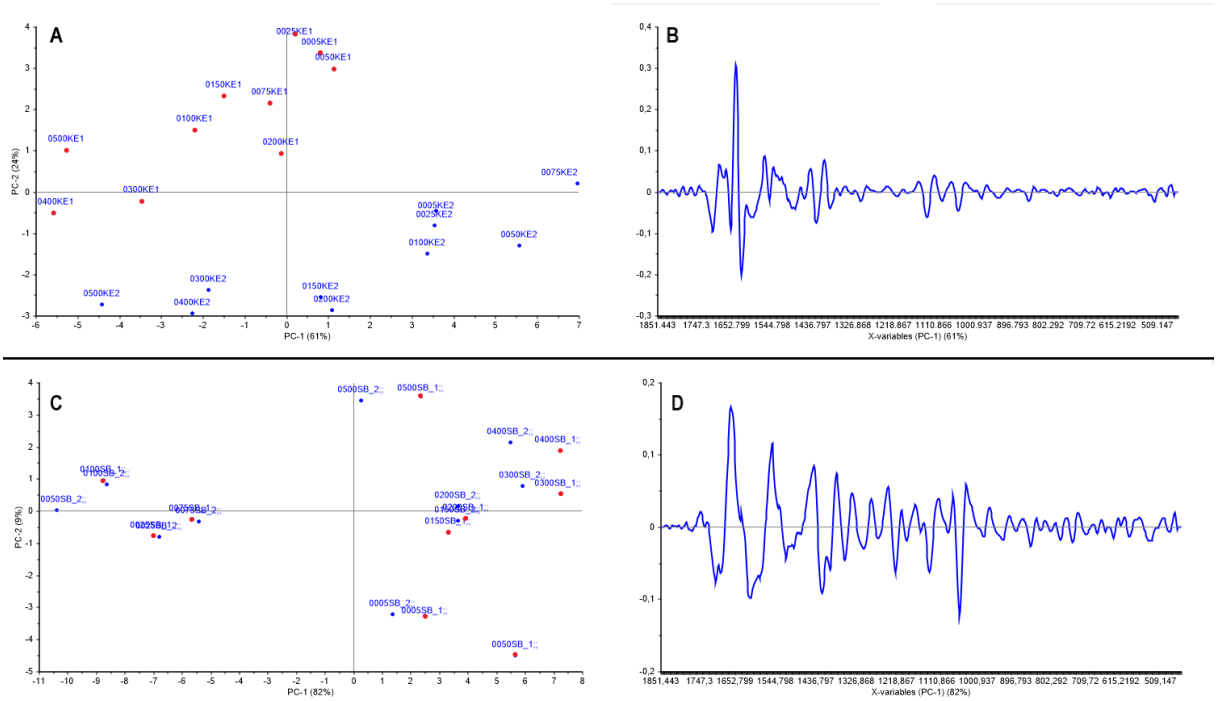

Figure 42. The PCA score plots of A) CF treated with Endocut-02 (KE) and B) loadings of the same series, while C) and D) show score plots and loadings of tendons treated with Bromelain (SB). The first series are marked with red dots and the duplicated series with blue dots.

The spectra in **Figure 43**, with the PCA score plot A) and loading B) shows the lab-scale end-products of all the materials treated with Endocut-02 and Bromelain. The amide I region expressed that Endocut-02 and Bromelain released different proteins from the CF. More of the terminal amino and carboxyl groups were formed when the CF was treated with Bromelain, which pointed to more cleaved peptides. The SEC analysis in section **4.2.2** also showed that Endocut-02 provided larger peptides than Bromelain. The heat-treated end-products had much higher absorption than the time series samples, particularly from the collagen-rich materials. The bond vibrations deriving from the collagen-rich materials clearly showed that the end-product deviated from the others with more extensive bands.

The most considerable variation was seen between tendons treated with Endocut-02 (SE) and CF treated with Bromelain (KB), which were on the far left and far right of score plot A) where the PC-1 accounted for 54% of the variation in the dataset. Also, variations along PC-1 showed that the most considerable variation between the same materials treated with Endocut-02 or Bromelain was SB and SE, while the least variation was observed between ME and MB. All the products treated with Endocut-02 were grouped to the top half of the score plot, while the

products treated with Bromelain grouped at the bottom half. PC-2 accounted for only 28% of the variation in the dataset. However, this grouping can still be seen as a logical trend since it was known that the two proteases selectivity towards the proteins were different. From the loading in B), the most considerable variation was connected to the amide I and II region as well as the -COO^- vibrations at ~1400 cm^{-1}. These are differences that have been shown for the vast majority of hydrolysates when treated with the two proteases.

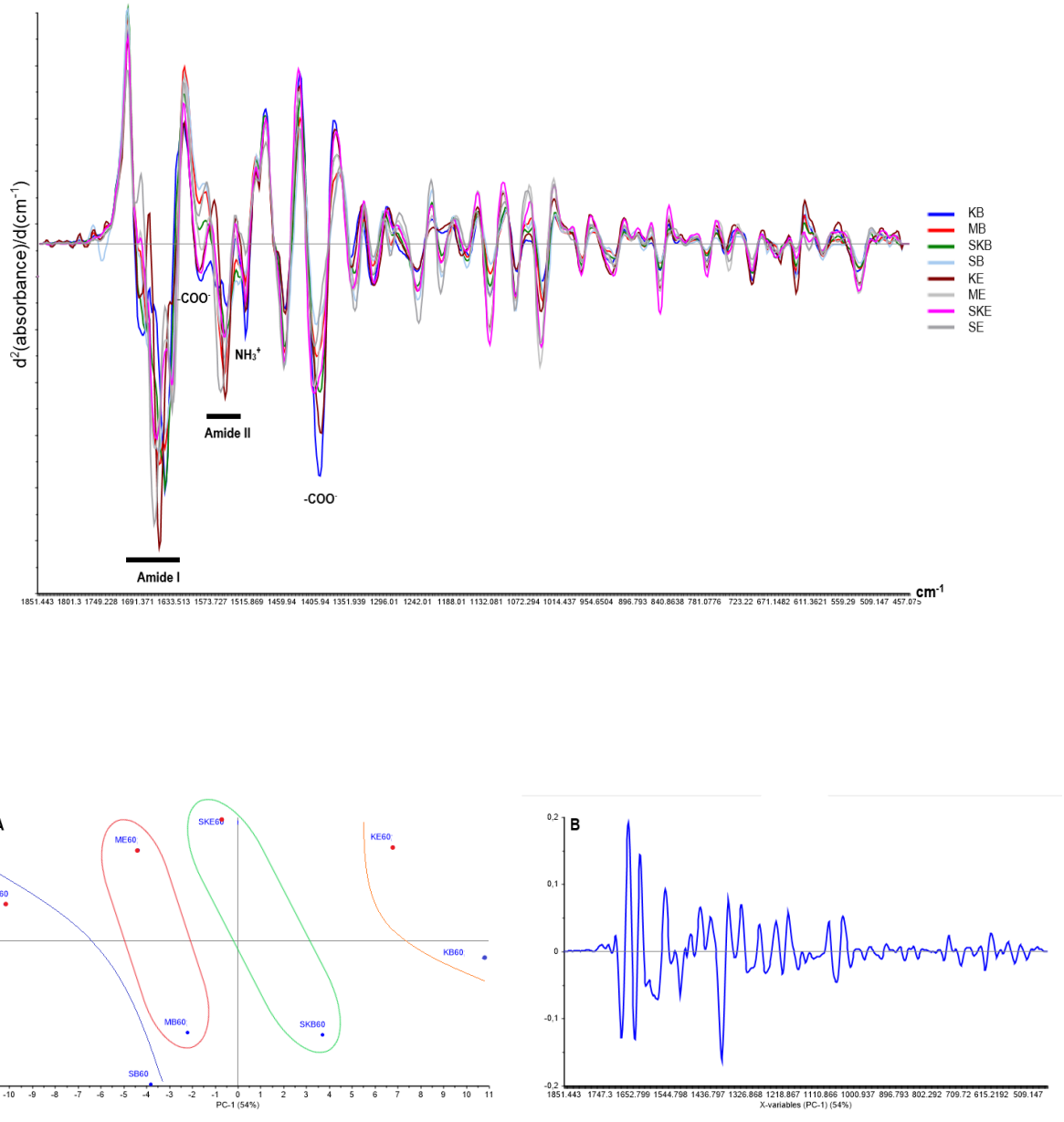

Figure 43. FTIR spectra of all the lab-scale end-products, KE, KB, SE, SB. SKE, SKB, ME, and MB, with the A) PCA score plot and B) loading. All the products treated with Endocut-02 are marked with red dots and the groupings are separated with different colors.

Since the hydrolysates would contain different compositions of proteins and peptides due to the materials complexity, it has been challenging to achieve reproducibility in the experiments. The poultry RRM contained bones, meat, tendons, and skin residues where the distribution differed from batch to batch. Even the CF would contain smaller parts of tendons. Therefore, the resulting FTIR spectra obtained from using the same materials and proteases, differed due to these variations. The main reason for the variations seen in the FTIR spectra was probably directly caused by differences in the collected time samples during the EPH. Some samples consisted primarily of the liquid phase, while others also contained parts of the solid phase. When introducing high heat to the materials in the deactivation step, it turned out that more proteins and peptides were released with solid materials present in the sample. That was mostly the case for collagen-rich materials, and since all except CF contained relatively high quantities of collagen, and this applied to the vast majority of samples.

4.2.3.8 Fourier-transform infrared spectroscopy – lab-scale enzymatic protein hydrolysis combining Endocut-02 and Bromelain

Previous studies have shown that a mixture of proteases could reveal different patterns than they do individually and that the best-suited "protease cocktail" is raw-material specific (125). A cocktail of proteases with broad selectivity could cleave more peptide bonds, expose new or several sites, and create peptides with alternate properties (140). The FTIR spectra showed that the lab-scale hydrolysates when combining the two proteases, provided different degradation of MDPR based on the order in which they were added to the EPH reaction. **Figure 44** show FTIR spectra of the duplicates of MDPR treated with a combination of Bromelain and Endocut-02. It turned out that the degradation of the proteins in the end-products was relatively similar, with some minor differences in some of the vibrations, as shown in D). However, the time series towards the end-products showed more significant variations. The difference between A) and C) was quite clear, especially in the amide I and II regions. The amide I stretch clearly stated that different proteins were released based on which of the proteases were added during the initial phase of the reaction. In the Amide II bands around ~1550 cm^{-1}, a mixture of in-plane N-H bending and C-N stretching (120) was more prominent in the C) spectra and almost absent in A).

The variation during time within the three series was studied by plotting the PC-1 scores obtained from PCA as a function of the hydrolysis time. This was done to study a possible correlation between PC-1 and the hydrolysis time. The study is shown in **Appendix 7.7.1** (Figure 67, A – C).

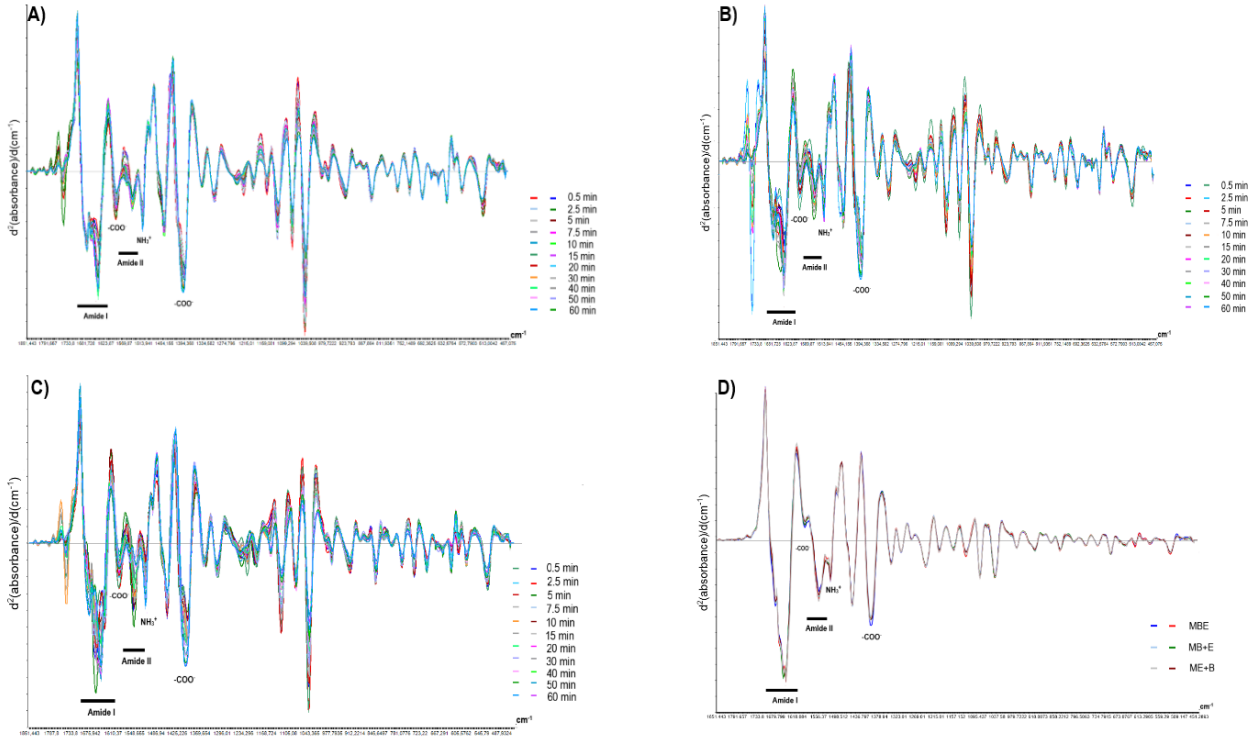

Figure 44. FTIR spectra of MDPR treated with a mix of Endocut-02 and Bromelain. The data was processed with the Savitzky-Golay algorithm creating a second derivative of the raw data and further normalized with SNV. A) MDPR treated with Bromelain + Endocut-02 from the initial, B) MDPR treated with Bromelain 30 minutes before Endocut-02, C) MDPR treated with Endocut-02 30 minutes before Bromelain was added to the reaction, and D) The products of all the 6 experiments.

In **Figure 45**, PCA scores for A) MBE, B) MB+E, and C) ME+B are shown. For MBE, the loadings are also included. For the MBE duplicate in A), the time series collected at the beginning of the EPH were grouped on the far bottom left of the score plot (green marking), the last samples that were taken out from the reactor grouped at the bottom right (orange), and the time series that were collected between 5-20 minutes is relatively high and in the center of the plot (blue). The spectra did not show major changes for the hydrolysates over time, but the PCA score plot revealed a distinct separation between the hydrolysates concerning the hydrolysis time. PC-1 accounted for the vast majority of the variations in this dataset by 84%,

where most of the variations were connected to the -COO^- vibrations in the ~1400 cm^{-1} region as well as some variations in the amide I and II regions. However, the largest variations seemed to be around ~1050-1000 cm^{-1}. No particular vibrations in this region are found to identify myofibrillar proteins or collagen, but the region between ~1200-800 cm^{-1} is referred to as the fingerprint region, where similar molecules can give different absorptions patterns (52). There can also be sugars, minerals, and salts in the hydrolysate products among the proteins and peptides. The vibrations at ~1050-1000 cm^{-1} can thus possibly be linked to sugar-phosphate bond vibrations (141). The score plot in B) and C) had a PC-1 that accounted for about 60% of the variations with inadequate groupings, especially the B) plot revealed unsufficient groupings with a cluster to the right that contained a spread variety of hydrolysates. In the C) plot, there was a prominent group on the far left with hydrolysates collected between 40-60 minutes, but the groups in the center and to the right were a little vaguer, although the trend revealed that the hydrolysates collected early in the EPH reaction grouped to the right.

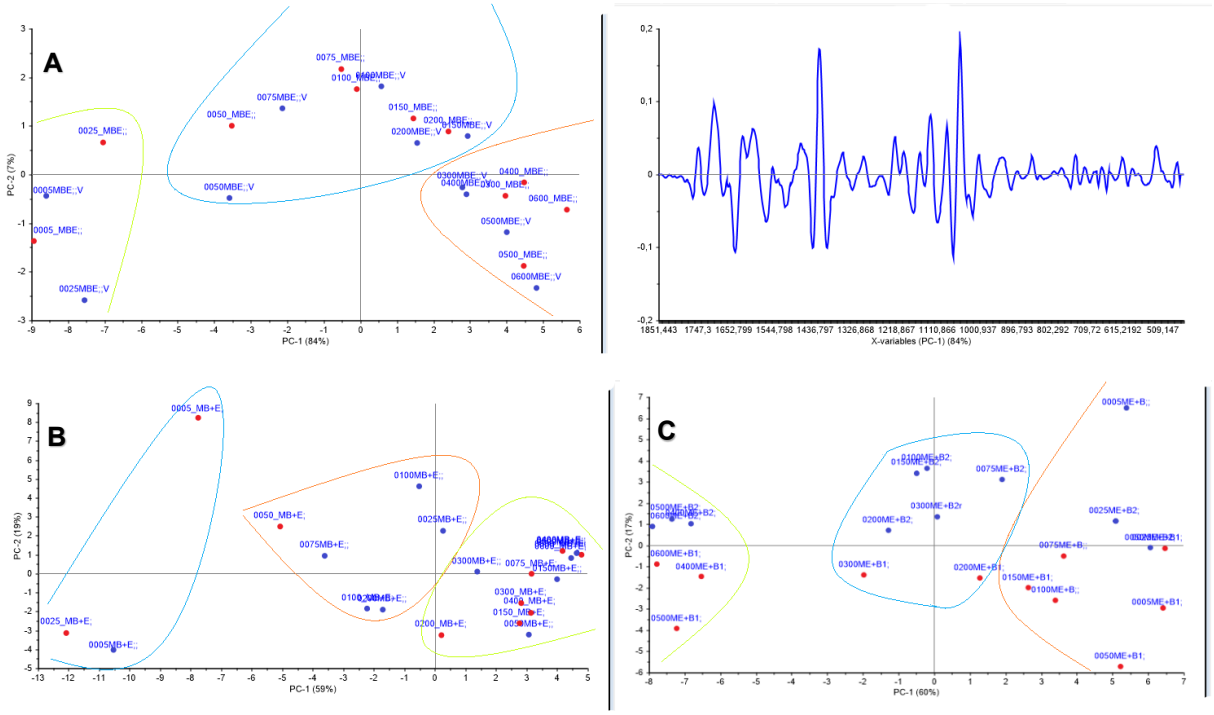

Figure 45. A) PCA score plot (left) and loadings (right) for MBE, with groupings separated with colors to clarify the variations between the hydrolysates that occur during the hydrolysis time. B) The score plots for MB+E and C) the score plot for ME+B, also with the colored separations.

The end-products from the six EPH reactions treated with a combination of both proteases are shown in **Figure 46**. The PCA score plot shows the MBE products marked in red, MB+E

marked with blue, and ME+B marked in yellow. MB+E was somewhat grouped, but MBE and ME+B were more spread and did not display any connection in the score plot. This spread was a natural result of MDPR treated with a combination of Endocut-02 and Bromelain. The two proteases have shown different selectivity towards the various parts of MDPR. Hence, the order in which the proteases were added would naturally be influencing the hydrolysate composition. Also, the composition of MDPR varied a lot in each EPH reaction, which further caused a variation within the duplicated series.

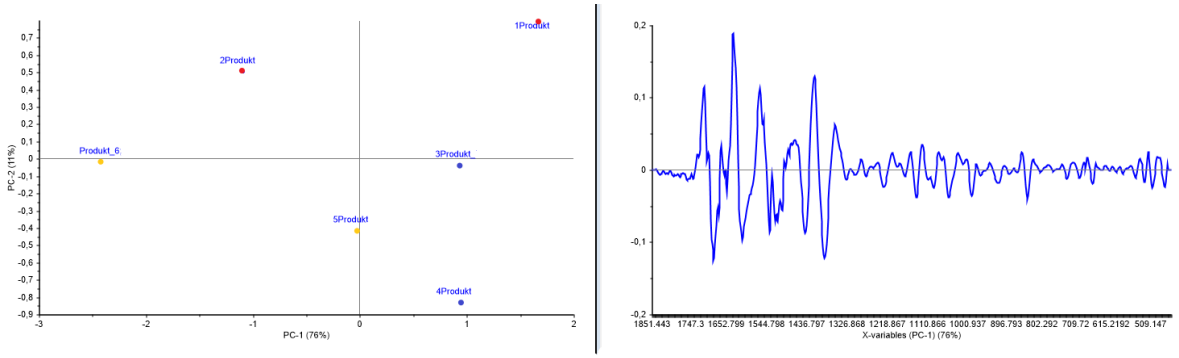

Figure 46. PCA scores and loadings for the final products after 60 minutes, from the mixed protease-treated MDPR. The MBE-products are marked in red, MB+E marked in blue, and the ME+B is marked yellow.

The end-products in spectra D) had a strongly present band in the amide I region, which probably is caused by the large-sized peptides released during heat-treatment. However, spectra A) – C) revealed that more of the terminal amino and carboxyl groups were produced during the hydrolysis, indicating that more of the proteins were degraded. Hence, the end products apparently contained a wide range of proteins and peptides of various sizes, but the large-sized peptides probably masked the small-sized peptides in the spectra.

*To sum up; it was observed that the most substantial differences between the materials treated with the two proteases appeared in the Amide I and II bond vibrations at ~1650 cm^{-1} and ~1550 cm^{-1} as well as the -NH_3^+ and -COO^- bond vibrations at ~1400 cm^{-1}, ~1500 cm^{-1}, and ~1580 cm^{-1}. The most significant variation in the lab-scale series treated with Endocut-02 or Bromelain was observed between SE and KB, and within the same RRM, SE and SB were most distant in the PCA score plot. For the lab-scale series of combined proteases, a different degradation pattern during hydrolysis time was observed regarding how the proteases were added. However, the end products showed almost identical spectra, matching the M_W during hydrolysis time profiles observed in section **4.4.2**, and the DH% during hydrolysis time in section **4.4.3**.*

5 General discussion, with challenges and improvements

This study aimed to optimize a lab-scale EPH process for better utilization of poultry RRM. Several analytical techniques were used to gain sufficient information about the proteins and peptides released during the EPH reactions and determine the protein yield of the lab-scale hydrolysates. The protein content (g) in the RRM was found by RMA (carried out by the ALS laboratory), and the protein content % was found in all the lab-scale hydrolysates by Dumas combustion analysis. Hence, from using the weight of the freeze-dried hydrolysates, together with the determined protein content from RMA and Dumas, the protein yield could be calculated for all the lab-scale hydrolysates, which was more industrial representative than the ER % determined during the preliminary study. The general discussion addresses the most important observations made during the study, with its challenges and suggested improvements.

Challenges and improvements of the lab-scale EPH process

During the first attempt at performing a lab-scale EPH, the collagen-rich materials were wrapped around the propeller during the reactions. Although the lab-scale EPH was optimized, a higher protein yield could be achieved if the materials were minced more thoroughly before the EPH was carried out. In this way, the substrate would have a larger surface area for the proteases to access, providing a higher protein yield. One drawback of grinding the materials more could be that the larger collagen peptides would not be solubilized since some of the larger peptides already had been broken during the grinding. Also, it depends on what the industry would want to do of pre-processing before the EPH. In this context, the protein yield relative to the costs associated with the pre-process would probably be a determining factor.

Through the lab-scale EPH with combined proteases, an increasing protease concentration did not result in a higher protein yield. Hence, an increasing concentration of the two proteases used in the present study would probably not affect the protein recovery. However, it cannot be ruled out that some of the other proteases used during the preliminary studies could have resulted in a higher protein yield. During the preliminary study, it was emphasized to find two proteases, which showed different selectivity against either myofibrillary proteins or collagen, and produced yield was not exclusively considered at the time. The most important outcome for the industry is to obtain a high yield from RRM that can be used in further applications. Fields of applications could be as a highly required protein and fat source for the globally growing population and, in general, provide an increased value of the RRM from the food industry.

Another value increase of the poultry RRM is biologically active components used in the pharmaceutical, cosmetic, or health food industry. However, before further use of the peptides, it is essential to provide information about the peptide composition produced through the EPH process.

One of the hypothesis at the beginning of the present study was that different proteins could be extracted from the poultry RRM within a defined time-frame during an EPH reaction. **Figure 47** illustrates how the two groups of proteins could be extracted individually from the same material (MDPR) but at different times during the EPH process. However, neither Endocut-02 nor Bromelain showed selectivity against just myofibrillary proteins or collagen. Instead, both proteases degraded both protein groups, which meant that the hypothesis illustrated in Figure 45 would not work in practice. Nevertheless, it was apparent that the degradation of the proteins was based on the two proteases' unique selectivity, which were reflected in the M_W profiles of the hydrolysates obtained from the separation by HP-SEC, and the structural differences in the hydrolysates that were shown in the FTIR spectra.

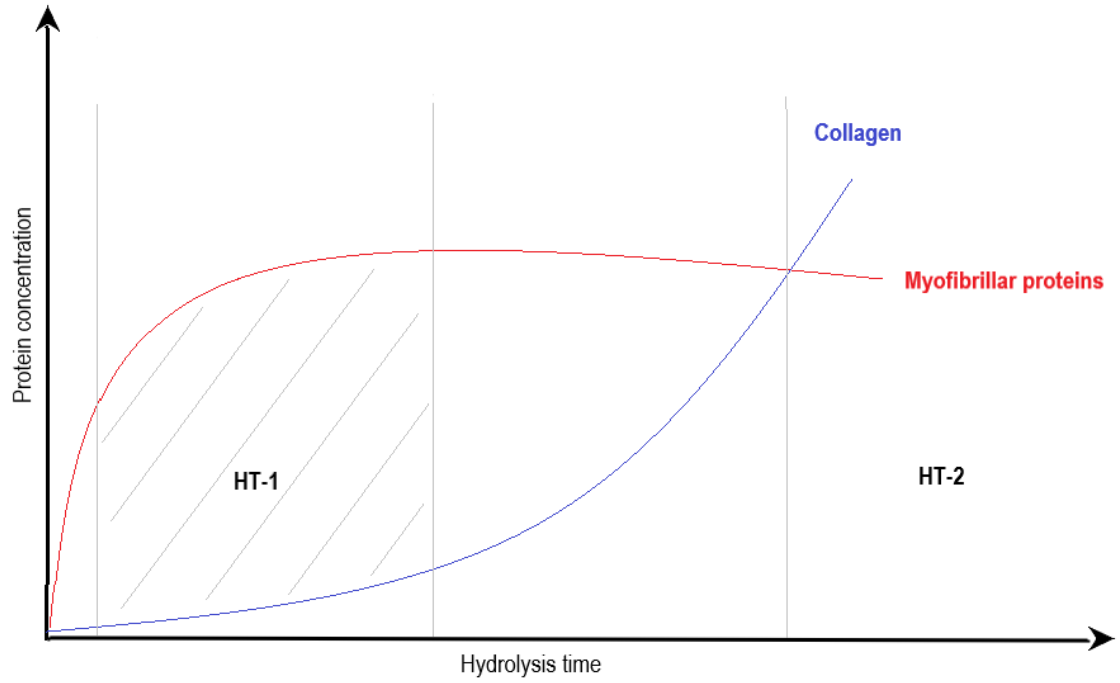

Figure 47. Graph of Endocut-02 and Bromelains degradation of myofibrillar proteins and collagen during hydrolysis time. Illustrates how myofibrillar proteins and collagen can be separated and extracted from MDPR in an EPH process at HT-1 or together at HT-2 (HT: Hydrolysis time), respectively.

Challenges and improvements during the hydrolysate analyses

During the study, one hypothesis was that large-sized peptides were released during heat-treatment. By combining HP-SEC and DH%, a low DH% with high M_W was shown for the end-products, while the hydrolysates collected before the end of reaction usually had a more normal peptide degradation profile with high DH% and low M_W. Furthermore, the HP-SEC chromatograms of collagen-rich materials such as tendons showed a distinct front of large peptides in the collagen-derived end-products. When the Hyp analysis showed minimal amounts of Hyp in all the hydrolysates between the initial phase and the end of the reaction, the hypothesis was strengthened with a sharp increase of Hyp in the end-products.

From studying the M_W of the materials treated with the two proteases, it was observed that Endocut-02 was releasing much larger peptides than Bromelain. Still, when combining the two proteases to the same solutions, the HP-SEC profiles of the end-products were almost identical, indicating that neither Endocut-02 nor Bromelain hindered the other from reaching their cleaving sites during the reactions. Moreover, the order in which the proteases were added did not affect the peptide profiles of the end-products.

A relatively large variation in protein yield was observed within the different series. Several replicates, providing a larger dataset, could decrease this variation and give a more accurate representation of the processed yield. Optimization of temperature and pH could have been investigated to see if a change in these parameters would affect the selectivity or activity of Endocut-02 and Bromelain. Earlier studies, where different temperatures and pH than used in the current study have revealed elevated Bromelain activity. From a process perspective, a disadvantage of adjusting the pH is that it usually requires the use of an acid or base that might result in high levels of salt in the final hydrolysate, which reduces the nutritional value of the product. Also, adjustments of the temperature may influence the nature of the proteins in the RRM. E.g., temperatures above 70 °C are reported to affect the proteins' secondary structure. Still, the advantage of raising the temperature considering the solubility of collagen is that higher temperatures could lead to an initial breakdown of the triple helix and a loss of the three-dimensional structure. In greater detail, since the tight configuration in the triple helix could protect the collagen molecule from the proteases, higher temperatures could result in a more accessible substrate and further lead to more solubilized collagen-peptides already from the EPH's initial phase.

The BioSep-SEC-s2000 column used during the separation of the hydrolysates was limited to separation of molecules between 1000 – 300 000 g/mol. That is, peptides above and below these sizes would not be properly separated. A two column-separation technique could be used to get a more extensive peptide separation of the hydrolysates. However, an additional column would provide a longer run time, which could be seen as a disadvantage. An alternative could be to separate the large-sized peptides from the smaller before they were injected into the HP-SEC system by, e.g., performing a membrane filtration and further use one column with the capacity to separate the largest peptides and one for separation of the smallest.

When analyzing the hydrolysates by FTIR, it was challenging to dilute the samples to the correct concentration and to put the correct film thickness onto the plate. One suggestion of improvement could be to perform Brix measurements of the hydrolysates in the preparatory work. Brix is measured using a refractometer that determines the degrees Brix (density) by measuring the refraction of light passing through the liquid sample (142). Brix measurement is a relatively rapid technique that can indicate the amount of dry matter in the liquid hydrolysates. Another alternative could be to resolve the freeze-dried hydrolysate instead of directly applying the liquid hydrolysate, which could provide better control of the concentration during the dilution step.

6 Conclusion and future work

Endocut-02 and Bromelain were chosen due to their selectivity towards collagen or myofibrillar proteins and provided the highest and lowest yield from tendons and CF, respectively. In the verification, the two proteases did not provide the same ER % as in the preliminary studies. However, the peptide distribution obtained from HP-SEC and the bond vibrations observed in the FTIR spectra revealed similar patterns as of the study by Dalsnes (107). A sample preparation method was developed for the collagen-rich hydrolysates, leading to collagen-peptide separation by HP-SEC without damaging the SEC-column.

Using a combination of HP-SEC, FTIR, RMA, DH%, Dumas, SDS-PAGE, and Hyp analyses provided quality parameters such as protein yield, M_W, DH%, and structural information regarding the hydrolysates peptide composition. Poultry RRM treated with each of the two proteases showed no major difference in protein yield % from using either Bromelain or Endocut-02, evident by a % RSD of 2.7 ≥ 10 % within the duplicated series. However, a large difference was observed by combining the two proteases, regardless of the order in which they were added. The main aim was to optimize an EPH process, using two different proteases with the possibility to enhance the protein yield, as illustrated in **Figure 48**, along with sub-goals and factors evaluated during the study. MDPR treated with a combination of both proteases did increase the protein yield by 13-20 %, with a % RSD of 1.6 ≥ 7.4 %, relative to the EPH using either Bromelain or Endocut-02

Due to the release of large-sized collagen peptides during the heated deactivation of collagen-rich materials, relative to the peptides released from myofibrillar proteins, the separation of the two protein groups could possibly be done after the reaction by, e.g., membrane filtration. Endocut-02 released proteins and protein-derivatives between an M_W of approximately 2000 – 5000 and 2000 – 11800 from CF and tendons, respectively, while Bromelain had a more relaxed selectivity towards the substrates, resulting in an M_W of approximately 1100 – 3000 and 1900 – 5500.

Repeatability: It was challenging to achieve good repeatability of the EPH processes due to the substrate's complexity with a composition of proteins from the complex materials used, which varied from each reaction.

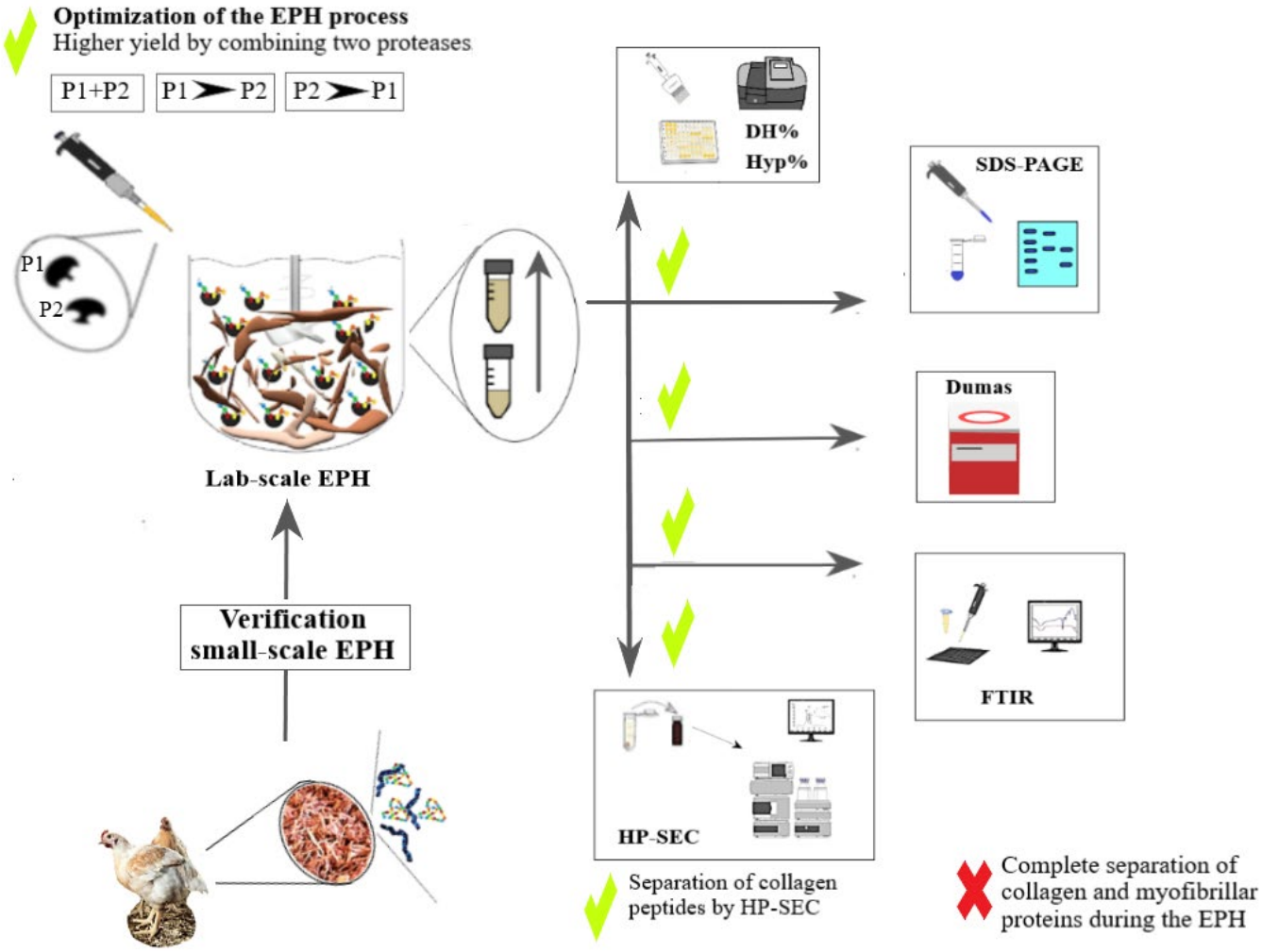

Figure 48. Overview of the aim, sub-goals, and factors that were evaluated during the present study. The optimized EPH process, using a combination of Bromelain and Endocut-02, provided a higher protein recovery from MDPR compared to using only one of the proteases. Product quality parameters were obtained by using a combination of classical biotechnological and analytical techniques, as illustrated.

The present study has been part of a larger project that will continue until the year 2022. The knowledge obtained during this study will be valuable in further research towards reaching a complete utilization of poultry RRM. However, the lab-scale EPH processing conditions need further optimization before being applied on an industrial scale.

6.1 Future work

During the present study, a lab-scale EPH process has been found that generated a higher yield using a combination of two proteases, and data have been presented where the peptide composition in the hydrolysates became more apparent. However, improvements can be made, and more information regarding the hydrolysates peptide composition can be obtained by using other analytical approaches, such as quantification of the hydrolysate products by, e.g., amino acid composition analyses, and identification of the proteins and protein derivatives by, e.g., LC-MS.

As mentioned in Section **5**, the focus was not exclusively on yield during the preliminary studies. Hence, it would be interesting to investigate whether the 23 proteases not used during the present study, could lead to a better protein yield. A combination of two proteases provided a higher protein recovery than each protease alone, which should be in mind in further investigation of other proteases.

The Amino acid composition (AAC) analyses requires approximately 1 µg of the sample, which has to be derivatized, usually in a pre-column before separation by RP-LC. However, several derivatization and separation principles can be used (143). AAC analysis could be done to quantify the proteins and protein-derivatives in the hydrolysates where the number of the individual residues present in the peptide, is characteristic for each peptide and protein (143). Hence, the AAC can reveal which proteins are degraded and released by the proteases and valuable information concerning future applications can be achieved (125).

Further investigation in identifying the proteins and protein-derivatives in the hydrolysates can provide valuable information concerning future applications and can be done through several separation and detection methods. MS is a useful tool for identifying proteins, peptides, and free amino acids in the hydrolysates. This is especially important in the search for bioactive peptides. Zeng, S. et al., searched for biologically active peptides from food proteins by HPLC ESI-MS/MS (144, 145). HPLC ESI-MS/MS is a simple, rapid, and sensitive method for analyzing peptides in complex samples. Several MS systems can be successfully used to identify larger peptides, such as Matrix-assisted Laser Desorption Ionization combined with Time of Flight analyzer (MALDI-TOF-MS). Khiari et al. used MALDI-TOF-MS to complement the SEC analyses and accurately determined the molar mass (g/mol) profile of

turkey head collagen peptides (54). Also, the use of ACN and TFA in the mobile phase, as in the present study, allows for successful SEC-MS experiments (89).

References

1. Kristoffersen KA. Expanding the analytical toolbox for characterization of proteolytic reactions: Advances in FTIR spectroscopy and classical methods [Philosophiae Doctor Thesis]. Ås, Norway: Norwegian University of Life Sciences; 2019.
2. Aspevik T, Oterhals A, Ronning SB, Altintzoglou T, Wubshet SG, Gildberg A, et al. Valorization of Proteins from Co- and By-Products from the Fish and Meat Industry. Top Curr Chem (Cham). 2017;375(3):53.
3. Mühlbradt T, Stensland PC, Kastmann PA, Singstad I, Hatling R, Koch PM. Innspill til en ny retning for Norge: Drømmeløftet 2016 Norway: Innovasjon Norge; 2016 [Available from: www.innovasjonnorge.no.
4. Lindberg D, Aaby K, Borge GIA, Haugen JE, Nilsson A, Rødbotten R, et al. Kartlegging av restråstoff fra jordbruket. Norway: Råvare og prosess, Mat og helse; 2016. Report No.: 67/2016.
5. Smith P, Howden M, Krug T, Masson-Delmotte V, Mbow C, Pörtner HO, et al. Climate Change and Land - An IPCC special report on climate change, desertification, land degradation, sustainable land management, food security, and greenhouse gas fluxes in terrestrial ecosystems. United States of America: Cambridge University Press; 2017.
6. Food and Agriculture Organization of the United Nations (FAO). Food Outlook - Biannual Report on Global Food Markets. 2019.
7. Food and Agriculture Organization of the United Nations (FAO). The State of Food and Agriculture: Climate Change, Agriculture and Food Security. 2016.
8. United Nations Environment. Global Environment Outlook (GEO-6). 2019.
9. United Nations Climate Change Secretariat. Climate action and support trends. 2019.
10. Smith P, Bustamante M, Ahammad H, Clark H, Dong H, Elsiddig EA, et al. Climate Change 2014: Mitigation of Climate Change. Constribution of Working group III to the Fifth Assessment Report of the Intergovernmental Panel on Climate Change. United States of America: Cambridge University Press; 2014.
11. Ahmad T, Ismail A, Ahmad SA, Khalil KA, Kumar Y, Adeyemi KD, et al. Recent advances on the role of process variables affecting gelatin yield and characteristics with special reference to enzymatic extraction: A review. Food Hydrocolloids. 2017;63:85-96.
12. Hart DJ, Hadad CM, Craine LE, Hart H, editors. Amino Acids, Peptides, and Proteins in Organic Chemistry: A Brief Course 13 ed. Belmont, United State of America: Brooks/Cole, Cengage Learning 2013.
13. Walsh G, editor. Protein Structure and Engineering in Proteins: Biochemistry and Biotechnology. 2 ed. United Kingdom: John Wiley & Sons, incorporated.; 2014.
14. Steward K. Amino Acids – the Building Blocks of Proteins. Technology Networks. 2019
15. Jackson M, Mantsch HH. The use and misuse of FTIR spectroscopy in the determination of protein structure. Crit Rev Biochem Mol Biol. 1995;30(2):95-120.
16. Luo Y, Matejic T, Ng C-K, Nunnally B, Porter T, Raso S, et al., editors. 8 - Characterization and Analysis of Biopharmaceutical Proteins. Separation Science and Technology: Academic Press; 2011.
17. Bowler BE. Residual structure in unfolded proteins. Curr Opin Struct Biol. 2012;22(1):4-13.
18. Arrondo JLR, Muga A, Castresana J, Goni FM. Quantitative studies of the structure of proteins in solution by fourier-transform infrared spectroscopy. Prog Biophys Mol Biol. 1993;59(1):23-56.
19. Lima RCL, Berg RS, Ronning SB, Afseth NK, Knutsen SH, Staerk D, et al. Peptides from chicken processing by-product inhibit DPP-IV and promote cellular glucose uptake: potential ingredients for T2D management. Food & Function. 2019;10(3):1619-28.
20. Xiong YL. Muscle proteins. Proteins in Food Processing. 2th ed. United States of America: Woodhead Publishing; 2018. p. 127-48.
21. Doherty MK, McLean L, Hayter JR, Pratt JM, Robertson DH, El-Shafei A, et al. The proteome of chicken skeletal muscle: changes in soluble protein expression during growth in a layer strain. Proteomics. 2004;4(7):2082-93.

22. Gross J. Collagen. Scientific American, a division of Nature America, Inc. 1961;204(5):120-34.
23. Ottani V, Raspanti M, Ruggeri A. Collagen structure and functional implications. Micron. 2001;32(3):251-60.
24. iStock. Istockphoto. Canada: Getty Images; 2020.
25. Liu D, Nikoo M, Boran G, Zhou P, Regenstein JM. Collagen and gelatin. Annu Rev Food Sci Technol. 2015;6:527-57.
26. Kadler KE, Holmes DF, Trotter JA, Chapman JA. Collagen fibrill formation. Biochem J. 1996;15(316):1-11.
27. Regenstein JM, Zhou P, editors. Collagen and gelatin from marine by-products in Maximising the Value of Marine By-Products. United States of America: Woodhead Publishing; 2007.
28. Gómez-Guillén MC, Giménez B, López-Caballero ME, Montero MP. Functional and bioactive properties of collagen and gelatin from alternative sources: A review. Food Hydrocolloids. 2011;25(8):1813-27.
29. Kempka AP, Ulson de Souza SMAG, Ulson de Souza AA, Prestes RC, Ogliari D. Influence of bloom number and plastifiers on gelatin matrices produced for enzyme immobilization. Brazilian Journal of Chemical Engineering 2014;31(1):95-108.
30. Nchienzia HA, Morawicki RO, Gadang VP. Enzymatic hydrolysis of poultry meal with endo- and exopeptidases. Poultry science. 2010;89(10):2273-80.
31. Karim AA, Bhat R. Fish gelatin: properties, challenges, and prospects as an alternative to mammalian gelatins. Food Hydrocolloids. 2009;23(3):563-76.
32. Kittiphattanabawon P, Benjakul S, Visessanguan W, Shahidi F. Effect of Extraction Temperature on Functional Properties and Antioxidative Activities of Gelatin from Shark Skin. Food and Bioprocess Technology. 2010;5(7):2646-54.
33. Phanturat P, Benjakul S, Visessanguan W, Roytrakul S. Use of pyloric caeca extract from bigeye snapper (Priacanthus macracanthus) for the production of gelatin hydrolysate with antioxidative activity. LWT - Food Science and Technology. 2010;43(1):86-97.
34. Lobo V, Patil A, Phatak A, Chandra N. Free radicals, antioxidants and functional foods: Impact on human health. Pharmacogn Rev. 2010;4(8):118-26.
35. Jridi M, Nasri R, Lassoued I, Souissi N, Mbarek A, Barkia A, et al. Chemical and biophysical properties of gelatins extracted from alkali-pretreated skin of cuttlefish (Sepia officinalis) using pepsin. Food Research International. 2013;54(2):1680-7.
36. GMIA. Gelatin-Handbook. In: America Gmio, editor. United States of America2019. p. 1-27.
37. Du L, Khiari Z, Pietrasik Z, Betti M. Physicochemical and functional properties of gelatins extracted from turkey and chicken heads. Poultry Science Association Inc. 2013;92(9):2463-74.
38. Gudipati V, Kannuchamy N, editors. Recovery of Gelatin with Improved Functionality from Seafood Processing Waste in Kim SK. (eds) Seafood Processing By-Products. United States of America: Springer, New York, NY; 2014.
39. Ward AG. The physical properties of gelatin solutions and gels. British Journal of Applied Physics. 1954;5(3):85-90.
40. Guo L, Colby RH, Lusignan CP, Whitesides TH. Kinetics of Triple Helix Formation in Semidilute Gelatin Solutions. Macromolecules. 2003;36(26):9999-10008.
41. Gray VA, Marques C, R. M, Ewart C, Riva T, M.D.R.T. J, et al. Use of Enzymes in the Dissolution Testing of Gelatin Capsules and Gelatin-Coated Tablets-Revisions to Dissolution and Disintegration and Dissolution of Dietary Supplements. Dissolution Technologies. 2014;21(4):6-18.
42. Barrett AJ. Proteases. Current Protocols in Protein Science. 2000;21(1):21.1.1-.1.12.
43. Rao MB, Tanksale, A.M., Ghatge, M.S., and Deshpande, V.V. Molecular and Biotechnological Aspects of Microbial Proteases. 1998;62(3):597-635.
44. Rutherfurd SM. Methodology for determining degree of hydrolysis of proteins in hydrolysates: A review. Journal of AOAC International. 2010;93(5):1515–22.
45. Taussig SJ, Batkin S. Bromelain, the enzyme complex of pineapple (Ananas comosus) and its clinical application. Journal of Ethnopharmacology. 1988;22:191-203.

46. Heinicke RM, Gortner WA. Stem bromelain: a new protease preparation from pineapple plants. Economic Botany. Economic Botany. 1957;11(3):225–34.
47. Tochi BN, Wang Z, Xu SY, Zhang W. Therapeutic Application of Pineapple Protease (Bromelain): A Review. Pakistan Journal of Nutrition. 2008;7(4):513-20.
48. Taylorzyme. Costumized enzyme solutions Denmark: Taylorzyme Aps; 2015 [Available from: https://tailorzyme.com/contact-tailorzyme/.
49. Sellami-Kamoun A, Haddar A, Ali Nel H, Ghorbel-Frikha B, Kanoun S, Nasri M. Stability of thermostable alkaline protease from Bacillus licheniformis RP1 in commercial solid laundry detergent formulations. Microbiol Res. 2008;163(3):299-306.
50. Jutamongkon R, Charoenrein S. Effect of Temperature on the Stability of Fruit Bromelain. Kasetsart J (Nat Sci). 2010;44(5):943-8.
51. Osamura T, Okuda M, Yamaguchi A, Ohtake K, Sakamoto K, Takimura Y. Variants of the industrially relevant protease KP-43 with suppressed activity under alkaline conditions developed using expanded genetic codes. Biochem Biophys Rep. 2019;17:93-6.
52. Bocker U, Wubshet SG, Lindberg D, Afseth NK. Fourier-transform infrared spectroscopy for characterization of protein chain reductions in enzymatic reactions. Analyst. 2017;142(15):2812-8.
53. Clemente A. Enzymatic Protein hydrolysates in human nutrision. Food Science & Technology. 2000;11(7):254-62.
54. Khiari Z, Ndagijimana M, Betti M. Low molecular weight bioactive peptides derived from the enzymatic hydrolysis of collagen after isoelectric solubilization/precipitation process of turkey by-products. Poultry Science A. 2014;93(9):2347-62.
55. Kobayashi H, Suzuki M, Kanayama N, Terao T. A soybean Kunitz trypsin inhibitor suppresses ovarian cancer cell invasion by blocking urokinase upregulation. Clin Exp Metastasis. 2004;21(2):159-66.
56. Hayes M. Biological Activities of Proteins and Marine-derived Peptides from Byproducts and Seaweeds. In: Kim S-K, editor. Marine Proteins and Peptides: John Wiley & Sons, Ltd; 2013. p. 139-65.
57. Kim S-K, Mendis E. Bioactive compounds from marine processing byproducts – A review. Food Research International. 2006;39(4):383-93.
58. Daliri EB, Oh DH, Lee BH. Bioactive Peptides. Foods. 2017;6(5):76-97.
59. Margot A, Flaschel E, Renken A. Empirical kinetic models for tryptic whey-protein hydrolysis. Process Biochemistry. 1997;32(3):217-23.
60. Folador JF, Karr-Lilienthal LK, Parsons CM, Bauer LL, Utterback PL, Schasteen CS, et al. Fish meals, fish components, and fish protein hydrolysates as potential ingredients in pet foods. J Anim Sci. 2006;84(10):2752-65.
61. Sathe SK, Teuber SS, Roux KH. Effects of food processing on the stability of food allergens. Biotechnol Adv. 2005;23(6):9-423.
62. Hugaas Rugeri. Dyrevelferdsrapport Norway: Norsk Kylling og Hugaas Rugeri; 2018 [Available from: https://docplayer.me/146434113-Dyrevelferdsrapport-norsk-kylling-og-hugaas-rugeri-2018.html.
63. Montowska M, Pospiech E. Species-specific expression of various proteins in meat tissue: proteomic analysis of raw and cooked meat and meat products made from beef, pork and selected poultry species. Food Chem. 2013;136(3-4):1461-9.
64. Baeza E, Salichon MR, Marche G, Wacrenier N, Dominguez B, Culioli J. Effects of age and sex on the structural, chemical and technological characteristics of mule duck meat. Br Poult Sci. 2000;41(3):300-7.
65. Haris PI, Severcan F. FTIR spectroscopic characterization of protein structure in aqueous and non-aqueous media. Journal of Molecular Catalysis B: Enzymatic. 1999;7(1-4):207-21.
66. Wubshet SG, Wold JP, Afseth NK, Böcker U, Lindberg D, Ihunegbo FN, et al. Feed-Forward Prediction of Product Qualities in Enzymatic Protein Hydrolysis of Poultry By-products: a Spectroscopic Approach. Food and Bioprocess Technology. 2018;11(11):2032-43.
67. Wubshet S, Lindberg D, Veiseth-Kent E, Kristoffersen KA, Böcker U, Washburn KE, et al., editors. Bioanalytical Aspects in Enzymatic Protein Hydrolysis of By-Products: Academic Press; 2019.

68. McClements DJ. Analysis of food products United States of America: University of Massachusetts: Department of Food Science; 2020 [Available from: https://people.umass.edu/~mcclemen/581Introduction.html.
69. ALS Laboratories UK. Analysetjenester innen miljø, inneklima, bygg og avfall, næringsmidler og produkter. United Kingdom: ALS Laboratories UK Ltd; 2020 [Available from: https://www.alsglobal.no/.
70. Ibanez E, Cifuentes A. New analytical techniques in food science. Crit Rev Food Sci Nutr. 2001;41(6):413-50.
71. Johnsen EF. Metodespesifikasjon: CHNS (DUMAS / total-nitrogen). In: akvakulturvitenskap Ifh-o, editor. Norway: NMBU; 2020. p. 1-2.
72. Thompson M, Owen L, Wilkinson K, Wood R, Damant A. A comparison of the Kjeldahl and Dumas methods for the determination of protein in foods, using data from a proficiency testing scheme. Analyst. 2002;127(12):1666-8.
73. Moore JC, DeVries JW, Lipp M, Griffiths JC, Abernethy DR. Total Protein Methods and Their Potential Utility to Reduce the Risk of Food Protein Adulteration. Comprehensive Reviews in Food Science and Food Safety. 2010;9(4):330-57.
74. Simonne AH, Simonne EH, Eitenmiller RR, Mills HA, Cresman III CP. Could the Dumas Method Replace the Kjeldahl Digestion for Nitrogen and Crude Protein Determinations in Foods? Journal of the Science of Food and Agriculture. 1997;73(1):39-45.
75. Miller EL, Bimbo AP, Barlow SM, Sheridan B. Repeatability and Reproducibility of Determination of the Nitrogen Content of Fishmeal by the Combustion (Dumas) Method and Comparison with the Kjeldahl Method: Interlaboratory Study. Journal of AOAC International. 2007;90(1):6-20.
76. Nielsen PM, Petersen D, Dambmann C. Improved Method for Determining Food Protein Degree of Hydrolysis. Journal of Food Science. 2001;66(5):642-6.
77. Hernandez MJM, Domingo EB, Camafias RMV, Alvarez-Coque MCG. Evaluation of the proteolysis degree with the o-phthalaldehyde[N-acetyl-L-cysteine reagent Fresenius` Journal of Analytical Chemistry. 1990;338(1):62-5.
78. Satake K, Okuyama T, Ohashi M, Shinoda T. The spectrophotometric determination of amine, amino acid and peptide with 2, 4, 6-trinitrobenzene 1-sulfonic acid. The Journal of Biochemistry. 1960;47(5):654-60.
79. Spellman D, McEvoy E, O'Cuinn G, FitzGerald RJ. Proteinase and exopeptidase hydrolysis of whey protein: Comparison of the TNBS, OPA and pH stat methods for quantification of degree of hydrolysis. International Dairy Journal. 2003;13(6):447-53.
80. Seibelsimon MJ, Robinscaren P, Gundberg M, editors. Biochemical Dynamics: Academic Press; 2007.
81. Avioli LV, Prockop DJ. Collagen degradation and the response to parathyroid extract in the intact rhesus monkey. J Clin Invest. 1967;46(2):217-24.
82. SIGMA-ALDRICH. Hydroxyproline Assay Kit. Technical Bulletin. United States of America: Sigma-Aldrich Co. LLC; 2020. p. 1-4.
83. Twyman RM. Principles of Proteomics. United States of America: Garland Science, Taylor & Francis Group, LLC; 2013.
84. Bio-Rad laboratories. A Guide to Polyacrylamide Gel Electrophoresis and Detection. 2017. p. 1-92.
85. Chrambach A, Rodbard D. Polyacrylamide Gel Electrophoresis. Science. 1971;172(3982):440-51.
86. Lundanes E, Reubsaet L, Greibrokk T. Chromatography - Basic principles, Sample Preparations and Related Methods. 1 ed. Germany: Wiley - VCH Verlag GmbH & Co. KGaA; 2014. 1-207 p.
87. Invitrogen by life technologies. NuPAGE®Technical Guide: General information and protocols for using the NuPAGE® electrophoresis system. United States of America: Life Technologies Corporation; 2010 p. 60.

88. Garcia MC. The effect of the mobile phase additives on sensitivity in the analysis of peptides and proteins by high-performance liquid chromatography-electrospray mass spectrometry. J Chromatogr B Analyt Technol Biomed Life Sci. 2005;825(2):111-23.
89. Fekete S, Beck A, Veuthey JL, Guillarme D. Theory and practice of size exclusion chromatography for the analysis of protein aggregates. J Pharm Biomed Anal. 2014;101:161-73.
90. Qian J, Tang Q, Cronin B, Markovich R, Rustum A. Development of a high performance size exclusion chromatography method to determine the stability of Human Serum Albumin in a lyophilized formulation of Interferon alfa-2b. J Chromatogr A. 2008;1194(1):48-56.
91. Josic D, Kovac S. Reversed-Phase High Performance Liquid Chromatography of Proteins. Current Protocols in Protein Science. 2010;61(1):1-22.
92. Barth HG, Boyes BE, Jackson C. Size Exclusion Chromatography and Related Separation Techniques. Analytical Chemistry. 1998;70(12):251-78.
93. Mori S, Barth HG. Size Exclusion Chromatography: Fundamental Concepts. Laboratory S, editor. Germany: Springer-Verlag Berlin Heidelberg; 1999. 234 p.
94. Striegel A, Yau WW, Kirkland JJ, Bly DD. Modern size-exclusion liquid chromatography: practice of gel permeation and gel filtration chromatography. 2 ed. United States of America: John Wiley & Sons; 2009. 496 p.
95. Hong P, Koza S, Bouvier ES. Size-Exclusion Chromatography for the Analysis of Protein Biotherapeutics and their Aggregates. J Liq Chromatogr Relat Technol. 2012;35(20):2923-50.
96. Tran BQ, Hernandez C, Waridel P, Potts A, Barblan J, Lisacek F, et al. Addressing Trypsin Bias in Large Scale (Phospho)proteome Analysis by Size Exclusion Chromatography and Secondary Digestion of Large Post-Trypsin Peptides. Journal of Proteome Research. 2011;10(2):800-11.
97. Johns PW, Jacobs WA, Phillips RR, McKenna RJ, O'Kane KA, McEwen JW. Characterisation of peptide molecular mass distribution in commercial hydrolysates and hydrolysate-based nutritional products. Food Chemistry. 2011;125(3):1041-50.
98. Zimmermann B, Kohler A. Optimizing Savitzky-Golay parameters for improving spectral resolution and quantification in infrared spectroscopy. Applied Spectroscopy. 2013;67(8):892-902.
99. Rintoul L, Panayiotou H, Kokot S, George G, Cash G, Frost R, et al. Fourier transform infrared spectrometry: a versatile technique for real world samples. Analyst. 1998;123(4):571–7.
100. Barth A. Infrared spectroscopy of proteins. Biochim Biophys Acta. 2007;1767(9):1073-101.
101. Siebert F. Infrared spectroscopy applied to biochemical and biological problems. Methods Enzymol. 1995;246:501-26.
102. Perkins WD, editor. Fourier Transform-Infrared Spectroscopy 1ed. United States of America: The Perkin-Elmer Corporation; 1986.
103. Hilderson HJ, Ralston GB, editors. Subcellular Biochemistry. Netherlands: Kluwer Academic Publishers Group; 1994.
104. McMurry J. Fundamentals of Organic Chemistry. 7 ed. United States of America: Brooks/Cole, Cengage Learning; 2011.
105. Hong H, Chaplot S, Chalamaiah M, Roy BC, Bruce HL, Wu J. Removing Cross-Linked Telopeptides Enhances the Production of Low-Molecular-Weight Collagen Peptides from Spent Hens. J Agric Food Chem. 2017;65(34):7491-9.
106. Prystupa DA, Donald AM. Infrared study of gelatin conformations in the gel and sol states. Polymer Gels and Networks. 1996;4(2).
107. Dalsnes MR. Enzymatic protein hydrolysis of residual raw materials from poultry: A study of proteases' selectivity toward collagen and myofibrillar proteins [Master`s thesis]. Trondhein, Norway: Norwegian University of Science and Technology Faculty of Natural Sciences; 2019.
108. Megazyme. Assay of endo-protease using azo-casein Ireland: Megazyme International Ireland; 2007 [Available from: https://www.megazyme.com/documents/Booklet/S-AZCAS_DATA.pdf.
109. Adler-Nissen J. Determination of the Degree of Hydrolysis of Food Protein Hydrolysates by Trinitrobenzenesulfonic Acid. Journal of Agricultural and Food Chemistry. 1979;27(6):1256–62.

110. Church FC, Swaisgood HE, Porter DH, Catignani GL. Spectrophotometric Assay Using o-Phthaldialdehyde for Determination of Proteolysis in Milk and Isolated Milk Proteins. Journal of Dairy Science. 1983;66(6):1219-27.
111. Kristoffersen KA, Hunnes LMG, Bøcker U, Lindberg D, Aafseth NK. Fourier-transform infrared spectroscopy as a tool to monitor the release of collagen derived peptides during enzymatic protein hydrolysis processing [unpublished work]. 2021.
112. Maleki MR, Mouazen AM, Ramon H, De Baerdemaeker J. Multiplicative Scatter Correction during On-line Measurement with Near Infrared Spectroscopy. Biosystems Engineering. 2007;96(3):427-33.
113. Barnes RJ, Dhanoa MS, S.J. L. Standard Normal Variate Transformation and De-Trending of Near-Infrared Diffuse Reflectance Spectra. Applied Spectroscopy. 1989;43(5):772–7.
114. Grisanti E, Totska M, Huber S, Krick Calderon C, Hohmann M, Lingenfelser D, et al. Dynamic Localized SNV, Peak SNV, and Partial Peak SNV: Novel Standardization Methods for Preprocessing of Spectroscopic Data Used in Predictive Modeling. Journal of Spectroscopy. 2018;2018:1-14.
115. Perisic N, Afseth NK, Ofstad R, Kohler A. Monitoring protein structural changes and hydration in bovine meat tissue due to salt substitutes by Fourier transform infrared (FTIR) microspectroscopy. J Agric Food Chem. 2011;59(18):10052-61.
116. Böcker U. Fourier-transform infrared microspectroscopy of muscle food - process-related changes in secondary structure of myofibrillar proteins and their relationships to meat functional properties [Philosophiae Doctor Thesis]. Ås, Norway: Norwegian University of Life Science; 2007.
117. Brown SD. Multivariate analysis in practice: A training package. Chemometrics. 1995;9(6):521-5.
118. Esbensen K, Schönkopf S, Midtgaard T. Multivariate Analysis in Practice. Journal of Chemometrics. 1994;9(6):441-531.
119. Wubshet SG, Mage I, Bocker U, Lindberg D, Knutsen SH, Rieder A, et al. Analytical methods - Calibration SEC: Supplementary material for FTIR as a rapid tool for monitoring average molecular weight during enzymatic protein hydrolysis of food processing by-products. In: Nofima AS Norwegian Institute of Food FaAR, editor. Norway2017.
120. Wubshet SG, Måge I, Böcker U, Lindberg D, Knutsen SH, Rieder A, et al. FTIR as a rapid tool for monitoring molecular weight distribution during enzymatic protein hydrolysis of food processing by-products. Analytical Methods. 2017;9(29):4247-54.
121. GE Healthcare. Maintenance and cleaning of size exclusion chromatography columns. United Kingdom: GE Healthcare UK; 2015. p. 1-7.
122. Elementar Analysensysteme GmbH. vario EL III CHNOS Elemental Analyzer: Operating Instructions. Germany: Elementar Analysensysteme GmbH; 2005. p. 1-59.
123. Franco DG, Spalanzani RN, Lima EE, Marchetti CR, Silva PO, Masui DC, et al. Biochemical properties of a serine protease fromAspergillus flavusand application in dehairing. Biocatalysis and Biotransformation. 2017;35(4):249-59.
124. Eason JR, Ryan D, Page B, Watson L, Coupe SA. Harvested broccoli (Brassica oleracea) responds to high carbon dioxide and low oxygen atmosphere by inducing stress-response genes. Postharvest Biology and Technology. 2007;43(3):358-65.
125. Lapena D, Vuoristo KS, Kosa G, Horn SJ, Eijsink VGH. Comparative Assessment of Enzymatic Hydrolysis for Valorization of Different Protein-Rich Industrial Byproducts. J Agric Food Chem. 2018;66(37):9738-49.
126. Singh SP, EEssary EO. Factors influencing dressing precentage and tissue comp. in broilers. Poultry Science. 1973;53(6):2143–7.
127. Grey TC, Robinson D, Jones JM, Stock SW, Thomas NL. Effect of age and sex on the composition of muscle and skin from a commercial broiler strain. Br Poult Sci. 1983;24(2):219-31.
128. Berri C, Wacrenier N, Millet E, Bihan-Duval L. Effect of Selection for Improved Body Composition on Muscle and Meat Characteristics of Broilers from Experimental and Commercial Lines. Poultry science. 2001;80(7):833-8.

129. Neuman RE, Logan MA. The Determination of Collagen and Elastin in Tissues. Journal of Biological Chemistry. 1950;186(2):549-56.
130. Koolmees PA, Bijker PG. Histometric and chemical methods for determining collagen in meats. Vet Q. 1985;7(2):84-90.
131. Lindberg D, et a. Effects of poultry raw material variation and choice of protease on protein hydrolysate quality [unpublished work]. 2020.
132. Shoulders MD, Raines RT. Collagen structure and stability. Annu Rev Biochem. 2009;78:929-58.
133. Mine K, Fuchihashi D. Labicons version 1.2 Labicons; 2020.
134. Deyl Z, I. M. Advanced separation methods for collagen parent a-chains, their polymers and fragments. J Chromatogr B Biomed Sci. 2000;739(1):3–31.
135. Sotelo CG, Comesaña MB, Ariza PR, Pérez-Martín RI. Characterization of Collagen from Different Discarded Fish Species of the West Coast of the Iberian Peninsula. Journal of Aquatic Food Product Technology. 2015;25(3):388-99.
136. Rabotyagova OS, Cebe P, Kaplan DL. Collagen Structural Hierarchy and Susceptibility to Degradation by Ultraviolet Radiation. Mater Sci Eng C Mater Biol Appl. 2008;28(8):1420-9.
137. Claeys E, Uytterhaegen L, Buts B, Demeyer D. Quantification of Beef Myofibrillar Proteins by SDS-PAGE Meat Science. 1995;39(2):177-93
138. Malaker SA, Pedram K, Ferracane MJ, Bensing BA, Krishnan V, Pett C, et al. The mucin-selective protease StcE enables molecular and functional analysis of human cancer-associated mucins. Proc Natl Acad Sci U S A. 2019;116(15):7278-87.
139. Shwetha S, Advitha P, Rajeswari P, Hariram N. Non-specific Subtilisin Producing Isolates KLU119 Cloning and Expression in pET24a Vector. J Mol Biol Biotech. 2017;2(3:9):1-7.
140. Aryee ANA, Agyei D, Udenigwe CC, editors. Proteins in Food Processing: Impact of processing on the chemistry and functionality of food proteins. 2 ed. United Kingdom: Woodhead Publishing; 2018.
141. Stuart BH. Infrared Spectroscopy : Fundamentals and Applications. Chichester, UK: John Wiley & Sons; 2004 [cited 2020 October 11th]. Available from: http://search.ebscohost.com.ezproxy.uio.no/login.aspx?direct=true&db=nlebk&AN=114408&site=ehost-live.
142. Mettler-Toledo. Brix Measurement and Brix Meters United Kingdom: Mettler-Toledo Ltd.; 2020 [Available from: https://www.mt.com/gb/en/home/perm-lp/product-organizations/ana/brix-meters.html.
143. Fountoulakis M, Lahm HW. Hydrolysis and amino acid composition analysis of proteins. Journal of Chromatography A. 1998;826(2):109-34.
144. Zeng SR, Wang YP, Bai XJ, Lin WL, Yang M, Xing HP. Determination of meaty peptide in enzymatic hydrolyzate of beef protein by HPLC-MS. Korean Journal of Chemical Engineering. 2008;25(5):1120-4.
145. Zeng SR, Wang YP, Zhang J, Yang M. Expression and identification of a small recombinant beefy meaty peptide secreted by the methylotrophic yeast Pichia pastoris. African Journal of Microbiology Research. 2010;4(24): 2754-62.

7 Appendix

7.1 Proteases used during the activity screening

Table 18. The 25 proteases used in the activity screening, with their optimal temperature- and pH-range, and genereral information of the proteases provided by the vendors (48).

Protease	Vendor	Activity	Food grade	General description	Form	pH	Temp ºC	Source
Alcalase 2.4L	Novozymes/Sigma	Endo/exo	no	Subtilisin A + 3 other enzymes	Liquid	7.0-10	30 - 70	B. licheniformis
Bromelain	ultra bio-logics	Endo	yes	lys-ala-tyr-glu (non spesific cystein prot)	Liquid	4.0 - 9.0	40 - 65	Ananas comosus
Corolase 2TS	AB enzymes/	Endo	yes	thermolysin (Ile - Leu - Val - Phe-NH2), extracellular neutral metalloprotease.	Liquid	6-9	up to 70	Bacillus stearothermophilus
Corolase 7090	AB Enzymes	Endo	yes	metallo endopeptidase	Liquid	6.5-7.5	45-70	Bacillus subtilis
ENDOCUT-01	Tailorzyme ApS	Endo	yes	neutral endo-protease	Liquid	6.0-8.0	45-55	controlled fermentation of Bacillus subtilis
ENDOCUT-02	Tailorzyme ApS	Endo	yes	alkaline protease, broad specificity	Liquid	(6)7,0-10	55-65	controlled fermentation of Bacillus Licheniformis
ENDOCUT-03	Tailorzyme ApS	Endo	yes	alkali endo-protease, extra high temperature and pH tolerance	Liquid	7-10	55-70	submerged fermentation of Bacillus Clausii? (06?)
Flavourzyme	Novozymes	Exo	no	aminopeptidase, dipeptidylpeptidase, endopeptidase, a-amylase	Liquid	5,0-7,0	35-65	Aspergillus oryzae
FoodPro 30L	DuPont-Danisco	Endo	yes	Alkaline Serine Endopeptidase	Liquid	7,5-10	45-65	Bacillus subtilis
FoodPro 51 FP	DuPont-Danisco	Endo/exo	yes	Reduce bitterness of protein hydrolysates, Improve protein yield. Meat, poultry, fish and vegetable protein hydrolysates	Powder	8.0-10.0	45-60	
FoodPro PNL	DuPont-Danisco	Endo	yes	Metallo Neutral Endopeptidase	Liquid	6.0-7.5	50-70	Bacillus amyloliquefaciens
FoodPro PNL	DuPont-Danisco	Endo	yes		Liquid	6.0-7.5	50-70	bacterial
MaxiPro AFP	DSM	Endo (+Exo?)	yes	aspergillopepsin	Liquid	1.5-3.5	45 - 55	Aspergillus niger
MaxiPro NPU	DSM	Endo	yes	metalloprotease	Liquid	5.5-7.5	35 - 55	Bacillus a myloliquefaciens (Japansk brosjyre)
PROMOD 144GL-100TU	Biocatalysts	Endo	yes	Ultra low sulphite papain (5 diff proteases)	Liquid	5,0-7,5	50-70	Carica papaya (papain)
PROMOD P950L	Biocatalysts	Endo	yes	Microbial alternative to papain	Liquid	5,0-7,0	50-60	Carica papaya (papain)
Protamex	Novozymes	Endo	yes	Trypsin, basillolysin, subtilisin	Powder	7.0 - 10?	35-60	Bacillus sp.
TAIL-10	Tailorzyme ApS	Endo	yes	Alkaline serine protease (subtilisin A), ficin, papain, pepsin. Alcalase-type	Liquid	7.0-9 (10)	30 - 70	B. licheniformis
Tail-189	Tailorzyme ApS	Collagenase	yes	?	Powder			
Tail-190	Tailorzyme ApS	Collagenase	yes	?	Powder			
Tail-191	Tailorzyme ApS	Collagenase	yes	?	Powder			
Tail-192	Tailorzyme ApS	Collagenase	yes	?	Powder			
Tail-193	Tailorzyme ApS	Collagenase	yes	?	Powder			
Tail-194	Tailorzyme ApS	Collagenase	yes	?	Powder			
Tail-197	Tailorzyme ApS	Collagenase	yes	?	Liquid			
VERON L	AB Enzymes	Endo	yes	proteolytic enzyme preparation based on papain (Sulfite max. 0.1%)	Liquid	5,0-7,5	50-70	Carica papaya (papain)

7.1.1 Protease concentration calculated from the activity screening

The dilution factor of all of the proteases was calculated based on the absorbance at 440 nm, providing a linear range in the area of approximately 0.10-1.5 OD. The extended calculations of Bromelain and Endocut-02 are included in **Table 19-20** and **Figure 49-50**, and the dilution factors for all the 25 proteases are presented in **Table 21**.

Table 19. The dilution factors and corresponding absorbance of Bromelain in the activity screening of azo-casein, found from measuring the absorbance at 440 nm.

Bromelain (1)		**Bromelain (2)**	
Conc. protease (µl)	Absorbans (OD)	Conc. protease (µl)	Absorbans (OD)
0.002	>3	0.0004	1.962
0.0004	1.984	0.0001	0.632
0.0001	0.623	0.00005	0.322

Table 20. The dilution factors and corresponding absorbance of Endocut-02 in the activity screening of azo-casein, found from measuring the absorbance at 440 nm.

Endocut 02 (1)		**Endocut 02 (2)**	
Conc. protease (µl)	Absorbans (OD)	Conc. protease (µl)	Absorbans (OD)
0.002	>3	0.0004	1.845
0.0004	1.846	0.0001	0.77
0.0001	0.626	0.00005	0.374

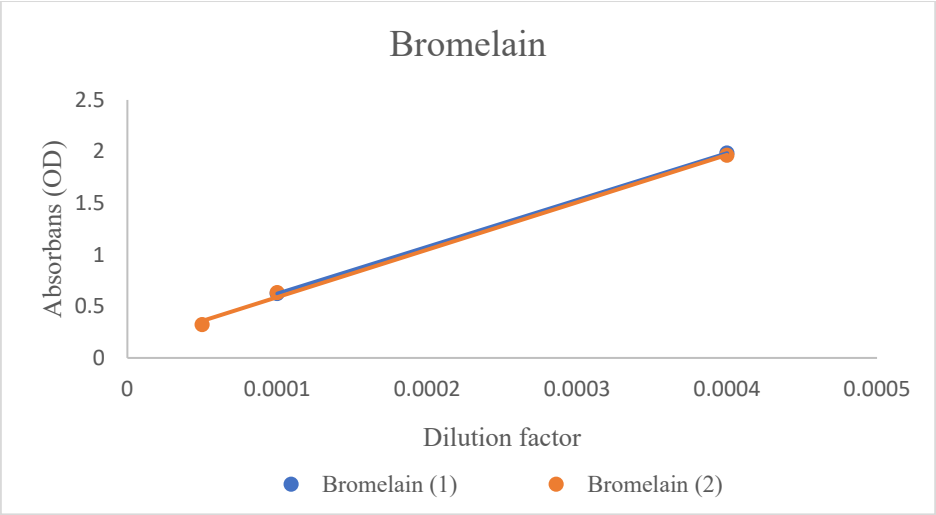

Figure 49. Absorbance as a function of the dilution factors for Bromelain, showing the linear regression with the dilution factor on the x-axis and the absorbance on the y-axis.

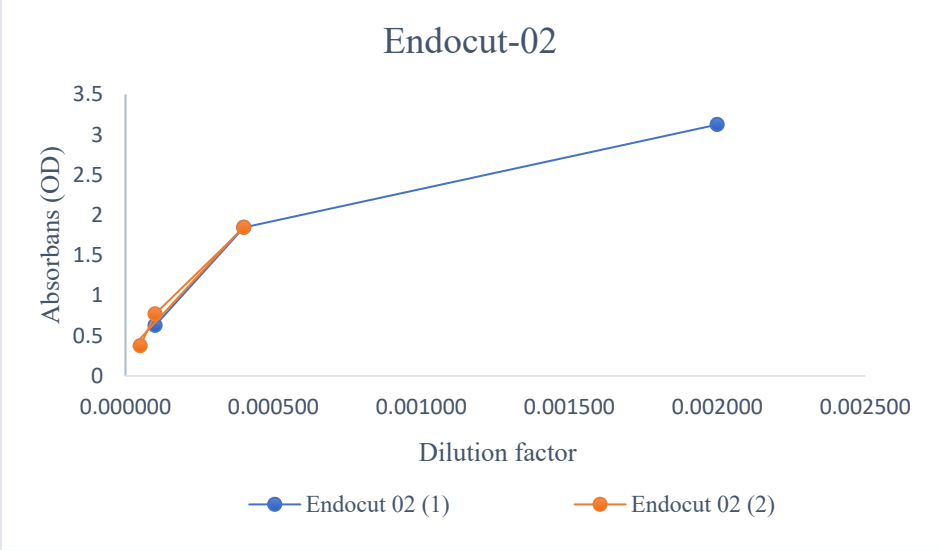

Figure 50. Absorbance as a function of the dilution factors for Endocut-02, showing the linear regression with the dilution factor on the x-axis and the absorbance on the y-axis.

Table 21. Protease concentrations for each of the 25 proteases after the activity screening towards azo-casein, calculated based on the dilution factor at OD = 1. Neutrase and MaxiPro NPU (marked in color) were rejected due to the need of high concentrations.

Protease	Dilution for Abs = 1	a	c	x when y = 1	Dilution factor	Deviation from arimetric mean	Amount of enzyme to add (µl el. mg/1000 µl)
Alcalase (Sigma bottle)		4.77E+03	-1.17E-01	2.34E-04	4.27E+03	8.68E-01	17.4
Bromelain	1.80E-04	9.18E+03	1.40E-01	9.36E-05	1.07E+04	3.47E-01	6.94
Bromelain new batch	1.80E-04	9.17E+03	1.01E-01	9.81E-05	1.02E+04	3.63E-01	7.27
Corolase 2TS	2.20E-03	8.91E+02	3.98E-03	1.12E-03	8.94E+02	4.15E+00	82.9
Corolase 7090	1.30E-03	1.52E+03	-2.14E-02	6.74E-04	1.48E+03	2.50E+00	50.0
ENDOCUT-01	2.00E-03	9.57E+02	-4.41E-03	1.05E-03	9.53E+02	3.89E+00	77.8
ENDOCUT-02	2.00E-04	8.00E+03	2.52E-01	9.35E-05	1.07E+04	3.46E-01	6.93
ENDOCUT-03	3.00E-04	6.70E+03	1.04E-01	1.34E-04	7.47E+03	4.96E-01	9.92
Flavourzyme/Sigma bottle	1.30E-03	1.58E+03	-3.01E-02	6.52E-04	1.53E+03	2.42E+00	48.3
FoodPro 30L (arried Jan 19)	2.50E-03	6.49E+03	1.04E-01	1.38E-04	7.24E+03	5.12E-01	10.2
FoodPro 51 FP	1.50E+00	1.20E+03	9.90E-02	7.53E-04	1.33E+03	2.79E+00	55.9
FoodPro PNL	1.40E-03	1.53E+03	-5.51E-02	6.89E-04	1.45E+03	2.55E+00	51.1
Protamex	1.20E-03	1.73E+03	-6.08E-02	6.14E-04	1.63E+03	2.28E+00	45.5
Neutrase	1.00E-02	4.90E+02	-3.71E-02	2.12E-03	4.72E+02	7.85E+00	157
MaxiPro NPU	4.00E-03	3.84E+02	-3.06E-02	2.69E-03	3.72E+02	9.95E+00	199
PROMOD 144GL-100TU	1.80E-03	1.19E+03	-4.31E-02	8.79E-04	1.14E+03	3.26E+00	65.1
PROMOD P950L	4.00E-04	4.67E+03	5.69E-02	2.02E-04	4.96E+03	7.48E-01	15.0
TAIL-10	1.80E-04	9.26E+03	1.24E-01	9.46E-05	1.06E+04	3.51E-01	7.01
Tail-189	7.50E-02	1.11E+04	1.37E-01	7.81E-05	1.28E+04	3.62E-01	7.23
Tail-190	4.00E-01	2.47E+03	2.17E-02	3.96E-04	2.53E+03	1.83E+00	36.6
Tail-191	2.50E-01	4.27E+03	-9.30E-02	2.56E-04	3.90E+03	1.19E+00	23.7
Tail-192	1.80E-01	4.44E+03	1.48E-01	1.92E-04	5.21E+03	8.88E-01	17.8
Tail-193	2.60E-01	4.03E+03	2.13E-01	1.95E-04	5.13E+03	9.03E-01	18.1
Tail-194	8.00E-01	1.01E+03	9.83E-02	8.96E-04	1.12E+03	4.15E+00	83.0
Tail-197	1.20E-03	1.89E+03	-1.05E-01	5.83E-04	1.71E+03	2.70E+00	54.0
VERON L	5.00E-04	4.05E+03	-1.34E-01	2.80E-04	3.57E+03	1.04E+00	20.8
Average dilution factor liquid protease					3.71E+03		
Average dilution factor solid protease					4.63E+03		

7.2 Protocols developed during the study

7.2.1 Protocol – Small-scale enzymatic protein hydrolysis

(in collaboration with Dalsnes, M. (107)).

Preparation of the samples: CF, tendons as well as a mix of the raw materials must be prepared before starting the experiment. Weigh the empty tubes, before 2.000 – 2.050 g of each raw material is added into a 10 mL tube (79x16mm, Sarstedt). Mark the tubes sufficiently before stored at -40 °C.

Prepare a protease solution of 34,5 µL Endocut-02 to 5000 µl Napi buffer 0.1 M pH 7.0, and 45,5 mg Bromelain to 5000 µL of the same buffer. This holds up to 6 samples, and a little extra. Upscale if necessary. Protease solution should be used within 2 hours, and bromelain solution must be stirred for 30 min. before use.

1. Defrost the tubes and mark them: 1) CF sample with Bromelain 2) CF sample with Endocut-02 3) tendons sample with Bromelain 4) tendons sample with Endocut-02 5) Mix with Bromelain 6) Mix with Endocut-02 7) Blank CF 8) Blank tendons 9) Blank mixed
2. Add 7.5 mL of 0.01 M sodium phosphate buffer pH 7.0 in each tube.
3. Pre-heat the samples:
   I) Bromelain in a water bath at 45 °C to achieve a sample temperature of 40 °C
   II) Endocut-02 in a water bath at 45 °C to achieve a sample temperature of 40 °C
4. When the optimum temperature is reached, add 1 mL of the protease solution into the tubes. Check if there is pH drop in blank solutions.
5. Fasten the tubes in the rotational mixer and place it in the heating cabinet at 42 °C for 60 and 180 minutes for Bromelain and Endocut-02, respectively.
6. When hydrolysis is finished, open the lids, and put the samples in a water bath at 95°C. Leave them for 15 minutes after reaching 90 °C, to inactivate the proteases.
7. Prepare and weigh filter papers (Ø 125 mm, 597, Whatman).
8. Filter the samples, starting with tendon, mixed and then the CF samples, with heated vacuum. Use a 50 mL falcon tube in the flask to collect the filtrated water phase.

9. After weighing, dry the empty tubes as well as the filter papers with residuals in a heating cabinet at 50 °C until completely dry. Weigh the solids again after dried, before stored in freezer at -20 °C.
10. Prepare the samples for analysis by using a 5 mL syringe (0.8x55 mm) to extract the water phase. Replace the needle with a 0.45 µL Millipore filter to filtrate it into SEC-vials and in Eppendorf tubes for the FTIR analysis, leaving at least 0.5 mL in each tube.

7.2.2 Protocol – Lab-scale enzymatic protein hydrolysis

This protocol has been performed on poultry RRM, Achilles tendons from turkey, CF, mixed CF + tendons, and MDPR.

Two proteases, ENDOCUT-02 and Bromelain, were used based on a previous small-scale screening on the same raw materials done by *Dalsnes, M., et al (2019)*. The following protocol was upscaled 166,5 times compared to the small-scale screening. The instrumentation was done by following the Hydrolysis protocol Reactor Ready (*Rein, M. and Lindberg, D., 2019*).

1. Weigh up 333 g of raw material and transfer it to the reactor with 667 mL of Milli-Q type 3 water.
2. Prepare protease solutions in a 15 mL falcon tube dissolving X mg or µL of protease in 10 mL water and rotate for 30 min. until homogenized.

Endocut-02: 6.9 µL • 166,5 = 1149 µL

Bromelain: 9.11 mg • 166,5 = 1517 mg

3. When the sample has reached a temperature of 40 °C, extract 15 mL of sample (blank sample) before adding the protease solution with a 5 mL pipette or a funnel. Rinse with a little water to get out the rest of the protease solution and prepare for the first sampling.
4. Extract 15 mL of sample after 0.5, 2.5, 5, 7.5, 10, 15, 20, 30, 40 and 50 minutes using a serological pipette (the entire tube + approx. 50 % of the serological pipettes volume) and transfer it into pre-weighed 50 mL falcon tubes. Rinse the pipette in H_2O x 3 between the sampling.
5. Use a special lid with a drilled hole to relieve pressure and microwave the sample for 20 seconds to start the boiling, before placing the sample in a water bath at 95 °C for 15 minutes. This step, from sampling to deactivation, goes fast!
6. After 60 minutes, transfer the final sample into beakers covered with cling film and microwave for 90 seconds (until boiling) followed by 15 minutes in a 95 °C water bath.

7. After the 60 min. samples are cooled, transfer to the two pre-weighed centrifuge containers and make sure that the weight is equal (within 0.5 g). Centrifuge at 4400 rpm for 15 min. The gelatin samples must be filtered directly after deactivation to avoid that the water phase is being stuck in the solid phase.

Extraction of water phase and filtration

1. Using a Büchner flask and funnel, filtrate the 11 x 15 mL samples through a pre-weighed filter paper (Ø 125 mm, 597, Whatman) into pre-weighed 50 mL falcon tubes. Weigh the liquid phase after filtration and incubate the filters, with the empty tubes, in the oven at 50 ºC overnight.

2. Using a large pre-weighed Büchner flask and funnel, filtrate the liquid phase of the 60 minutes sample through a pre-weighed self-made filter paper. For the gelatin samples, use a large sieve over the funnel to collect the solid phase. Weigh all the filtered liquid phases and incubate the gelatin-filters in oven. If a fat layer occurs at the top of the liquid phase, use a separating funnel to collect and weigh this phase as well.

3. Extract the supernatant from all samples using a 5 mL syringe and needle (0.8x55mm). Replace the needle with a 0.45 µL Millipore filter to filtrate it into Eppendorf tubes and vials (only CF samples in vials), leaving at least 0.5 mL in each tube.

4. Weigh the solid phase from the containers, as well as the dried filters and tubes from the incubation.

5. Store the solid phase from the containers, as well as the dried filters, and tubes with filtered supernatant in a freezer at -20 ºC.

7.2.3 Protocol – Sodium dodecyl sulfate – Polyacrylamide gel electrophoresis

Analysis of various peptides from hydrolysis of poultry raw material residues were carried out using SDS-PAGE, following a procedure from Invitrogen.

1. Prepare samples:
    - In eppendorf tubes, weigh-in 15 – 50 mg solid phase material from the hydrolysis, depending on the material and protease used in the hydrolysis reaction
    - Add 1 mL deionized water and heat the samples under stirring, at 50 ºC and 800 rpm for 30 min.
    - Centrifuge the samples in 10 min. at 3200 rpm and 25 ºC
    - Transfer the supernatant to new eppendorf tubes
    - Transfer 20 µL sample to new tubes and add 20 µL 2x treatment buffer with DTT and bromophenol blue, and place the solutions in a heated stirrer at 50 ºC and 400 rpm for 15 min.

2. Prepare buffer solution to run SDS-PAGE, 500 mL

    - 20X NuPAGE® SDS Running Buffer: 25 mL
    - Deionized water: 475 mL
    - Total volume: 500 mL

3. Place the gel NuPage 12 %TC, in the chamber with the application-side inwards. Remember to remove the application safety lid and the tape at the bottom front of the cassette.

4. Check if the chamber is leaking, by pouring some buffer in the middle of the chamber. If not, pour in the rest of the buffer and start the application of protein marker and sample solutions in the wells.

    Protein marker, 3 µL
    Sample solution, 5 – 10 µL

5. Put on the lid, plug in the wires, and turn on the instrument.
    - Instrument settings:

    200V, 125 mA, 25W and reaction time ~ 40 min. Stop the reaction before the fragments reach the bottom of the cassette

6. To release the gel from the cassette, gently bend the inside of the lid around the entire edge with a spatula. When the lid is loose, carefully remove and loosen the gel around the entire edge. Then start loosening the gel from the plate by using a wet spatula. Place the gel in a vessel and add dye. The gel should not dry or be touched with anything but the spatula to prevent it from breaking and getting fingerprints.

7. After one hour in the vessel, the staining solution is replaced with a dye-removing solution. A paper ball can be placed in the corner for more effective discoloration. The vessel is then being microwaved in, 2 x 20 seconds. The solution is changed after approx. 30 min. This is done 2-3 times before the gel is placed in deionized water for an hour. The gel can then be scanned using an Epson instrument.

7.3 Raw material analysis provided by ALS laboratories UK

Table 22. The composition of Hyp, ash, water content, protein, fat, carbohydrates and energy in various materials from poultry raw material residues, determined by RMA (69).

ELEMENT	SAMPLE	CF (1)	CF (2)	Tendons (1)	Tendons (2)	MDPR (1)	MDPR (2)
Sampling Date		5/11/2020	5/11/2020	5/11/2020	5/11/2020	5/11/2020	5/11/2020
Hydroksyproline	g/100g	0.06	0.05	3.24	2.86	1.020	1.010
Ash	g/100g	1.20	1.20	5.60	4.50	1.600	2.000
Water content	g/100g	73.4	73.7	56.5	60.6	58.40	59.00
Protein	g/100g	22.2	22.5	31.7	30.1	19.20	20.70
Fat	g/100g	2.60	2.50	4.80	4.40	19.70	19.70
Totale carbohydrates	g/100 g	0.60	0.10	1.40	0.40	1.100	<0.1
Energy	kJ/100 g	484	477	740	681	1074	1081
Energy	kcal/100 g	115	113	176	162	259.0	260.0

7.4 Dumas combustion analysis – nitrogen content in the lab-scale hydrolysates

Table 23-32 shows the nitrogen content (N [%]) of all the lab-scale hydrolysates [mg] determined by Dumas, with calculations of the protein content (Prot. [%]) using a conversion factor of 6.25.

7.4.1 Nitrogen content in the lab-scale hydrolysates treated with Bromelain or Endocut-02

Table 23. Nitrogen content determined from the hydrolysate products, and converted to protein content using the protein factor. The lab-scale hydrolysates from MDPR treated with Endocut-02 (ME1: first series, ME2: duplicated series).

Name	Weight [mg]	Method	N [%]	Prot. factor	Prot. [%]
LMGH20_0005ME1	5.02	5mg90s	11.8	6.25	73.9
LMGH20_0025ME1	4.84	5mg90s	12.3	6.25	76.7
LMGH20_0050ME1	4.61	5mg90s	12.6	6.25	78.8
LMGH20_0075ME1	4.87	5mg90s	12.7	6.25	79.1
LMGH20_0100ME1	4.81	5mg90s	11.4	6.25	71.4
LMGH20_0150ME1	5.09	5mg90s	12.3	6.25	76.8
LMGH20_0200ME1	5.19	5mg90s	12.2	6.25	76.5
LMGH20_0300ME1	5.01	5mg90s	12.3	6.25	77.1
LMGH20_0400ME1	4.61	5mg90s	11.7	6.25	72.9
LMGH20_0500ME1	5.31	5mg90s	11.4	6.25	71.4
LMGH20_0600ME1	4.72	5mg90s	14.4	6.25	89.8
LMGH20_0005ME2	4.91	5mg90s	9.8	6.25	61.2
LMGH20_0025ME2	4.48	5mg90s	12.5	6.25	78.0
LMGH20_0050ME2	5.07	5mg90s	11.5	6.25	71.8
LMGH20_0075ME2	4.77	5mg90s	12.2	6.25	76.0
LMGH20_0100ME2	4.85	5mg90s	12.2	6.25	76.4
LMGH20_0150ME2	4.61	5mg90s	12.0	6.25	75.3
LMGH20_0200ME2	5.14	5mg90s	12.1	6.25	75.8
LMGH20_0300ME2	4.23	5mg90s	12.3	6.25	76.8
LMGH20_0400ME2	5.17	5mg90s	11.8	6.25	73.6
LMGH20_0500ME2	4.72	5mg90s	12.1	6.25	75.7
LMGH20_0600ME2	4.85	5mg90s	14.4	6.25	90.1

Table 24. Nitrogen content determined from the hydrolysate products, and converted to protein content using the protein factor. The lab-scale hydrolysates from MDPR treated with Bromelain (MB1: first series, MB2: duplicated series).

Name	Weight [mg]	Method	N [%]	Prot. factor	Prot. [%]
LMGH20_0005MB1	4.61	5mg90s	11.2	6.25	70.2
LMGH20_0025MB1	4.92	5mg90s	12.1	6.25	75.4
LMGH20_0050MB1	4.69	5mg90s	12.2	6.25	76.5
LMGH20_0075MB1	4.66	5mg90s	11.3	6.25	70.5
LMGH20_0100MB1	4.73	5mg90s	12.7	6.25	79.0
LMGH20_0150MB1	5.32	5mg90s	12.9	6.25	80.5
LMGH20_0200MB1	5.33	5mg90s	12.8	6.25	79.7
LMGH20_0300MB1	4.85	5mg90s	12.8	6.25	80.0
LMGH20_0400MB1	4.63	5mg90s	13.0	6.25	81.2
LMGH20_0500MB1	5.00	5mg90s	13.2	6.25	82.4
LMGH20_0600MB1	4.85	5mg90s	14.6	6.25	91.5
LMGH20_0005MB2	4.86	5mg90s	10.2	6.25	64.0
LMGH20_0025MB2	5.29	5mg90s	11.9	6.25	74.6
LMGH20_0050MB2	5.25	5mg90s	11.8	6.25	74.0
LMGH20_0075MB2	4.62	5mg90s	12.3	6.25	77.0
LMGH20_0100MB2	4.93	5mg90s	12.4	6.25	77.3
LMGH20_0150MB2	4.78	5mg90s	12.4	6.25	77.7
LMGH20_0200MB2	4.56	5mg90s	12.5	6.25	78.1
LMGH20_0300MB2	4.84	5mg90s	13.6	6.25	85.0
LMGH20_0400MB2	5.30	5mg90s	12.4	6.25	77.2
LMGH20_0500MB2	4.91	5mg90s	12.8	6.25	79.7
LMGH20_0600MB2	5.09	5mg90s	14.6	6.25	91.4

Table 25. Nitrogen content determined from the hydrolysate products, and converted to protein content using the protein factor. The lab-scale hydrolysates from tendons treated with Endocut-02 (SE1: first series, SE2: duplicated series).

Name	Weight [mg]	Method	N [%]	Prot. factor	Prot. [%]
LMGH20_0005SE1	5.12	5mg90s	9.2	6.25	57.6
LMGH20_0025SE1	4.63	5mg90s	10.6	6.25	66.2
LMGH20_0050SE1	5.07	5mg90s	11.5	6.25	71.9
LMGH20_0075SE1	4.66	5mg90s	10.8	6.25	67.5
LMGH20_0100SE1	5.03	5mg90s	10.7	6.25	67.0
LMGH20_0150SE1	4.92	5mg90s	12.4	6.25	77.7
LMGH20_0200SE1	4.49	5mg90s	11.3	6.25	70.4
LMGH20_0300SE1	5.07	5mg90s	10.7	6.25	66.7
LMGH20_0400SE1	4.62	5mg90s	12.2	6.25	76.5
LMGH20_0500SE1	4.65	5mg90s	10.8	6.25	67.2
LMGH20_0600SE1	4.63	5mg90s	15.0	6.25	93.8
LMGH20_0005SE2	4.98	5mg90s	11.0	6.25	68.8
LMGH20_0025SE2	4.76	5mg90s	10.7	6.25	66.6
LMGH20_0075SE2	4.77	5mg90s	10.8	6.25	67.5
LMGH20_0100SE2	5.05	5mg90s	11.0	6.25	68.7
LMGH20_0150SE2	5.00	5mg90s	12.1	6.25	75.5
LMGH20_0200SE2	4.72	5mg90s	10.6	6.25	66.5
LMGH20_0300SE2	4.71	5mg90s	10.7	6.25	66.9
LMGH20_0400SE2	4.84	5mg90s	11.7	6.25	73.1
LMGH20_0500SE2	5.03	5mg90s	11.2	6.25	70.2
LMGH20_0600SE2	4.71	5mg90s	14.7	6.25	91.8

Table 26. Nitrogen content determined from the hydrolysate products, and converted to protein content using the protein factor. The lab-scale hydrolysates from tendons treated with Bromelain (SB1: first series, SB2: duplicated series).

Name	Weight [mg]	Method	N [%]	Prot. factor	Prot. [%]
LMGH20_0005SB1	4.68	5mg90s	11.3	6.25	70.4
LMGH20_0025SB1	4.50	5mg90s	13.2	6.25	82.5
LMGH20_0050SB1	4.54	5mg90s	14.8	6.25	92.4
LMGH20_0075SB1	4.77	5mg90s	12.5	6.25	78.2
LMGH20_0100SB1	4.89	5mg90s	13.7	6.25	85.3
LMGH20_0150SB1	4.65	5mg90s	12.1	6.25	75.7
LMGH20_0200SB1	5.05	5mg90s	11.5	6.25	71.8
LMGH20_0300SB1	4.57	5mg90s	11.5	6.25	71.9
LMGH20_0400SB1	4.63	5mg90s	11.6	6.25	72.3
LMGH20_0500SB1	4.56	5mg90s	12.5	6.25	78.0
LMGH20_0600SB1	4.68	5mg90s	15.4	6.25	96.0
LMGH20_0005SB2	4.82	5mg90s	9.7	6.25	60.5
LMGH20_0025SB2	4.83	5mg90s	10.1	6.25	62.9
LMGH20_0050SB2	4.89	5mg90s	10.8	6.25	67.4
LMGH20_0075SB2	4.57	5mg90s	11.7	6.25	73.3
LMGH20_0100SB2	4.81	5mg90s	11.2	6.25	70.2
LMGH20_0150SB2	4.86	5mg90s	10.7	6.25	67.1
LMGH20_0200SB2	4.86	5mg90s	11.1	6.25	69.6
LMGH20_0300SB2	4.73	5mg90s	11.4	6.25	71.2
LMGH20_0400SB2	4.59	5mg90s	11.7	6.25	73.2
LMGH20_0500SB2	4.41	5mg90s	11.8	6.25	73.8
LMGH20_0600SB2	4.53	5mg90s	15.6	6.25	97.8

Table 27. Nitrogen content determined from the hydrolysate products, and converted to protein content using the protein factor. The lab-scale hydrolysates from CF treated with Endocut-02 (KE1: first series, KE2: duplicated series).

Name	Weight [mg]	Method	N [%]	Prot. factor	Prot. [%]
LMGH20_0005KE1	5.10	5mg90s	12.3	6.25	76.9
LMGH20_0025KE1	5.00	5mg90s	13.0	6.25	81.4
LMGH20_0050KE1	4.80	5mg90s	12.5	6.25	77.8
LMGH20_0075KE1	5.25	5mg90s	13.0	6.25	81.3
LMGH20_0100KE1	4.88	5mg90s	13.0	6.25	81.4
LMGH20_0150KE1	4.77	5mg90s	13.3	6.25	83.3
LMGH20_0200KE1	4.68	5mg90s	12.9	6.25	80.7
LMGH20_0300KE1	4.69	5mg90s	12.7	6.25	79.5
LMGH20_0400KE1	4.54	5mg90s	14.0	6.25	87.7
LMGH20_0500KE1	4.68	5mg90s	13.5	6.25	84.4
LMGH20_0600KE1	5.26	5mg90s	14.4	6.25	89.8
LMGH20_0005KE2	5.09	5mg90s	13.0	6.25	81.0
LMGH20_0025KE2	4.70	5mg90s	13.1	6.25	81.9
LMGH20_0050KE2	5.09	5mg90s	13.0	6.25	81.4
LMGH20_0075KE2	4.47	5mg90s	12.4	6.25	77.3
LMGH20_0100KE2	5.01	5mg90s	13.2	6.25	82.5
LMGH20_0150KE2	4.66	5mg90s	13.8	6.25	86.2
LMGH20_0200KE2	4.95	5mg90s	13.5	6.25	84.3
LMGH20_0300KE2	5.09	5mg90s	13.3	6.25	83.2
LMGH20_0400KE2	5.07	5mg90s	13.7	6.25	85.4
LMGH20_0500KE2	4.90	5mg90s	14.0	6.25	87.6
LMGH20_0600KE2	4.82	5mg90s	14.0	6.25	87.5

Table 28. Nitrogen content determined from the hydrolysate products, and converted to protein content using the protein factor. The lab-scale hydrolysates from CF treated with Bromelain (KB1: first series, KB2: duplicated series).

Name	Weight [mg]	Method	N [%]	Prot. factor	Prot. [%]
LMGH20_0005KB1	4.67	5mg90s	13.5	6.25	84.4
LMGH20_0025KB1	4.59	5mg90s	13.4	6.25	83.9
LMGH20_0050KB1	4.39	5mg90s	13.3	6.25	83.0
LMGH20_0075KB1	4.90	5mg90s	12.8	6.25	79.7
LMGH20_0100KB1	4.84	5mg90s	13.7	6.25	85.8
LMGH20_0150KB1	4.76	5mg90s	13.6	6.25	84.9
LMGH20_0200KB1	4.55	5mg90s	13.9	6.25	87.0
LMGH20_0300KB1	4.63	5mg90s	14.2	6.25	89.0
LMGH20_0400KB1	4.56	5mg90s	14.3	6.25	89.5
LMGH20_0500KB1	4.88	5mg90s	14.6	6.25	91.2
LMGH20_0600KB1	4.40	5mg90s	13.8	6.25	86.3
LMGH20_0005KB2	5.12	5mg90s	12.0	6.25	74.9
LMGH20_0025KB2	4.99	5mg90s	12.2	6.25	76.4
LMGH20_0050KB2	4.97	5mg90s	13.7	6.25	85.3
LMGH20_0075KB2	5.09	5mg90s	13.5	6.25	84.3
LMGH20_0100KB2	4.43	5mg90s	13.9	6.25	87.1
LMGH20_0150KB2	5.06	5mg90s	12.9	6.25	80.7
LMGH20_0200KB2	4.71	5mg90s	14.3	6.25	89.6
LMGH20_0300KB2	4.59	5mg90s	13.7	6.25	85.8
LMGH20_0400KB2	4.56	5mg90s	14.4	6.25	89.7
LMGH20_0500KB2	5.04	5mg90s	13.8	6.25	86.4
LMGH20_0600KB2	4.97	5mg90s	14.5	6.25	90.3

Table 29. Nitrogen content determined from the hydrolysate products, and converted to protein content using the protein factor. The lab-scale hydrolysates from artificial MDPR (SKB1: first series of artificial MDPR treated with Bromelain, SKB2: second series, and SKE1: Artificial MDPR treated with Endocut-02, SKE2: *).

Name	Weight [mg]	Method	N [%]	Prot. factor	Prot. [%]
LMGH20_0005SKB1	4.59	5mg90s	12.6	6.25	78.5
LMGH20_0025SKB1	4.93	5mg90s	12.9	6.25	80.5
LMGH20_0050SKB1	4.87	5mg90s	12.7	6.25	79.2
LMGH20_0075SKB1	4.79	5mg90s	13.6	6.25	84.7
LMGH20_0100SKB1	4.64	5mg90s	13.2	6.25	82.4
LMGH20_0150SKB1	4.59	5mg90s	13.3	6.25	83.1
LMGH20_0200SKB1	4.84	5mg90s	13.5	6.25	84.5
LMGH20_0300SKB1	5.19	5mg90s	13.1	6.25	82.0
LMGH20_0400SKB1	4.95	5mg90s	13.5	6.25	84.2
LMGH20_0500SKB1	5.17	5mg90s	13.0	6.25	81.4
LMGH20_0600SKB1	4.71	5mg90s	14.6	6.25	91.0
LMGH20_0005SKB2	4.66	5mg90s	13.5	6.25	84.5
LMGH20_0025SKB2	4.95	5mg90s	14.3	6.25	89.1
LMGH20_0050SKB2	4.80	5mg90s	14.1	6.25	87.9
LMGH20_0075SKB2	4.92	5mg90s	14.4	6.25	89.7
LMGH20_0100SKB2	4.88	5mg90s	14.1	6.25	88.4
LMGH20_0150SKB2	4.60	5mg90s	14.0	6.25	87.2
LMGH20_0200SKB2	4.94	5mg90s	13.8	6.25	86.1
LMGH20_0300SKB2	4.63	5mg90s	13.4	6.25	83.5
LMGH20_0400SKB2	5.15	5mg90s	13.8	6.25	86.4
LMGH20_0500SKB2	4.48	5mg90s	14.0	6.25	87.5
LMGH20_0600SKB2	5.03	5mg90s	14.7	6.25	91.9
LMGH20_0005SKE1	4.67	5mg90s	12.6	6.25	78.4
LMGH20_0025SKE1	5.05	5mg90s	12.4	6.25	77.7
LMGH20_0050SKE1	4.66	5mg90s	12.9	6.25	80.3
LMGH20_0075SKE1	4.55	5mg90s	11.0	6.25	68.8
LMGH20_0100SKE1	4.75	5mg90s	12.9	6.25	80.6
LMGH20_0150SKE1	4.55	5mg90s	13.4	6.25	83.4
LMGH20_0200SKE1	4.74	5mg90s	13.2	6.25	82.4
LMGH20_0300SKE1	4.67	5mg90s	13.4	6.25	83.5
LMGH20_0400SKE1	5.14	5mg90s	12.4	6.25	77.6
LMGH20_0500SKE1	5.09	5mg90s	12.6	6.25	78.8
LMGH20_0600SKE1	4.59	5mg90s	14.1	6.25	88.2

**The duplicated SKE series was not detected due to an error in the Dumas instrument. It was decided not to prepare a new sample set as these samples were not seen as necessary during the present study.*

7.4.2 Nitrogen content in the lab-scale hydrolysates treated with a combination of Bromelain and Endocut-02

Table 30. Nitrogen content determined from the hydrolysate products, and converted to protein content using the protein factor. The lab-scale hydrolysates from MDPR treated with Bromelain+Endocut-02 (MBE1: first series, MBE2: second series).

Name	Weight [mg]	Method	N [%]	Prot. factor	Prot. [%]
LMGH20_0005MBE1	4.46	5mg90s	10.9	6.25	68.2
LMGH20_0025MBE1	4.99	5mg90s	11.4	6.25	71.0
LMGH20_0050MBE1	4.67	5mg90s	12.3	6.25	76.9
LMGH20_0075MBE1	4.76	5mg90s	12.9	6.25	80.4
LMGH20_0100MBE1	4.85	5mg90s	13.0	6.25	81.1
LMGH20_0150MBE1	4.69	5mg90s	13.2	6.25	82.5
LMGH20_0200MBE1	4.50	5mg90s	11.6	6.25	72.6
LMGH20_0300MBE1	4.93	5mg90s	13.2	6.25	82.7
LMGH20_0400MBE1	4.72	5mg90s	13.6	6.25	84.8
LMGH20_0500MBE1	4.65	5mg90s	13.7	6.25	85.7
LMGH20_0600MBE1	4.34	5mg90s	13.5	6.25	84.4
LMGH20_ProdMBE1	5.11	5mg90s	15.2	6.25	94.9
LMGH20_0005MBE2	4.69	5mg90s	10.9	6.25	68.3
LMGH20_0025MBE2	4.52	5mg90s	11.8	6.25	73.6
LMGH20_0050MBE2	4.79	5mg90s	12.2	6.25	76.5
LMGH20_0075MBE2	4.56	5mg90s	12.4	6.25	77.4
LMGH20_0100MBE2	4.96	5mg90s	13.0	6.25	80.9
LMGH20_0150MBE2	4.86	5mg90s	13.3	6.25	83.1
LMGH20_0200MBE2	4.56	5mg90s	13.1	6.25	82.1
LMGH20_0300MBE2	5.08	5mg90s	13.4	6.25	83.5
LMGH20_0400MBE2	4.64	5mg90s	13.3	6.25	83.2
LMGH20_0500MBE2	4.48	5mg90s	13.7	6.25	85.3
LMGH20_0600MBE2	4.81	5mg90s	13.7	6.25	85.7
LMGH20_ProdMBE2	4.98	5mg90s	15.2	6.25	95.2

Table 31. Nitrogen content determined from the hydrolysate products, and converted to protein content using the protein factor. The lab-scale hydrolysates from MDPR treated with Bromelain → Endocut-02 (MB+E1: first series, MB+E2: second series).

Name	Weight [mg]	Method	N [%]	Prot. factor	Prot. [%]
LMGH20_0005MB+E1	5.12	5mg90s	11.4	6.25	71.0
LMGH20_0025MB+E1	4.77	5mg90s	12.7	6.25	79.1
LMGH20_0050MB+E1	4.80	5mg90s	12.1	6.25	75.4
LMGH20_0075MB+E1	4.77	5mg90s	12.5	6.25	78.2
LMGH20_0100MB+E1	4.84	5mg90s	12.6	6.25	78.4
LMGH20_0150MB+E1	4.53	5mg90s	13.6	6.25	85.2
LMGH20_0200MB+E1	4.69	5mg90s	13.1	6.25	81.9
LMGH20_0300MB+E1	4.43	5mg90s	13.2	6.25	82.8
LMGH20_0400MB+E1	4.79	5mg90s	13.2	6.25	82.5
LMGH20_0500MB+E1	4.83	5mg90s	13.2	6.25	82.5
LMGH20_0600MB+E1	4.56	5mg90s	13.4	6.25	83.5
LMGH20_ProdMB+E1	4.63	5mg90s	15.1	6.25	94.6
LMGH20_0005MB+E2	4.73	5mg90s	10.7	6.25	67.1
LMGH20_0025MB+E2	5.09	5mg90s	11.4	6.25	70.9
LMGH20_0050MB+E2	4.58	5mg90s	13.5	6.25	84.6
LMGH20_0075MB+E2	4.90	5mg90s	13.5	6.25	84.6
LMGH20_0100MB+E2	5.02	5mg90s	13.0	6.25	81.0
LMGH20_0150MB+E2	4.71	5mg90s	13.7	6.25	85.6
LMGH20_0200MB+E2	4.32	5mg90s	13.3	6.25	83.4
LMGH20_0300MB+E2	5.08	5mg90s	13.7	6.25	85.4
LMGH20_0400MB+E2	4.56	5mg90s	13.5	6.25	84.1
LMGH20_0500MB+E2	4.55	5mg90s	13.5	6.25	84.4
LMGH20_0600MB+E2	4.87	5mg90s	13.5	6.25	84.6
LMGH20_ProdMB+E2	4.92	5mg90s	15.4	6.25	96.4

Table 32. Nitrogen content determined from the hydrolysate products, and converted to protein content using the protein factor. The lab-scale hydrolysates from MDPR treated with Endocut-02 → Bromelain (ME+B1: first series, ME+B2: second series).

Name	Weight [mg]	Method	N [%]	Prot. factor	Prot. [%]
LMGH20_0005ME+B1	5.02	5mg90s	12.7	6.25	79.4
LMGH20_0025ME+B1	4.92	5mg90s	12.7	6.25	79.3
LMGH20_0050ME+B1	4.83	5mg90s	13.1	6.25	81.6
LMGH20_0075ME+B1	4.55	5mg90s	13.5	6.25	84.2
LMGH20_0100ME+B1	5.19	5mg90s	13.1	6.25	82.1
LMGH20_0150ME+B1	4.87	5mg90s	13.4	6.25	83.5
LMGH20_0200ME+B1	4.85	5mg90s	13.2	6.25	82.5
LMGH20_0300ME+B1	5.01	5mg90s	13.6	6.25	84.8
LMGH20_0400ME+B1	4.47	5mg90s	13.2	6.25	82.8
LMGH20_0500ME+B1	4.68	5mg90s	13.9	6.25	86.9
LMGH20_0600ME+B1	4.51	5mg90s	13.9	6.25	86.8
LMGH20_ProdME+B1	4.78	5mg90s	15.4	6.25	96.2
LMGH20_0005ME+B2	4.69	5mg90s	11.2	6.25	69.8
LMGH20_0025ME+B2	4.89	5mg90s	12.0	6.25	75.0
LMGH20_0050ME+B2	4.76	5mg90s	12.8	6.25	80.3
LMGH20_0075ME+B2	5.02	5mg90s	12.5	6.25	78.3
LMGH20_0100ME+B2	4.50	5mg90s	12.7	6.25	79.1
LMGH20_0150ME+B2	4.82	5mg90s	12.6	6.25	78.7
LMGH20_0200ME+B2	5.05	5mg90s	12.8	6.25	79.7
LMGH20_0300ME+B2	4.82	5mg90s	13.7	6.25	85.7
LMGH20_0400ME+B2	4.74	5mg90s	13.5	6.25	84.6
LMGH20_0500ME+B2	4.63	5mg90s	13.8	6.25	86.4
LMGH20_0600ME+B2	4.62	5mg90s	13.4	6.25	83.5
LMGH20_ProdME+B2	4.56	5mg90s	15.3	6.25	95.8

7.5 Calculations of the small- and Lab-scale hydrolysates

7.5.1 Values for determining the ER % for the small-scale hydrolysates

The values used for calculating the ER% from the verification of Dalsnes 12mL are given in **Table 33,** using ~2.000 g of the various RRM in the small-scale EPH.

Table 33. The values used for calculating the ER% where the total yield % represents the weight yield before subtracting the background reaction. The weighed RRM used in the EPH was included in the calculations.

Endocut-02					
RRM	Water content (%)	Background reaction (%)	Sediment weight (dry) [g]	Total yield %	ER %
Tendons	58	16	0.9	31	15
CF	75	8.5	0.5	13	4.4
MDPR	59	3.2	0.8	52	49
Artificial MDPR	66	0.6	0.7	30	30
Bromelain					
RRM	Water content (%)	Background reaction (%)	Sample weight (dry) [g]	Total yield %	ER %
Tendons	58	16	0.9	45	29
CF	75	9.1	0.5	48	39
MDPR	59	4.4	0.8	42	37
Artificial MDPR	66	1.0	0.7	45	44

7.5.2 Values for determining the protein yield % for the lab-scale hydrolysates

The values used for the calculations of protein yield % in the lab-scale hydrolysates are shown in **Table 34**, using ~333 g of the various RRM in the EPH with single protease-treatment, and ~250 g MDPR in the EPH with combined protease-treatment.

Table 34. The values presented in the table were used for determining the protein yield %. The weighed RRM used in the EPH was included in the calculations.

Protease	Lab-scale products	Total liquid phase (g)	Hydrolysate (g)	Protein (w/v) %	Protein in raw material (w/w)	Calculated protein (w/w)	Protein Yield %
Endocut-02	CF 1	772	15	90	0.22	0.09	39
Endocut-02	CF 2	702	12	88	0.22	0.08	34
Bromelain	CF 1	704	19	91	0.22	0.12	52
Bromelain	CF 2	636	17	92	0.22	0.10	45
Endocut-02	Tendons 1	504	30	94	0.31	0.11	36
Endocut-02	Tendons 2	768	22	92	0.31	0.14	44
Bromelain	Tendons 1	766	28	96	0.31	0.18	59
Bromelain	Tendons 2	753	22	98	0.31	0.15	49
Endocut-02	Artificial MDPR 1	595	15	88	0.27	0.10	36
Endocut-02	Artificial MDPR 2	715	16	88	0.27	0.11	40
Bromelain	Artificial MDPR 1	749	20	91	0.27	0.13	48
Bromelain	Artificial MDPR 2	739	19	92	0.27	0.14	54
Endocut-02	MDPR 1	704	20	90	0.20	0.11	54
Endocut-02	MDPR 2	716	15	90	0.20	0.10	51
Bromelain	MDPR 1	701	18	91	0.20	0.11	57
Bromelain	MDPR 2	680	19	91	0.20	0.11	54
Both	MBE1	556	17	95	0.20	0.12	60
Both	MBE2	543	13	95	0.20	0.14	69
Both	MB+E1	528	14	95	0.20	0.14	68
Both	MB+E2	544	12	96	0.20	0.14	70
Both	ME+B1	540	16	96	0.20	0.15	76
Both	ME+B2	505	12	96	0.20	0.13	65

7.5.3 F-test and student`s t-Test for the lab-scale hydrolysates treated with a combination of Endocut-02 and Bromelain

For the MBE/MB+E (**Table 35**), MB+E/ME+B (**Table 36**), and ME+B/MBE (**Table 37**) series, an F-test followed by an unpaired one-tailed t-Test was done to reveal the possible significant difference between the three ways of adding the combination of Bromelain and Endocut-02, regarding the protein yield %.

Table 35. F-test and t-Test for MBE and MB+E

F-Test: Two selections for variances		
	MBE	*MB+E*
Mean	64.3	69.3
Variance	37.5	2.47
Observations	2.00	2.00
fg	1.00	1.00
F	15.2	
P(F<=f) one-tail	0.16	
F-critical, one-tail	161	

t-Test two sample assuming equal variances

	MBE	*MB+E*
Mean	64.3	69.3
Variance	37.5	2.47
Observations	2.00	2.00
Pooled variance	20.0	
Hypothesized Mean difference	0.00	
fg	2.00	
t-Stat	-1.11	
P(T<=t) one-tail	0.19	
T-critical, one-tail	2.92	
P(T<=t) two-tail	0.38	
T-critical, two-tail	4.30	

Table 36. F-test and t-Test for MBE and ME+B

F-Test: Two selections for variances		
	MBE	*ME+B*
Mean	64.3	70.7
Variance	37.5	55.3
Observations	2.00	2.00
fg	1.00	1.00
F	0.68	
P(F<=f) one-tail	0.44	
F-critical, one-tail	0.01	

t-Test two sample assuming equal variances

	MBE	*ME+B*
Mean	64.3	70.7
Variance	37.5	55.3
Observations	2.00	2.00
Pooled variance	0.00	
Hypothesized Mean difference	2.00	
fg	-0.94	
t-Stat	0.22	
P(T<=t) one-tail	2.92	
T-critical, one-tail	0.45	
P(T<=t) two-tail	4.30	

Table 37. F-test and t-Test for MB+E and ME+B

F-Test: Two selections for variances		
	MB+E	*ME+B*
Mean	69.3	70.7
Variance	2.47	55.3
Observations	2.00	2.00
fg	1.00	1.00
F	0.04	
P(F<=f) one-tail	0.13	
F-critical, one-tail	0.01	

t-Test two sample assuming equal variances

	MB+E	*ME+B*
Mean	69.3	70.7
Variance	2.47	55.3
Observations	2.00	2.00
Pooled variance	0.00	
Hypothesized Mean difference	1.00	
fg	-0.27	
t-Stat	0.42	
P(T<=t) one-tail	6.31	
T-critical, one-tail	0.83	
P(T<=t) two-tail	12.7	

7.6 Degree of hydrolysis during hydrolysis time

The DH% was plottet against the hydrolysis time to observe the degradation pattern for each RRM during time. This was done to reveal possible deviations from the normal DH% trend, which is a steady to increased DH% with increasing hydrolysis time. **Figure 51-55** (A – B, -C) shows the DH% during hydrolysis time (min) for all the lab-scale series. Trendlines are included.

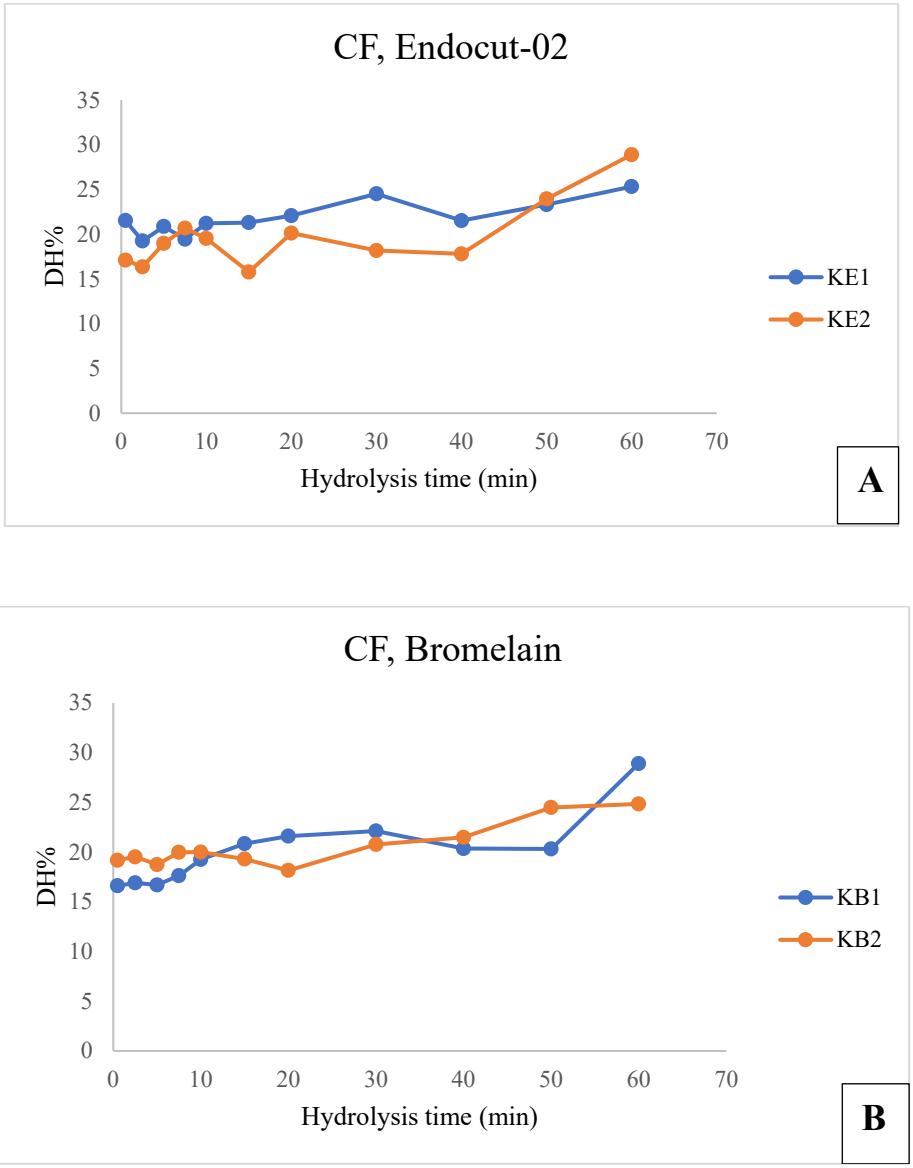

Figure 51. Graph with trendlines of the DH% during hydrolysis time of A) CF treated with Endocut-02, and B) CF treated with Bromelain, with the hydrolysis time on the x-axis and the DH% on the y-axis.

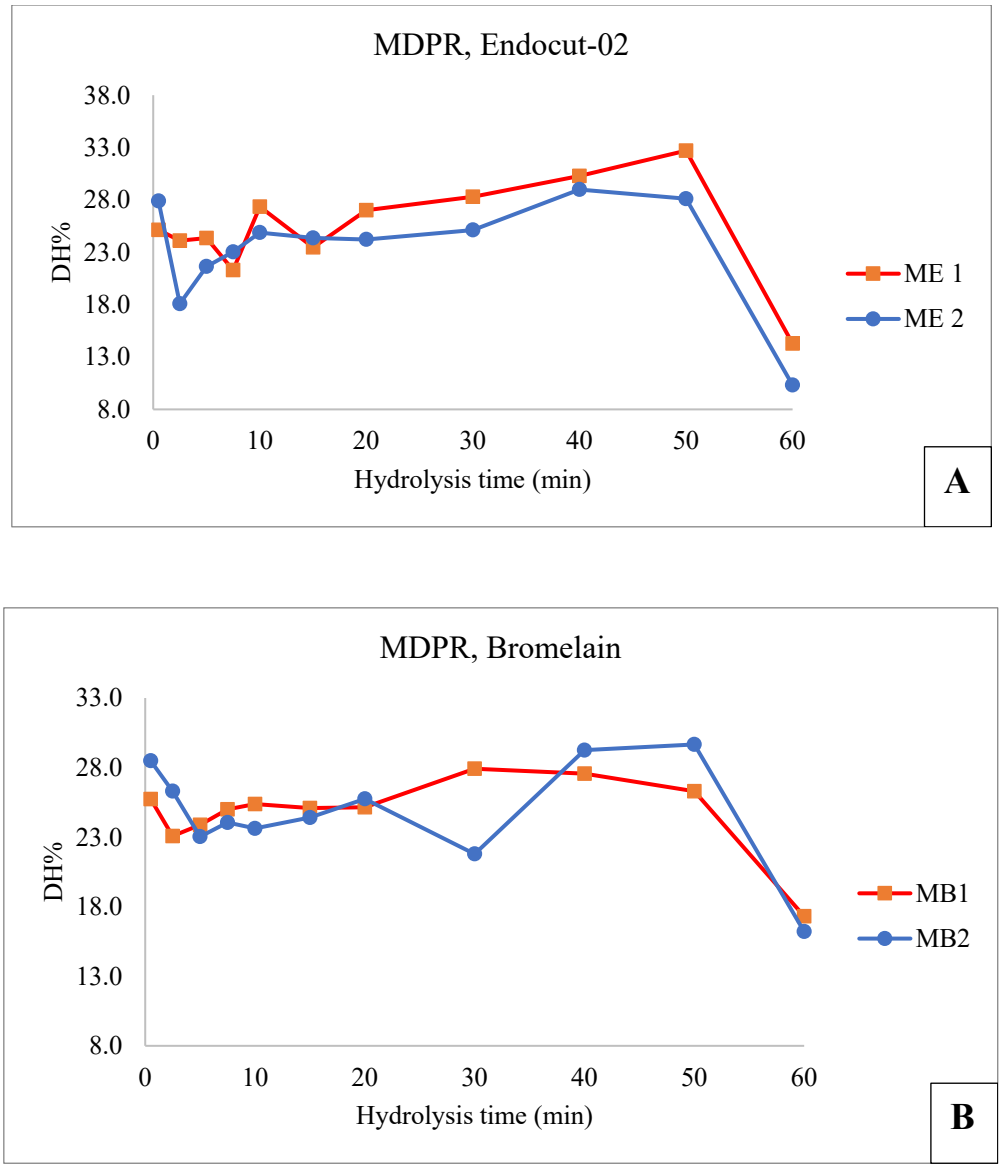

Figure 52. Graph with trendlines of the DH% during hydrolysis time of A) MDPR treated with Endocut-02, and B) MDPR treated with Bromelain, with the hydrolysis time on the x-axis and the DH% on the y-axis.

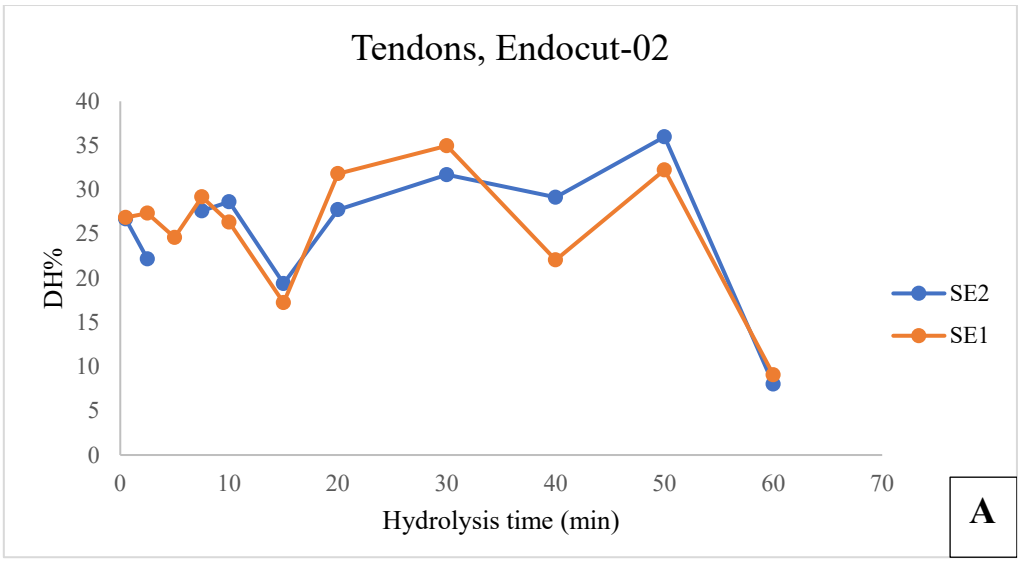

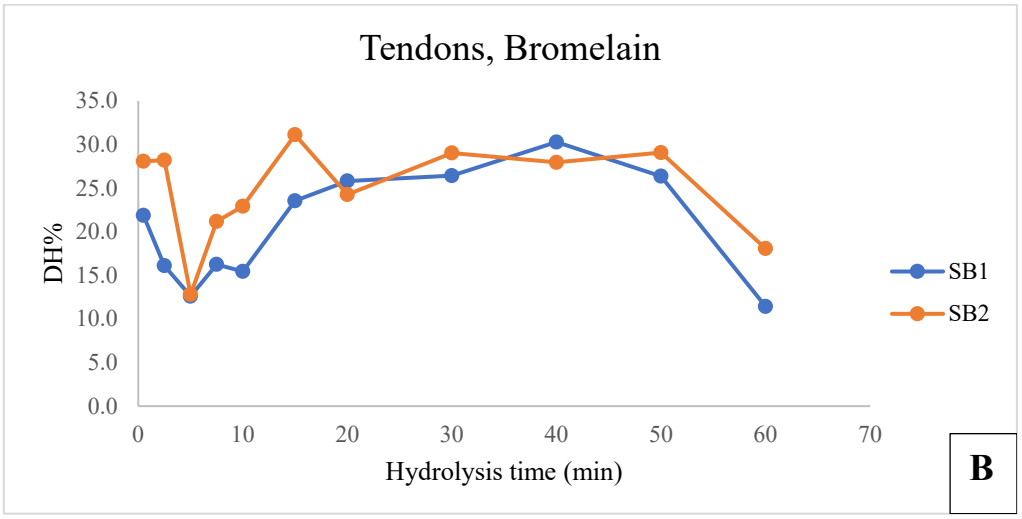

Figure 53. Graph with trendlines of the DH% during hydrolysis time of A) tendons treated with Endocut-02, and B) tendons treated with Bromelain, with the hydrolysis time on the x-axis and the DH% on the y-axis.

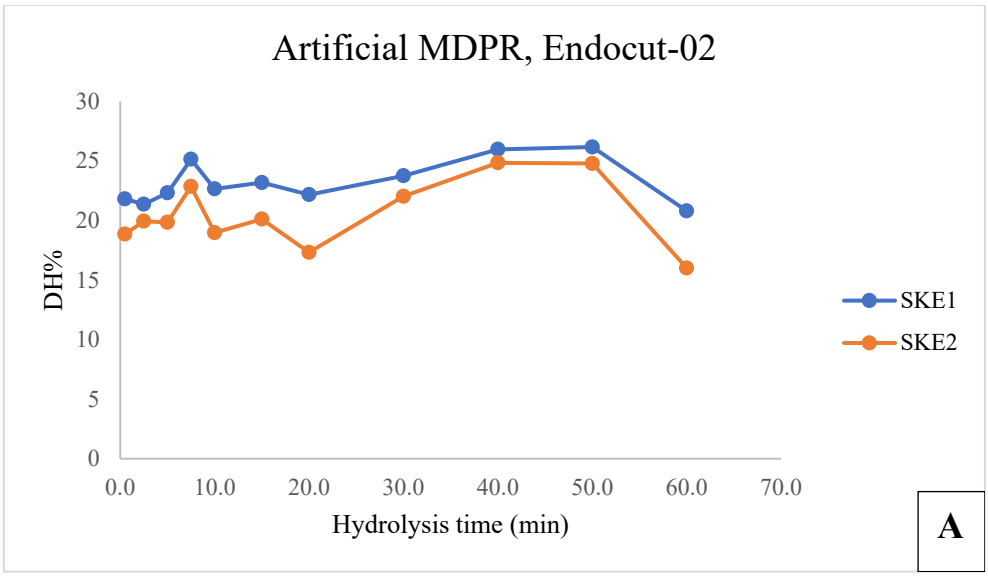

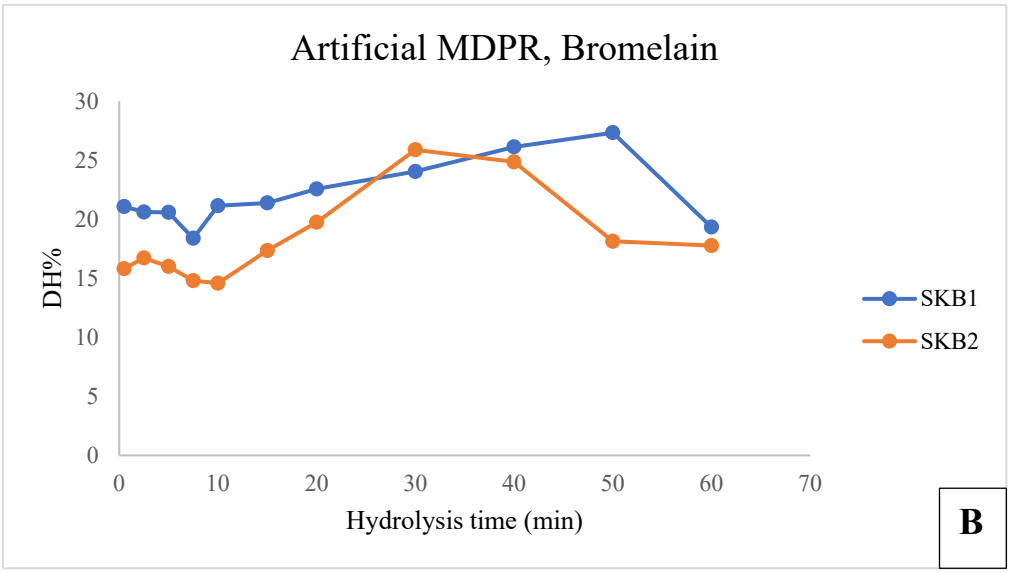

Figure 54. Graph with trendlines of the DH% during hydrolysis time of A) Artificial MDPR treated with Endocut-02, and B) Artificial MDPR treated with Bromelain, with the hydrolysis time on the x-axis and the DH% on the y-axis.

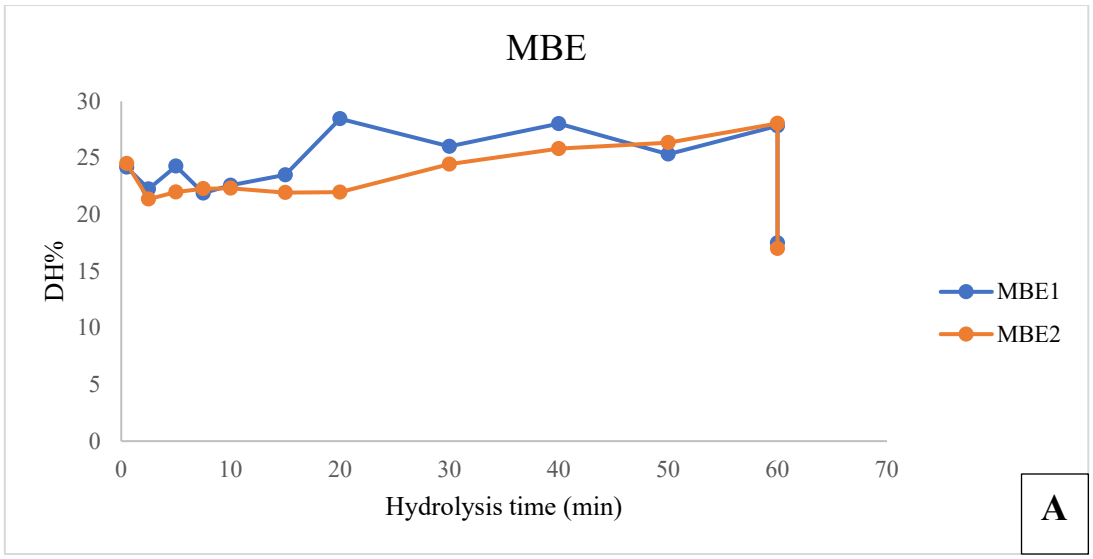

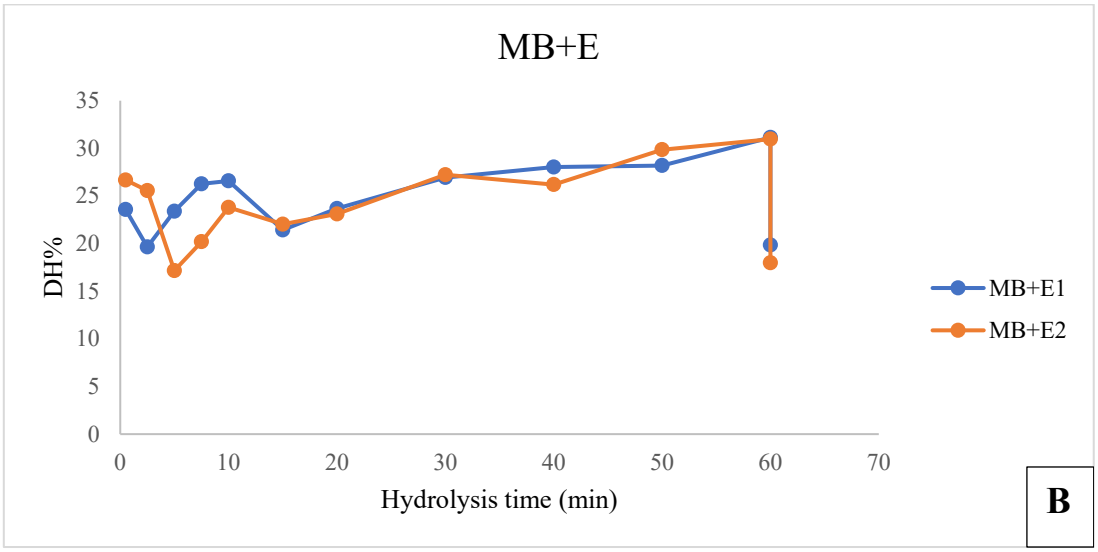

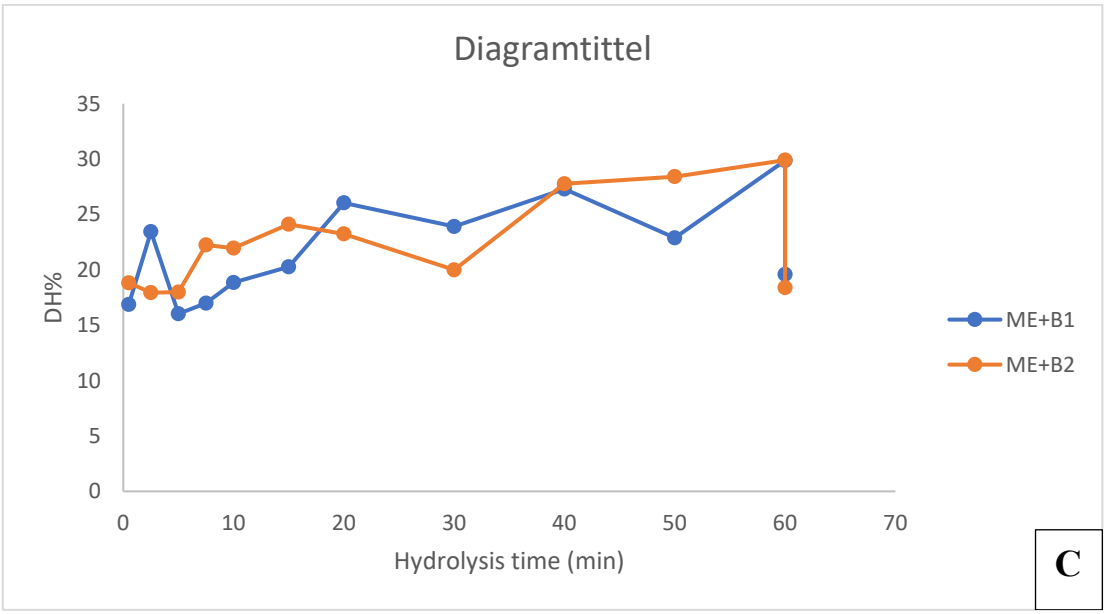

Figure 55. Graph of the DH% during hydrolysis time of A) MBE, B) MB+E, and C) ME+B with the hydrolysis time on the x-axis and the DH% on the y-axis. End-products are included.

7.7 Fourier-transform infrared analysis of the small- and lab-scale series

The spectra and the PCA score plots and loadings that were not included in section **4** are given in **Figure 56-66**. The spectra have been studied, but they are not presented with vibrational bond ranges in the appendix.

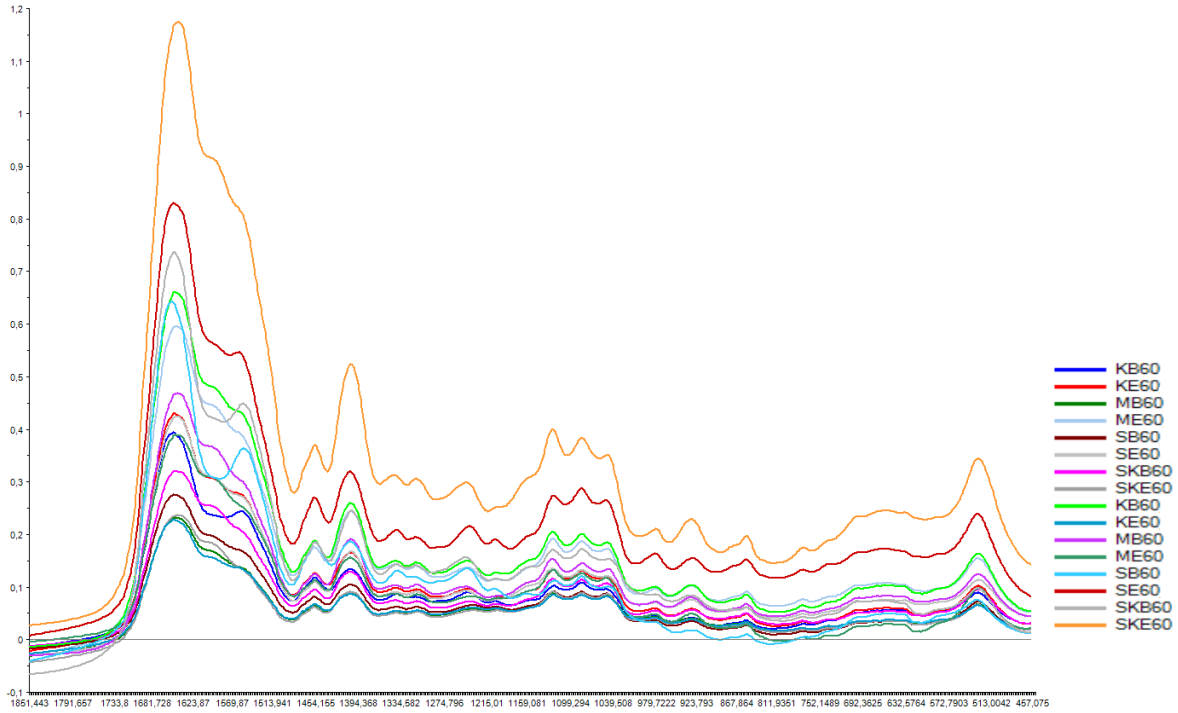

Figure 56. Raw spectra of the hydrolysates from the small-scale EPH

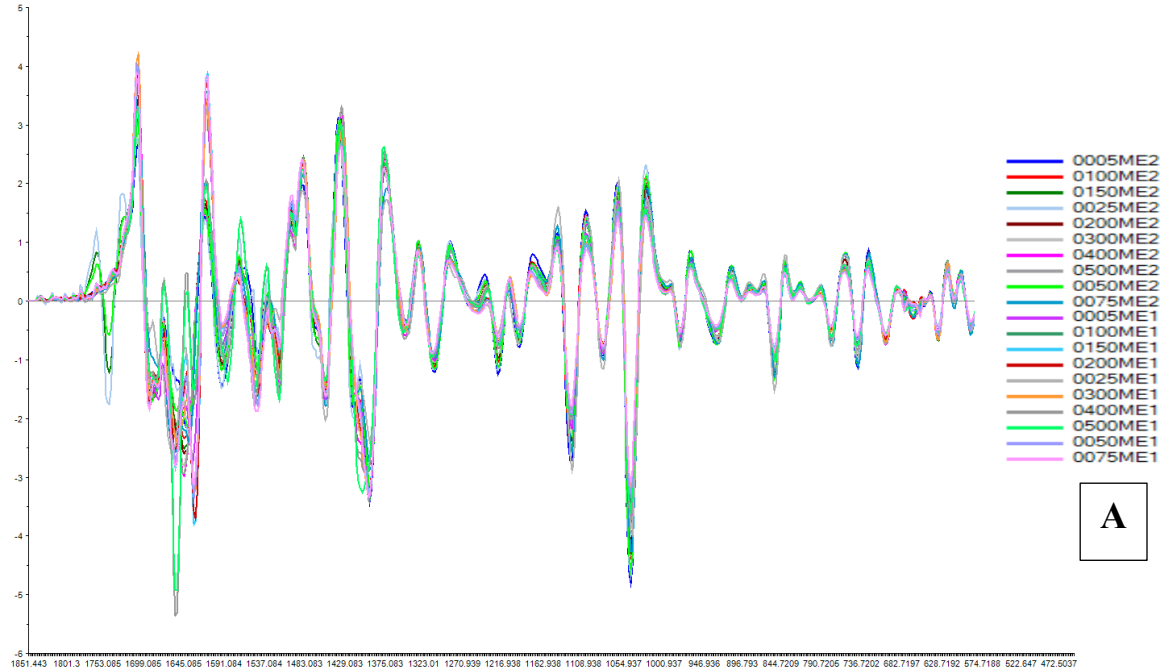

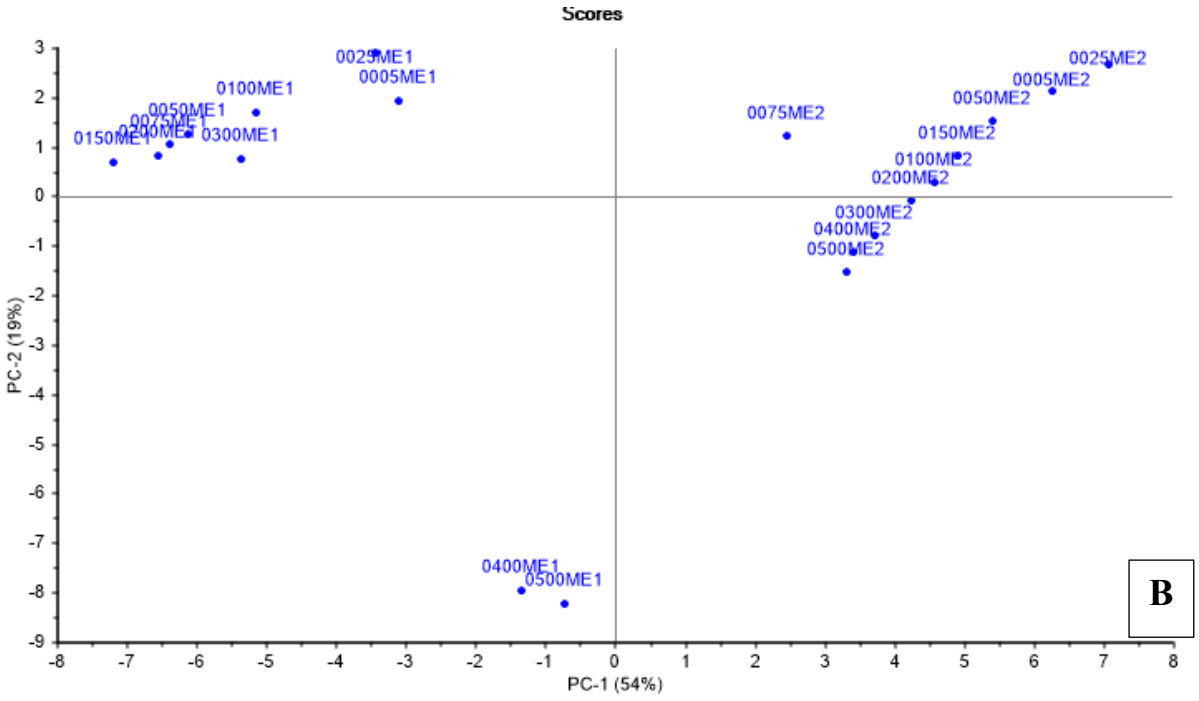

Figure 57. A) The SNV normalized second derivative spectra of the lab-scale series from MDPR treated with Endocut-02, with B) the PCA score plot.

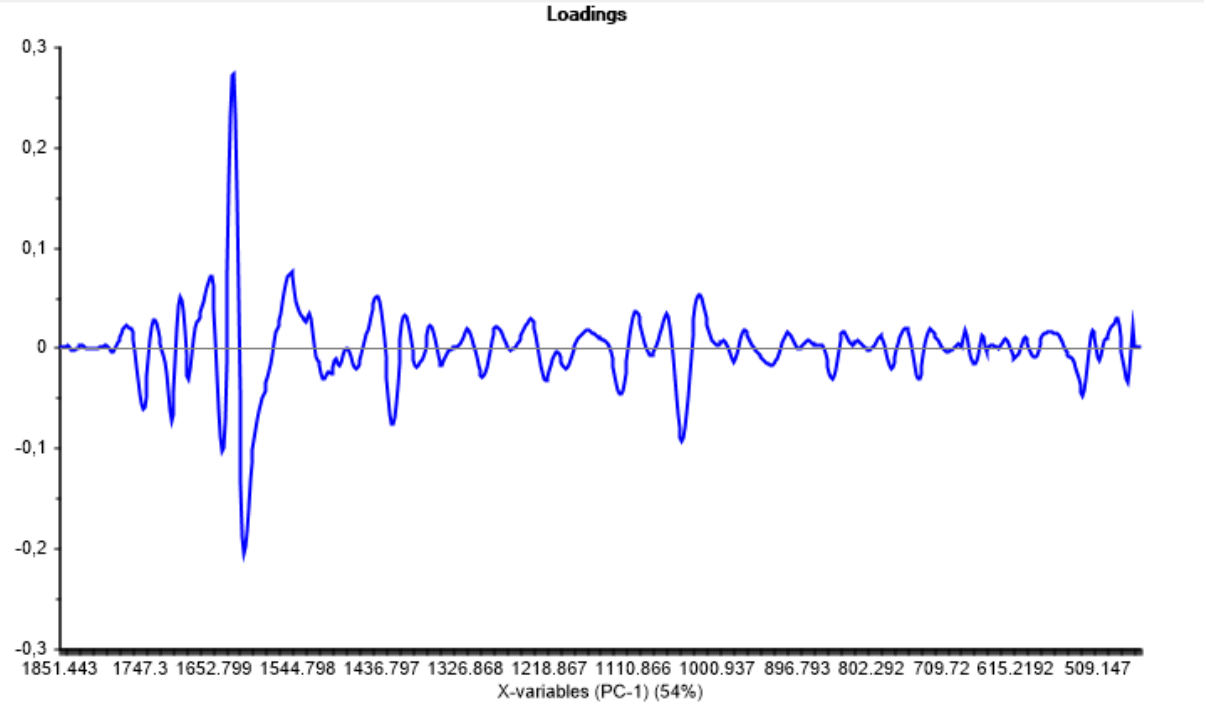

Figure 58. The PCA loading that corresponds to **Figure 57**, MDPR treated with Endocut-02.

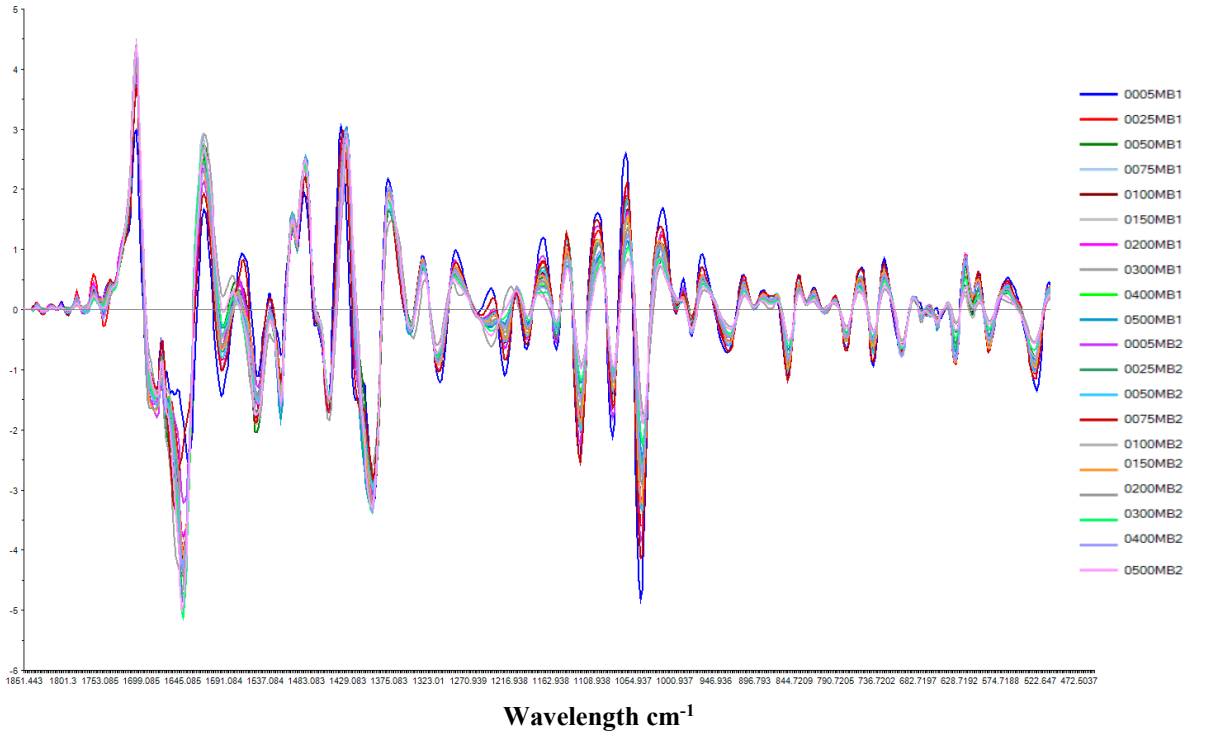

Figure 59. The SNV normalized second derivative spectra of the lab-scale series from MDPR treated with Bromelain.

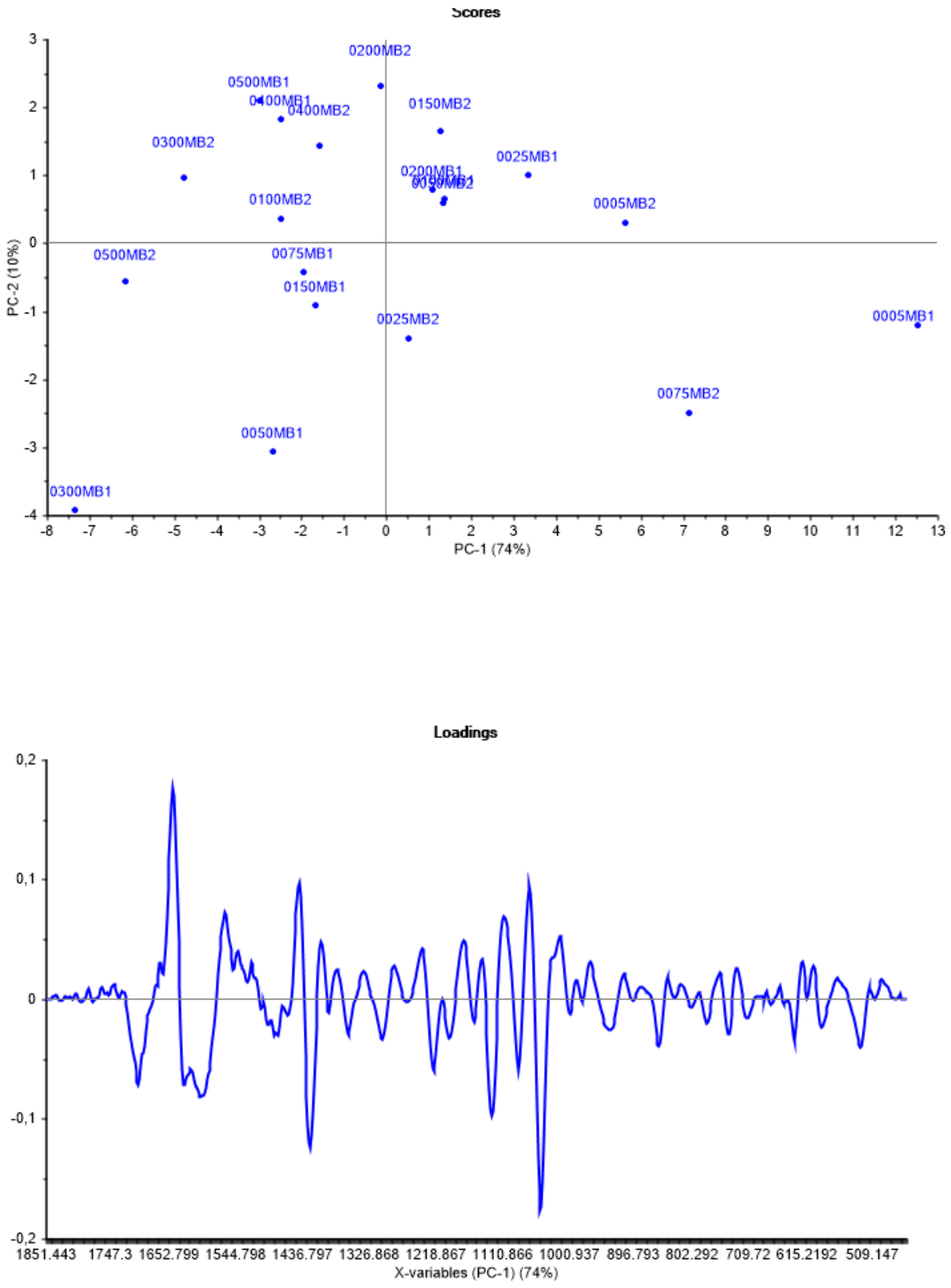

Figure 60. The PCA score plot and loading that corresponds to **Figure 59,** MDPR treated with Bromelain.

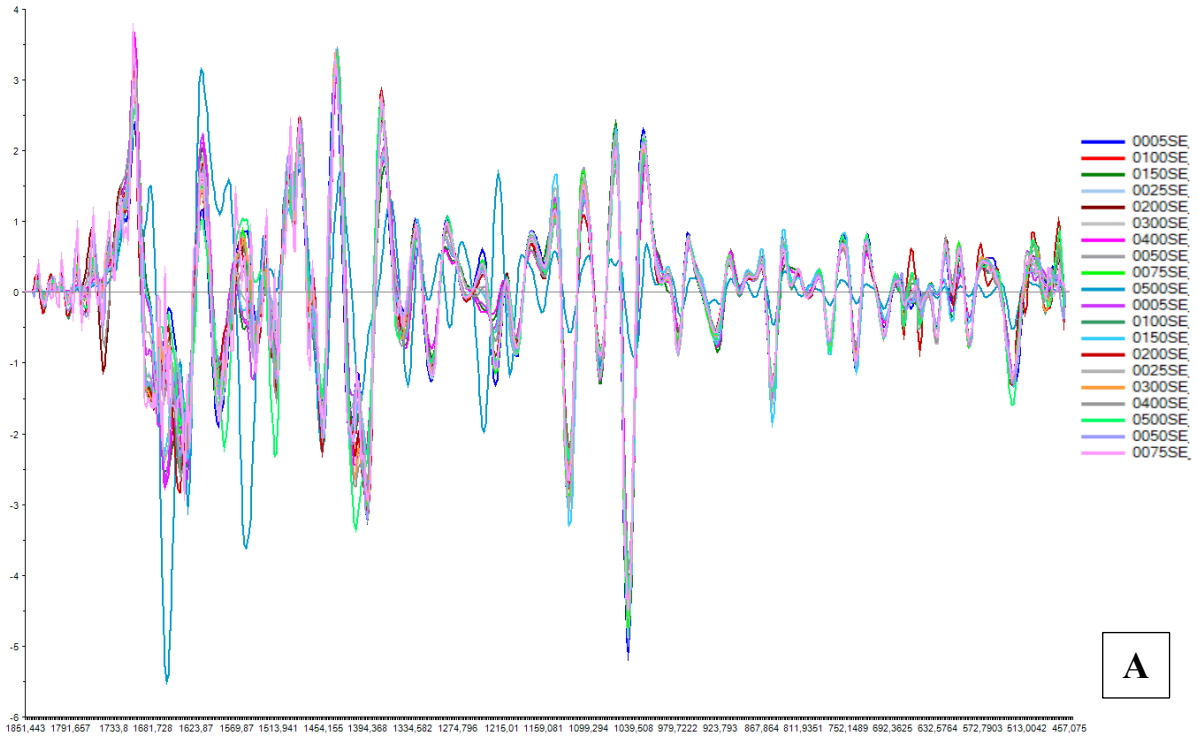

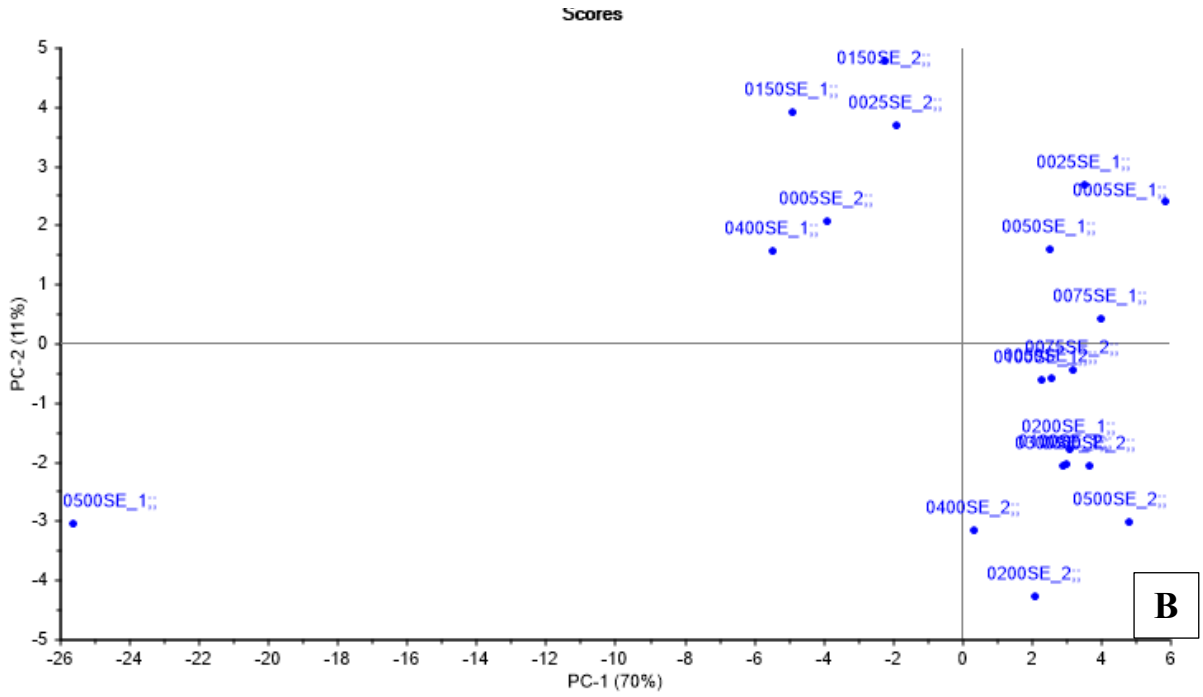

Figure 61. A) the SNV normalized second derivative spectra of tendons treated with Endocut-02, and B) the PCA score plot.

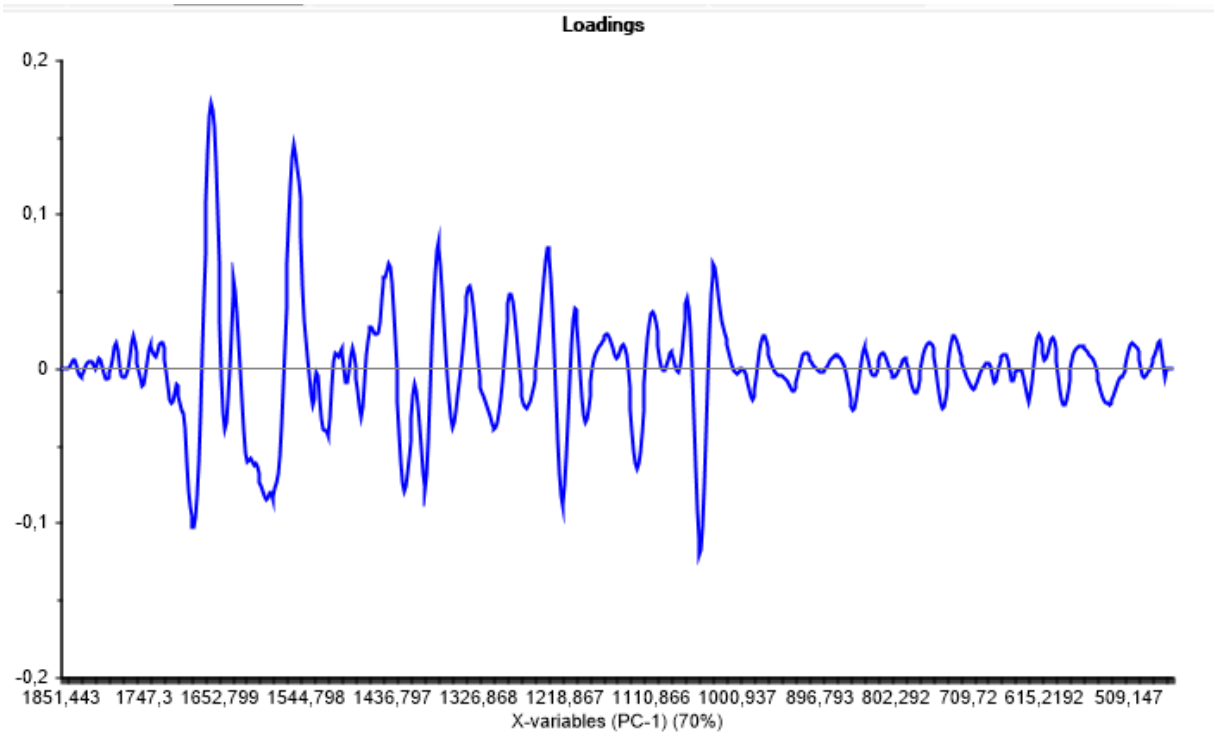

Figure 62. The PCA loading that corresponds with **Figure 61 (A-B)**, of tendons treated with Endocut-02.

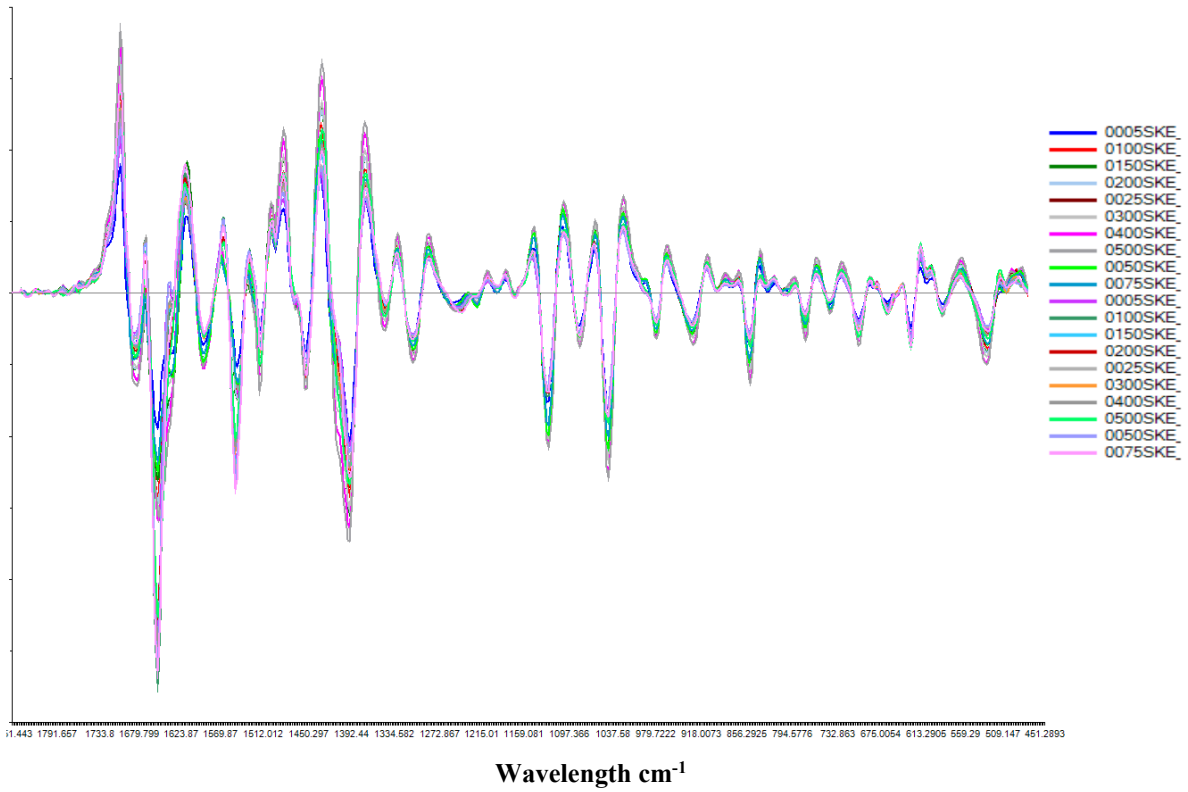

Figure 63. The SNV normalized second derivative spectra of artificial MDPR treated with Endocut-02.

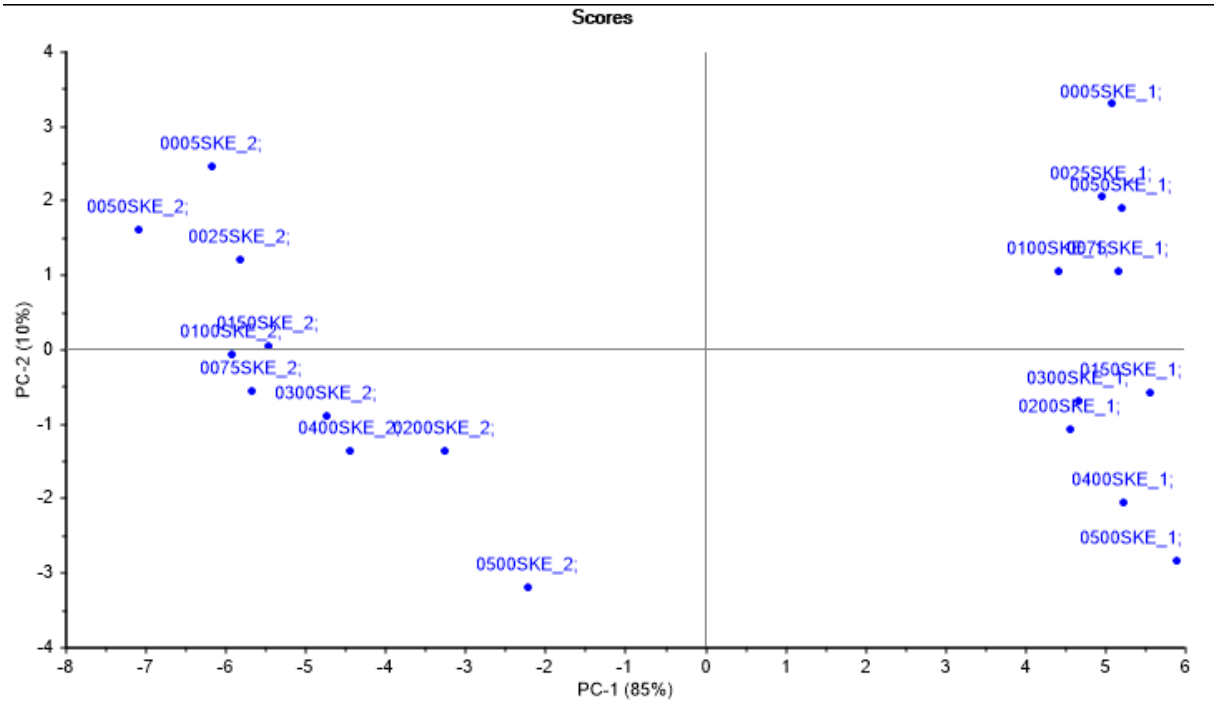

Figure 64. The PCA score plot that corresponds with **Figure 63,** of artificial MDPR treated with Endocut-02.

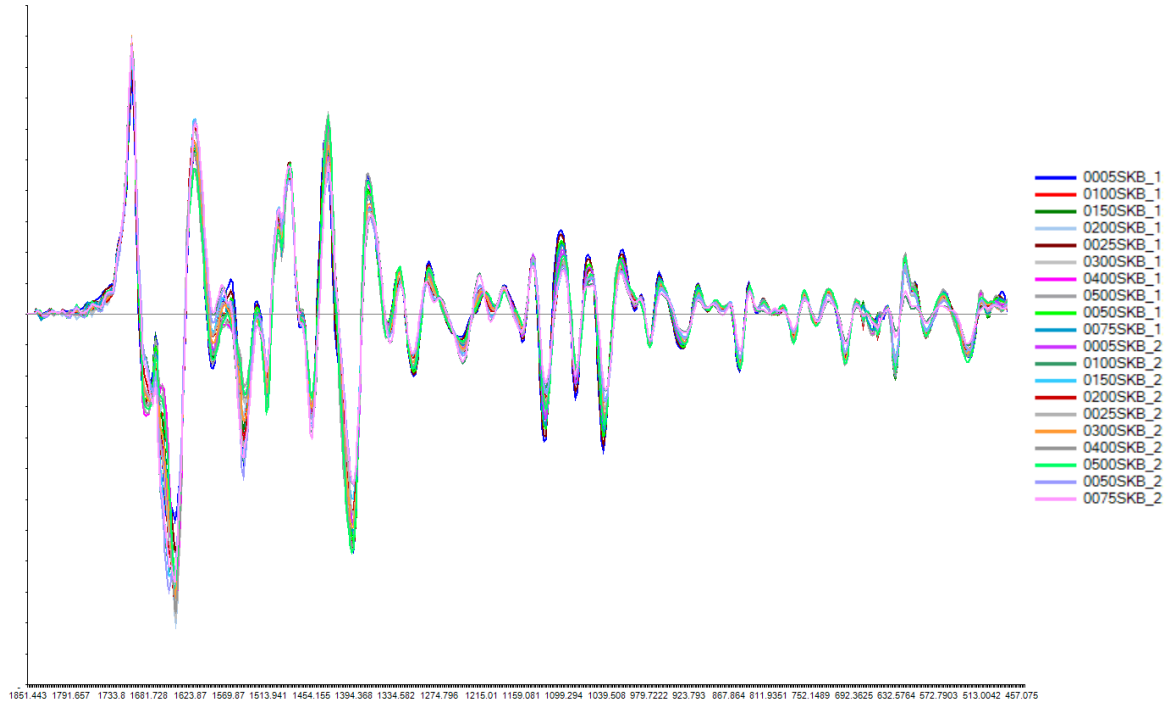

Wavelength cm^{-1}

Figure 65. The SNV normalized second derivative spectra of the lab-scale series with artificial MDPR treated with Bromelain.

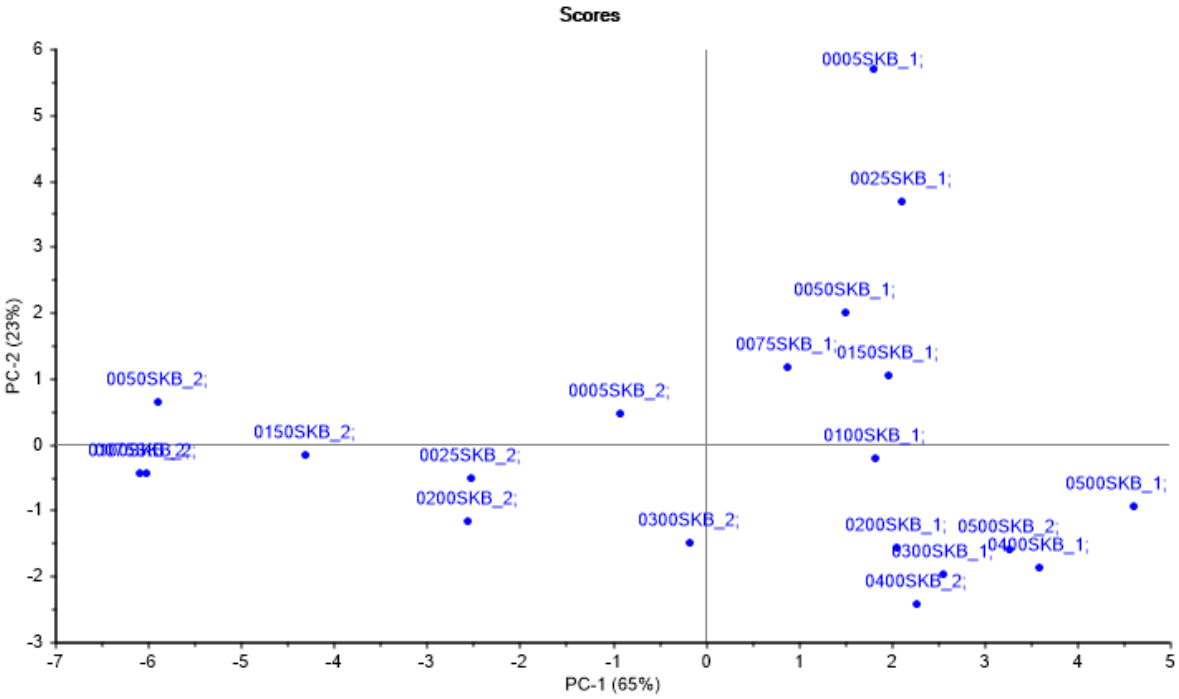

Figure 66. The PCA score plot that corresponds with **Figure 65,** artificial MDPR treated with Bromelain.

7.7.1 The variation during hydrolysis time revealed by principle component-1

It may seem like there was a correlation between PC-1 and the hydrolysis time, shown in **Figure 67**, A) – C). The graphs of the duplicated series were close throughout the reaction. If it is true that there is a correlation, it could be assumed that these reactions have had relatively good repeatability. A rapid change at the beginning of the reaction was observed, particularly in A) and B), which was reduced with the hydrolysis time. The rapid change from the experimental start could be explained by the fact that a higher kinetic movement happened at the beginning of the reaction when all the proteases were available to cleave the peptide chains. Also, a slow release of the small peptides towards the end of the hydrolysis has been observed earlier. However, an abrupt decrease in graph B) was shown at 30 minutes when Bromelain was added to the reaction, which was interesting. With the knowledge obtained throughout the study, there may seem like there is a correlation between PC-1 and the hydrolysis time, revealing a pattern where Bromelain, which is more relaxed than Endocut-02, solubilized the proteins at a higher pace than Endocut-02.

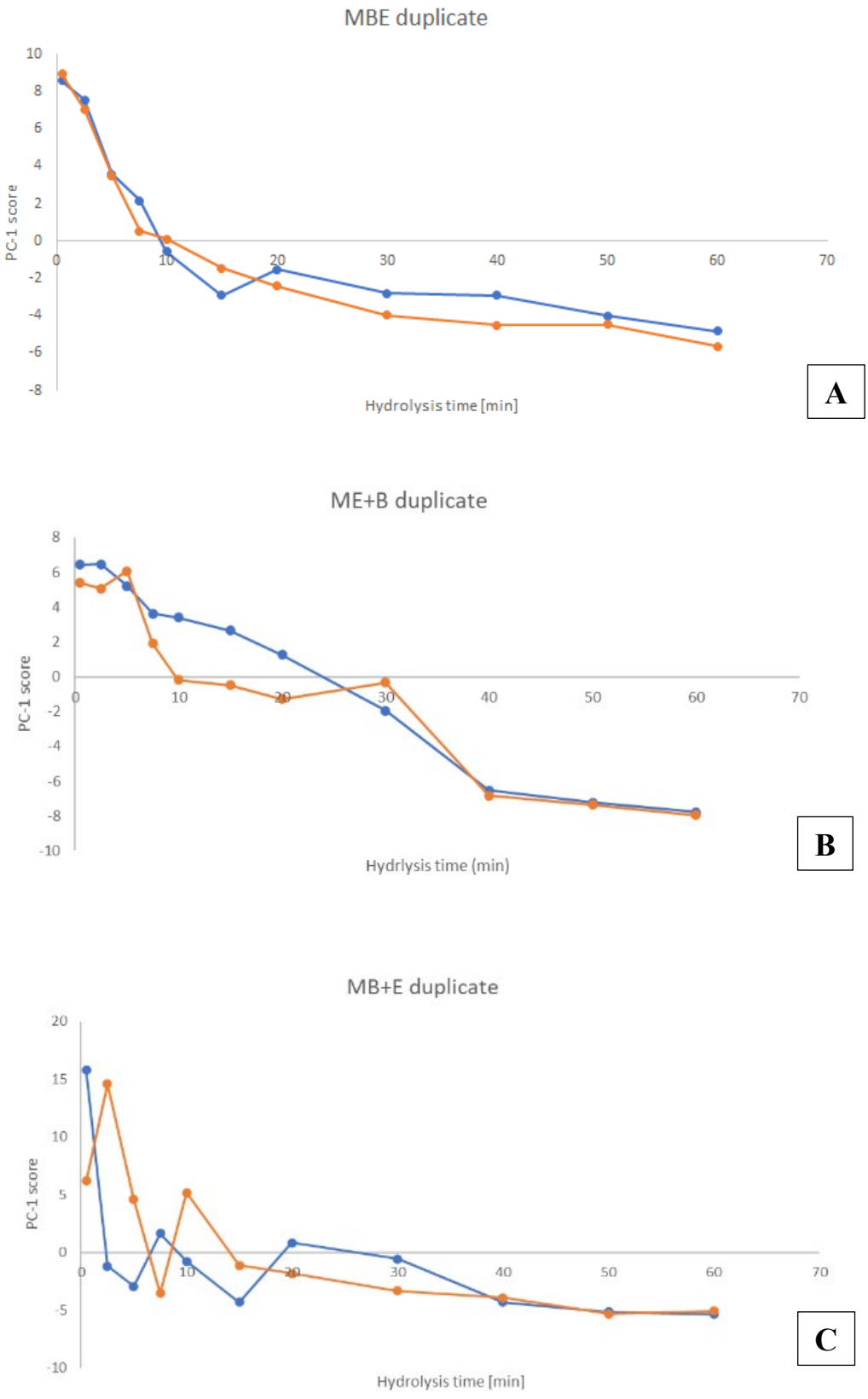

Figure 67. The correlation between the PC-1 scores and the hydrolysis time (min) for A) MBE, B) ME+B, and C) MB+E. Trendlines are included.

7.8 High performance size – exclusion chromatography

The lab-scale series chromatograms that were not included in section **4**, are shown in **Figure 68-73.** The chromatograms have been studied, but the figures are not presented with fractions in the appendix.

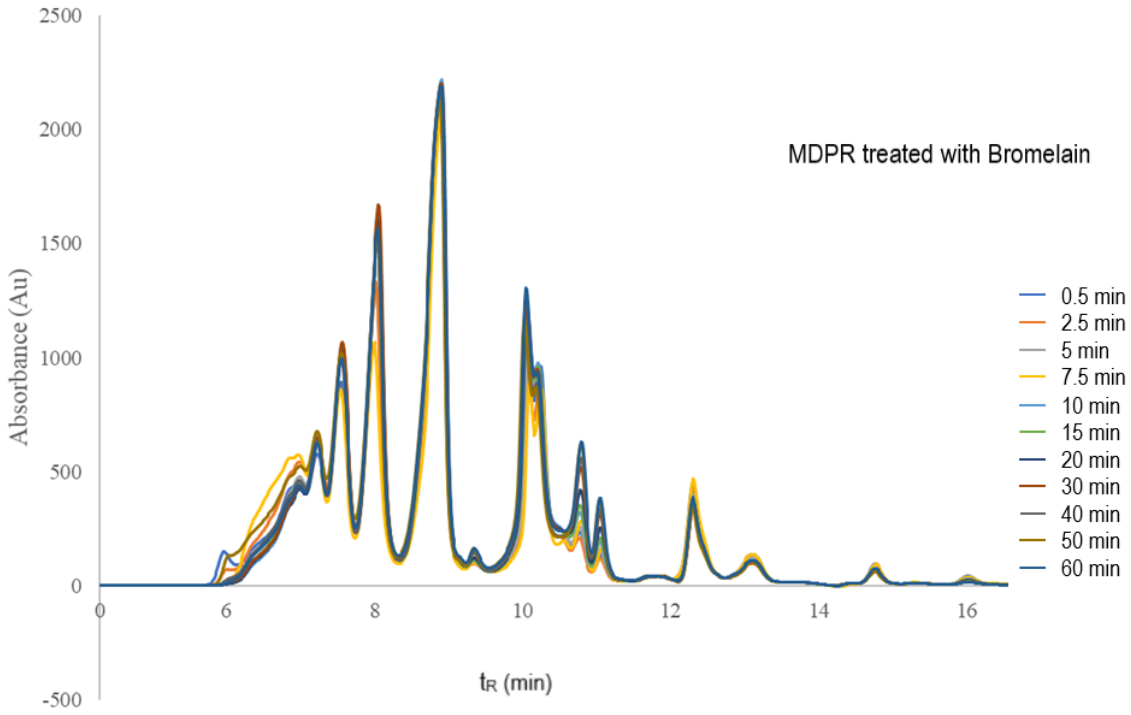

Figure 68. Chromatograms of MDPR treated with Bromelain, with retention time (min) on the x-axis and the Absorbance (Au) on the y-axis.

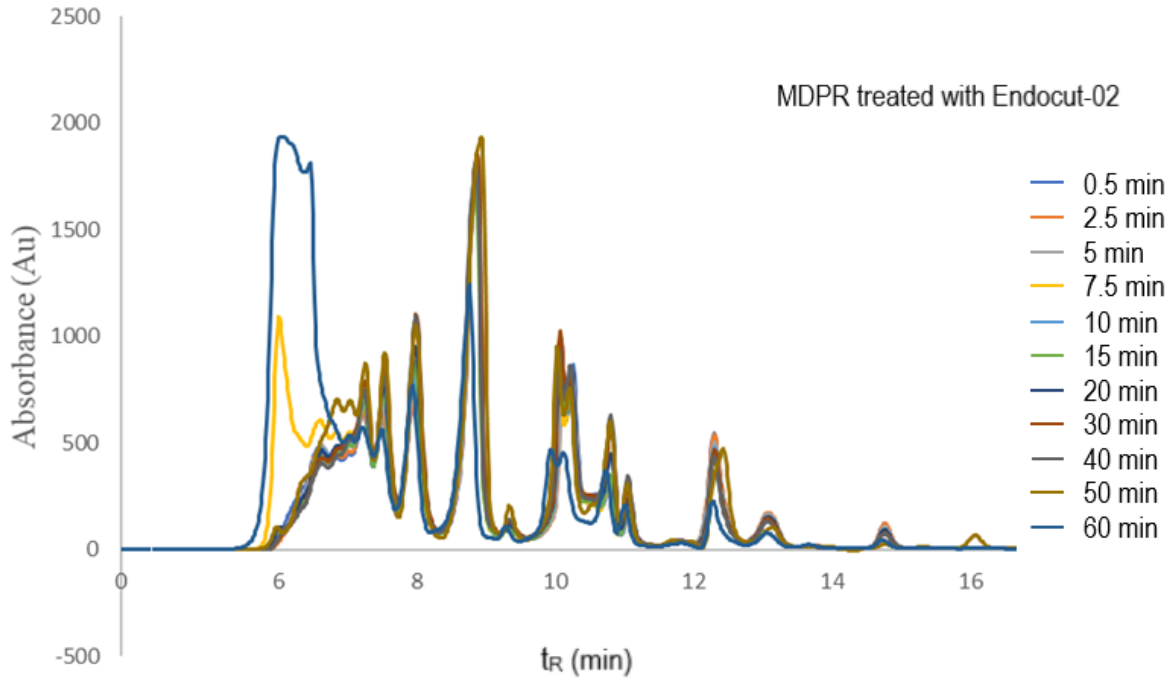

Figure 69. Chromatograms of MDPR treated with Endocut-02, with retention time (min) on the x-axis and the Absorbance (Au) on the y-axis.

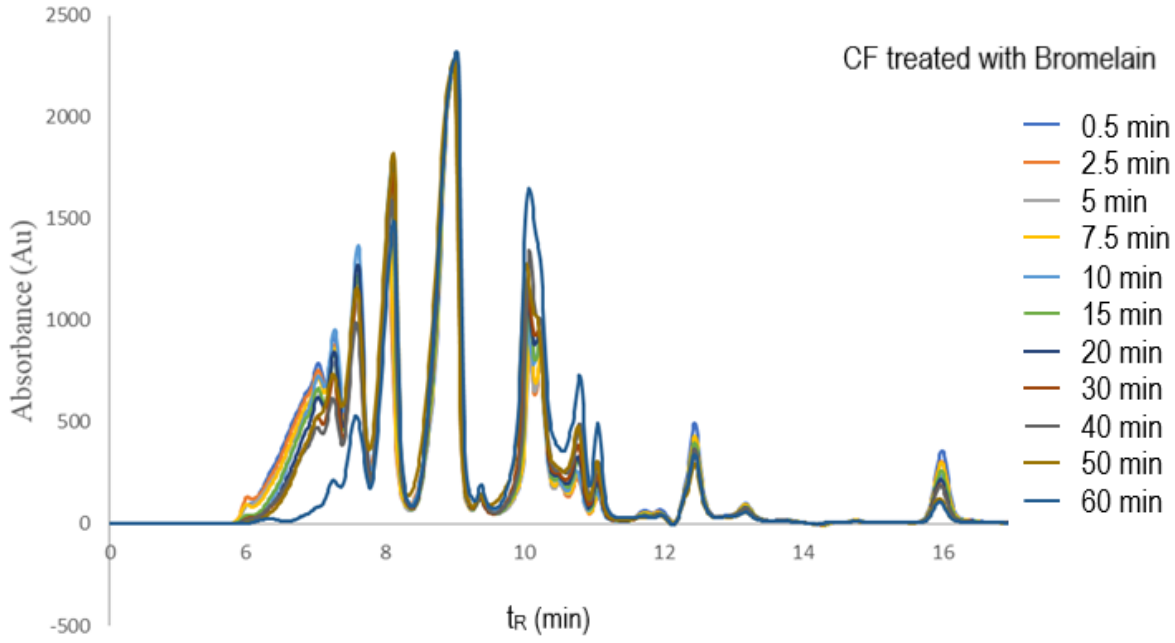

Figure 70. Chromatograms of CF treated with Bromelain, with retention time (min) on the x-axis and the Absorbance (Au) on the y-axis.

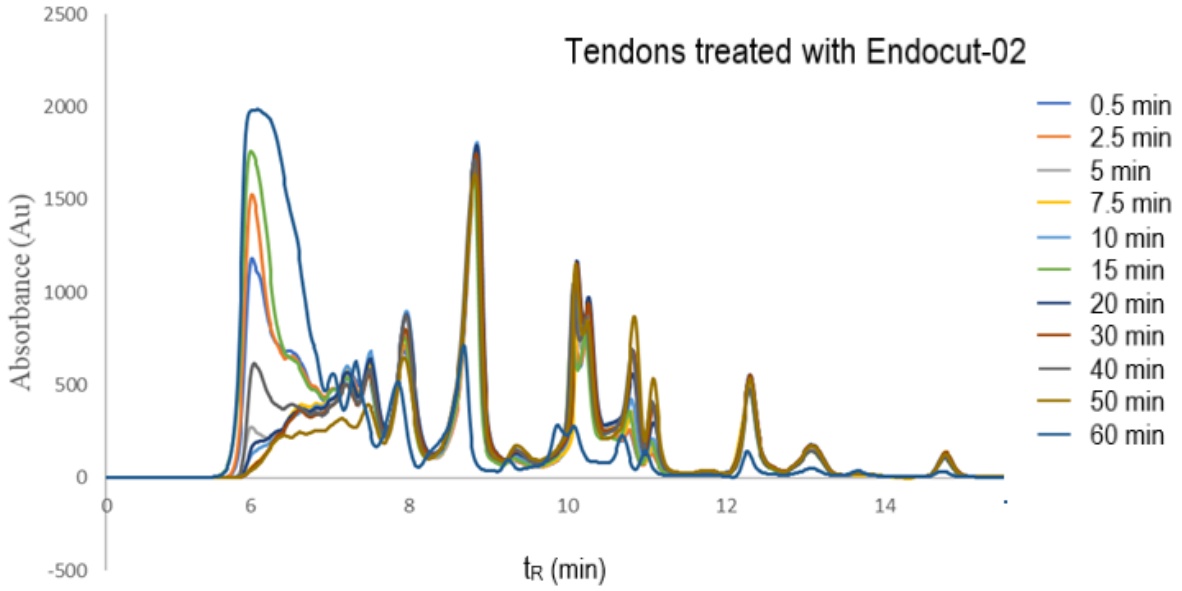

Figure 71. Chromatograms of tendons treated with Endocut-02, with retention time (min) on the x-axis and the Absorbance (Au) on the y-axis.

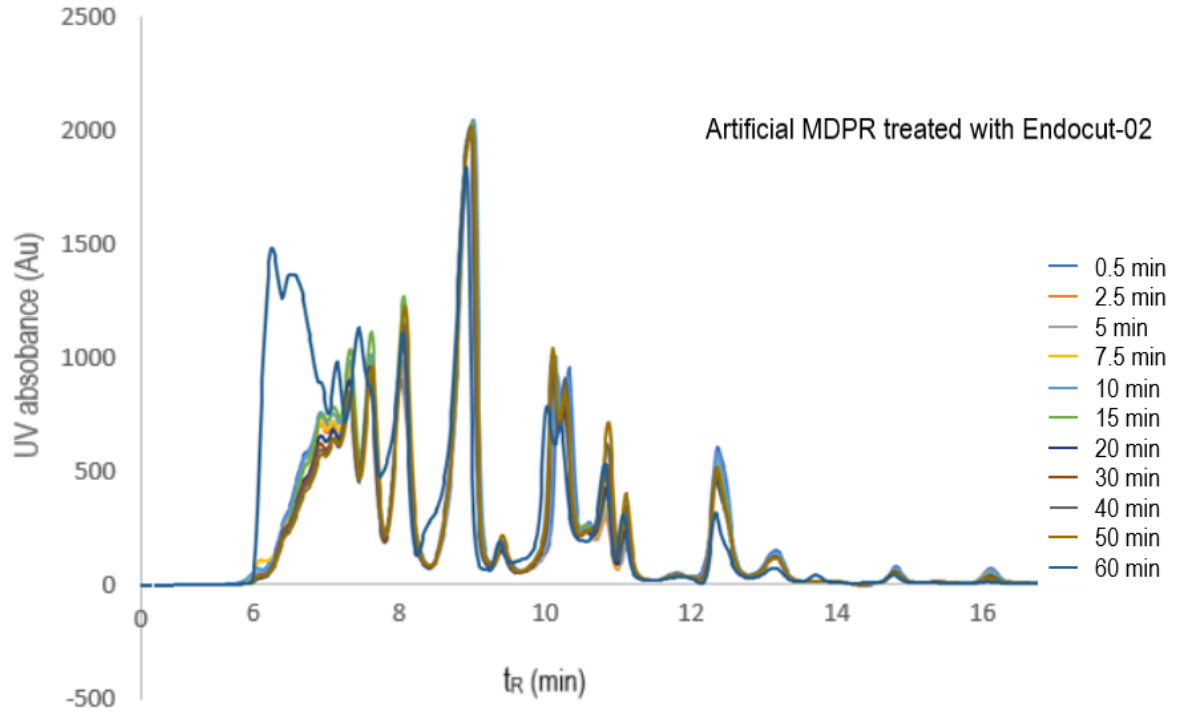

Figure 72. Chromatograms of artificial MDPR treated with Endocut-02, with retention time (min) on the x-axis and the Absorbance (Au) on the y-axis.

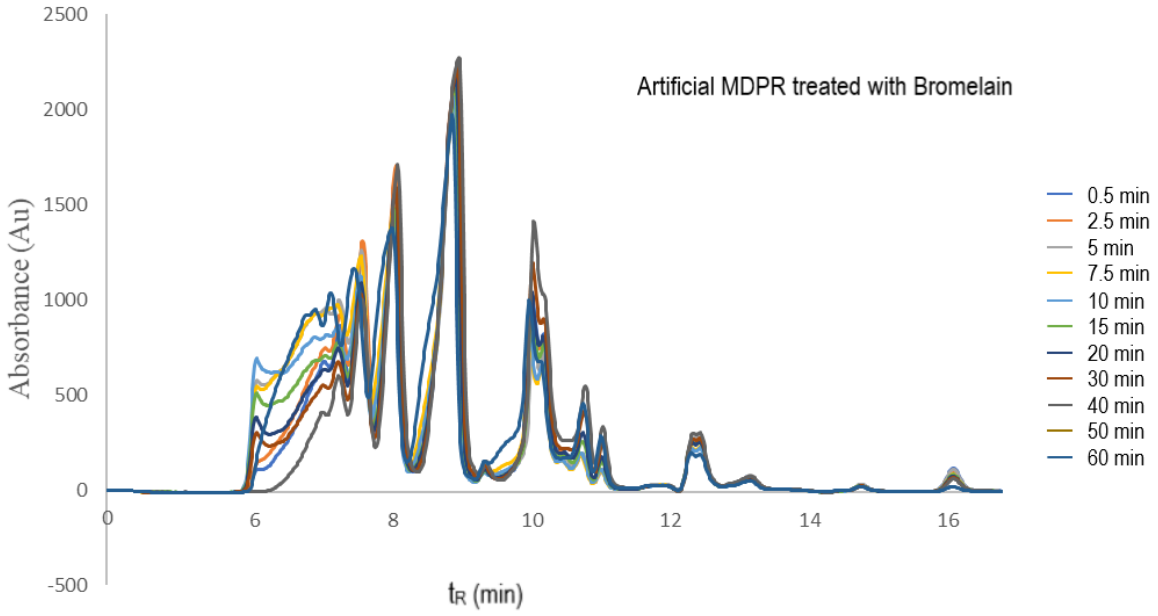

Figure 73. Chromatograms of artificial MDPR treated with Bromelain, with retention time (min) on the x-axis and the Absorbance (Au) on the y-axis.

7.9 Images from the enzymatic protein hydrolysis process

A set of images from the EPH process, with a brief description below each image.

CF before grinding

Tendons

MDPR

CF grinded

Small-scale EPH

Lab-scale EPH

Deactivation

Dried sediment

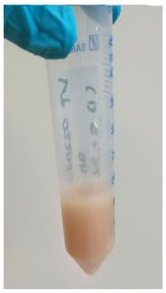

Time series sample

Sediment (MBE)

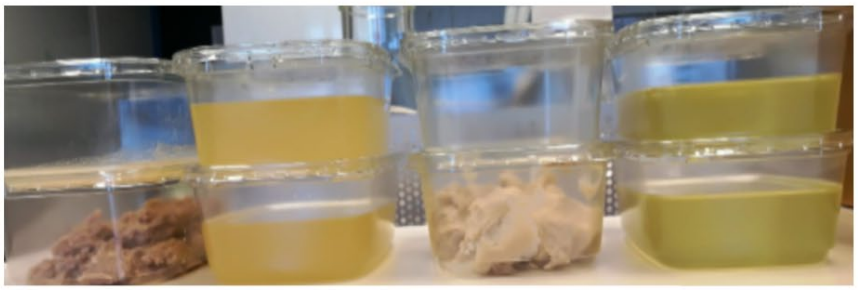

Sediment (MB) | Liquid (MB) | Sediment (KB) | Liquid (KB)

8 Poster presented at Bioprosp_19 «Unlocking the potential of biomolecules from marine environments,» Tromsø 2019.

Bioprosp_19, 25-27 Feb., Tromsø, Norway

Development of novel cascade technologies enabling optimal utilization of marine and animal by-products – the NOTABLY approach

D. Lindberg*[1], S.G. Wubshet[1], M. R. Dalsnes[1], L. M. G. Hunnes[1], J. Döring[1], U. Böcker[1], K. A. Kristoffersen[1], N. K. Afseth[1]

*Email: Diana.Lindberg@Nofima.no, Tel: +47 64 97 02 07
[1] Dept.. Raw Materials and Process, Nofima AS, Norwegian Institute of Food, Fisheries and Aquaculture Research, NO-1433 Ås, Norway

During enzymatic protein hydrolysis (EPH), enzymes are added to by-products to facilitate breakdown of proteins to smaller peptides and amino acids. Currently, this is followed by downstream recovery of three crude fractions: peptides, lipids and a collagen- and mineral-rich low value sediment. However, by-products from marine and animal origin are not limited to three components only, but consist a multitude of different proteins and other biological molecules. In the NOTABLY project (NRC no. 280709), multistep bioprocessing will be used for total utilization of two types of by-products: cod heads and mechanically deboned poultry residue (MDPR). Both displays a high degree of chemical complexity due to an abundance of connective tissue and bones. The goal of the project is the development of new cascade processes enabling the recovery of several high-value components from one process line. A precise break-down of complex materials, enabling the recovery of concentrated high-value products, calls for a thorough understanding of the specific activity of enzymes towards each component present. In this study we thus present a methodological approach for enzyme screening towards "pure" components of poultry and cod residues.

Approach

The evaluation of single enzyme activities on raw material components is based on a two-step approach. In the first step, a screening of the activity of each protease yields a number signifying enzyme activity in comparison to the others, based on an azo-casein substrate assay. In the next step, a second screening is performed using the proteases on "real" sample substrates, consisting of pure components of by-products. The amount of protease used in the second screening is "normalized" based on the activity in the first screening step.

Materials & methods

The first-step enzyme activity screening was performed by use of the Azo-casein assay (S-AZCAS 12/07, Megazyme International Ireland, Ireland) according to protocol. The proteases used were selected based on information on that they would display sufficient activity at pH 7, and are either defined as general proteases or collagenases.

The enzyme list comprised Endocut 1-3, 10 189-194 & 197 from Tailorzyme ApS (Denmark); Alcalase, Protamex, Neutrase & Flavourzyme from Novozymes ApS (Denmark); Veron L, Corolase 2TS & 7090 from AB Enzymes GmbH (Germany); Promod 144 GL-100TU & 9950L from Biocatalysts LtD (UK); Maxipro NPU from DSM (The Netherlands); Foodpro 30L, 51FP & PNL from Dupont/Danisco (USA).

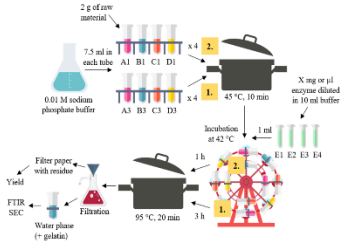

Figure 1. Flow chart of the second screening

The resulting activities for liquid and powder enzymes were compared, and normalized amounts were added to the reaction mixtures in the second step screening of activity on real raw materials. For the approach development, ground meat, bones and mechanically deboned carcass from chicken and well as cut turkey tendons were used. The screening protocol is outlined in Fig. 1.

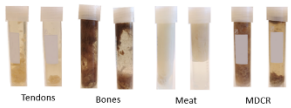

Figure 2. Example pictures after decomposition of the raw materials, using different two different enzymes for each material type.

The proteases were allowed to react for 1 and 3 hours, respectively (see Fig 2). For all reaction mixtures, proteases were deactivated by heating. Product characterization was based on yield (i.e. weight of remaining substrate) as well as analysis of the aqueous phase using Fourier-transform Infrared spectroscopy (FTIR) and Size-Exclusion Chromatography (SEC).

Results enzyme screening

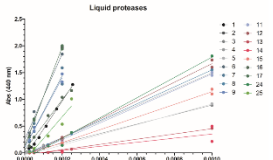

Figure 3. The resulting end-absorbances after the Megazyme Azo-casein assay (40 °C, 10 min , pH 7), using liquid enzymes at different concentrations.

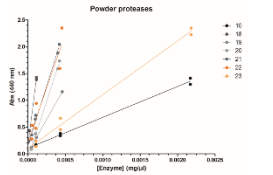

Figure 4. The resulting end-absorbances after the Megazyme Azo-casein assay (40 °C, 10 min, pH 7), using powder enzymes at different concentrations.

There is a large variation in protease activity shown after measurements with the azo-casein assay. When using the linear regression results to calculate how much of each protease is needed to reach "the same" activity level, at y=1, the difference between the highest and lowest acting proteases differ with a factor of 28 times for the liquid protease products, and a factor of 11 for the powder products.

These factors were used to calculate the amount of protease added in the next step. For the measurements on raw materials to the right, the factors are 2.7 times between proteases 1 and 21 (same amount) to protease 8, and 1.3 times to protease 20.

Result raw materials screening

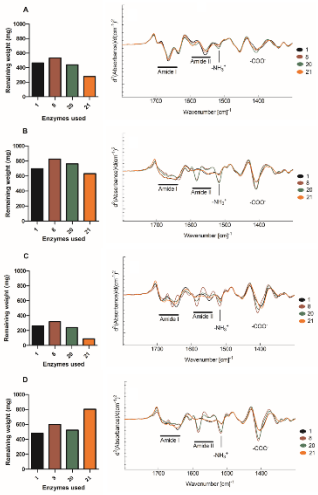

Figure 5. Results from hydrolysis with proteases 1 and 8 (liquids), as well as 20 and 21 (powder), presented as remaining amount of raw material (left). Materials are A) Achilles tendon; B) bones; C) meat, and D) MDCR. To the right, for materials A-D, the resulting FTIR spectra of each of the proteases used.

In spite of normalizing activity based on the azo-casein assay, expected differences in activity are seen in both remaining amount of raw material. There are also clear differences in the FTIR spectra, based on both raw materials and between single proteases in hydrolysis of different raw materials.

Acknowledgements

The Notably project is a research project during years 2018-2021, granted by the Norwegian research council (NRC grant no. 280709)

- Marte R. Dalsnes is currently a MSc student at NTNU under the supervision of Dr. Eva Falch.
- Maria G. Hunnes is currently a MSc student at UiO under the supervision of Prof. Elsa Lundanes.
- Julia Döring is currently a MSc student at Copenhagen University under the supervision of Assoc. Prof. Karsten Olsen.

Conclusions

A clear difference in protease activity of are shown, irrespective of substrate.

- Although the presented approach is based on normalizing protease activity based on a pre-screening, the hydrolysis of different materials leads to expected differences in the degradation of protein-rich by-products

The raw material FTIR spektra differs between substrate materials, as does the spectra of each hydrolysate resulting from using different proteases of the single raw material components.

Nofima AS, NO-9291 Tromsø, Norway, Tel: +47 77 62 90 00, www.nofima.no/en/, post@nofima.no - Norwegian Institute of Food, Fisheries and Aquaculture Research